INFORMATION TO USERS

This manuscript has been reproduced from the microfilm master. UMI films the text directly from the original or copy submitted. Thus, some thesis and dissertation copies are in typewriter face, while others may be from any type of computer printer.

The quality of this reproduction is dependent upon the quality of the copy submitted. Broken or indistinct print, colored or poor quality illustrations and photographs, print bleedthrough, substandard margins, and improper alignment can adversely affect reproduction.

In the unlikely event that the author did not send UMI a complete manuscript and there are missing pages, these will be noted. Also, if unauthorized copyright material had to be removed, a note will indicate the deletion.

Oversize materials (e.g., maps, drawings, charts) are reproduced by sectioning the original, beginning at the upper left-hand corner and continuing from left to right in equal sections with small overlaps.

Photographs included in the original manuscript have been reproduced xerographically in this copy. Higher quality 6" x 9" black and white photographic prints are available for any photographs or illustrations appearing in this copy for an additional charge. Contact UMI directly to order.

Bell & Howell Information and Learning
300 North Zeeb Road, Ann Arbor, MI 48106-1346 USA

UMI®
800-521-0600

Université d'Ottawa · University of Ottawa

ABSTRACT

Mixed metal organometallic complexes with oxide co-ligands may serve as useful models for platinum metal catalysts on early transition metal oxide supports. Reaction of the electronically unsaturated hydride containing cluster $[H_2Os_3(CO)_{10}]$ with $[W(C{\equiv}CPh)(O)_2(Cp^*)]$ afforded the μ-oxo, μ-hydrido, μ-vinylidene cluster $[Os_3W(\mu\text{-}H)(\mu\text{-}\eta^1\text{-}C{=}CHPh)(CO)_{10}(O)(\mu\text{-}O)(Cp^*)]$ **1** via a process involving acetylide and oxide coordination to the Os_3 framework and transfer of a hydride ligand to the unsaturated hydrocarbyl.

Under thermal conditions, cluster **1** undergoes smooth decarbonylation concomitant with the formation of a novel μ_3-oxo ligand to afford $[Os_3W(\mu\text{-}H)(\textit{trans}\text{-}\mu\text{-}\eta^1\text{-}C{=}CHPh)(CO)_9(O)(Cp^*)(\mu_3\text{-}O)]$ **2**. Under photolysis, **2** isomerizes in high yield to a second μ_3-oxo, μ-vinylidene complex $[Os_3W(\mu\text{-}H)(\textit{cis}\text{-}\mu\text{-}\eta^1\text{-}C{=}CHPh)(CO)_9(O)(Cp^*)(\mu_3\text{-}O)]$ **3**.

Under photolytic conditions, the μ-hydrido ligand of **1** is transferred over to the μ-vinylidene ligand resulting in the formation of a $\mu\text{-}\eta^1,\eta^2$-vinyl ligand in $[Os_3W(CO)_{10}(O)(\mu\text{-}\eta^1,\eta^2\text{-}CH{=}CHPh\{\textit{W-Os}\})(\mu\text{-}O)(Cp^*)]$ **4**. Cluster **4** reacts under photolytic conditions with dihydrogen gas in a non-regioselective manner to produce two clusters, $[Os_3W(\mu\text{-}H)(\textit{anti}\text{-}\mu\text{-}\eta^1\text{-}CHCH_2Ph)(CO)_9(O)(Cp^*)(\mu_3\text{-}O)]$ **5** and $[Os_3W(\mu\text{-}H)(\textit{gauche}\text{-}\mu\text{-}\eta^1\text{-}CHCH_2Ph)(CO)_9(O)(Cp^*)(\mu_3\text{-}O)]$ **6**, bearing a μ_3-oxo ligand and a μ-alkylidene organic fragment.

The complexes **1**, **4**, **5** and **6** resemble species proposed as intermediates on hydrogenation catalysts. A rational next step in such a catalyzed reduction process would be the elimination of the organic fragment from the metal framework. However in this study no evidence supporting such chemical behavior was observed. Nevertheless interesting clusters bearing no hydrocarbyl fragments were isolated from a related experiment. Thermolysis of **4** led to the isolation of two clusters, $[Os_3W(\mu\text{-}H)(CO)_9(\mu\text{-}O)_2(Cp^*)]$ **9** and $[Os_3W(CO)_8(\mu\text{-}O)_2(Cp^*)]_2$ **12**, without hydrocarbyl units. The metal framework of **12** consists of a rare Os_6 rhombic raft and a packing diagram suggested the presence of a layered $W(O)_2|Os_6|W(O)_2$

lattice. This reaction also led to the isolation of an additional four clusters demonstrating various bonding modes for both the $[W(O)_2(Cp^*)]$ fragment and the vinyl ligand on a Os_3 skeleton. As suggested by TLC analysis and infrared spectroscopy, the first complex formed upon thermolysis of **4** is $[Os_3W(CO)_9(\mu\text{-}O)_2(\mu\text{-}\eta^1,\eta^2\text{-}CH{=}CHPh\{W\text{-}Os\})(Cp^*)]$ **7** which further isomerizes to $[Os_3W(CO)_9(\mu\text{-}O)_2(\mu\text{-}\eta^1,\eta^2\text{-}CH{=}CHPh\{Os\cdots Os\})(Cp^*)]$ **8**. The reaction of **8** with carbon monoxide liberated during previous reaction steps led to the isolation of $[Os_3W(CO)_{10}(O)(\mu\text{-}\eta^1,\eta^2\text{-}CH{=}CHPh\{Os\text{-}Os\})(\mu\text{-}O)(Cp^*)]$ **10** which also reacts with one molecule of carbon monoxide to provide $[Os_3W(\eta^1\text{-}CH{=}CHPh)(CO)_{11}(O)(\mu\text{-}O)(Cp^*)]$ **11**.

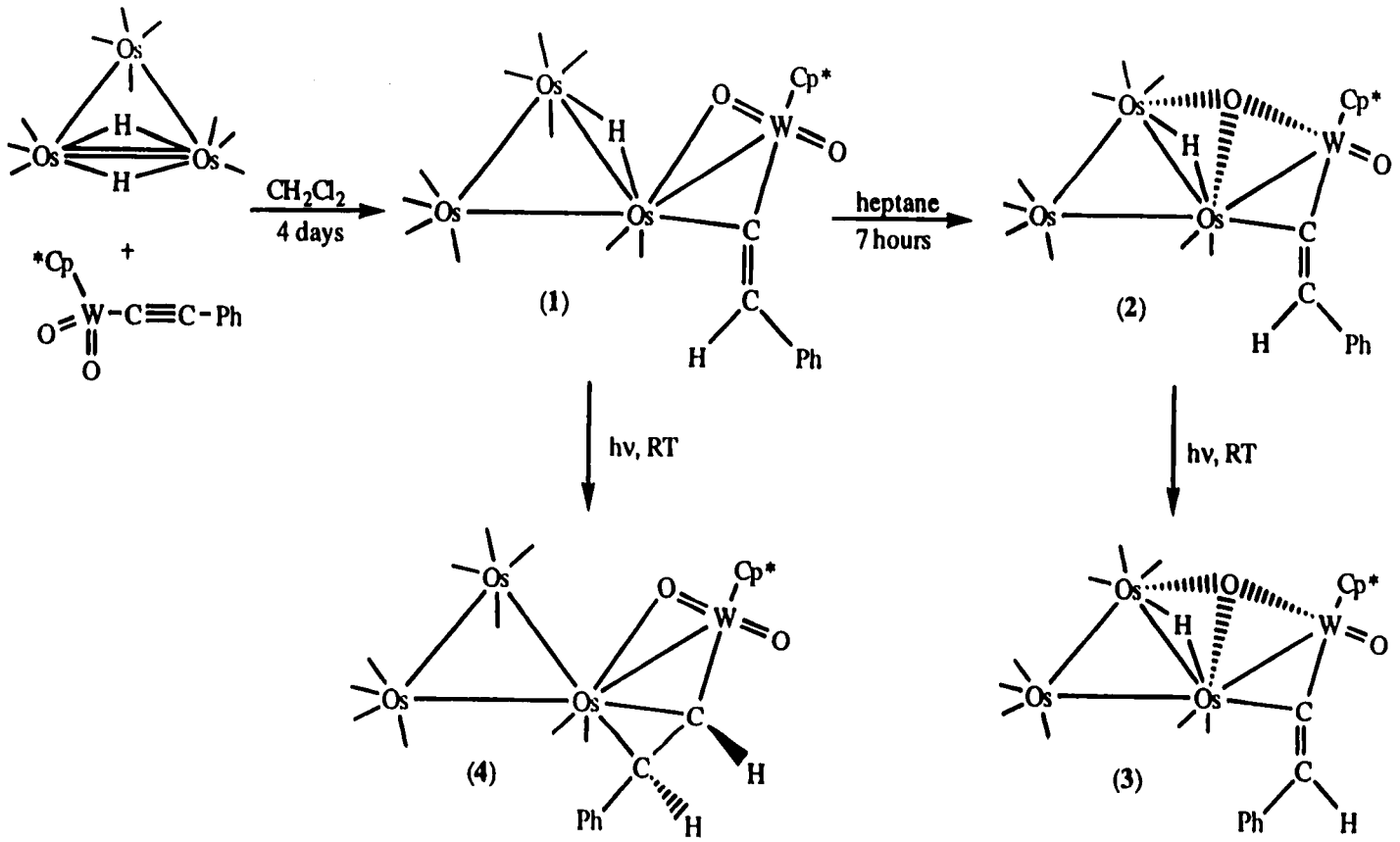

Abstract summary scheme.

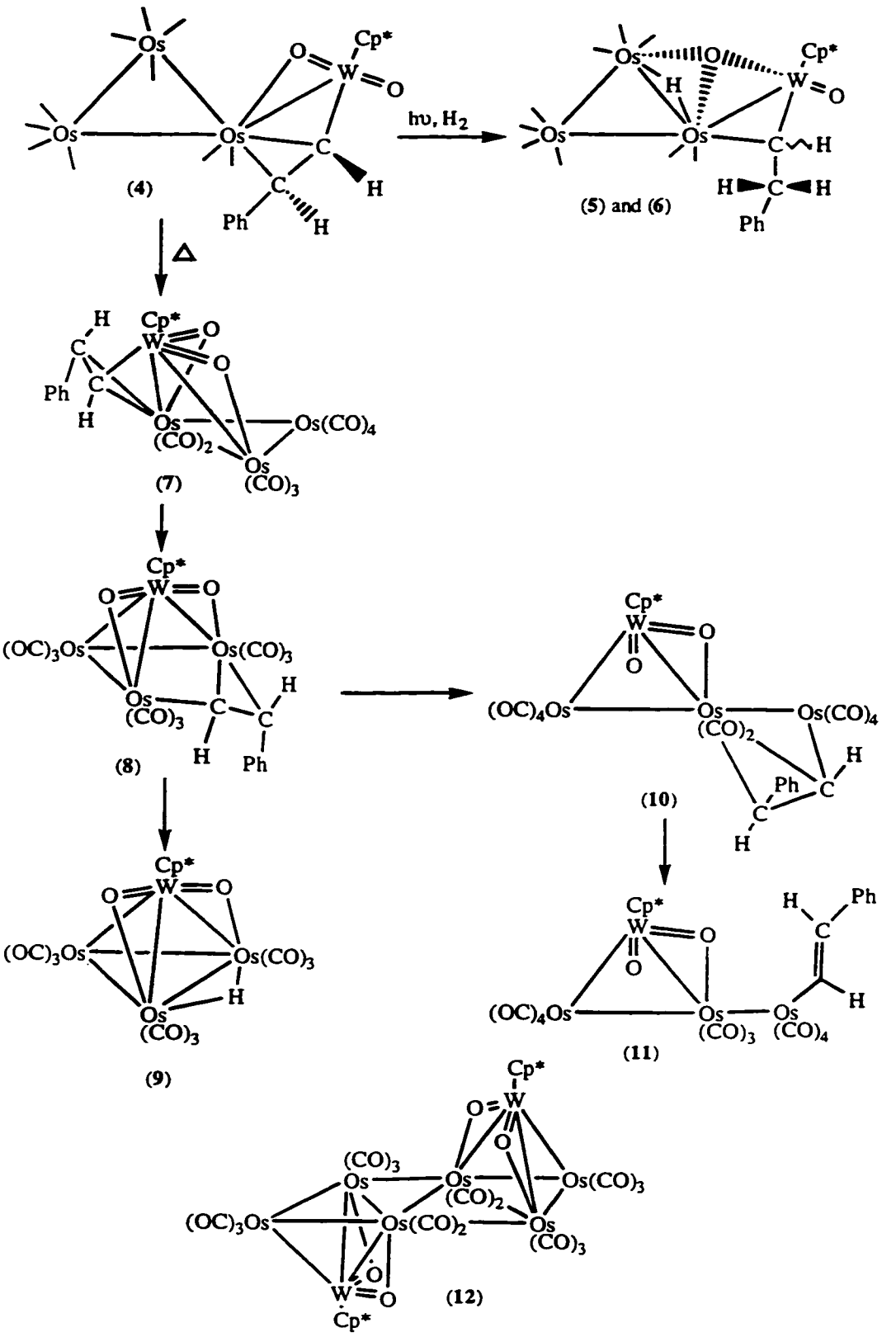

Abstract (continued)

ACKNOWLEDGEMENTS

I would like to express my gratitude to my supervisor, Dr Arthur J. Carty for providing me with the opportunity to join his research group, and for his support, guidance and encouragement over the course of these studies.

I would also like to thank the members of the group for their continuous support. Dr John H. Yamamoto is acknowledged for the many helpful discussions about this project. Dr Paul J. Low is also thanked for his assistance and useful suggestions. Your help has been greatly appreciated. Finally, I would like to thank the latest addition to the group, Mrs. Ludmila Scoles for her good humor and her constant supply of fudge!

Dr Gary D. Enright and Dr Konstantin A. Udachin both deserve special thanks for helping me with the crystallographic studies. The NMR studies wouldn't have been completed without the assistance of Don Leek. Special thanks for the ^{2}H NMR studies and the beneficial suggestions.

Mrs. Paulette Vineham also deserves many thanks for her many efforts spent trying to keep me informed with the administrative "work" at the university. All your efforts were greatly appreciated.

To my fiancé and my mother whose support, encouragement and understanding have been crucial for the completion of this work.

TABLE OF CONTENTS

LIST OF TABLES

LIST OF FIGURES

LIST OF SCHEMES

LIST OF ABBREVIATIONS

Å	Angstrom
br	broad (IR, NMR)
C_α	alpha carbon
C_β	beta carbon
cod	cyclooctadiene
Cp	cyclopentadienyl
Cp*	pentamethyl-cyclopentadienyl
d	doublet
dd	doublet of doublets
δ	NMR scale
Δ	heat
η^n	n-hapto
$\{^1H\}$	proton decoupled
Hz	Hertz
HMQC	heteronuclear multiple quantum correlation
HOMO	highest occupied molecular orbital
IR	infrared
LUMO	lowest unoccupied molecular orbital
m	medium (IR) multiplet (NMR)
mg	milligram
MHz	Mega Hertz
min	minutes
mmol	millimole
mL	millilitre
MS	mass spectrometry
NMR	nuclear magnetic resonance
Ph	phenyl
ppm	parts per million
π	pi (bond)
q	quartet
R	organic side group
s	strong (IR), singlet (NMR)
sh	shoulder
t	triplet
T	temperature
TLC	thin layer chromatography
vw	very weak
w	weak

LIST OF APPENDICES

LIST OF COMPOUNDS

1	$[Os_3W(\mu\text{-}H)(\mu\text{-}\eta^1\text{-}C{=}CHPh)(CO)_{10}(O)(\mu\text{-}O)(Cp^*)]$
2	$[Os_3W(\mu\text{-}H)(\textit{trans}\text{-}\mu\text{-}\eta^1\text{-}C{=}CHPh)(CO)_9(O)(Cp^*)(\mu_3\text{-}O)]$
3	$[Os_3W(\mu\text{-}H)(\textit{cis}\text{-}\mu\text{-}\eta^1\text{-}C{=}CHPh)(CO)_9(O)(Cp^*)(\mu_3\text{-}O)]$
4	$[Os_3W(CO)_{10}(O)(\mu\text{-}\eta^1,\eta^2\text{-}CH{=}CHPh\{\textit{W-Os}\})(\mu\text{-}O)(Cp^*)]$
5	$[Os_3W(\mu\text{-}H)(\textit{anti}\text{-}\mu\text{-}\eta^1\text{-}CHCH_2Ph)(CO)_9(O)(Cp^*)(\mu_3\text{-}O)]$
6	$[Os_3W(\mu\text{-}H)(\textit{gauche}\text{-}\mu\text{-}\eta^1\text{-}CHCH_2Ph)(CO)_9(O)(Cp^*)(\mu_3\text{-}O)]$
7	$[Os_3W(CO)_9(\mu\text{-}O)_2(\mu\text{-}\eta^1,\eta^2\text{-}CH{=}CHPh\{\textit{W-Os}\})(Cp^*)]$
8	$[Os_3W(CO)_9(\mu\text{-}O)_2(\mu\text{-}\eta^1,\eta^2\text{-}CH{=}CHPh\{\textit{Os}\cdots\textit{Os}\})(Cp^*)]$
9	$[Os_3W(\mu\text{-}H)(CO)_9(\mu\text{-}O)_2(Cp^*)]$
10	$[Os_3W(CO)_{10}(O)(\mu\text{-}\eta^1,\eta^2\text{-}CH{=}CHPh\{\textit{Os-Os}\})(\mu\text{-}O)(Cp^*)]$
11	$[Os_3W(\eta^1\text{-}CH{=}CHPh)(CO)_{11}(O)(\mu\text{-}O)(Cp^*)]$
12	$[Os_3W(CO)_8(\mu\text{-}O)_2(Cp^*)]_2$

Chapter One

Introduction

1.1 Early high-late low oxidation state mixed metal complexes

Heteronuclear (or mixed-metal) metal-metal bonded compounds are defined as compounds containing at least one metal-metal bond between dissimilar metals.[1] Since 1960, hundreds of di- and polynuclear complexes have been prepared in which different transition metals are directly bonded to one another. Of these, compounds which contain both early and late transition metals are by far the least common, mainly because of the different reactivity properties and ligand affinities of early and late metals.

1.1.1 Electronic characteristics and ligand affinities of early metals and late metals

The maximum binding energies associated with the transition elements in their bulk states occur near the center of the transition series, which corresponds to half-filled *d* and *s* valence bands. In molecular cluster compounds, the most stable metal cores will be those in which the M-L distribution mimics this arrangement.[2] Consequently, cluster compounds of the earlier transition metal elements are generally associated with ligands capable of donating additional electrons to the metal based bonding molecular orbitals, namely π-donor ligands. In contrast, clusters of the later transition metals form more stable complexes in the presence of π-acceptor ligands. These ligands withdraw electron density from the cluster and as a result depopulate skeletal molecular orbitals which otherwise would have been metal-metal antibonding.

1.1.1.1 Early metals and π-donor ligands

Complexes of the early transition metals often feature the metals in high oxidation states. Early metals are generally considered to be electron poor and tend to attract electron density from the ligands. Therefore, the most stable early transition metal complexes feature π-donor ligands such as amines (NR_2^-), alkoxide (OR^-), oxo (O^{2-}), sulfide (S^{2-}), bromide

(Br^-), iodide (I^-), fluoride (F^-) and chloride (Cl^-). Early metals are also termed oxophilic (literally: having an affinity for oxygen). Alternatively, π-donor ligands are often called hard ligands in allusion to their low polarizability. The ligands are π-donors since filled *p* orbitals of π-type symmetry remain available following the σ-bond formation. These *p* orbitals are capable of overlapping with empty metal based d_π orbitals associated with early transition metal compounds. This secondary π-bonding interaction strengthens the M-L bond.

1.1.1.2 Late metals and π-acid ligands

Late metals are often found in low oxidation states in their organometallic compounds. Late metals possess more *d* electrons than their early metal counterparts and are termed electron rich. As a result, late metals form more stable complexes with π-acid (or π-acceptor) ligands. Examples of π-acceptor ligands include carbon monoxide (CO), isocyanides (-NC), nitric oxide (NO), phosphines (PR_3), alkenes ($R_2C{=}CR_2$), alkynes ($RC{\equiv}CR$), arenes, carbenes (R_2C:) and carbynes (RC:). Each of these ligands possesses a filled orbital that acts as a σ-donor and empty orbitals of the appropriate symmetry to overlap with a filled d_π orbital of the metal. These orbitals are almost always the highest filled (HOMO) and lowest unoccupied (LUMO) of the ligand respectively. Consequently d_π electrons that were initially metal-centered are delocalized over the ligands resulting in the donation of electron density from the metal to the ligands. This phenomenon is called backbonding. Since late metals in a reduced state already have a high electron density, acceptance of further electrons from pure σ-donors would be disfavored. By backbonding, the electron density on the metal can be decreased.

The most important ligand for stabilizing cluster compounds of the later transition metals is carbon monoxide. It is an excellent π-acid not only due to the presence of empty π^* orbitals but also because of its capability of occupying terminal, edge-bridging, or face-capping positions in a cluster. Furthermore, this ligand behaves as a two-electron ligand in each of these bonding situations which explains the very low activation energies found for terminal to bridging intramolecular exchange processes.

1.1.2 Synergy between metals

The interest in the area of polynuclear heterometallic clusters was largely stimulated by the unique and highly selective chemical transformations that were expected to result from the combinations of metals having diverse chemical and electronic properties.[3] The possible interaction between adjacent metals is particularly interesting for catalytic systems. For example, the ability of one metal to react with a small organic molecule can be modified electronically and/or sterically by the presence of a second metal center. This results in enhanced or diminished overall catalytic activity or a change in product selectivity.[4] The availability of coordination sites on both type of metals each having their own specific properties, may also modify the catalytic properties. Hence, the differences in electronic and steric requirements for reactant coordination to the different metals can undoubtedly result in novel multiple site catalysis, manifesting itself in higher catalyst activities and/or different product selectivity.[4]

1.1.3 Literature survey of early-late heterometallic clusters

This overview is intended to survey types of reactions leading to the synthesis of early-late heteronuclear clusters. In order to keep this discussion to a reasonable length only representative examples of reactions will be presented. The synthetic strategies are divided into four main sections: ligand substitution reactions, addition reactions, bridge-assisted reactions, and metal-metal exchange reactions. It also has been necessary to adhere to a specific definition of an early-late heteronuclear cluster, and the following criteria have been set.

(1) By definition, a cluster must contain at least three metals, and a portion of the cluster must contain a closed polyhedron.
(2) Metals belonging to groups 3-6 are considered early metals.
(3) Metals belonging to groups 8-12 are regarded as late metals.
(4) Metals of group 7 are either early or late depending on the combination in which it is involved.

Several review articles have been published that might be of interest for more detailed discussion. Shapley and Comstock published an article on hydrocarbyl ligand derivatives of

group 6-group 9 heterometallic clusters.[5] The Comprehensive Organometallic Chemistry II series also has a volume dedicated to heteronuclear complexes, including a chapter by Chi where early-late combinations are discussed.[6]

1.1.3.1 Ligand substitution reactions

The replacement of one or more ligands on a transition metal center by another ligand or metal fragment is referred to as a ligand substitution reaction. In these cluster synthesis reactions a metal-containing nucleophile is combined with a metal complex that contains a good leaving group (Equation (1)).[6]

$$[ML_n] + [M'L_m]^{x-} \rightarrow [MM'L_{n+m-1}]^{x-} + L \quad (1)$$

Carbon monoxide is the neutral ligand displaced most frequently as it is so widely occurring. The usual reaction is between a carbonylmetallate and a neutral metal carbonyl complex. For example, carbonylmetallates react with dimeric carbonyls to yield early-late clusters, as illustrated by the reaction shown in Equation (2) where M = Mo or W.[7]

$$2[M(CO)_3Cp]^- + [Fe_2(CO)_9] \rightarrow [M_2Fe_2(CO)_{10}(Cp)_2]^{2-} \quad (2)$$

Dahl and co-workers also used this approach to prepare a series of trigonal bipyramidal clusters of the general formula $[M_2Ni_3(CO)_{16}]^{2-}$ (M = W, Cr or Mo) via the reaction shown in Equation (3).[8]

$$[M_2(CO)_{10}]^{2-} + 3[Ni(CO)_4] \rightarrow [M_2Ni_3(CO)_{16}]^{2-} \quad (3)$$

The products of Equations (2)-(3) are not those expected from a one-to-one combination of reagents. For this reason, the products formed in these reactions are often unpredictable.

Halides are the most commonly displaced anionic ligands. Carbonylmetallates will displace a halide from a metal halide complex to yield neutral metal-metal bonded species. Cluster compounds can be obtained with di- and polyhalide complexes or with dimeric carbonylmetallates. Examples of this synthetic technique are shown in Equations (4)[9] and (5)[10].

$$[Co_3(CO)_{10}]^- + [MCl(CO)_3(Cp)] \rightarrow [MCo_3(CO)_{11}(Cp)] \quad (4)$$

$$2[Mo(CO)_3(Cp)]^- + [PtCl_2(PPh_3)_2] \rightarrow [Mo_2Pt_2(CO)_6(PPh_3)_2(Cp)_2] \quad (5)$$

where M = Mo or W. There are few examples of this type of reaction, essentially because of the low availability of dimeric dianions and dimeric dihalides.

1.1.3.2 Addition reactions

Addition reactions are restricted to formally unsaturated complexes (e.g., 16-electron mononuclear metal complexes, 32-electron binuclear metal complexes, compounds containing multiple bonds, etc.).[6] These compounds can accept a ML_n fragment without the elimination of a ligand and the reactions may be described as a simple addition of reagents parts. This approach to early-late metal combinations is based on an analogy between the addition of metal nucleophiles to olefins, metal carbenes and M-M double bonds and similarly the addition of nucleophiles to alkynes, metal carbynes and metal-metal triple bonds. The reactions with metal carbene and carbyne complexes will be discussed in Section 1.1.3.3 as these are more properly called bridge-assisted reactions in that the organic ligand ends up as a bridging ligand.

The dinuclear complex $[CoW(CO)_7Cp^*]$ adds to $[Cp^*(CO)_2W{\equiv}W(CO)_2Cp^*]$ which contains a tungsten-tungsten triple bond. A saturated tetranuclear complex $[CoW_3(CO)_9(Cp^*)_3]$ consisting of a tetrahedral cluster with one cobalt and three tungsten atoms was formed (Equation (6)).[11] The unsaturated (32-electron) dihydride complex $[Re_2(\mu\text{-}H)_2(CO)_8]$ reacts with the mononuclear metal complex $[Pt(cod)_2]$ to yield the triangular complex $[PtRe_2(\mu\text{-}H)_2(CO)_8(cod)]$ (Equation (7)).[12]

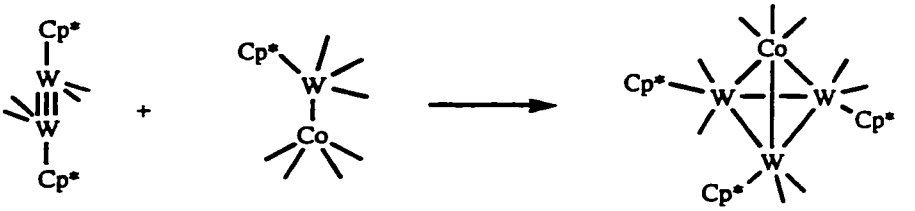

(6)

$$[Re_2(\mu\text{-}H)_2(CO)_8] + [Pt(cod)_2] \longrightarrow$$

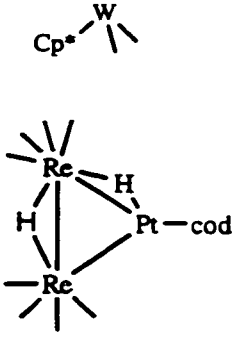

(7)

1.1.3.3 Bridge-assisted reactions

Another approach to the synthesis of early-late cluster compounds is to use bridging ligands derived from main group elements. Bridging ligands can be obtained via two different pathways: (1) the addition of a metal fragment to a ligand on a second metal complex and (2) the oxidative addition of a reactive bond on a ligand in one complex to a second complex.[6]

The addition of a metal fragment to a ligand present on a second metal complex usually involves the loss of a ligand and the formation of a bond between the metal atom of that complex and the ligand of the second complex. In its simplest form this bond will be of the donor-acceptor type and initially no metal-metal bond will be formed. Driven by subsequent ligand elimination, the close proximity of the metal atoms favors the formation of a metal-metal bond. For example, most bridging sulfido ligands contain a lone pair of electrons which is very effective for the capture of metal carbonyl fragments. For example, the loss of CO under UV irradiation from the compounds $[W(CO)_5L]$, where L = CO or PMe_2Ph , will lead to the addition of the remaining fragment to one of the sulfido ligands in the molecule $[Fe_3(CO)_9(\mu_3\text{-}S)_2]$. Subsequent decarbonylation can lead to incorporation of the tungsten atom into the metal cluster (Equation (8)).[13]

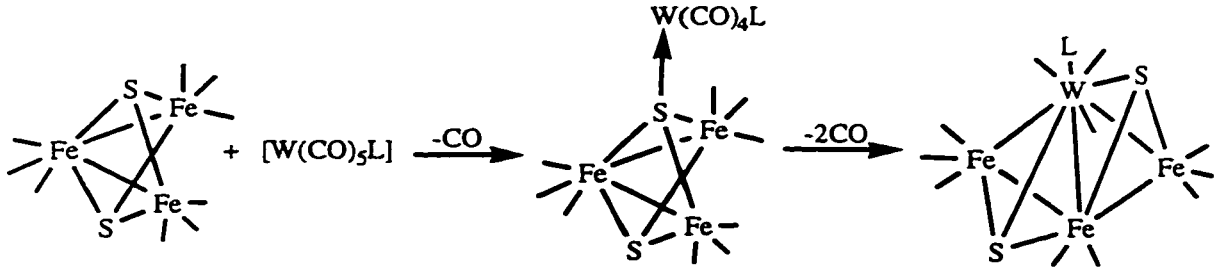

(8)

As expected, compounds with unsaturated metal-metal bonds will readily add to complexes containing ligands with lone pairs of electrons (Equation (9)).[14]

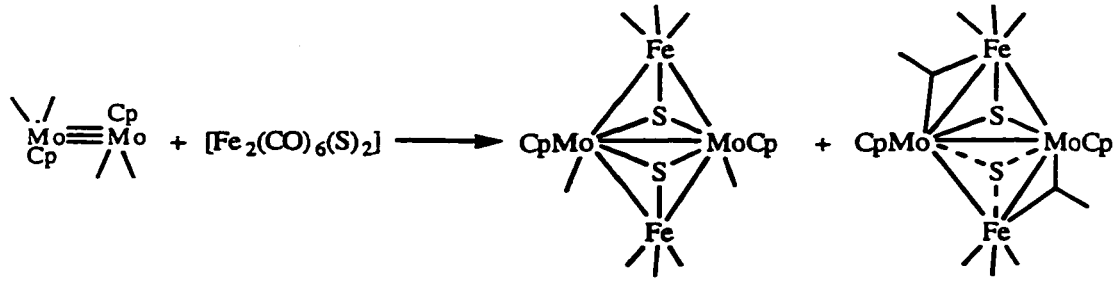

(9)

The nucleophilic site need not be a lone pair of electrons on a single atom. The possibility of adding metal-containing groupings across metal-carbon multiple bonds was the object of many studies in the 1980s.[15] Heteronuclear metal clusters may be obtained from the addition of metal groupings to alkylidyne complexes. These complexes containing metal-carbon multiple bonds may be viewed as ligands for early-late metal combinations. For example, $[W(\equiv C\text{-Tol})(CO)_2(Cp)]$ reacts with $[Co_2(CO)_8]$ to yield the trinuclear cluster complex $[Co_2W(CO)_8(\mu_3\text{-C-Tol})(Cp)]$ that has a triply bridging alkylidyne ligand (Equation (10)).[16]

$$[W(\equiv C\text{-Tol})(CO)_2(Cp)] + [Co_2(CO)_8] \longrightarrow$$ 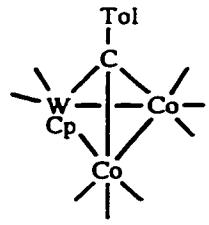 (10)

Replacement of the cyclopentadienyl ligand in $[W(\equiv C\text{-R})(CO)_2(Cp)]$ with the doubly negatively charged carbaborane ligands such as $[1,2\text{-}C_2B_9H_9Me_2]^{2-}$ or $[1,2\text{-}C_2B_9H_{11}]^{2-}$ yields the negatively charged alkylidyne complexes $[W(\equiv C\text{-R})(CO)_2(1.2\text{-}C_2B_9H_9Me_2)]^-$ and $[W(\equiv C\text{-R})(CO)_2(1.2\text{-}C_2B_9H_{11})]^-$, where R = Me, Ph, Tol, or $2,6\text{-}C_6H_3Me_2$. Both the unsaturation of the W≡C fragment and good nucleophicity of B-H have been found to be very useful for preparing clusters containing heteronuclear metal-metal bonds. For example, $[W(\equiv C\text{-Tol})(CO)_2(1.2\text{-}C_2B_9H_9Me_2)]^-$ reacts with $[Co_2(CO)_8]$ to yield the anionic heterotrinuclear complex $[WCo_2(CO)_6(\mu_3\text{-C-Tol})(1,2\text{-}C_2B_9H_9Me_2)]^-$ in which two of the *exo*-B-H bonds of the $1,2\text{-}C_2B_9H_9Me_2$ ligand formed three-center two-electron bonding interactions to the neighboring cobalt atoms.[17]

Metal fragments and polynuclear metal fragments can also be captured by the π-bonds of uncoordinated and unsaturated hydrocarbon groupings, such as acetylides -C≡CR and allenyl ligands, leading to the formation of new metal-metal bonds. The reaction of the propargyl complexes $[MCH_2C{\equiv}CPh]$, where M = $Mo(CO)_3Cp$ or $W(CO)_3Cp$ with $[Co_2(CO)_8]$ provides an excellent example of the capture of a dimetal fragment by the uncoordinated acetylenic π-bonds of a propargyl group (Equation (11)).[18] The acetylenic

fragment adds to the dicobalt group in the well known μ-⊥ coordination mode. No new metal-metal bonds were formed, but when the compounds were treated with H^+ a cobalt fragment was eliminated, the propargyl ligand was converted to a bridging alkyne, and the heterobinuclear alkyne complexes $[CoM(\mu\text{-}MeC_2Ph)(CO)_5Cp]$, where M = Mo or W, were formed.

$$[Co_2(CO)_8] + [W(CH_2C{\equiv}CPh)(CO)_3(Cp)] \longrightarrow \text{ 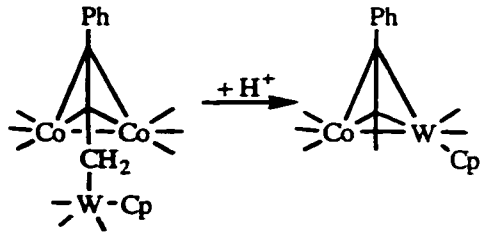 } \quad (11)$$

Oxidative addition of a reactive bond on a ligand in one complex to a second complex is another type of bridge-assisted reaction. Hence, unsaturated metal carbonyl fragments can be inserted into reactive E-X bonds on ligands, where E is a main group element and X is a substituent (e.g., H or Cl). Subsequent ligand elimination often allows for the isolation of complexes containing metal-metal bonds. Complexes containing secondary phosphine ligands have been shown to follow this reaction pathway. For example, the reaction of the complexes $[M(CO)_5(PPh_2H)]$, where M = Cr, Mo, or W, with the compounds $[Pt(PR_3)_2(C_2H_4)]$, where R = Ph or Et, yielded the products $[MPt(\mu\text{-}H)(CO)_4(PR_3)_2(\mu\text{-}PPh_2)]$ containing bridging PPh_2 and H ligands (Equation (12)).[19]

$$[M(CO)_5(PPh_2H)] + [Pt(PR_3)_2(C_2H_4)] \rightarrow [MPt(\mu\text{-}H)(CO)_4(PR_3)_2(\mu\text{-}PPh_2)] \quad (12)$$

Thiol ligands (SH) can also react by oxidative addition. An example of such a reaction is shown in Equation (13).[20] The reaction of the thiol group in $[W(CO)_3(SH)(Cp)]$ with $[Os_3(CO)_{11}(NCMe)]$ produced the sulfur-bridged "open" cluster complex $[Os_3W(\mu\text{-}H)(CO)_{13}(\mu_3\text{-}S)(Cp)]$. Thermolysis of this compound leads to the elimination of two moles of CO and the subsequent formation of three W-Os bonds to yield the complex $[Os_3W(\mu\text{-}H)(CO)_{11}(\mu_3\text{-}S)(Cp)]$. The formation of the one additional W-Os bond is compensated by the cleavage of one Os-Os bond.

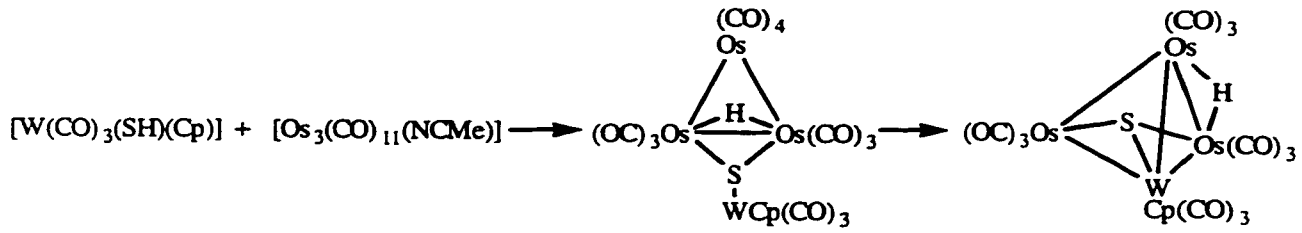

(13)

1.1.3.4 Metal-metal exchange reactions

In metal-metal exchange reactions, one or more metal-ligand groups present in a cluster are replaced by different metal-ligand groups to produce a new cluster containing still the same number of metal atoms.[6] However, these reactions usually follow a two-step process involving the coordination of a metal-ligand group, followed by the subsequent elimination of a different metal fragment. Most of these reactions involve steps that have been described in the preceding sections. Sometimes, the isolation of the enlarged intermediate(s) is possible and provides valuable mechanistic information.

Metal carbonyl anions can displace metal groups in certain ligand-bridged clusters. For example, the reaction of the prochiral cluster complex $[Co_2Ru(CO)_9(\mu_3\text{-PPh})]$ with $[W(CO)_3Cp]^-$ yielded the chiral complex $[CoRuW(CO)_8(\mu_3\text{-PPh})Cp]$ where one of the cobalt fragments was replaced by a $[W(CO)_2Cp]$ group.[21] Alkyne- and vinylidene-bridged cluster complexes have also undergone this type of reaction.[22] Furthermore complexes containing triply-bridging alkylidyne ligands can undergo multiple metal exchange processes. For example, the complex $[Co_3(CO)_9(\mu_3\text{-CR})]$ reacts with the anions $[M(CO)_3Cp]^-$, where M = Mo or W, to yield the products $[MCo_2(CO)_8(\mu_3\text{-CR})Cp]$ and $[M_2Co(CO)_7(\mu_3\text{-CR})(Cp)_2]$ by a single or a double exchange process depending on the stoichiometry of the reaction.[23] The $AsMe_2$ ligand can also be used in a bridge-assisted manner. For example, the reaction of complexes such as $[M(CO)_3(AsMe_2)Cp]$ where M = Mo or W with $[Co_3(CO)_9(\mu_3\text{-CR})]$ resulted in the displacement of a CO ligand and the subsequent coordination of the arsenic atom. A $Co(CO)_3AsMe_2$ group was then eliminated and a $CpM(CO)_2$ fragment entered the cluster allowing for the formation of heteronuclear metal-metal bonds.[24]

The reaction of acetylide complexes with trinuclear complexes has also been shown to yield the exchange products. For example, the acetylide complexes $[M^1(\mu\text{-}C{\equiv}CR)(CO)_3Cp]$, where M^1 = Mo or W and R = Ph, C_6H_4F, C_6H_4OMe, Bu^t, or Pr, reacted with the trinuclear complexes $[Os_3(CO)_{10}(NCMe)_2]$ or $[Ru_3(CO)_{12}]$ to produce $[M^1M^2_2(CO)_8(\mu_3\text{-}C{\equiv}CR)Cp]$, where M^1 = Mo and M^2 = Ru or M^1 = W and M^2 = Ru or Os, which contains a triply-bridging acetylide ligand.[25] Since the elements of the third-row transition series form the strongest metal-metal bonds, the reaction of $[W(C{\equiv}CPh)(CO)_3Cp]$ with $[Os_3(CO)_{10}(NCMe)_2]$ lead to the isolation of the tetranuclear intermediate $[WOs_3(CO)_{11}(\mu_3\text{-}C{\equiv}CPh)Cp]$. This tetranuclear product was converted to the trinuclear product $[WOs_2(CO)_8(\mu_3\text{-}C{\equiv}CPh)Cp]$ in a good yield under thermolytic conditions in the presence of CO at a pressure of 207 kPa.

In a few cases, the expanded clusters were isolated and structurally characterized. These intermediates can provide valuable insight into the mechanism of the reaction. For example, $[Ru_3(CO)_{10}(\mu_3\text{-}S)]$ reacted with $[Cp(CO)_2Mo{\equiv}Mo(CO)_2Cp]$ to yield the double exchange product $[Mo_2Ru(CO)_7(\mu_3\text{-}S)(Cp)_2]$.[26] However, small amounts of the pentanuclear cluster complex $[Ru_3Mo_2(CO)_{12}(\mu_4\text{-}S)(Cp)_2]$ which consists of a square pyramidal cluster of five metal atoms with a quadruply bridging sulfido ligand, were isolated. This complex was shown to be an intermediate in the bridge-assisted metal exchange reaction and was formed by the insertion of the unsaturated Mo≡Mo grouping into one of the Ru-S bonds.

1.2 Mixed metal complexes with oxide ligands

There has been considerable interest in recent years in the synthesis of organometallic complexes containing both oxygen and hydrocarbon ligands as they are thought to be suitable models for reactions that occur on the surface of metals during heterogeneous catalytic processes.[27] The difficulties encountered during the characterization of heterogeneous catalysts render a complete understanding of the structure of the catalyst almost impossible. It is a common belief that transition metal clusters may contribute to a fuller understanding

by modeling the interaction present in heterogeneous catalysts. Burwell made the first connections between heterogeneous catalysts and organometallics[28] while Earl Muetterties made analogies between ligands bound to clusters and those on surfaces.[29] Investigators of this area now refer to their field of research as "surface organometallic chemistry" and they hope to develop molecular approaches to surface catalysis.[30]

Polynuclear systems are of particular interest as they are expected to improve the current understanding of the possible coordination modes of oxygen atoms bound to surfaces, in addition to explaining the role of the oxo ligand in the enhanced reactivity of cluster-bound hydrocarbon fragments.[31] Hence, it is expected that the elucidation of the reactivity and structural features of these oxo clusters will provide insights on how oxo ligands bond to the metal atoms and how they react with adjacent hydrocarbon ligands. As a result, catalyst preparation would become a more efficient process due to the knowledge of the chemistries of the precursors, the supports and the conditions for their interaction and activation.

1.2.1 Oxo ligands in organometallic chemistry

The oxo group, formally considered as the radical O (2-electron donor) or dianion O^{2-}, (a 4-electron donor) is an extremely versatile ligand and plays an important role in organometallic chemistry. The binding modes available for the oxo ligands are various since it is capable of binding as either a terminal group to a metal (M=O) (2 electron donor) or bridging 2, 3, 4 or 5 metal atoms.[32] Bridging oxygen atoms are designated as (μ-O) (for dinuclear bridging), (μ_3-O), (μ_4-O) or (μ_5-O) and they act as a 2, 4 or 6 electron donors, respectively. Organometallic oxo complexes feature mainly metals of Groups 4 to 7 (Group 7 being confined to rhenium). A few examples from the lanthanides and actinides and some clusters containing metals from Groups 8 and 9 are also known.[39] Only one monomeric complex, $[Os(CH_2SiMe_3)_4(O)]$, from Group 8 is known.[33] The main types of organic ligands present on organometallic oxo compounds are η-C_5R_5, alkyls or aryls.[39] Carbonyls are also fairly common in clusters containing oxygen atoms.

Fischer and co-workers seem to have been the first group to report their investigation on the oxidation of organometallic complexes with dioxygen. They prepared both $[VCl_2(O)Cp]$ and $[CrOCp]_4$.[34] The true structure of the latter as $[Cr(\mu_3\text{-}O)Cp]_4$ was only realized much later.[35] The interest of several groups in organometallic oxo compounds led to the preparation of several complexes including $[cis\text{-}\{Mo(O)Cp\}_2(\mu\text{-}O)_2]$ by Green,[36] $[\{TiCl_2Cp\}_2(\mu\text{-}O)]$ by Corradini and Allegra,[37] and $[VCl_2(O)(\eta^1\text{-}Ph)]$ by Reichle and Carrick[38]. Following these early studies very few complexes were isolated. Most were obtained serendipitously (by inadvertent admission of air into a reaction mixture) or as unexpected products from the reaction between an organometallic compound and a reagent containing oxygen. Only recently have a greater number of different types of organometallic oxo compounds been prepared. Nonetheless it is more accurate to describe synthetic methods for several types of compounds as being the rational exploitation of serendipitous or unexpected discoveries rather than planned syntheses.[39] The first CO containing organometallic oxo cluster to be characterized was $[Os(CO)_3(\mu_3\text{-}O)]_4$ in 1966.[40] However, the first monomeric oxocarbonyl with a terminal [M=O] group, $[WCl_2(PMePh_2)_2(CO)(O)]$, and its ethylene analog, $[WCl_2(PMePh_2)_2(\eta^2\text{-}C_2H_4)(O)]$ were discovered only recently.[41]

1.2.2 Oxide supported late metal catalysts

The interest in mixed-metal catalysts was prompted by the fundamental importance and industrial relevance of heterogeneous catalysts.[42] Alumina-supported platinum-rhenium, is one of the most important commercial bimetallic catalysts.[43] It is used in the catalytic reforming of petroleum naphthas. Oxide-supported Pt, Pt-Sn and Pt-Ir systems are also used in reforming.[43,44] The major reactions encountered in the reforming of saturated hydrocarbons include isomerization, dehydrogenation and dehydrocyclization to afford aromatic hydrocarbons, which improves the octane rating of gasolines. Hydrogenolysis of alkanes and cycloalkanes to produce low molecular weight alkanes is another important type of reaction in reforming. These reactions are illustrated in Scheme 1.1.[42(a)]

In industrial catalysts, the metals (about 1 wt %) are found dispersed on the surface of the support. The reaction conditions for reforming include temperatures of 700-800 K and

pressures of 10-30 atm. While the metals catalyze dehydrogenation and dehydrocyclization reactions, the support, which is acidic, plays a role in catalyzing isomerization.[42(a)] Since the support takes an active role in catalysis, the catalysts are considered as bifunctional. The

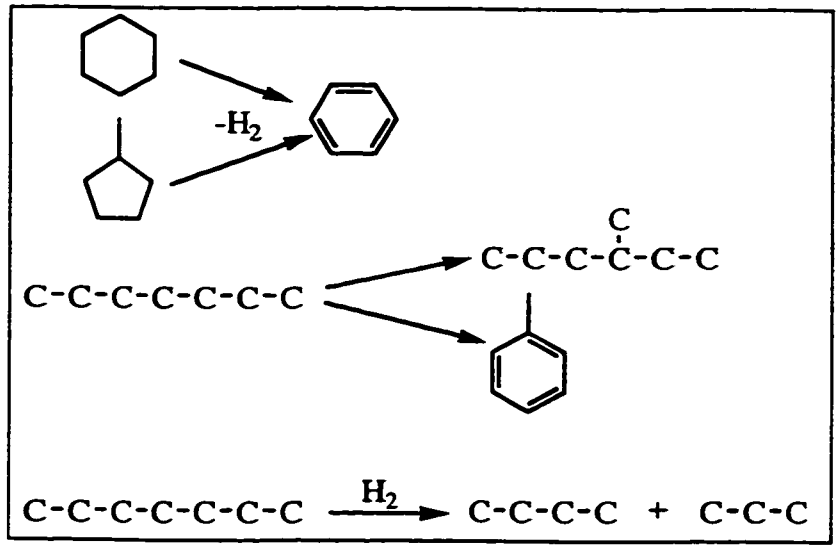

Scheme 1.1 Typical reactions in catalytic reforming.

bimetallic Pt-Re catalysts are prepared by a multiple step technique involving impregnation of alumina with aqueous solutions of compounds such as H_2PtCl_6 and NH_4ReO_4, followed by calcination in an oxygen atmosphere and then reduction under hydrogen.[42(a)] Recently an alternative approach to the formation of bimetallic catalysts such as Pt-Re/Al_2O_3 involves the use of mixed-metal cluster complexes as precursors.[45] An example is the preparation of Pt-Re/Al_2O_3 from $[PtRe_2(CO)_{12}]$.[46] This promising new method might favor desirable bimetallic interaction in the final form of the catalysts, due to the retention of the Pt-Re metal-metal bonds in the cluster.

The Pt-Re catalyst was introduced about two decades ago.[47] Since that time its important role as a commercial catalyst has encouraged numerous investigations.[44(a),43,48] Many questions are still being debated including the nature of the interaction between the two metals, the role of rhenium in maintaining catalytic activity and the oxidation state of rhenium.[42(a)] The oxidation state of Pt in the reduced catalysts is widely accepted to be zero.[42(a)] However, the question of the oxidation state of Re in the reduced catalysts remains

unresolved.[42(a)] Another significant issue is the nature of the interaction if any between the two metals in the reduced catalyst. The results from various studies are controversial, but there is more evidence supporting the presence of Pt-Re interactions.[42(a)]

The synthesis of Pt-Re clusters and the studies of model reactions have provided much information on the structure and reactivity of the Pt-Re catalysts. Puddephatt and co-workers synthesized complexes containing either ReOPt bridges or Pt-Re bonds which provided models for the binding of platinum to rhenium modified alumina surfaces.[42(a)] The complex $[Pt_3(\mu_3\text{-}CO)(\mu\text{-}dppm)_3]^{2+}$ reacted with $[Re(CO)_5]^-$ to yield the new heterometallic cation $[Pt_3\{Re(CO)_3\}(\mu\text{-}dppm)_3]^+$ (**A**). Oxidation of complex **A** using the reagents Me_3NO, O_2 or H_2O_2[49] afforded the series of oxo clusters $[Pt_3\{Re(CO)_3\}(\mu_3\text{-}O)_n(\mu\text{-}dppm)_3]^+$, (**B**), n = 1; (**C**), n = 2; (**D**), n = 3 under mild conditions. Conversely, the reaction of **A** with O_2 under high temperatures gave $[Pt_3(ReO_3)(\mu\text{-}dppm)_3]^+$ **E** via the intermediacy of **C**. Complex **E** is the first example of a cluster containing metals in widely different oxidation states (Scheme 1.2). The conversion of **A** to **E** simply involves the replacement of the three carbonyl ligands in **1** by the three terminal oxo ligands in **E**. Since both CO and the terminal oxo ligand are formally two-electron donors, the overall cluster counts in **A** and **E** are the same at 54-electrons.

Complex **A** reacted with Me_3NO in a 1:1 mole ratio to produce the mono-oxo cluster **B**. Further exposure of cluster **B** to Me_3NO or O_2 afforded the dioxo cluster **C** which was also obtained directly by the reaction of **A** with O_2. The latter reaction appears to mimic dissociative chemisorption of O_2 on a metal surface and it was also the first example of oxidative addition of O_2 to a metal cluster to give a bis(μ_3-O) cluster. Complex **C** was an intermediate formed during the preparation of the trioxo cluster **D** via the treatment of **A** with H_2O_2.

The effect of metal oxidation state was demonstrated by the different selectivity of complexes **A** and **E** towards ligand addition.[50] For example, the reaction of cluster **E** with

donor ligands occurred at the Pt_3 center which afforded complexes **F** and **G** (Scheme 1.3).[50] In contrast complex **A** reacted with neutral ligands at the Re center as shown in Scheme 1.4.

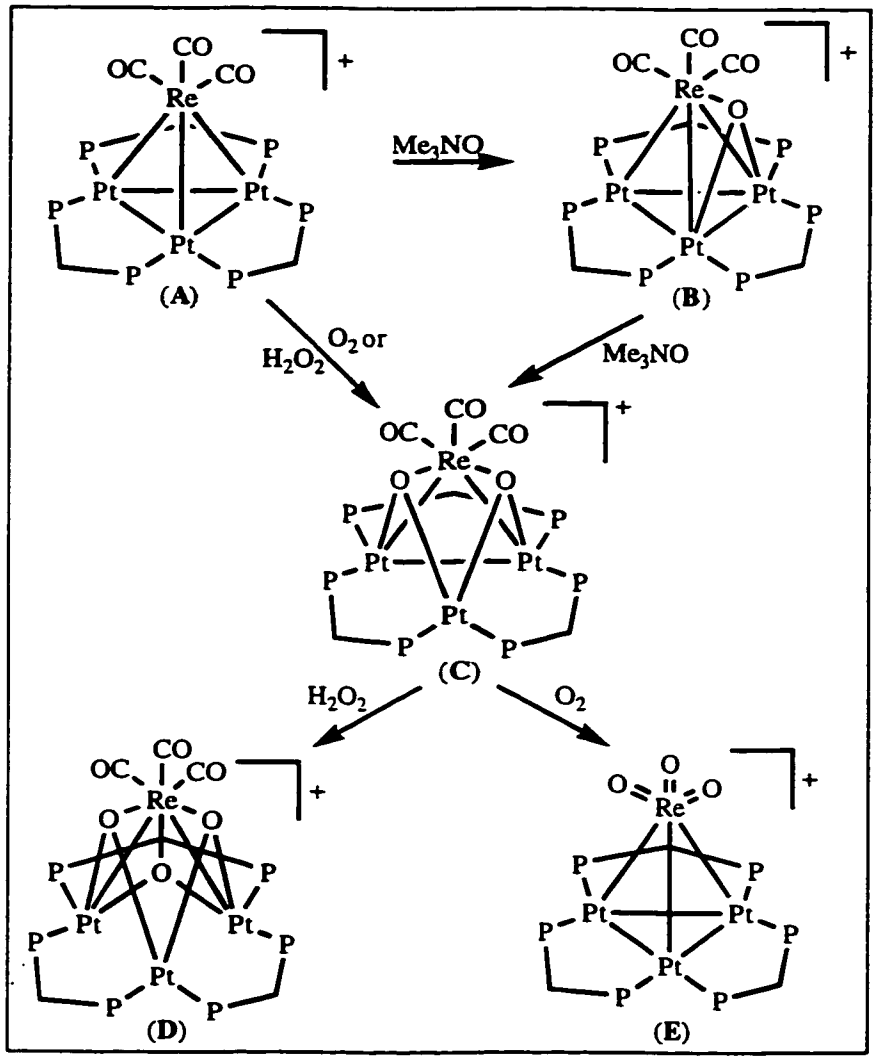

Scheme 1.2 Reactivity of $[Pt_3\{Re(CO)_3\}(\mu\text{-dppm})_3]^+$.

In the case of Pt-Re/Al_2O_3 catalysts, further reactivity differentials were observed for the two oxidation states of the rhenium present on the surfaces of the reduced catalyst. Re(0) is found to chemisorb CO while Re(IV) shows no such activity.[51] Clusters **A** and **E** and their respective selectivity towards ligand addition were considered to model this effect.

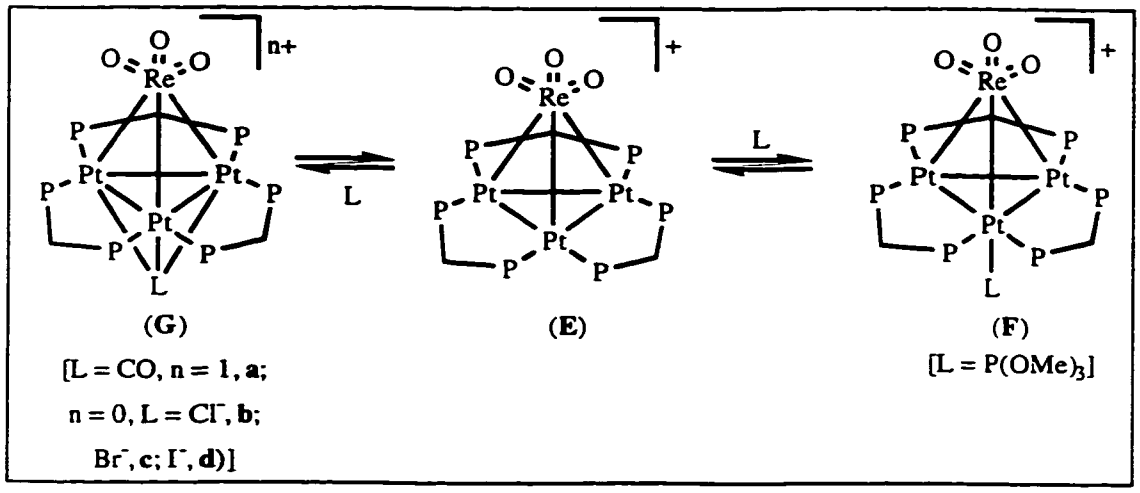

Scheme 1.3 Selectivity of $[Pt_3(ReO_3)(\mu\text{-dppm})_3]^+$ towards ligand addition.

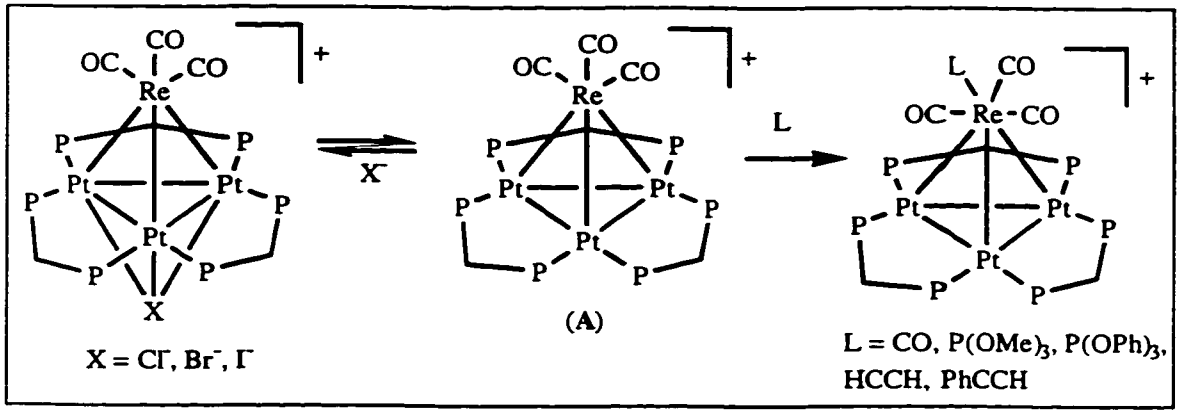

Scheme 1.4 Selectivity of $[Pt_3\{Re(CO)_3\}(\mu\text{-dppm})_3]^+$ towards ligand addition.

1.2.3 Synthesis of oxo-bridged mixed-metal complexes

Transition metal carbonyl oxide complexes have been prepared by four different methods: C-O bond scission, direct oxidation, addition of $[W(C{\equiv}CPh)(CO)_3Cp]$ to the unsaturated oxo complex $[Re(O)(\mu\text{-}O)Cp^*]_2$ and by reacting $[W(C{\equiv}CPh)(O)_2Cp^*]$ with metal carbonyls.

1.2.3.1 C-O bond scission

A number of heteropolynuclear carbonyl cluster compounds containing bridging oxo ligands are known where the oxygen bridge originated from the breakdown of an oxygen containing group in a precursor molecule.[32]

The first synthesis of mixed metal complexes containing oxo ligands involved the transformation, under thermolytic conditions, of an activated carbonyl group to an oxo ligand in a mixed metal carbonyl cluster. The complex $[Os_3W(CO)_{11}(\mu_3\text{-}\eta^2\text{-}C(O)CH_2Tol)(Cp)]$ (**H**) was obtained from the coupling of $[H_2Os_3(CO)_{10}]$ with $[W(CO)_2(\equiv CTol)Cp]$.[52] The bridging dihapto acyl ligand of **H** was formed after the insertion of a CO ligand into the M-CTol linkage of $[W(CO)_3(\equiv CTol)Cp]$. The lengthened and hence "activated" CO allows for the scission of the acyl C-O bond upon heating resulting in the formation of the μ-oxo-alkylidyne complex $[Os_3W(CO)_6(\mu_3\text{-}CCH_2Tol)(\mu\text{-}O)Cp]$ (**I**) (Scheme 1.5).[53] The shorter length of the W-O (1.812(7) Å) bond compared to the Os-O bond (2.169(8) Å) strongly suggest the donor-acceptor mode W=O:→Os for this oxo bridge. The nearly coplanar butterfly arrangement of WOs_3 atoms in complex **H** has changed to a pseudo-tetrahedral array in the oxo-bridged product **I**. The oxo ligand bridges a WOs edge adjacent to the WOs_2 face capped by the alkylidyne ligand. It contributes four electrons (neutral atom counting scheme) to the overall 60 cluster valence electrons complex.

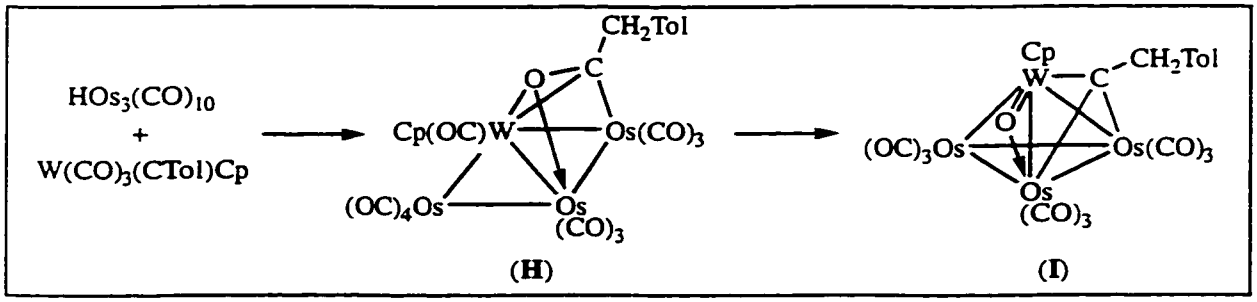

Scheme 1.5 Reactivity of $[H_2Os_3(CO)_{10}]$ with $[W(CO)_2(\equiv CTol)Cp]$.

The oxo cluster $[Ru_3W_2(CO)_{11}(O)(\mu_5\text{-}C)(Cp)_2]$ (**K**) is also formed via the direct scission of a C-O bond.[54] The pentanuclear cluster $[Ru_3W_2(CO)_{13}(Cp)_2]$ (**J**), obtained from the thermolysis of $[Ru_3W(H)(CO)_{12}(Cp)]$ with an excess of $[W(H)(CO)_3(Cp)]$, eliminated one CO in refluxing toluene to afford the oxo-carbido complex $[Ru_3W_2(CO)_{11}(O)(\mu_5\text{-}C)(Cp)_2]$ (**K**) in 22% yield. Two additional derivatives $[Ru_3W_2(CO)_{11}(O)(\mu_5\text{-}C)(LL')]$ ((**L**), L=L'=Cp*; (**M**), L=Cp and L'=Cp*) were obtained from the condensation of $[Ru_3W(H)(CO)_{12}(L)]$ and $[W(H)(CO)_3(L')]$ (L=L'=Cp*; L=L'=Cp, Cp*) through the

consecutive elimination of one H_2 and three CO ligands. The structures of **K**, **L** and **M** can all be described as wingtip-bridged butterflies. The carbido atom is bonded to all transition metal atoms, and the oxo ligand is coordinated to the WCp apex. The clusters **K-M** possess 76 valence electrons which is consistent with known carbido clusters adopting similar geometry. In order to obtain this count, the oxo ligand is considered as a four-electron donor. This donor ability suggests a W≡O multiple bonding interaction which is supported by a short W-O distance (1.697(5) Å). The formation of the strong W≡O multiple bond undoubtedly provides an additional driving force for the C-O cleavage process. Based on experimental evidence, the following reaction path was proposed (Scheme 1.6).[54]

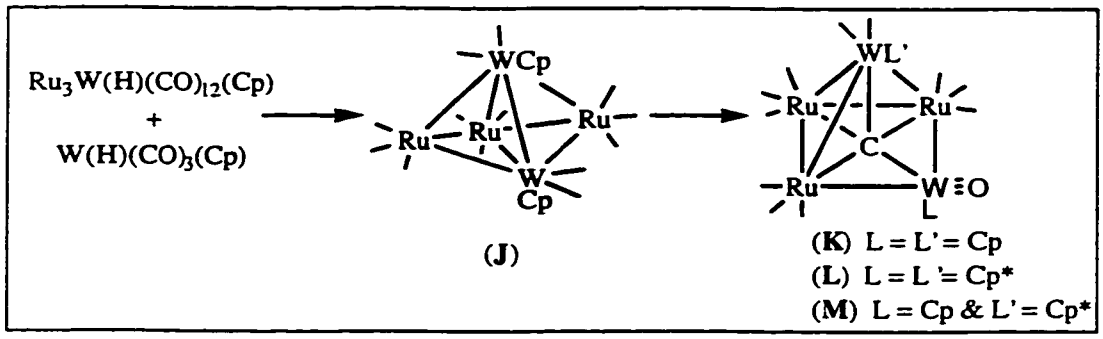

Scheme 1.6 Reactivity of $[Ru_3W(H)(CO)_2(Cp)]$ with $W(H)(CO)_3(Cp)]$.

The tetranuclear ketenyl compound $[Os_3W(\mu\text{-}H)(CO)_{13}\{C(O)CH_2\}(Cp)]$ (**N**), available via condensation of $[Os_3(CO)_{10}(NCMe)_2]$ with the aldehyde complex $[W(CH_2CHO)(CO)_3(Cp)]$, also provides mixed metal oxo complexes.[55] The pyrolysis of **N** gave a dark brown pentanuclear oxo-ethylidyne compound $[Os_3W_2(\mu\text{-}H)(CO)_9(\mu_3\text{-}CCH_3)(\mu\text{-}O)(Cp)_2]$ (**O**) in 10% yield and a red oxo-ethylidyne $[Os_4W(CO)_{12}(\mu_3\text{-}CCH_3)(\mu\text{-}O)(Cp)]$ (**P**) in 11% yield (Scheme 1.7).[55]

Complex (**O**) has a W_2Os_3 square-pyramidal arrangement. The W-W bond distance (W-W' = 2.552(2) Å) suggests a W-W double bond while the bond length of the W-O bonds (W-O = 1.88(2) Å) indicates a bond order of 1.5. Considering the neutral oxo ligand as a four-electron donor, the authors calculated that this molecule possessed 72 cluster valence electrons. This electron counting is in agreement with the expected count for a square

pyramidal cluster with one metal-metal double bond and seven single bonds. The metal core of (**P**) consists of a WOs_4 trigonal-bipyramidal arrangement. The oxo ligand bridges a W-Os edge with a short W-O distance (W-O = 1.82(3) Å) and a long Os-O distance (Os-O = 2.13(3) Å). These bonding parameters suggest that the oxo ligand adopts the asymmetrical W=O:→Os bonding mode and serves as a four-electron donor. However, using this concept brings the total number of valence electrons for this cluster to 74, which is two electrons in excess of the expected count for a cluster with a trigonal-bipyramidal geometry (nine M-M bonds). In this work the cleavage of the ketenyl C-O bond and concurrent thermally induced formation of a pair of oxo and ethylidine ligands was unambiguously established. These C-O bond cleavage reactions are probably favored by the generation of strong multiple bonding between tungsten and oxygen atoms.[55]

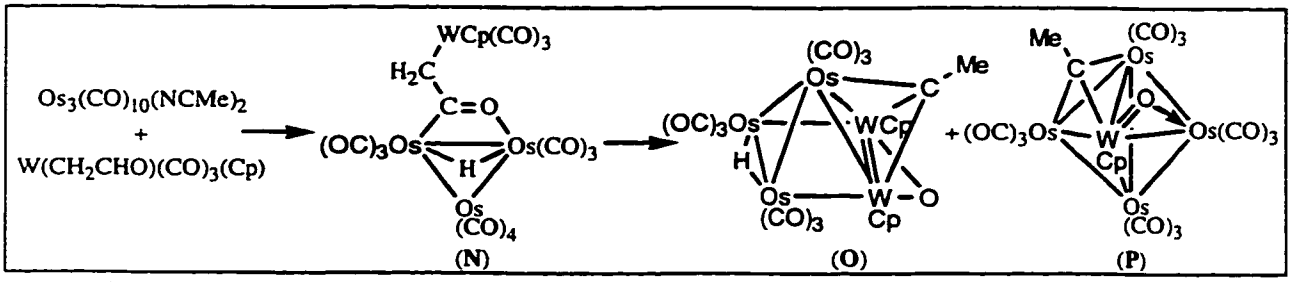

Scheme 1.7 Reactivity of $[Os_3(CO)_{10}(NCMe)_2]$ with $[W(CH_2CHO)(CO)_3(Cp)]$.

1.2.3.2 Direct oxidation

Another synthetic method used to transform a CO group into an oxo ligand involves the exposure of a mixed metal carbonyl complex to an oxygen or nitrous oxide atmosphere. For example, the WRe_2 acetylide cluster $[Re_2W(CO)_9(C{\equiv}CPh)(Cp^*)]$ (**Q**) prepared by combining $[Re_2(CO)_8(NCMe)_2]$ and $[W(C{\equiv}CPh)(CO)_3(Cp^*)]$, formed the oxo-acetylide cluster $[Re_2W(CO)_8(CCPh)(O)(Cp^*)]$ (**R**) upon exposure to an atmosphere of oxygen or nitrous oxide.[27,31,56]

The acetylide ligand of **R** adopts a novel $\mu_3,\eta^1,\eta^1,\eta^2$-mode, in which the α-carbon is bonded to all three metal atoms, but the β-carbon is linked only to the W atom. The carbenic character of the latter is substantial. The terminal oxo ligand is attached to the tungsten atom

and the resulting W-O vector is perpendicular to the plane defined by the metal atoms and the acetylide ligand.[27]

Further reactivity differential has been explored between $[Re_2W(CO)_9(C{\equiv}CPh)(Cp^*)]$ (**Q**) and $[Re_2W(CO)_8(CCPh)(O)(Cp^*)]$ (**R**). The oxo complex **R** undergoes fragmentation upon treatment with thiophenol in toluene to afford a dinuclear complex $[ReW(\mu\text{-}H)(CO)_4(CCPh)(O)(Cp^*)]$. The corresponding reaction with **Q** only afforded addition products, giving cluster compounds $[Re_2W(CO)_8(\mu_3\text{-}SPh)(CH{=}CPh)(Cp^*)]$ and $[Re_2W(CO)_7(\mu_3\text{-}SPh)(CH{=}CPh)(Cp^*)]$ as the final products. Such divergence in reactivity between **Q** and **R** provided further evidence of the influence of the oxo ligand on the chemical reactivities.[56]

1.2.3.3 Addition of $[W(C{\equiv}CPh)(CO)_3(Cp)]$ to the unsaturated oxo complex $[Cp^*Re(O)(\mu\text{-}O)]_2$

The reaction of the rhenium dioxo dimer $[Re(O)(\mu\text{-}O)(Cp^*)]_2$ with the tungsten acetylide complex $[W(C{\equiv}CPh)(CO)_3(Cp)]$ afforded the dark green oxo-acetylide compound $[ReW(\mu\text{-}C_2Ph)(CO)_2(O)(Cp)(Cp^*)]$ (**S**) in 52% yield, in addition to a small amount of a second oxo-acetylide compound $[ReW(\mu\text{-}C_2Ph)(CO)_2(O)(Cp)(Cp^*)]$ (**T**) (Scheme 1.8). Complex **T** is a thermodynamically more stable isomer formed via the intermetal migration of an oxo ligand. The W-O multiple bond interaction in **T** is stronger than the Re-O bonding in **S**. This experimental fact indicates that the isomerization **S** → **T** is driven by the difference in M-O bond strengths.[57]

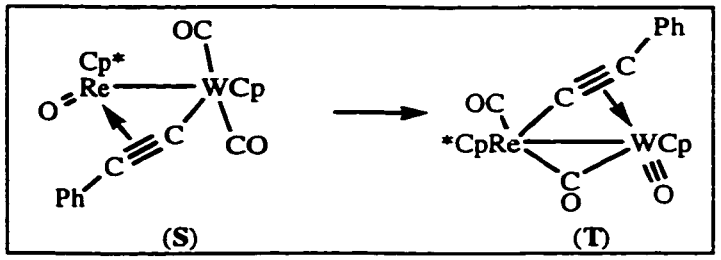

Scheme 1.8 Intermetal migration of an oxo ligand.

1.2.3.4 Reactivity of [W(C≡CPh)(O)$_2$(Cp*)] with metal carbonyls

The previous preparations pose some problems because most of the oxo carbonyl cluster compounds described were formed adventitiously. It was therefore of interest to develop a more systematic methodology of generating these compounds through combination of a metal oxo complex and a carbonyl cluster template. One target molecule which can be used in assembling such cluster molecules, is the dioxo acetylide compound with formula [W(C≡CR)(O)$_2$(L)], where L = Cp or Cp*; R = alkyl or aryl groups.[58]

The synthetic strategy developed involves the coordination of an early-metal oxo acetylide [W(C≡CPh)(O)$_2$(Cp*)] with a late-metal carbonyl alkyne acceptor fragment. This method utilizes the strong π-coordinating ability of an acetylide ligand to deliver a high oxidation state early-metal oxo fragment to a late-metal, low oxidation state carbonyl center. The products obtained via this methodology acquire a W(O)$_2$(Cp*) fragment from their starting materials. As a result, their structural and reactivity properties will differ greatly from those previously reported which only contained one oxo ligand in either edge-bridging or terminal mode (Section 1.2.3.1).[59]

The first examples of mixed metal clusters obtained via this synthetic strategy were WRu complexes.[60] The open face of [Ru$_4$(CO)$_{13}$(μ_3-PPh)] was used to coordinate the acetylide ligand of [W(C≡CPh)(O)$_2$(Cp*)]. One major product was obtained with the formula [Ru$_4$W(CO)$_{10}$(O)(μ-O)(μ_4-PPh)(CCPh)(Cp*)] (**U**). The reactivity of **U** was investigated. It was found that the direct reaction of **U** with toluene and with excess [Ru$_3$(CO)$_{12}$] in toluene gave respectively the toluene-substituted derivative [Ru$_4$W(CO)$_7$(O)(μ-O)(μ_4-PPh)(CCPh)(Cp*)(C$_7$H$_8$)] (**V**) and the hexametallic complex [Ru$_5$W(CO)$_{12}$(O)(μ-O)(μ_4-PPh)(CCPh)(Cp*)] (**W**) (Scheme 1.9).

The nature of the W(O)$_2$(Cp*) moiety and its bonding to the ruthenium framework was of particular interest. The W(O)$_2$(Cp*) fragment possessed local structural features resembling those present in the 16-electron mononuclear oxo alkyl complexes

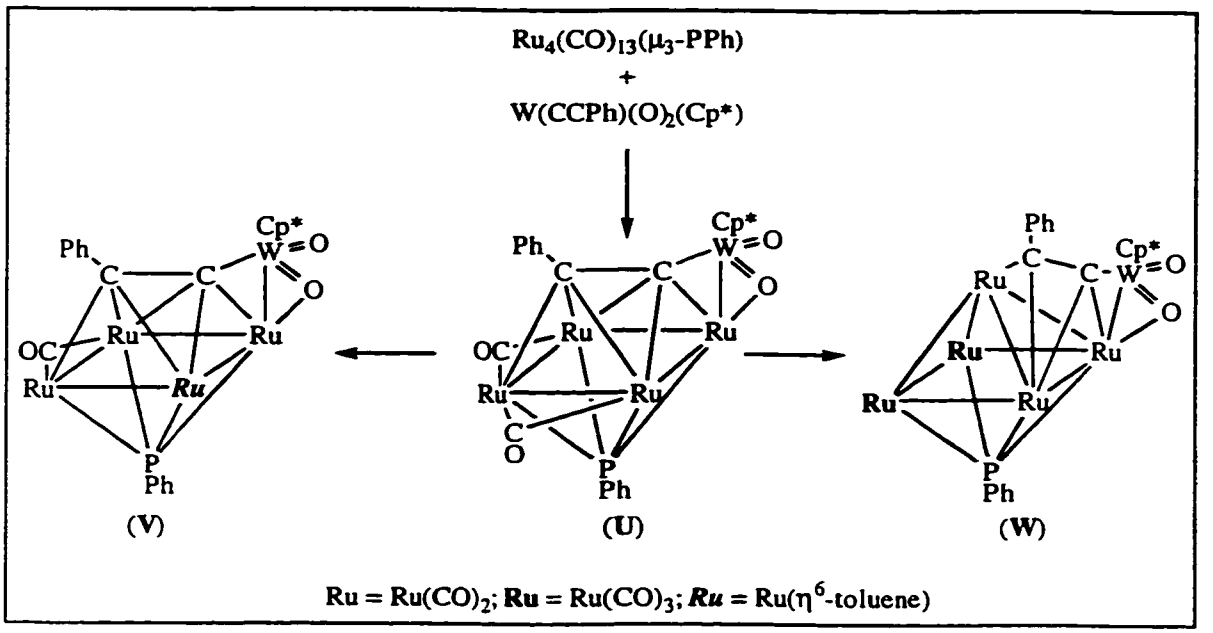

Scheme 1.9 Reactivity of $[Ru_4(CO)_{13}(\mu_3\text{-PPh})]$ with $[W(C{\equiv}CPh)(O)_2(Cp^*)]$.

$[W(CH_2SiMe_3)(O)_2(L)]$, L = Cp and Cp* which formally contained tungsten in its highest oxidation state of VI with two W=O double bonds. In contrast, complex (**U**) has a W atom with one of the oxo ligands within bonding distance from Ru. The oxo ligand is believed to serve as a π-donor to the 16-electron W center. Indeed, this type of interaction is supported by the short W-O distance (1.793(5) Å) which is also encountered in the W=O:→Os fragment of the $Os_3W(\mu\text{-O})$ clusters and suggests retention of the W=O multiple bonding. The modest lengthening (0.084(5) Å) of the W=O distance for the bridging oxo ligand versus the terminal oxo ligand in (**S**) provided further evidence for the presence of such bonding. Hence, structural data and electron counting suggested that both the bridging and the terminal oxo ligands possess W=O double bonds. The bonding mode of the terminal oxo ligand is different from the one present in the related monooxotungsten-containing cluster complexes in which the terminal oxo ligand instead adopts a formal triply bonded mode to the tungsten atom. This unusual bonding arises from the presence of only two valence orbitals on tungsten, which can be utilized to accept π-electrons from the oxo ligands.[60]

Reactivity differentials were observed between the W(VI) dioxo center [W(C≡CPh)(O)$_2$(Cp*)] and the W(II) center [W(C≡CPh)(CO)$_3$(Cp*)]. The reaction of [W(C≡CPh)(O)$_2$(Cp*)] with [Ru$_4$(CO)$_{13}$(μ_3-PPh)] produced complex (**U**) while in the lower oxidation state case, a [W(C$_2$Ph)(CO)(Cp*)] fragment caps the nido Ru$_4$P framework with incorporation of the tungsten into an octahedral Ru$_4$WP skeleton.[60]

The strategy of combining a dioxo acetylide complex [W(C≡CPh)(O)$_2$(Cp*)] with a late-metal carbonyl alkyne acceptor fragment also provided WOs$_3$ oxo complexes.[59] The labile ligand of the bis acetonitrile complex [Os$_3$(CO)$_{10}$(NCMe)$_2$] was used as the entry point to coordinate the acetylide ligand of [W(C≡CPh)(O)$_2$(Cp*)] which yielded the heterometallic acetylide cluster compound [Os$_3$W(CO)$_9$(μ-O)$_2$(μ-CCPh)(Cp*)] (**X**) (Scheme 1.10). The metal arrangement of **X** consists of a WOs$_3$ butterfly. This complex was characterized by the presence of two bridging oxo ligands located on two W-Os bonds of nearly equal length (2.981(2) and 3.014(2) Å). The bond lengths to the oxo ligands (av. W-O = 1.76(3) Å, Os-O = 2.13(3) Å) resembled that of the W=O:→Os bonding mode observed previously.[59]

Complex **X** reacted with dihydrogen resulting in the elimination of the acetylide ligand and the formation of the compound [Os$_3$W(μ-H)(CO)$_9$(μ-O)$_2$(Cp*)] (**Y**). The metal skeleton of **Y** now consists of a WOs$_3$ tetrahedron with a bridging hydride on the unique Os-Os edge. A better understanding of the reactivity of complex **X** was obtained by studying its reaction with carbon monoxide which produced a spiked triangular complex [Os$_3$W(C≡CPh)(CO)$_{11}$(O)(μ-O)(Cp*)] (**Z**) and a small amount of acetylide complex [W(C≡CPh)(O)$_2$(Cp*)] (Scheme 1.10). Complex **Z** is produced by addition of two CO molecules. Of particular interest, the structure of **Z** revealed the formation of a terminal acetylide group on the Os atom from a bridging acetylide ligand and the shifting of one edge-bridging oxo ligand to the terminal mode.

Finally, it was found that thermolysis of **Z** regenerated **X** in high yield. This reactivity pattern indicated to the authors the capacity of the acetylide and the terminal oxo ligands to act as good multiple electron donors. Both ligands can stabilize an unsaturated

cluster resulting from CO elimination by forming an edge-bridge ligand (i.e. μ-η^2-CCPh and μ-O modes) via the donation of π-electrons or lone pair electrons respectively.[59]

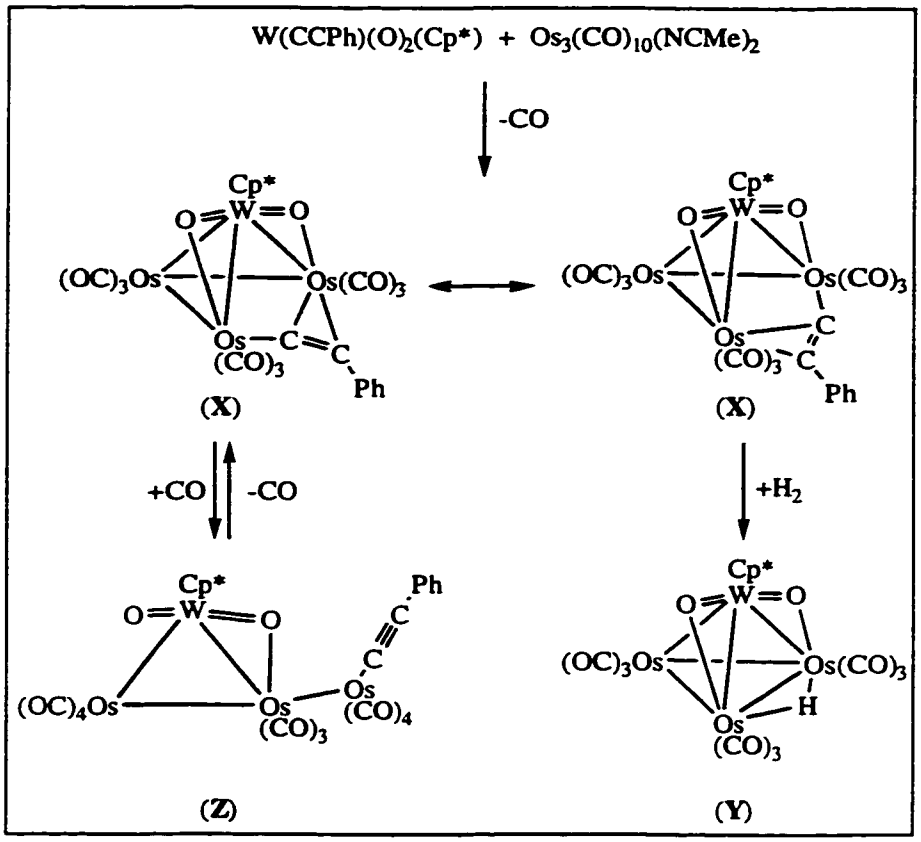

Scheme 1.10 Reactivity of $[Os_3(CO)_{10}(NCMe)_2]$ with $[W(C{\equiv}CPh)(O)_2(Cp^*)]$.

It is again interesting to note that there exists a difference in reactivity between the W(VI) $[W(C{\equiv}CPh)(O)_2(Cp^*)]$ and W(II) $[W(C{\equiv}CPh)(CO)_3(Cp^*)]$ towards $[Os_3(CO)_{10}(NCMe)_2]$. The yields for the former are greatly improved over the latter for similar cluster building reactions. The key factor in improving the yields is related to the electron withdrawing capability of the $W(O)_2(Cp^*)$ fragment which decreases the relative energy of the acetylide π^*-orbitals and therefore increases the metal-to-acetylide ligand back π-bonding.[59]

1.3 Objectives of the thesis

This thesis is focused on the area of oxide bridged early-late metal organometallics as models for platinum metals on oxide supports. Complexes of high oxidation state "oxophilic" metals and low oxidation state metals with π-acid ligands are usually considered to be at opposite extremes of the spectrum of transition metal organometallic compounds. However, group VIII metals on oxide supports are some of the most widely used heterogeneous catalysts. Thus, the combination of oxo early-metal organometallics with late-metal carbonyl compounds offers the opportunity to explore, *inter alia*, the generation of bimetallic or polymetallic models for oxide-supported platinum metal catalysts and the physical and chemical behavior of organometallic compounds of metals in highly disparate oxidation states.

Earlier in this chapter it was pointed out that certain early-late bimetallic catalysts were effective in hydrocarbon reforming. These processes undoubtedly involve hydrogen migration from substrate to metal to ligand and/or hydrogen transfer from hydrocarbon to support to metal. We know very little about these transformations. Some pertinent questions are: (a) If, as seems likely, late metal-hydrogen and metal-carbon bonds are formed in reactions between supported bimetallics and hydrocarbons (saturated and unsaturated), can model mixed metal oxide clusters bearing hydride and hydrocarbyl ligands be prepared? What types of reactivity, particularly hydrogen transfer reactions, do they undergo? (b) In the hydrogenation of mixed metal complexes with oxide and hydride ligands is hydrogen transfer to the oxide (the "supporting" ligand) a competitive process? Can μ-OH ligands be observed? (c) What are the likely products of transfer of M-H or μ-H ligands from a bimetallic or polymetallic fragment onto an unsaturated hydrocarbyl? Is there any specificity in this transfer? (d) Many intermediates, for example metal-alkenyl, metal-alkylidene, metal alkyl/aryl can be envisaged as potential products of cluster oxide hydride to unsaturated ligand migrations. Can such species be isolated and sequentially transformed?

The objectives of this thesis were therefore: 1) to synthesize and characterize new examples of early-late oxide bridged organometallic clusters from the coordinatively

unsaturated dihydride cluster $H_2Os_3(CO)_{10}$, 2) to examine the possibility of intramolecular hydrogen transfer from a low oxidation state metal to the hydrocarbyl or alternatively to the oxo functionality of the early transition metal, and 3) to probe whether oxide bridged early late metal clusters might serve as models for the hydrogenation of an alkyne on an oxide supported platinum metal surface.

Throughout this thesis, the following questions will be addressed. The transfer of hydrides onto the hydrocarbyl fragment of a cluster will be explored in order to get a better understanding of the reduction process. The characterization of complexes formed in the hydrogenation sequence will allow the identification of possible intermediates on a hydrogenation catalyst. Finally, the role of the oxide ligands, not as a hydrogen acceptor but as a potential donor via the different coordination modes (μ_2 and μ_3 bonded oxygen to help create coordination sites) will provide a more detailed understanding of the reactivity of organometallic oxo complexes.

1.4 General experimental

1.4.1 General conditions

All reactions were carried out under dry high purity nitrogen using standard Schlenk techniques. Solvents for reactions were distilled under nitrogen from appropriate drying agents prior to use. Heptane, hexane and octane were dried over sodium/benzophenone. Methylene chloride was collected after refluxing over P_2O_5. Preparative TLC was performed on 20 x 20 cm glass plates coated with silica gel (CAMAG DSF-5, 0.5 mm thick). All reactions were monitored by infrared spectroscopy (carbonyl region). Literature methods were used to prepare $[H_2Os_3(CO)_{10}]$,[61] $[D_2Os_3(CO)_{10}]$[61] and $[W(C{\equiv}CPh)(O)_2(Cp^*)]$.[58] Other reagents were purchased and used as received.

1.4.2 Instrumental conditions

Infrared spectra were recorded on a BioRad FTS-40A spectrometer, using matched calcium fluoride solution cells of 0.5 mm path length. NMR spectra were recorded on a

Bruker DRX-400 (^{1}H 400.13 MHz, ^{13}C 100.61 MHz) in $CDCl_3$ and referenced against the residual proton or carbon of deuterated solvent. FAB-MS were obtained on a JEOL AX505 spectrometer, using Xe as the exciting gas, FAB gun voltage 6 kV, accelerating potential 3 kV, and *m*-nitrobenzylalcohol matrix. Microanalyses were performed by Mrs. Ann Webb at the NRC's Institute for Biological Sciences, 100 Sussex Dr, Ottawa, Ontario, K1A 0R6, Canada.

1.4.3 Crystallography

This section summarizes the general techniques and conditions used for all crystallography experiments. Specific conditions used to obtain single crystals suitable for crystallographic study for each complex are described in the Experimental Section of the appropriate chapters. These sections also contain pertinent information for each crystallographic experiment including the final agreement (R and R_w) values obtained. More information about each experiment is provided in the Appendices.

Diffraction measurements were carried out at the NRC's Steacie Institute of Molecular Sciences on a Siemens SMART CCD automatic diffractometer using graphite-monochromated Mo-Kα (λ = 0.7107$_3$ Å) radiation. The SMART CCD automatic search, center, index and least-squares routines were used to determine the unit cell parameters from randomly selected reflections. Data processing was carried out on a Pentium II computer using the NRCVAX structure solving library obtained from the National Research Council of Canada, Ottawa, Ontario. Neutral atom scattering factors were taken from the standard references. Anomalous dispersion corrections were applied to all non-hydrogen atoms. Lorentz/polarization (Lp) and absorption corrections were applied to the data for all of the structures. Full matrix least-squares refinements minimized the functions: $\Sigma_{hkl}w(|F_o|-|F_c|)^2$ where $w = 1/\sigma(F_o)^2$, $\sigma(F_o) = \sigma(F^2_o)/2F_o$ and $\sigma(F^2_o) = [\sigma(I_{raw})^2 + (0.02I_{net})^2]^{1/2}/Lp$.

1.5 References

1. Roberts, D.A.; Geoffroy, G.L. In *Comprehensive Organometallic Chemistry: The Synthesis, Reactions, and Structures of Organometallic Compounds*; Wilkinson, G., Gordon, F., Stone, A., Eds.; Oxford: New York, 1982; Volume 6, Chapter 40.

2. Michael, D.; Mingos, P.; May, A.S. In *The Chemistry of Metal Cluster Complexes;* Shriver, D.F., Kaesz, H.D., Adams, R.D., Eds.; VCH: New York, 1990; p 14.

3. Chi, Y.; Chiang, S.-J.; Su, C.-J. In *The Synergy Between Dynamics and Reactivity at Clusters and Surfaces, NATO ASI Series C: Mathematical and Physical Sciences - Advanced Study Institute;* Farrugia, L.J., Ed.; Kluwer Academic Publishers: Netherlands, 1995; Volume 465, pp 113-124.

4. Rosenberg, E.; Laine, R. In *Catalysis by Di- and Polynuclear Metal Cluster Complexes*; Adams, R.D., Cotton, F.A., Eds.; Wiley-VCH: New-York, 1998; pp 17-23.

5. Comstock, M.C.; Shapley, J.R. *Coord. Chem. Rev.* **1995**, 143, 501.

6. *Comprehensive Organometallic Chemistry II: A Review of the Literature 1982-1994*; Abel, E.W., Stone, F.G.A., Wilkinson, G., Eds.; Oxford: New York, 1995; Volume 10.

7. Hsieh, A.T.T.; Mays, M.J. *J. Organomet. Chem.* **1972**, 39, 157.

8. Ruff, J.K.; White Jr., R.P.; Dahl, L.F. *J. Am. Chem. Soc.* **1971**, 93, 2159.

9. Schmid, G.; Bartl, K.; Boese, R. *Z. Naturforsch. Teil B* **1977**, 32, 1277.

10. Braunstein, P.; Dehand, J.; Nennig, J.F. *J. Organomet. Chem.* **1975**, 92, 117.

11. Chetcuti, M.J.; Gordon, J.C.; Fanwick, P.E. *Inorg. Chem.* **1990**, 29, 3781.

12. Antognazza, P.; Beringhelli, T.; D'Alfonso, G.; Minoja, A. *Organometallics* **1992**, 11, 1777.

13. Adams, R.D.; Babin, J.E.; Wang, J.-G.; Wu, W. *Inorg. Chem.* **1989**, 28, 703.

14. Curtis, M.D. *Polyhedron* **1987**, 6, 759.

15. (a) Stone, F.G.A. *Angew. Chem., Int. Ed. Engl.* **1984**, 23, 89. (b) Stone, F.G.A. *Philos. Trans. R. Soc. London, Ser. A* **1982**, 308, 87. (c) Stone, F.G.A. *Adv. Organomet. Chem.* **1990**, 31, 53.

16. Chetcuti, M.J.; Chetcuti, P.A.M.; Jeffery, J.C.; Mills, R.M.; Mitrprachachon, P.; Pickering, S.J.; Stone, F.G.A.; Woodward, P. *J. Chem. Soc., Dalton Trans.* **1982**, 699.

17. Stone, F.G.A. *Adv. Organomet. Chem.* **1990**, 31, 53.

18. Wido, T.; Young, G.H.; Wojcicki, A.; Calligaris, M.; Nardin, G. *Organometallics* **1988**, 7, 452.

19. Powell, J.; Gregg, M.R.; Sawyer, J.F. *Inorg. Chem.* **1989**, 28, 4451.

20. Süss-Fink, G.; Thewalt, U.; Klein, H.P. *J. Organomet. Chem.* **1984**, 262, 315.

21. Mani, D.; Vahrenkamp, H. *Chem. Ber.* **1986**, 119, 3639.

22. Albiez, T.; Bernhardt, W.; Von Schnering, C.; Roland, E.; Bantel, H.; Vahrenkamp, H. *Chem. Ber.* **1987**, 120, 241.

23. Blumhofer, R.; Fischer, K.; Vahrenkamp, H. *Chem. Ber.* **1986**, 119, 194.

24 Vahrenkamp, H. *Comments Inorg. Chem.* **1985**,4, 253.

25. Hwang, D.-K.; Chi, Y.; Peng, S.-M.; Lee, G.-H. *Organometallics* **1990**, 9, 2709.

26. Adams, R.D.; Babin, J.E.; Tasi, M. *Organometallics* **1988**, 7, 219.

27. Chi, Y.; Wu, H.-L.; Chen, C.-C.; Su, C.-J.; Peng, S.-M.; Lee, G.-H. *Organometallics* **1997**, 16, 2434.

28. (a) Burwell Jr., R.L. In *Chem. and Eng. News*, Aug. 22, 1966. (b) Basolo, F.; Burwell Jr., R.L. In *Catalysis Progress in Research;* Plenum Press: New York, 1973; p 51.

29. (a) Muetterties, E.L. *Bull. Soc. Chim. Belg.* **1975**, 84, 959. (b) Muetterties, E.L. *Bull. Soc. Chim. Belg.* **1976**, 85, 451. (c) Muetterties, E.L. *Science* **1977**, 196, 839.

30. (a) *Metal Clusters in Catalysis*; Gates, C., Guczi, L., Knözinger, H., Eds.; Elsevier: Amsterdam; 1986; 648 p. (b) *Surface Organometallic Chemistry: Molecular Approaches to Surface Catalysis, NATO ASI Series C.*; Basset, J.-M., Bates, B.C., et. al., Eds.; Kluwer Academic Publishers, Dordrecht, Boston and London, 1988; Volume 231, 330 p.

31. Chi, Y.; Cheng, P.-S.; Wu, H.-L.; Hwang, D.-K.; Su, P.-C.; Peng, S.-M.; Lee, G.-H. *J. Chem. Soc., Chem. Commun.* **1994**, 1839.

32. West, B.O. *Polyhedron* **1989**, 8, 219.

33. Alves, A.S.; Moore, D.S.; Andersen, R.A.; Wilkinson, G. *Polyhedron* **1982**, 1, 83.

34. Fischer, E.O.; Ulm, K.; Fritz, H.P. *Chem. Ber.* **1960**, 93, 2167.

35. Bottomley, F.; Paez, D.E.; White, P.S. *J. Am. Chem. Soc.* **1981**, 103, 5581.

36. Cousins, M.; Green, M.L.H. *J. Chem. Soc.* **1964**, 1567.

37. Corradini, P.; Allegra, G. *J. Am. Chem. Soc.* **1959**, 81, 5510.

38. Carrick, W.L.; Reichle, W.T.; Pennella, F.; Smith, J.J. *J. Am. Chem. Soc.* **1960**, 82, 3887.

39. Bottomley, F.; Sutin, L. *Adv. Organomet. Chem.* **1988**, 28, 339.

40. (a) Johnson, B.F.G.; Lewis, J.; Williams, I.G.; Wilson, J. *Chem Commun.* **1966**, 391. (b) Bright, D.A. *J. Chem. Soc., Chem. Commun.* **1970**, 1169.

41. Su, F.-M.; Cooper, C.; Geib, S.J.; Rheingold, A.L.; Mayer, J.M. *J. Am. Chem. Soc.* **1986**, 108, 3545.

42. (a) Xiao, J.; Puddephatt, R. J. *Coord. Chem. Rev.* **1995**, 143, 457-500. (b) Braunstein, P.; Rosé, J. In *Catalysis by Di- and Polynuclear Metal Cluster Complexes*; Adams, R.D., Cotton, F.A., Eds.; Wiley-VCH: New-York, 1998; pp 443-508.

43. Sinfelt, J.H. In *Bimetallic Catalysts: Discoveries, Concepts and Applications;* Wiley, New York, 1983; 164 p.

44. (a) Klabunde, K.J.; Li, Y.-X. In *Selectivity in Catalysis*; Davis, M.E., Suib, S.L., Eds; American Chemical Society: Washington, DC, 1993; pp 88-108. (b) Biswas, J.; Bickle, G.M.; Gray, P.G.; Do, D.D.; Barbier, J. *Catal. Rev. Sci. Eng.* **1988**, 30, 161.

45. Adams, R.D.; Herrmann, W.A. *Polyhedron* **1988**, 7, 2255.

46. Fung, A.S.; McDevitt, M.R.; Tooley, P.A.; Kelley, M.J.; Knoingsberger, D.C.; Gates, B.C. *J. Catal.* **1993**, 140, 190.

47. Kluksdahl, H.E. *US Patent* **1968**, 3415, 737.

48. (a) Biswas, J.; Bickle, G.M.; Gray, P.G.; Do, D.D.; Barbier, J. *Catal. Rev. Sci. Eng.* **1988**, 30, 161. (b) Sinfelt, J.H. *Acc. Chem. Res.* **1987**, 20, 134. (c) Ponec, V. *Adv. Catal.* **1983**, 32, 149.

49. (a) Xiao, J.; Vittal, J.J.; Puddephatt, R.J.; Manojlovic-Muir, Lj.; Muir, K.W. *J. Am. Chem. Soc.* **1993**, 115, 7882. (b) Xiao, J.; Puddephatt, R.J.; Manojlovic-Muir, Lj.; Muir, K.W. *J. Am. Chem. Soc.* **1994**, 116, 1129. (c) Choi, M.-G., Angelici, R.J. *J. Am. Chem. Soc.* **1991**, 113, 5651.

50. Jennings, M.C.; Schoettel, G.; Puddephatt, R.J. *Organometallics* **1991**, 10, 580.

51. Nacheff, M.S.; Kraus, L.S.; Ichikawa, M.; Hoffman, B.M.; Butt, J.B.; Sachtler, W.M.H. *J. Catal.* **1987**, 106, 263.

52. Park, J.T.; Shapley, J.R.; Churchill, M.R.; Bueno, C. *Inorg. Chem.* **1983**, 22, 1579.

53. Churchill, M.R.; Ziller, J.W.; Beanan, L.R. *J. Organomet. Chem.* **1985**, 287, 235.

54. Su, C.-J.; Su, P.-C.; Chi, Y.; Peng, S.-M.; Lee, G.-H. *J. Am. Chem. Soc.* **1996**, 118, 3289.

55. Gong, J.-H.; Hwang, D.-K.; Tsay, C.W.; Chi, Y.; Peng, S.-M.; Lee, G.-H. *Organometallics* **1994**, 13, 1720.

56. (a) Chi, Y.; Wu, H.-L.; Peng, S.-M.; Lee, G.-H. *J. Chem. Soc., Dalton Trans.* **1997**, 1931. (b) Wu, H.-L; Lu, G.-L.; Chi, Y.; Farrugia, L. J.; Peng, S.-M.; Lee, G.-H. *Inorg. Chem.* **1996**, 35, 6015.

57. Lai, N.-S.; Tu, W.-C.; Chi, Y.; Peng, S.-M.; Lee, G.-H. *Organometallics* **1994**, 13, 4652.

58. Shiu, C.-W.; Su, C.-J.; Pin, C.-W.; Chi, Y.; Peng, S.-M.; Lee, G.-H. *J. Organomet. Chem.* **1997**, 545-546, 151.

59. Shiu, C.-W.; Chi, Y.; Carty, A.J.; Peng, S.-M.; Lee, G.-H. *Organometallics* **1997**, 16, 5368.

60. Blenkiron, P.; Carty, A.J.; Peng, S.-M.; Lee, G.-H.; Su, C.-J.; Shiu, C.-W.; Chi, Y. *Organometallics* **1997**, 16, 519.

61. Knox, S.A.R.; Koepke, J.W.; Andrews, M.A.; Kaesz, H.D. *J. Am. Chem. Soc.* **1975**, 97, 3942.

Chapter Two

Synthesis and reactivity of $[Os_3W(\mu\text{-}H)(\mu\text{-}\eta^1\text{-}C{=}CHPh)(CO)_{10}(O)(\mu\text{-}O)Cp^*]$ 1

2.1 Introduction

In this chapter the generation of new mixed early-late metal oxo bridged hydrocarbyl complexes via the strategy of reacting an early metal oxo acetylide $[W(C{\equiv}CPh)(O)_2(Cp^*)]$ with $[H_2Os_3(CO)_{10}]$ is explored. The early metal compound $[W(C{\equiv}CPh)(O)_2(Cp^*)]$ has a strongly coordinating π-acceptor ligand -C≡CPh and the late metal fragment $[H_2Os_3(CO)_{10}]$ is known to have an affinity for alkynes.

The use of a metal carbonyl cluster containing hydrides as the hydrocarbyl acceptor fragment may provide different avenues for interesting chemical transformations. Indeed, the reaction of alkynes with di- and polynuclear hydrido-metal complexes has been extensively developed as a strategy for synthetic routes into μ-vinyl (-CR=CHR') (Scheme 2.1) and μ-allyl ($-C_3H_3RR'$) bridged systems.[1]

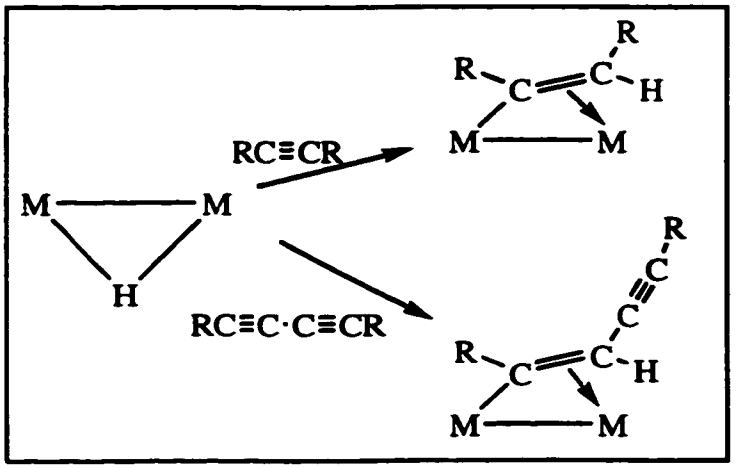

Scheme 2.1 Reaction chemistry of alkyne ligands and hydride containing clusters.

The cluster $[H_2Os_3(CO)_{10}]$ represents an ideal candidate to explore the reactivity of metal carbonyl clusters containing hydrides with the early metal oxo-acetylide complex $[W(C{\equiv}CPh)(O)_2(Cp^*)]$. The unsaturation associated with $[H_2Os_3(CO)_{10}]$ may serve as the coordination site for the acetylide ligand which would deliver in the process an early metal oxo fragment to the late metal complex.[2] The 46 electron cluster $[H_2Os_3(CO)_{10}]$ is electron deficient by two electrons. This deficiency is responsible in large part for the rich and diverse chemistry associated with $[H_2Os_3(CO)_{10}]$.

The $[H_2Os_3(CO)_{10}]$ cluster reacts with nucleophiles. The addition process involves a shift of one bridging hydride into a terminal position, leading to the 48 electron species $[Os_3H(\mu\text{-}H)(CO)_{10}L]$. The incoming ligand L occupies either an axial or an equatorial site, depending on its steric bulk.[3] $[H_2Os_3(CO)_{10}]$ also adds electrophiles. Addition of electrophiles E to $[H_2Os_3(CO)_{10}]$ can remove unsaturation if the radical E can behave as a three-electron donor.

The unsaturated cluster $[H_2Os_3(CO)_{10}]$ also undergoes insertion reactions with alkynes. For example, $[H_2Os_3(CO)_{10}]$ reacts with $PhC{\equiv}CPh$ quantitatively at room temperature to give $[Os_3(H)(CO)_{10}\{\mu\text{-}CPhC(H)Ph\}]$, which contains an edge-bridging (σ-π) alkenyl group.[1(e),4] Interestingly, the more reactive alkyne $CF_3C{\equiv}CCF_3$ reacts with $[H_2Os_3(CO)_{10}]$ to give $[Os_3(H)(CO)_{10}\{\mu_3\text{-}C(CF_3)C(H)CF_3\}]$, which contains a triply-bridging bis-trifluoromethylalkenyl group.[5]

Also of interest is the ability of $[H_2Os_3(CO)_{10}]$ to add a variety of metal containing groups to yield higher nuclearity heteronuclear cluster complexes. The following examples show the addition of *d*-block metals as triply bridging fragments to produce Os_3M tetrahedral clusters (60 cluster valence electrons). The compounds in this series consist mostly of an $Os_3(CO)_9$ framework to which is attached a transition metal atom with various bridging ligands (hydride, CO, vinylidene, oxide, sulfide, alkylidene, or alkyne) (Equation 2.1 and 2.2).

$$H_2Os_3(CO)_{10} + Pt(C_2H_4)_2PR_3 \longrightarrow$$

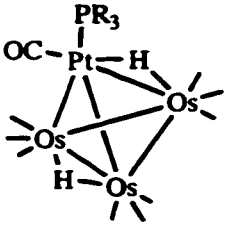

(2.1)[6]

$$H_2Os_3(CO)_{10} + CpCo(CO)_2 \longrightarrow$$

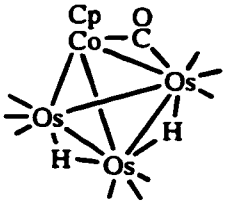

(2.2)[7]

As a result of both the unsaturation and the presence of hydride ligands, $[H_2Os_3(CO)_{10}]$ can be regarded as a model catalyst for hydrocarbon transformations. Thus Deeming and Hasso proposed a catalytic cycle for the isomerization of olefins by $[H_2Os_3(CO)_{10}]$ (Scheme 2.2).

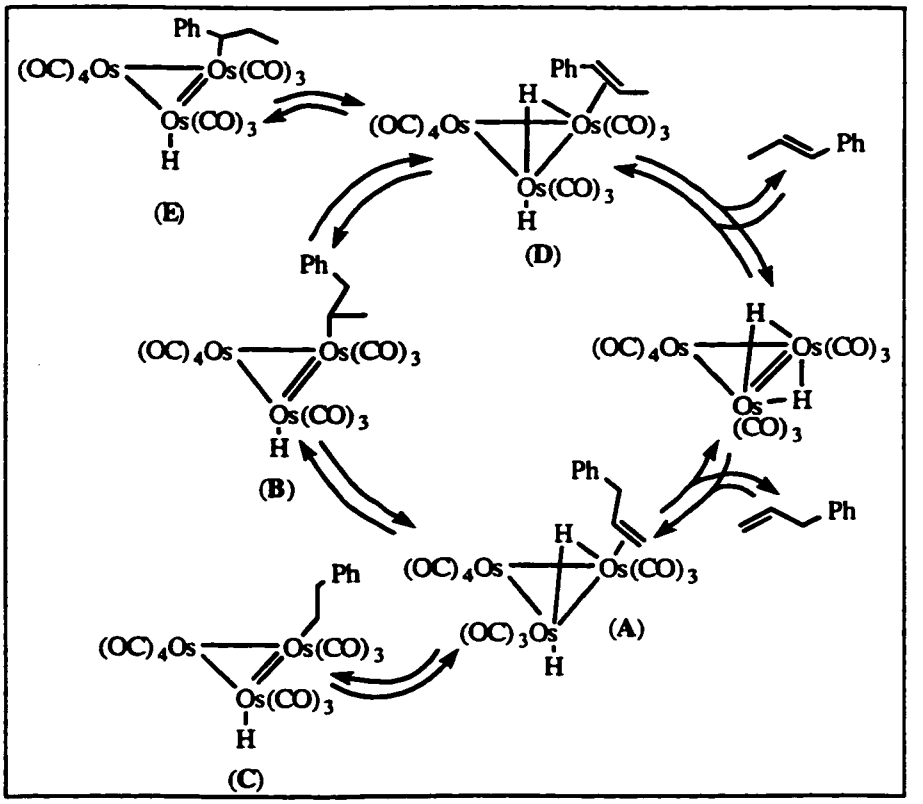

Scheme 2.2 Proposed catalytic cycle for the isomerization of olefins.

It is assumed that $[H_2Os_3(CO)_{10}]$ adds to the alkene to give the η^2-alkene complex **A** of which phosphine analogs have been synthesized and characterized.[8] This η^2-alkene complex **A** can transfer a hydrogen atom from the metal framework to the coordinated olefin to give the hydridoalkyl complex **B** or **C**. With diethyl fumarate or dimethyl maleate, a hydridoalkyl cluster of the type $[Os_3H\{CH(CH_2COOEt)(COOEt)\}(CO)_{10}]$, in which the ester function helps to stabilize the system, could be characterized.[8] The reverse hydrogen transfer from **B** gives **D**, from which the isomerized alkene can be eliminated.

The ability of $[H_2Os_3(CO)_{10}]$ to catalyze the hydrogenation of an alkyne to an alkene by a trinuclear osmium cluster has been proposed[9] and demonstrated for a trifluoromethyl-substituted substrate (Scheme 2.3).

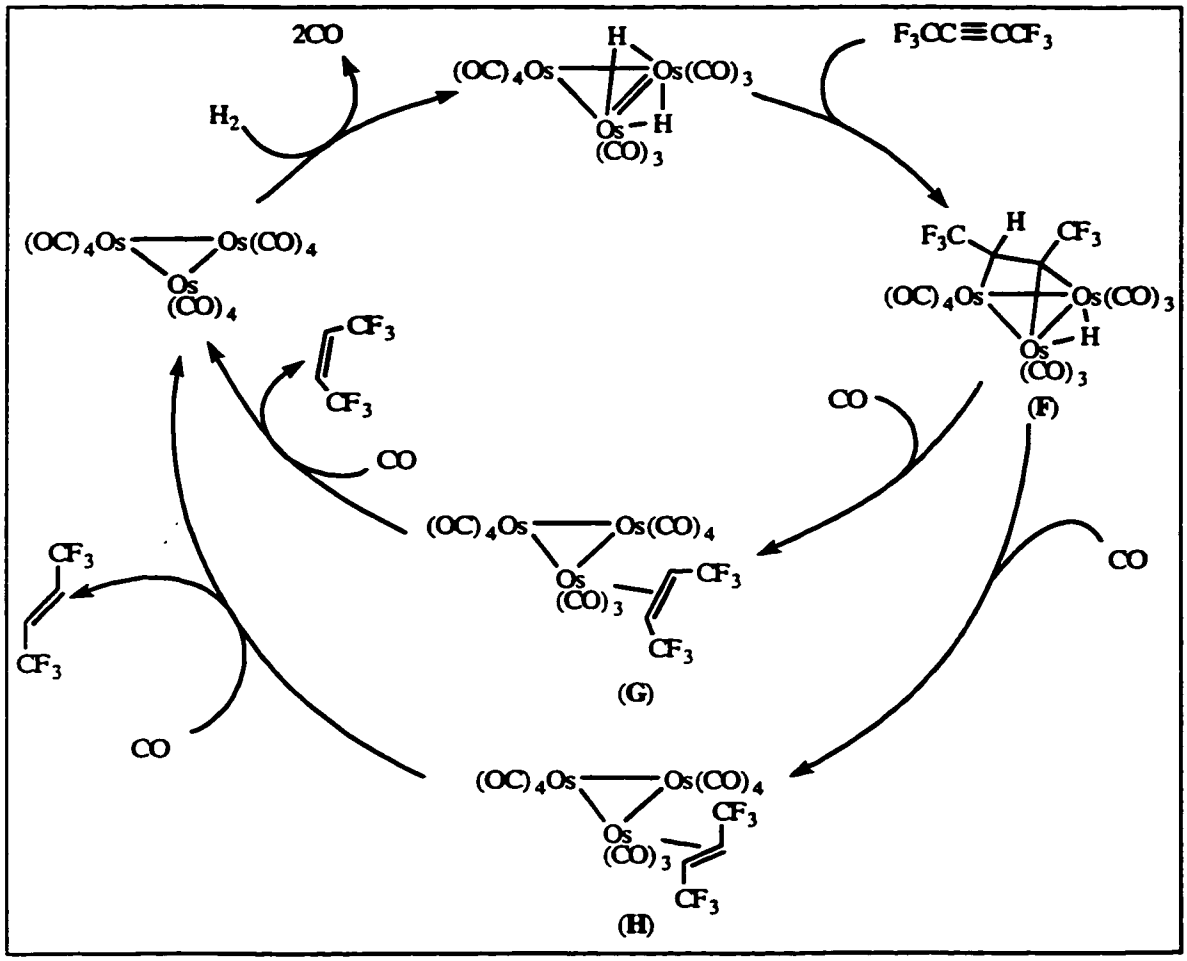

Scheme 2.3 Proposed mechanism for the hydrogenation of bis(trifluoromethyl)-acetylene.

The hydrido cluster $[H_2Os_3(CO)_{10}]$ adds bis(trifluoromethyl) acetylene to give cluster **F**, which itself takes up carbon monoxide to give a 1:1 mixture of the alkene complexes **G** and **H**. These complexes can be reacted separately with CO to generate $Os_3(CO)_{12}$ quantitatively with loss of the corresponding (*E*)- and (*Z*)-alkanes. The cycle is completed by the known[10] hydrogenation of $[Os_3(CO)_{12}]$ to $[H_2Os_3(CO)_{10}]$.

2.2 Results and discussion

2.2.1 Summary

The reaction between $[H_2Os_3(CO)_{10}]$ and 1.2 equivalents of $[W(C{\equiv}CPh)(O)_2(Cp^*)]$ in refluxing dichloromethane resulted in a color change from purple to dark orange after four days in the dark. A new complex $[Os_3W(\mu\text{-}H)(\mu\text{-}\eta^1\text{-}C{=}CHPh)(CO)_{10}(O)(\mu\text{-}O)(Cp^*)]$ (**1**) was isolated showing a selective transfer of hydride to the organic moiety yielding a compound containing a vinylidene ligand with a phenyl ligand *trans* to the Os(1) atom.

Attempts to transfer the bridging hydride of **1** under thermal conditions lead to the isolation of $[Os_3W(\mu\text{-}H)(\textit{trans}\text{-}\mu\text{-}\eta^1\text{-}C{=}CHPh)(CO)_9(O)(Cp^*)(\mu_3\text{-}O)]$ (**2**). Hence **1** readily undergoes CO loss, concomitant with the formation of a triply bridging oxo ligand to afford **2**. This μ_3-O coordination mode is unprecedented in heteronuclear WOs_3 complexes. However, triply bridging oxo ligands have been previously located on homonuclear clusters such as $[Ru_3(CO)_3(\mu_3\text{-}CO)(\mu\text{-}dppm)_3(\mu_3\text{-}O)]$,[11] $[Fe_3(CO)_9(\mu_3\text{-}O)]^{2-}$,[12] $[Os_6(CO)_{18}(\mu_3\text{-}CO)(\mu_3\text{-}O)]$,[13] and heteronuclear complexes. Examples of the latter include $[Pt_3\{Re(CO)_3\}(\mu_3\text{-}O)_2(\mu\text{-}dppm)_3]^+$,[14] $[FeMo_2(CO)_7(\mu_3\text{-}O)(Cp^*)_2]$[15] and $[MFe_2(CO)_8(\mu\text{-}RS)(\mu_3\text{-}O)(Cp)]$ (M = Mo, W)[16].

Exposure of **2** to a 60 W tungsten incandescent light resulted in the isomerization of the vinylidene ligand to produce $[Os_3W(\mu\text{-}H)(\textit{cis}\text{-}\mu\text{-}\eta^1\text{-}C{=}CHPh)(CO)_9(O)(Cp^*)(\mu_3\text{-}O)]$ (**3**).

To our knowledge, such selective photo-induced isomerization of a vinylidene ligand has not been reported previously in the literature.

The bridging hydride present on **1** was found to be readily transferred to the hydrocarbyl fragment upon exposure of the complex to a 60W tungsten incandescent light at room temperature, resulting in the formation of $[Os_3W(CO)_{10}(O)(\mu\text{-}\eta^1,\eta^2\text{-}CH{=}CHPh\{W\text{-}Os\})(\mu\text{-}O)(Cp^*)]$ (**4**). This photo-induced H-migration is without literature precedence. The conversion of **1** to **4** represents the first light induced transfer of a single hydride from a metal framework to a bridging vinylidene resulting in the formation of a bridging vinyl ligand. The compounds **1**, **2**, **3** and **4** have been fully characterized by IR, ^1H and ^{13}C spectroscopies and single crystal X-ray structure determinations in each case. Satisfactory elemental analyses were also obtained.

This proposed sequential addition of H_2 was further supported by D_2 labeling experiments. Treatment of $[W(C{\equiv}CPh)(O)_2(Cp^*)]$ with $[D_2Os_3(CO)_{10}]$ afforded the labeled complexes $[Os_3W(\mu\text{-}D)(\mu\text{-}\eta^1\text{-}C{=}CDPh)(CO)_{10}(O)(\mu\text{-}O)(Cp^*)]$ (**1d**) and $[Os_3W(CO)_{10}(O)(\mu\text{-}\eta^1,\eta^2\text{-}CD{=}CDPh\{W\text{-}Os\})(\mu\text{-}O)(Cp^*)]$ (**4d**). These compounds were thoroughly characterized by IR, ^1H, and ^2H spectroscopies and elemental analysis.

2.2.2 Synthesis of $[Os_3W(\mu\text{-}H)(\mu\text{-}\eta^1\text{-}C{=}CHPh)(CO)_{10}(O)(\mu\text{-}O)(Cp^*)]$ 1

Complex **1** was obtained from the reaction of $[W(C{\equiv}CPh)(O)_2(Cp^*)]$ with $[H_2Os_3(CO)_{10}]$ (Scheme 2.4). This synthetic route is an example of a recently established strategy from work in this laboratory[2a] and elsewhere[2b] for attaching a metal oxo fragment to a late metal center via the coordination of a metal oxo-acetylide or other unsaturated hydrocarbyl to a late metal hydrocarbyl acceptor. This reaction may be a general one adaptable to the synthesis of a range of late metal clusters in relatively high yields (67% for cluster **1**).

2.2.2.1 Spectroscopic features of 1

The infrared spectrum of the crystalline compound **1** showed terminal carbonyl stretching bands at 2132 (w), 2078 (vs), 2060 (s), 2049 (vs), 2029 (m), 2018 (m), 2005 (m), 1998 (m), 1982 (w) and 1944 (w) cm^{-1}. The FAB mass spectrum was characterized by an $[M]^+$ ion at *m/z* 1305 suggesting the simple addition of $[W(C{\equiv}CPh)(O)_2(Cp^*)]$ to $[H_2Os_3(CO)_{10}]$. The ^1H NMR spectrum exhibited signals at δ 9.27 and at −18.01 in addition to the expected Ph and Cp* resonances. The ^1H NMR spectrum of the hydrido-vinylidene complex $[Os_3(\mu\text{-}H)(\mu\text{-}Br)(\mu\text{-}\eta^1\text{-}C{=}CHPh)(CO)_9]$ exhibited similar resonances at δ 9.11 and −11.25 which were characteristic of a vinylidene and hydride protons respectively.[17] The ^{13}C NMR spectrum showed two signals at δ 148.0 and 144.2 attributed to the hydrocarbyl fragment. A Heteronuclear Multiple Quantum Correlation (HMQC) experiment was used to establish the $^{13}C/^1H$ coupled systems. This experiment was carried out on a sample of **1** in order to distinguish between the C_α and C_β of the hydrocarbyl fragment. The singlet at δ_H 9.27 has a cross-peak (i.e. coupling correlation) with the resonance at δ_c 148.0. Thus, the signals at δ_C 144.2 and 148.0 are attributed to the C_α and C_β of the vinylidene, respectively.

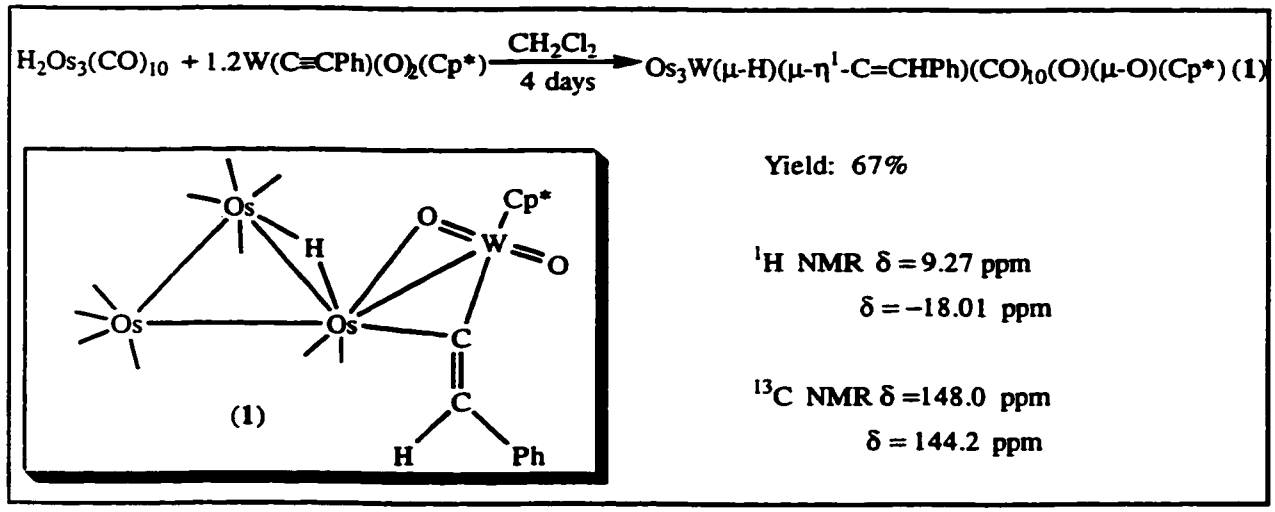

Scheme 2.4 The synthesis of $[Os_3W(\mu\text{-}H)(\mu\text{-}\eta^1\text{-}C{=}CHPh)(CO)_{10}(O)(\mu\text{-}O)(Cp^*)]$ **1**.

2.2.2.2 X-ray structure of 1

The structure of **1** was confirmed by an X-ray crystal structure determination. The molecular structure of $[Os_3W(\mu\text{-}H)(\mu\text{-}\eta^1\text{-}C{=}CHPh)(CO)_{10}(O)(\mu\text{-}O)(Cp^*)]$ (**1**) is shown as an ORTEP plot in Figure 2.1. Selected bond lengths and angles are summarized in Table 2.1. The metal framework consists of a triangle of three osmium atoms, which is spiked by a tungsten atom at Os(1). The Os(2) and Os(3) atoms carry four CO groups while Os(1) has two CO groups completing the usual octahedral geometry about each metals. Within the Os_3 triangle, two of the Os-Os edges (Os(1)-Os(3) = 2.8529(4) Å and Os(2)-Os(3) = 2.9025(4) Å) are almost equal and are close to the range of values expected for a single Os-Os bond (cf. Os-Os = 2.877 Å in $Os_3(CO)_{12}$),[3b] while the Os(1)-Os(2) separation (2.9995(4) Å) is substantially greater. A difference Fourier map revealed the presence of a bridging hydride between Os(1) and Os(2) (Os(1)-H(1) = 1.84(6) Å and Os(2)-H(1) = 1.62(7) Å). The location of the bridging hydride in this complex is supported by the observation that bridging hydride ligands typically cause an expansion of the bridged metal-metal bond length relative to non-bridged analogues.[3b,3c,18] It should also be noted that the presence of bridging hydrides forces any adjacent equatorial carbonyl ligands away from the center of the bridged metal-metal bond resulting in the enlargement of the Os-Os-C(O) angles.[19] The Os-Os-C(O) angles of the equatorial carbonyl ligands associated with Os(1)-Os(3) and Os(2)-Os(3) bonds are less than 100°, while the Os(1)-Os(2)-C(21) angle is substantially greater (Os(1)-Os(2)-C(21) = 118.1(2)°) (Appendix A.1).

A vinylidene ligand [C(1)=C(2)] bridges the W-Os(1) vector in a $\mu\text{-}\eta^1$ fashion (W-C(1) = 2.031(6) Å and Os(1)-C(1) = 2.200(6) Å), which is similar to the situation observed in $[Os_3W(\mu\text{-}\eta^1\text{-}C{=}CH(p\text{-}Tol))(CO)_9(\mu\text{-}O)(Cp)]$ (W-C = 2.08(4) Å and Os-C = 2.15(4) Å).[20] The vinylidene ligand features a phenyl substituent *trans* to Os(1) and dihedral angles of W-C(1)-C(2)-C(3) = -8.5(4)° and Os(1)-C(1)-C(2)-C(3) = -170.0(10)°. The C(1)-C(2) bond distance (1.319(9) Å) may be compared with the corresponding values in vinylidene complexes such as $[Os_3(\mu\text{-}H)(\mu\text{-}Br)(\mu\text{-}\eta^1\text{-}C{=}CHPh)(CO)_9]$ (C-C = 1.37(2) Å)[17] where the vinylidene ligand bridges also two metal centers in a $\mu\text{-}\eta^1$ fashion.

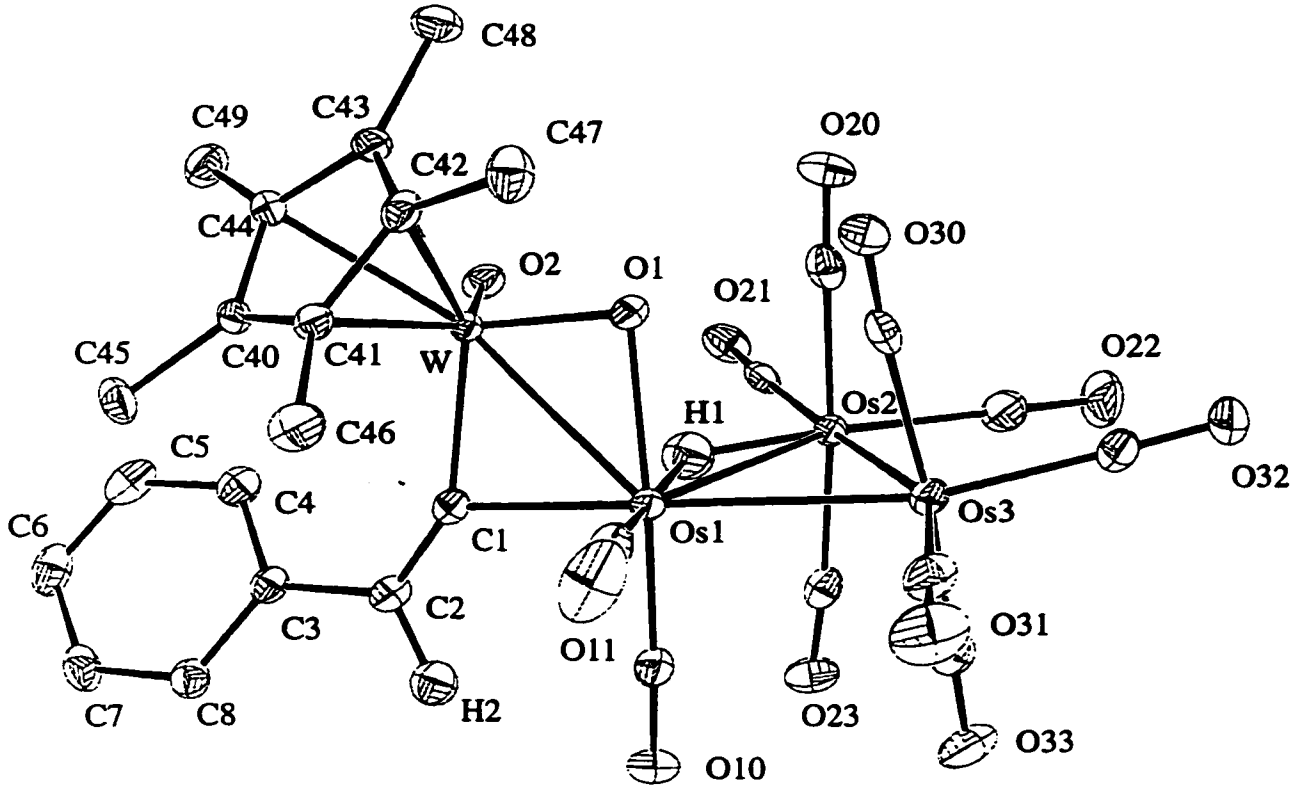

Figure 2.1 The molecular structure of $[Os_3W(\mu\text{-}H)(\mu\text{-}\eta^1\text{-}C{=}CHPh)(CO)_{10}(O)(\mu\text{-}O)(Cp^*)]$ **1**.

Table 2.1 Selected bond lengths (Å) and angles (deg) for **1**.

Lengths			
Os(2)-Os(3)	2.9025(4)	W-O(2)	1.711(4)
Os(2)-Os(1)	2.9995(4)	W-O(1)	1.844(4)
Os(3)-Os(1)	2.8529(4)	W-C(1)	2.031(6)
W-Os(1)	2.7586(3)	Os(1)-C(1)	2.200(6)
Os(1)-O(1)	2.110(4)	C(1)-C(2)	1.319(9)
Angles			
Os(2)-Os(1)-Os(3)	59.402(8)	Os(1)-C(1)-W	81.3(2)
Os(1)-Os(2)-Os(3)	57.785(8)	W-C(1)-C(2)	148.6(5)
Os(1)-Os(3)-Os(2)	62.813(9)	Os(1)-C(1)-C(2)	128.9(4)
Os(2)-Os(1)-W	98.04(1)	C(1)-C(2)-C(3)	126.8(6)
Os(3)-Os(1)-W	132.90(1)	Os(2)-Os(1)-O(1)	82.5(1)
Os(1)-O(1)-W	88.2(2)	Os(3)-Os(1)-O(1)	91.8(1)
O(1)-W-O(2)	106.2(2)		

The W-O(1)-Os(1) bridge is characterized by a short tungsten-oxygen bond length of W-O(1) = 1.844(4) Å and a comparatively long osmium-oxygen bond length of Os(1)-O(1) = 2.110(4) Å; the angle Os(1)-O(1)-W is 88.2(2)°. This data is in agreement with the description of the bridge in terms of a W=O:→Os system in which the oxo functionality serves as a 2 electron donor to the osmium atom. An analogous bonding mode has been found previously in the related molecule $[Os_3W(\eta^1\text{-}C{\equiv}CPh)(CO)_{11}(O)(\mu\text{-}O)(Cp^*)]$ (W-O = 1.83(1) Å, Os-O = 2.15(1) Å; W-O-Os = 95.1(5)°) and several other complexes.[2b] Parameters for the OsW(μ-O) portions of these clusters are compared in Table 2.2. A typical W-Os bond distance in unbridged heterobimetallic complexes is ~ 3.037 (1) Å.[21] The W-Os bond distance obtained for the first six complexes included in Table 2.2 illustrates that the presence of a bridging oxo ligand between the W and Os atoms results in a shortening of the W-Os bond (avg. 2.926 (2) Å). The bridging hydrocarbyl ligands of these complexes are linked uniquely to the tungsten atom of the OsW(μ-O) fragment or are bridging two osmium atoms of the metal framework. The addition of another bridge on a W-Os vector bearing already an oxo ligand leads to a further contraction of the W-Os bond, as demonstrated by both $[Os_3W(CO)_9(\mu_3\text{-}C\text{-}CH_2Tol)(\mu\text{-}O)(Cp)]$ and **1**, which were shown to have a shorter W-Os bond distance and a smaller W-O-Os angle than the previous six complexes mentioned in Table 2.2. In the case of $[Os_3W(\mu\text{-}H)(CO)_8(\mu_3\text{-}\eta^2\text{-}C_2H_2)(\mu\text{-}O)(Cp)]$ (Table 2.2), the W-Os vector is part of the triangular WOs_2 face capped by the sterically undemanding $\mu_3\text{-}\eta^2\text{-}C_2H_2$ ligand, which does not lead to a contraction of the W-Os vector.[20]

The neutral bridging oxo ligand in complex **1** serves as a net four electron donor. With all metal atoms and ligands treated as formally neutral, cluster **1** is electron precise with an overall 64 cluster valence electrons as expected for a spiked triangular metal framework (4 M-M bonds).

2.2.3 Synthesis of $[Os_3W(\mu\text{-}H)(\textit{trans}\text{-}\mu\text{-}\eta^1\text{-}C{=}CHPh)(CO)_9(O)(Cp^*)(\mu_3\text{-}O)]$ 2

A heptane solution of complex **1** was heated at 100°C for 7 hours resulting in a color change from orange to red (Scheme 2.5). Red crystals of $[Os_3W(\mu\text{-}H)(\textit{trans}\text{-}\mu\text{-}\eta^1\text{-}$

Table 2.2 Dimensions of OsW(μ-O) systems in WOs_3 clusters.

Complex	*d*(W=O), Å	*d*(Os-O), Å	*d*(W-Os), Å	W-O-Os, deg
$Os_3W(CO)_9(\mu_3\text{-}C\text{-}CH_2Tol)(\mu\text{-}O)Cp^{*}$[2b]	1.83(1)	2.15(1)	2.942(1)	95.1(5)
$Os_3W(\mu\text{-}Cl)(CO)_9(\mu\text{-}CHCH_2Tol)(\mu O)Cp$[22]	1.786(9)	2.126(8)	2.987(1)	99.2(4)
$Os_3W(\mu\text{-}H)(CO)_9\ (\mu\text{-}CHCH_2Tol)(\mu O)Cp$[22]	1.74(2)	2.17(2)	2.916(1)	96.0(7)
$Os_3W(\mu\text{-}H)(\mu\text{-}C{=}CHTol)(CO)_9(\mu\text{-}O)Cp$[20]	1.79(2)	2.13(2)	2.868(2)	93.6(9)
$Os_3W(\mu\text{-}\eta^1,\eta^2\text{-}C{\equiv}CPh)(CO)_9(\mu\text{-}O)_2Cp^{*}$[2b]	1.76(3)	2.13(3)	2.998(2)	101(1)
$Os_3W(\mu\text{-}H)(CO)_9(\mu\text{-}O)_2Cp$[23]	1.79(3)	2.09(3)	2.887(3)	N/A
$Os_3W(\mu\text{-}H)(CO)_8(\mu_3\text{-}\eta^2\text{-}C_2H_2)(\mu\text{-}O)Cp$[24]	1.761(8)	2.200(8)	2.885(1)	92.8(4)
$Os_3W(CO)_9(\mu_3\text{-}C\text{-}CH_2Tol)(\mu\text{-}O)Cp$[25]	1.812(7)	2.169(8)	2.663(1)	83.5(3)
$Os_3W(\mu\text{-}H)(\mu\text{-}\eta^1\text{-}C{=}CHPh)(CO)_{10}(O)(\mu\text{-}O)Cp^{*}$ (1)	1.844(4)	2.110(4)	2.7586(3)	88.2(2)
$Os_3W(CO)_{10}(O)(\mu\text{-}\eta^1,\eta^2\text{-}CH{=}CHPh)(\mu\text{-}O)Cp^{*}$ (4)	1.817(5)	2.167(5)	2.8257(4)	89.9(2)

C=CHPh)(CO)$_9$(O)(Cp*)(μ_3-O)] (**2**) were obtained from slow evaporation of a 1/1 CH_2Cl_2/hexane solution at room temperature. This reaction is an example of a thermally induced loss of CO followed by structural rearrangement.

2.2.3.1 Spectroscopic features of 2

The infrared spectrum of this crystalline compound showed the characteristic absorption of terminal carbonyl function as bands at 2093 (m), 2056 (vs), 2031 (w), 2017 (vs), 2012 (s), 2005 (m), 1997 (m), 1980 (w) and 1959 (w) cm^{-1}. The ^1H NMR spectrum of **2** displayed the two anticipated resonances for the Ph and Cp* ligands. In addition, the ^1H NMR spectrum exhibited two singlets (δ 9.60 and –13.65) similar to those of the parent cluster **1**. These two resonances are characteristic of vinylidene and hydride protons respectively. The ^{13}C NMR spectrum of **2** exhibited, in addition to peaks for CO, Ph and Cp* ligands, two peaks at δ 143.7 and 146.8 ppm characteristic of C_α and C_β shifts observed for vinylidene ligands (cf. Complex **1**). The parent ion peak in the FAB mass spectrum is located at *m/z* 1277 suggesting the loss of a carbonyl ligand from **1**.

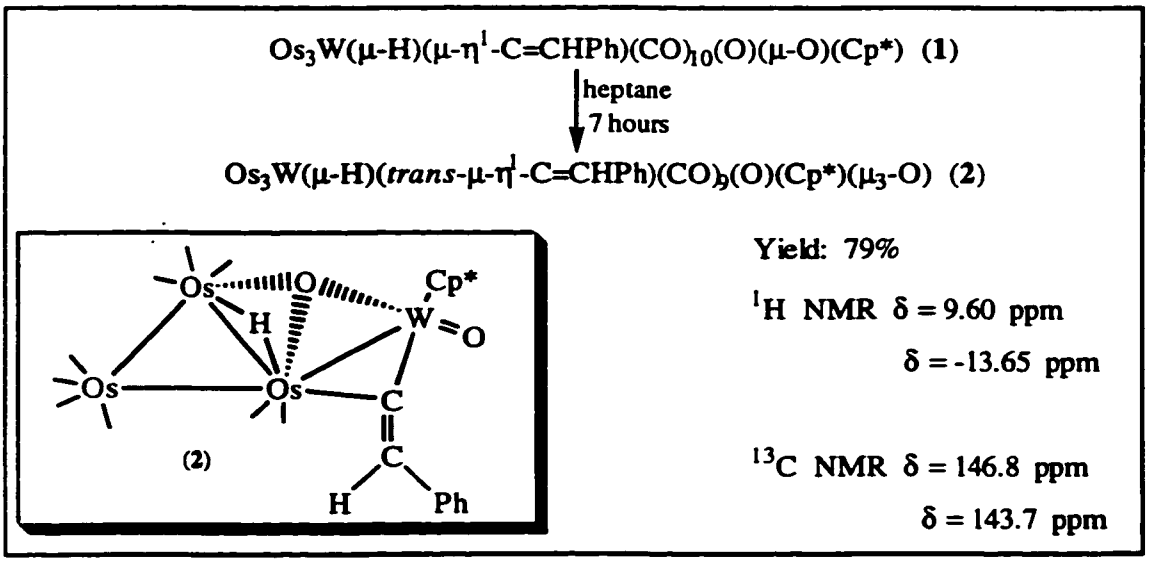

Scheme 2.5 The synthesis of [Os$_3$W(μ-H)(*trans*-μ-η^1-C=CHPh)(CO)$_9$(O)(Cp*)(μ_3-O)] **2**.

2.2.3.2 X-ray structure of 2

The red crystals of $[Os_3W(\mu\text{-}H)(trans\text{-}\mu\text{-}\eta^1\text{-}C{=}CHPh)(CO)_9(O)(Cp^*)(\mu_3\text{-}O)]$ (**2**) were studied crystallographically. The crystal structure of **2** is shown as an ORTEP plot in Figure 2.2. Selected structural parameters are listed in Table 2.3. The metal framework of **2** consists of a closed triangle of osmium atoms with a single tungsten atom spiked at Os(1). Within the Os_3 triangle, the three Os-Os bonds (Os(1)-Os(2) = 2.8139(5) Å, Os(1)-Os(3) = 2.8120(6) Å and Os(2)-Os(3) = 2.8373(6) Å) are of almost equal length. Cluster **2** has a total of nine terminal carbonyl groups distributed in the following manner: Os(1), two; Os(2), four; Os(3), three. The geometry about Os(1), Os(2) and Os(3) is distorted octahedral as indicated by the C-Os-C angles (C(10)-Os(1)-C(11) = 89.3(4)°; C(21)-Os(2)-C(22) = 95.5(4)°, C(20)-Os(2)-C(21) = 91.2(4)°, C(21)-Os(2)-C(23) = 166.0(4)°; C(30)-Os(3)-C(31) = 95.9(4)°, C(30)-Os(3)-C(32) = 91.1(4)°, C(31)-Os(3)-C(32) = 90.4(4)°). The parameters associated with the carbonyl ligands (Os-CO = 1.881(9) – 1.96(1) Å; C-O = 1.12(1) – 1.15(1) Å and Os-C-O = 171.69(8) – 179.7(9)°) are within the expected ranges.[20] Nonetheless, the presence of the triply bridging oxo ligand results in significant differences in the orientation of the carbonyl groups around the Os(3) atom. The μ_3-O ligand induces a rotation of the carbonyl ligands attached to Os(3) resulting in a staggered conformation compared to the carbonyl ligands of Os(2). The following dihedral angles (C(23)-Os(2)-Os(3)-O(1) = 42.2(7)°, C(22)-Os(2)-Os(3)-C(31) = 38.8(9)° and C(21)-Os(2)-Os(3)-C(32) = 43.6(8)°) suggest that carbonyl ligands on Os(3) are shifted from their respective positions on Os(2) by an average of 41.5(8)°.

A vinylidene ligand ($\mu\text{-}\eta^1\text{-}C{=}CHPh$) is sigma bonded to both the W and Os(1) atoms (W-C(1) = 2.024(8) Å, Os(1)-C(1) = 2.194(8) Å and C(1)-C(2) = 1.33(1) Å; Os(1)-C(1)-W = 80.0(3)°). A phenyl substituent present on the vinylidene ligand is located *trans* to the Os(1) atom as indicated by the dihedral angles of (W-C(1)-C(2)-C(3) = 169.7(2)° and Os(1)-C(1)-C(2)-C(3) = -4.1(7)°). The geometry of the vinylidene ligand of **2** is thus very similar to that of the parent cluster **1**.

The most important and striking feature of this cluster is the unexpected formation of a μ_3-O ligand which prior to this work was unprecedented for oxo ligands of a $[W(O)_2(Cp^*)]$ fragment. The μ_3-O ligand of **2** bridges the following three atoms: Os(1), Os(3) and W. The bond distances and angles associated with the $[Os_3W(\mu_3\text{-}O)]$ fraction are: W-O(1) = 1.959(5) Å; Os(1)-O(1) = 2.098(5) Å; Os(3)-O(1) = 2.158(5) Å; Os(1)-Os(2) = 2.8139(5) Å; Os(1)-Os(3) = 2.8120(6) Å; Os(2)-Os(3) = 2.8373(6) Å; Os(1)-O(1)-W = 83.9(2)° and Os(3)-O(1)-W = 118.8(2)°. The comparison of these structural features with those of the $[Os_3W(\mu\text{-}O)]$ fragment present in **1** reveals several important points. First, the μ_3-O ligand in **2** spans the shortest Os-Os bond, in keeping with the conclusion that μ-oxo ligands lead to a contraction of M-M bonds, as observed in **1**. Secondly, the W-Os(1) bond distance in **2** is shorter and the W-O(1)-Os(1) angle is smaller than in **1**. Finally, the triply bridging coordination mode of the oxo ligand has caused a lengthening of the W-O(1) bond length compared to that in **1** [**1**, 1.844(4) Å; **2**, 1.959(5) Å]. Conversely, the Os(1)-O(1) and Os(3)-O(1) bond distances present in **2** are similar to those found in **1** and also in other related clusters (Table 2.2).

The W-O(1) bond length of 1.959(5) Å in **1** resembles the predicted W-O single bond length of ≈ 1.98 Å (from *r*(W) 1.32 Å and *r*(O) 0.66 Å).[20] Nonetheless it also falls within the range expected for W-O bond lengths present in tungsten-alkoxide complexes, $[W(C_3Et_3)\{O\text{-}2,6\text{-}C_6H_3(i\text{-}Pr)_2\}_3]$ (W-O 1.885(6)-2.008(6) Å),[26] $[W(C_3Et_3)\{OCH(CF_3)_2\}_3]$ (W-O 1.93(1)-1.98(1) Å)[27] and $[W\{C(t\text{-}Bu)CHC(t\text{-}Bu)\}\{OCH(CF_3)_2\}_3]$ (W-O 1.954(7)-1.959(7) Å).[28] These latter complexes were found to possess some oxygen-tungsten π-donation which may indicate the presence of a tungsten-osmium double bond in complex **2**. Conversely, the Os-O bond distances are slightly longer than expected for a single bond (*r*(Os) + *r*(O) = 2.08 Å) and may be regarded as donor bond, i.e., O:→Os.[20] However the possibility that the Os(1)-O(1) linkage consist of a single bond may not be discarded.

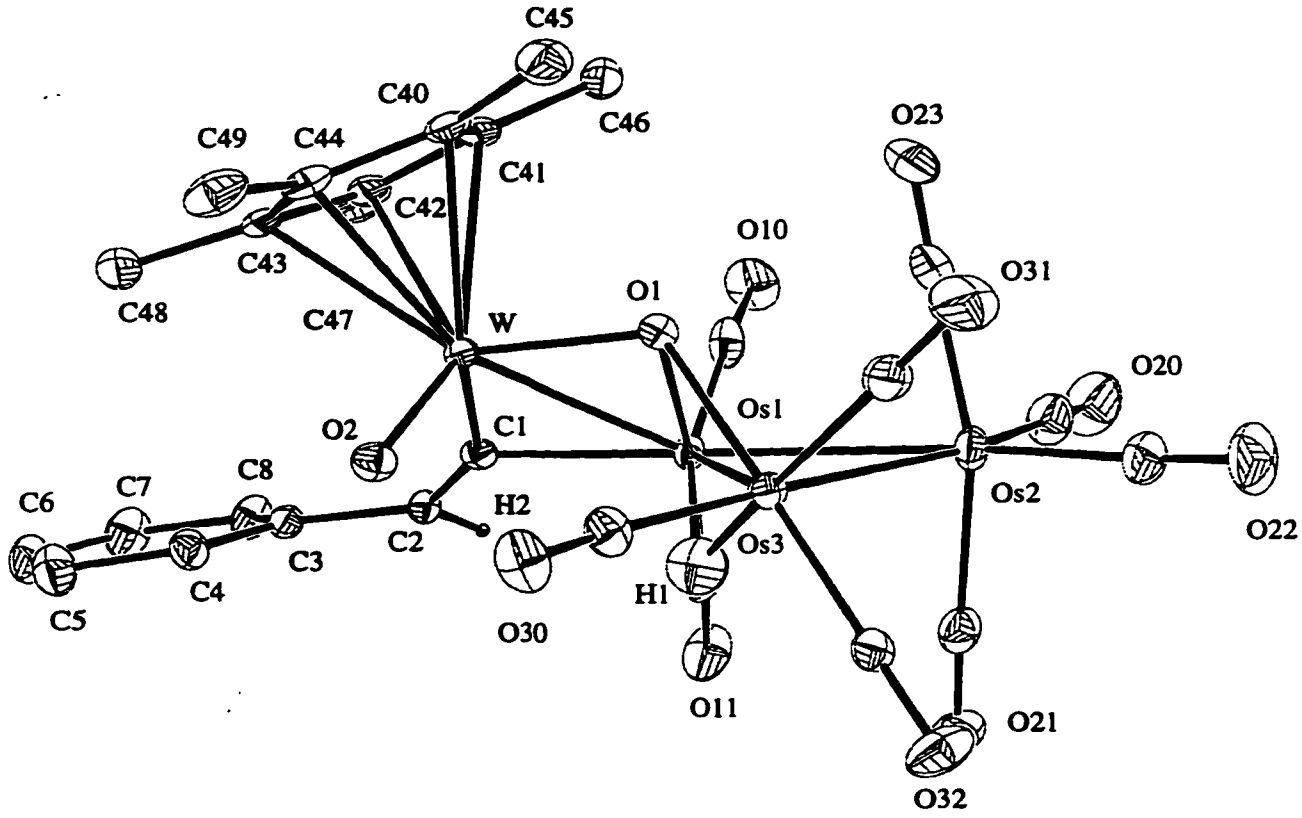

Figure 2.2 The structure of $[Os_3W(\mu\text{-}H)(\textit{trans}\text{-}\mu\text{-}\eta^1\text{-}C{=}CHPh)(CO)_9(O)(Cp^*)(\mu_3\text{-}O)]$ **2**.

Table 2.3 Selected bond lengths (Å) and angles (deg) for **2**.

		Lengths	
Os(2)-Os(3)	2.8373(6)	W-O(2)	1.721(5)
Os(2)-Os(1)	2.8139(5)	W-O(1)	1.959(5)
Os(3)-Os(1)	2.8120(6)	W-C(1)	2.024(8)
W-Os(1)	2.7129(5)	Os(1)-C(1)	2.194(8)
Os(1)-O(1)	2.098(5)	C(1)-C(2)	1.33(1)
Os(3)-O(1)	2.158(5)		
		Angles	
Os(2)-Os(1)-Os(3)	60.57(1)	O(1)-W-O(2)	109.2(2)
Os(1)-Os(2)-Os(3)	59.68(2)	Os(1)-C(1)-W	80.0(3)
Os(1)-Os(3)-Os(2)	59.75(1)	W-C(1)-C(2)	150.6(6)
Os(2)-Os(1)-W	131.32(2)	Os(1)-C(1)-C(2)	129.3(6)
Os(3)-Os(1)-W	79.80(1)	C(1)-C(2)-C(3)	127.3(8)
Os(1)-O(1)-W	83.9(2)	Os(2)-Os(1)-O(1)	85.7(2)
Os(3)-O(1)-W	118.8(2)	Os(3)-Os(1)-O(1)	49.6(1)

Therefore, we can interpret the bonding of the μ_3-oxo ligand in terms of either one of the following two descriptions. In the first instance, the oxide ligand is doubly bonded to the tungsten atom and donates a lone pair of electrons to both Os(1) and Os(3) as depicted in Figure 2.3(a). In this case the μ_3-O ligand acts as a six electron donor and **2** is electron precise with an overall 64 cluster valence electrons as expected for a spiked triangular core of metals.

An alternative description of the bonding of the oxo ligand to the three metal atoms is illustrated in Figure 2.3(b). In this instance the oxide ligand is a 4 electron donor contributing one electron to tungsten, one to Os(1) and having a 2 electron donor acceptor linkage to Os(2). Using this description, **2** is electron deficient by two electrons with an overall 62 cluster valence electrons.

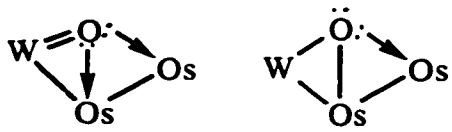

(a) (b)

Figure 2.3 Bonding interaction in $[Os_2W(\mu_3\text{-}O)]$.

It is emphasized that both descriptions of the bonding mode of the oxo ligand are formalized representations. Complex **2** illustrates the difficulties that may be encountered in formal cluster valence electron counting. Hence the μ_3-O ligand in **2** may be formally regarded as either a four or a six electron donor. The ambiguities encountered in the formal electron count of **2** are also found in the other clusters containing a triply bridging oxo ligand prepared during this study. In no case does the structural details provide a clear distinction between the interpretations of the oxo bonding modes. For convenience, the μ_3-O ligand is regarded as a six electron donor, resulting in electron precise clusters throughout the remainder of this thesis.

Both the electron count and the ^{1}H NMR spectra suggested the presence of a bridging hydride on the metal cluster. The position of the bridging hydride was determined using the

XHYDEX program of Orpen.[29] The optimized hydride positions are calculated from the structural parameters of non-hydrogen atoms by minimizing the potential energy function defined by intra-molecular interactions between postulated hydride positions and other non-bonded atoms, subject to bond length constraints. On this basis, the hydride ligand detected by NMR was calculated to lie in an asymmetric fashion on the Os(1)-Os(3) vector. The bond distances obtained (Os(1)-H(1) = 1.8548(4) Å and Os(3)-H(1) = 1.6082(4) Å) are similar to those found from a difference map in **1** (Os(1)-H(1) = 1.84(6) Å and Os(2)-H(1) = 1.62(7) Å). Figure 2.2 suggests that the hydride is located opposite to the triply bridging oxo ligand when the plane defined by Os(1), Os(2) and Os(3) is taken as reference. In complex **2** the expansion of the metal-metal bond that may be expected due to the presence of the bridging hydride ligand is counteracted by the contraction associated with the presence of the bridging oxo ligand on the Os(1)-Os(3) vector. However, an enlargement of the Os-Os-C(O) angles in **2** was observed. The largest Os-Os-C(O) angle in **2** is Os(1)-Os(3)-C(30) = 117.2(3)° compared to Os(3)-Os(2)-C(22) = 98.1(3)° and Os(1)-Os(2)-C(20) = 104.0(3)°. This may be further evidence of the presence of a bridging hydride ligand on the Os(1)-Os(3) bond. The exact contribution of the hydride ligand to the enlargement of the Os(1)-Os(3)-C(30) angle is unknown due to the presence of a μ_3-O ligand on the same M-M bond.

2.2.4 Synthesis of [$Os_3W(\mu\text{-}H)(cis\text{-}\mu\text{-}\eta^1\text{-}C{=}CHPh)(CO)_9(O)(Cp^*)(\mu_3\text{-}O)$] 3

When a hexane solution of **2** was exposed to light at room temperature for 15 hours a color change from red to orange occurred (Scheme 2.6). Orange crystals of [$Os_3W(\mu\text{-}H)(cis\text{-}\mu\text{-}\eta^1\text{-}C{=}CHPh)(CO)_9(O)(Cp^*)(\mu_3\text{-}O)$] (**3**) were obtained from slow evaporation of a 1/1 CH_2Cl_2/hexane mixture at room temperature in 70% yield.

2.2.4.1 Spectroscopic features of 3

The infrared spectrum showed the characteristic terminal carbonyl stretching bands at 2094 (m), 2057 (vs), 2022 (s), 2013 (m), 2006 (m), 1998 (m), 1980 (w) and 1959 (w) cm^{-1}. The symmetry of the terminal carbonyl absorptions implies a structure similar to **2**. The anticipated resonances for the Cp* and Ph ligands were located in the ^1H and ^{13}C NMR

spectra of **3**. The ^{1}H NMR spectrum of **3** exhibited two resonances (δ 9.66 and −14.11) similar to those of the parent cluster **2** indicating the retention of the hydride and vinylidene protons. The ^{13}C NMR spectrum showed two peaks at δ 145.8 and 143.5 present in the parent compound and characteristic of a vinylidene fragment, in addition to resonances between δ 185.7 and 174.8 for CO groups. Retention of the molecular mass on going from **2** to **3** was indicated by the observation of a molecular ion at *m/z* 1277 in the FAB mass spectrum. Hence a complex bearing strong structural similarities to **2** was expected.

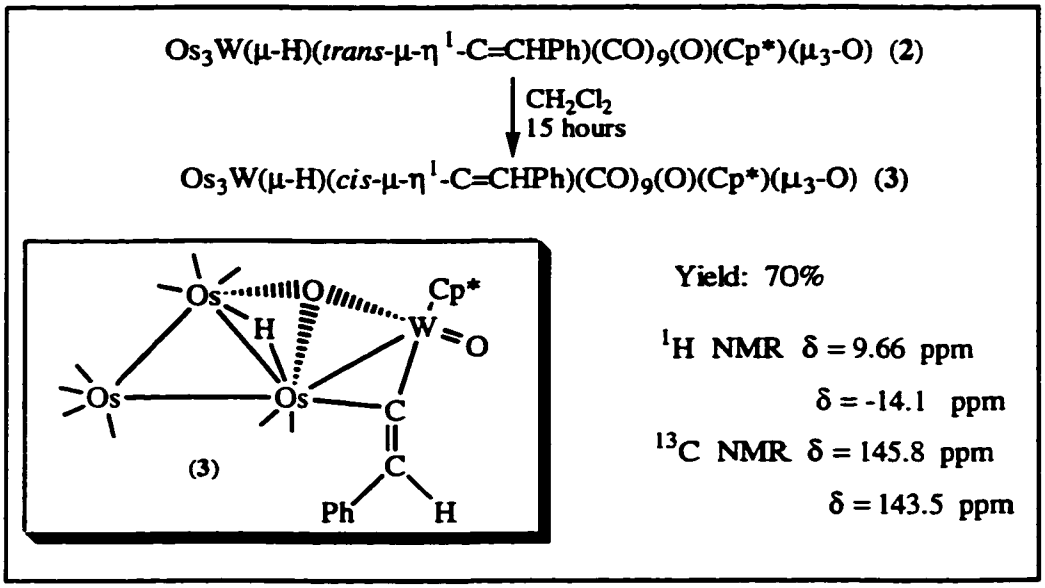

Scheme 2.6 The synthesis of [$Os_3W(\mu\text{-}H)(cis\text{-}\mu\text{-}\eta^1\text{-}C{=}CHPh)(CO)_9(O)(Cp^*)(\mu_3\text{-}O)$] **3**.

2.2.4.2 X-ray analysis of 3

An X-ray crystal structure study was undertaken in order to determine the main differences between cluster **2** and **3**. The ORTEP plot of compound **3** is shown in Figure 2.4 and selected bond lengths and angles are summarized in Table 2.4. Figure 2.4 illustrates a metal framework essentially identical to that of **2**. Hence **3** consists of a triangle of osmium atoms with one tungsten atom bonded to Os(1). The Os-Os bond distances (Os(1)-Os(2) = 2.8296(8) Å, Os(1)-Os(3) = 2.8031(9) Å and Os(2)-Os(3) = 2.8322(9) Å) and the carbonyl distributions are similar to the parent cluster **2**. The μ_3-O ligand of **3** also induces a rotation of the carbonyl ligands about Os(3) resulting in a staggered conformation relative to the

disposition of CO ligands about Os(2). A study of the dihedral angles indicated a shifting of the carbonyl ligands on Os(3) from their respective positions on Os(2) by an average of 40(1)° (C(20)-Os(2)-Os(3)-O(1) = 44.6(8)°, C(21)-Os(2)-Os(3)-C(31) = 35(1)° and C(22)-Os(2)-Os(3)-C(32) = 39(1)°). This value strongly resembles the one obtained for **2** (41.5(8)°).

An oxo ligand caps a face by linking the Os(1), Os(3) and W atoms (vide infra). The two osmium-oxygen bond distances are similar (Os(1)-O(1) = 2.113(9) Å and Os(3)-O(1) = 2.163(9) Å) and may be regarded as a lone pair donation from the oxygen to the osmium atoms. The W-O(1) bond length in **3** is 1.966(9) Å which resembles that of **2**, and may be considered as a W-O double bond. Also characteristic of a μ_3-O ligand on a WOs_3 metal framework is the induced contraction of the Os(1)-Os(3) vector compared with the other Os-Os bond distances of cluster **3**. The μ_3-O ligand contributes six electrons to the expected 64 outer valence electrons cluster.

The XHYDEX program[29] provided the location of a bridging hydride between the Os(1) and Os(3) atoms (Os(1)-H(1) = 1.8535(6) Å and Os(3)-H(1) = 1.6082(6) Å), which was similar to the location of the hydride ligand on **2**. The presence of a bridging hydride on cluster **3** was supported by the electron count and a ^1H resonance in the hydride region. Furthermore, the Os-Os-C(O) angles agreed with the calculated position as the Os(1)-Os(3)-C(30) angle was the largest (Os(1)-Os(2)-C(23) = 97.6(5)°, Os(3)-Os(2)-C(21) = 104.7(5)° and Os(1)-Os(3)-C(30) = 117.0(5)°).

The major difference between complexes **2** and **3** resides in the stereochemistry of the vinylidene ligand. A vinylidene ligand [C(1)=C(2)] bridges the W-Os(1) vector in a μ-η^1 fashion (W-C(1) = 2.05(2) Å, Os(1)-C(1) = 2.16(1) and C(1)-C(2) = 1.29(2) Å) in **3**. A phenyl substituent of the vinylidene ligand is located *cis* to Os(1) with dihedral angles of W-C(1)-C(2)-C(3) = -176(3)° and Os(1)-C(1)-C(2)-C(3) = -11(1). Hence, the *trans*-vinylidene ligand of complex **2** undergoes a facile rotation along the C(1)=C(2) axis leading to the formation of the *cis* isomer **3**.

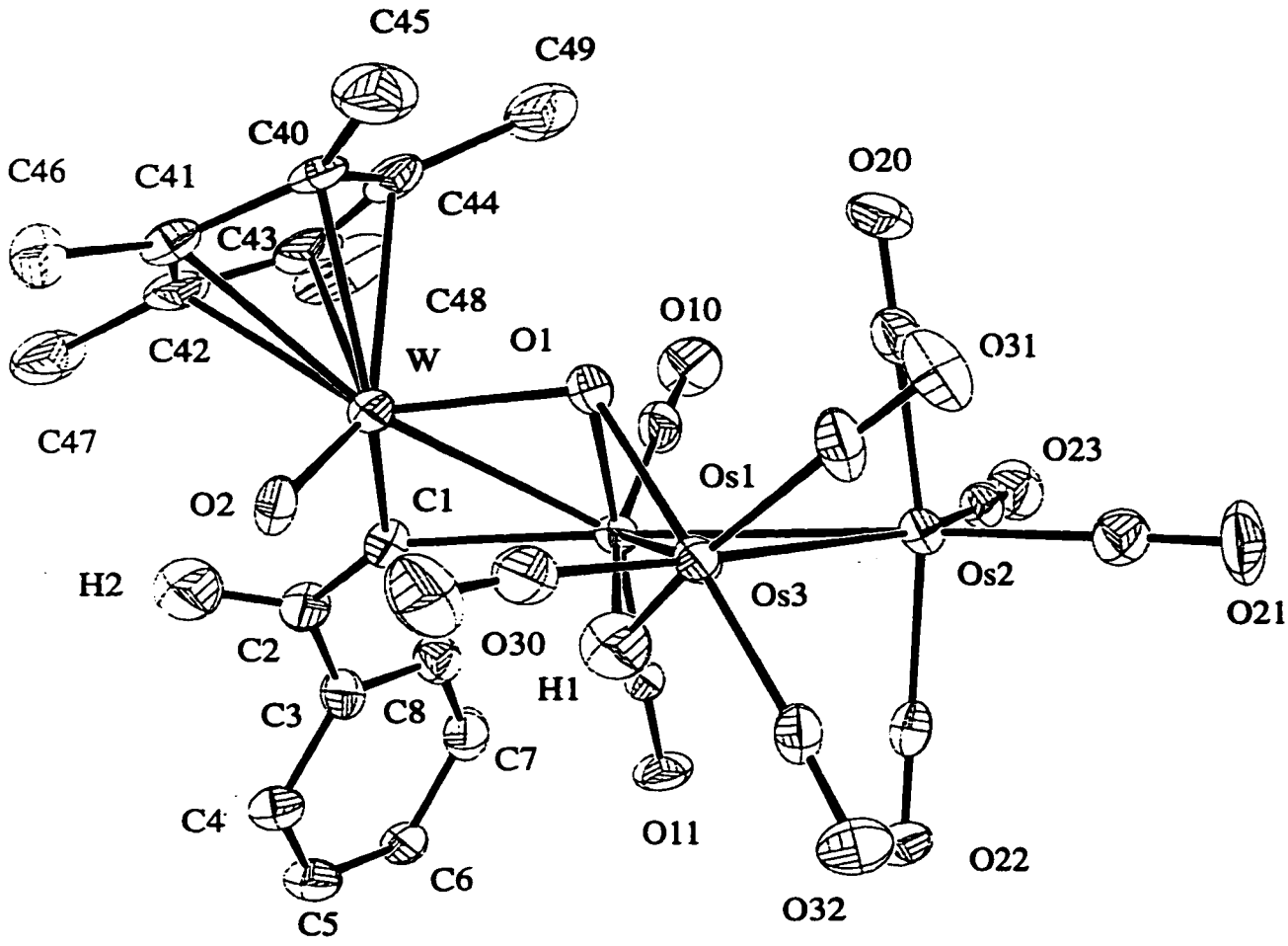

Figure 2.4 The molecular structure of $[Os_3W(\mu\text{-}H)(cis\text{-}\mu\text{-}\eta^1\text{-}C{=}CHPh)(CO)_9(O)(Cp^*)(\mu_3\text{-}O)]$ **3**.

Table 2.4 Selected bond lengths (Å) and angles (deg) for **3**.

		Lengths	
Os(2)-Os(3)	2.8322(9)	W-O(2)	1.70(1)
Os(2)-Os(1)	2.8296(8)	W-O(1)	1.966(9)
Os(3)-Os(1)	2.8031(9)	W-C(1)	2.05(2)
W-Os(1)	2.7123(9)	Os(1)-C(1)	2.16(1)
Os(1)-O(1)	2.113(9)	C(1)-C(2)	1.29(2)
Os(3)-O(1)	2.163(9)		
		Angles	
Os(2)-Os(1)-Os(3)	60.37(2)	O(1)-W-O(2)	107.9(4)
Os(1)-Os(2)-Os(3)	59.35(2)	Os(1)-C(1)-W	80.2(5)
Os(1)-Os(3)-Os(2)	60.28(2)	W-C(1)-C(2)	139(1)
Os(2)-Os(1)-W	130.13(3)	Os(1)-C(1)-C(2)	140(1)
Os(3)-Os(1)-W	79.66(3)	C(1)-C(2)-C(3)	129(2)
Os(1)-O(1)-W	83.3(3)	Os(2)-Os(1)-O(1)	84.3(2)
Os(3)-O(1)-W	117.6(4)	Os(3)-Os(1)-O(1)	49.8(2)

2.2.5 Synthesis of $[Os_3W(CO)_{10}(O)(\mu\text{-}\eta^1,\eta^2\text{-}CH{=}CHPh\{W\text{-}Os\})(\mu\text{-}O)(Cp^*)]$ 4

Complex **1** was found to be extremely light sensitive in solution. Exposure of a hexane solution of **1** to light at room temperature for 12 hours resulted in a color change from orange to red. Red crystals of $[Os_3W(CO)_{10}(O)(\mu\text{-}\eta^1,\eta^2\text{-}CH{=}CHPh\{W\text{-}Os\})(\mu\text{-}O)(Cp^*)]$ (**4**) were obtained from slow evaporation of a 1/1 CH_2Cl_2/hexane mixture at room temperature in 87% yield (Scheme 2.7).

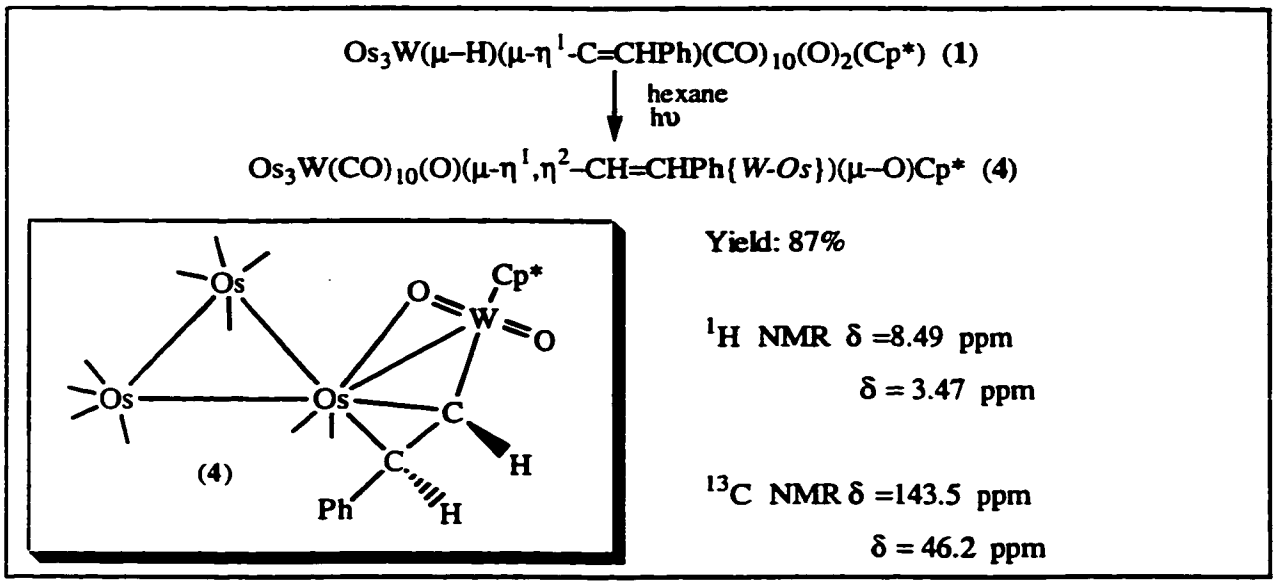

Scheme 2.7 The synthesis of $[Os_3W(CO)_{10}(O)(\mu\text{-}\eta^1,\eta^2\text{-}CH{=}CHPh\{W\text{-}Os\})(\mu\text{-}O)(Cp^*)]$ **4**.

2.2.5.1 Spectroscopic features of 4

The infrared spectrum of the crystalline compound **4** showed terminal carbonyl stretching bands at 2112 (m), 2064 (m), 2036 (vs), 2013 (m), 2003 (w), 1983 (vw), 1971 (vw) and 1943 (vw) cm^{-1}. A molecular ion at *m/z* 1305 in the FAB mass spectrum was observed, indicating that both complexes **1** and **4** had the same molecular weight. The ^1H and ^{13}C NMR spectra contained the anticipated resonances for the Ph and Cp* ligands. In addition, the ^1H NMR spectrum indicated the absence of hydride signals and the presence of two doublets (δ 8.49 and 3.47 ppm (J = 12 Hz)) in the olefinic region. The ^{13}C NMR spectrum was characterized by two signals at δ 143.5 and 46.2. The shifting of one highfield signal present in complex **1** to 46.2 suggested the transformation of the vinylidene ligand. An X-ray structural analysis provided full details of the molecular structure.

2.2.5.2 X-ray analysis of 4

The molecular structure of complex **4** is illustrated in Figure 2.5 and selected bond lengths and angles are summarized in Table 2.5. The metal framework of **4** like that of **1**, **2** and **3** above, consists of a triangle of osmium atoms with one tungsten atom bonded to Os(1). Like complex **1**, the Os(2) and Os(3) atoms carry four carbonyl groups while Os(1) has two CO groups in the usual octahedral conformation. The three Os-Os bonds assembling the Os_3 triangle (Os(1)-Os(2) = 2.8529(5) Å, Os(1)-Os(3) = 2.8660(5) Å and Os(2)-Os(3) = 2.8664(7) Å) are almost of equal length and again typical of values associated with a single Os-Os bond. Clearly the molecular geometry of **4** resembles that of the precursor **1**, but in contrast to **1** there is no elongated Os-Os bond. This is additional evidence (vide infra) for the transfer of a bridging hydride from an Os-Os bond onto the vinylidene group present in **1**.

The vinyl ligand is linked to both the W and Os(1) atoms via a σ-bond to tungsten and a π-interaction with Os(1). Key bond lengths are: W-C(1) = 2.053(8) Å, Os(1)-C(1) = 2.217(8) Å and Os(1)-C(2) = 2.302(9) Å. A useful indication of the strength of olefin-metal bonding is provided by the "bent-back" angles at C(1) and C(2). It is known that C=C ligands can form metallocycle or π-donor type adducts. In the case where the vinyl ligand is involved in a π-donor type interaction, the vinyl group retains appreciable double-bond character with sp^2 hybridized carbons (Scheme 2.8).[30] To the contrary, metallocycles are characterized by: 1) C-C bond distances approaching those of normal C-C single bonds, and 2) near sp^3 hybridization of the carbon atoms attached to the metal (Scheme 2.8).[30] Nonetheless, the metallocycle view and the π-donor view are not mutually exclusive but rather complementary, with a smooth gradation of one description into the other. In complex **4**, the angles W-C(1)-C(2) = 116.3(6)° and C(1)-C(2)-C(3) = 123.8(8)° suggest a simple coordination of the vinyl ligand to the Os(1) atom. The η^2-coordination weakens the π bonding in the vinyl group due to back-donation from the metal into antibonding orbitals on the olefin resulting in the elongation of the C(1)-C(2) double bond (1.45(1) Å).[30]

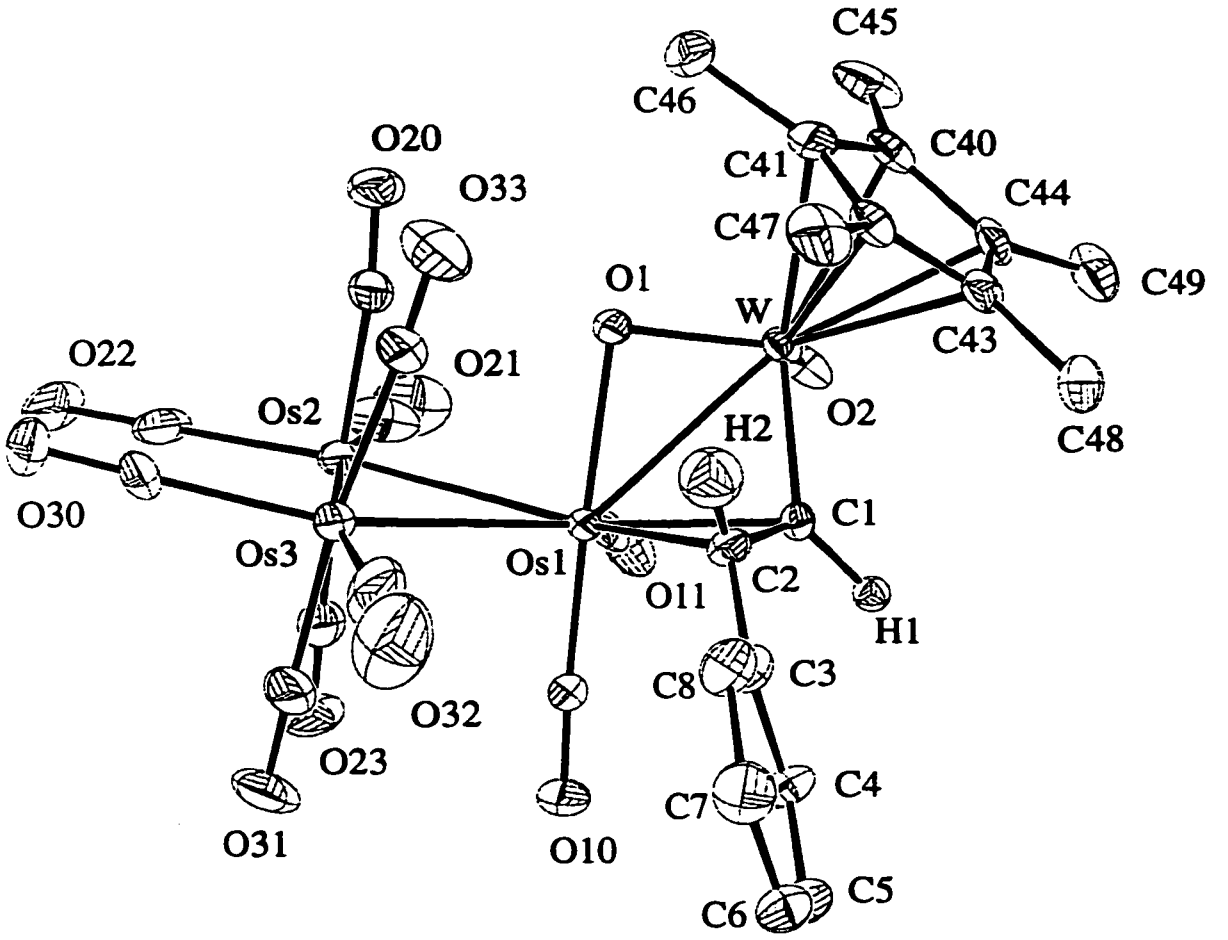

Figure 2.5 The molecular structure of $[Os_3W(CO)_{10}(O)(\mu\text{-}\eta^1,\eta^2\text{-}CH{=}CHPh\{W\text{-}Os\})(\mu\text{-}O)(Cp^*)]$ **4**.

Table 2.5 Selected bond lengths (Å) and angles (deg) for **4**.

Lengths			
Os(2)-Os(3)	2.8664(7)	W-O(1)	1.817(5)
Os(1)-Os(2)	2.8529(5)	W-C(1)	2.053(8)
Os(1)-Os(3)	2.8660(5)	Os(1)-C(1)	2.217(8)
W-Os(1)	2.8257(4)	Os(1)-C(2)	2.302(9)
Os(1)-O(1)	2.167(5)	C(1)-C(2)	1.45(1)
W-O(2)	1.714(6)		
Angles			
Os(2)-Os(1)-Os(3)	60.16(2)	Os(1)-C(1)-W	82.8(3)
Os(1)-Os(2)-Os(3)	60.15(1)	W-C(1)-C(2)	116.3(6)
Os(1)-Os(3)-Os(2)	59.69(1)	Os(1)-C(1)-C(2)	74.5(5)
Os(2)-Os(1)-W	114.94(2)	Os(1)-C(2)-C(1)	68.1(5)
Os(3)-Os(1)-W	128.19(2)	C(1)-C(2)-C(3)	123.8(8)
Os(1)-O(1)-W	89.9(2)	Os(2)-Os(1)-O(1)	84.4(2)
O(1)-W-O(2)	115.0(3)	Os(3)-Os(1)-O(1)	91.3(2)

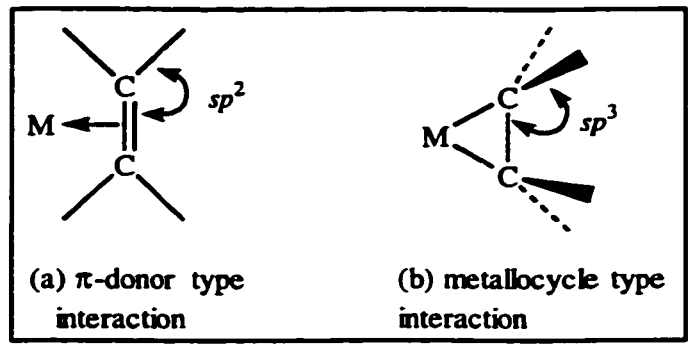

(a) π-donor type interaction (b) metallocycle type interaction

Scheme 2.8 Possible interactions in compounds with C=C bonds.

The bridging mode of the oxo ligand (W-O(1) = 1.817(5) Å, Os(1)-O(1) = 2.167(5) Å; Os(1)-O(1)-W = 89.9(2)°) is very similar to that in complex **1** and best described as a W=O:→Os interaction. The presence of a bridging μ-η^1,η^2-CH=CHPh ligand on the W-Os vector bridged by the oxo ligand also leads to a shortening of the W-Os bond distance and a smaller W-O-Os angle compared to some previously characterized complexes described in Table 2.2.

Such *trans* hydrogenations of acetylide ligands in heterometallic carbonyl clusters have only recently been reported in the literature. For example $[Re_2W(\mu\text{-}H)_2(CO)_6(\mu\text{-}O)(C{\equiv}CPh)(Cp^*)]$ underwent a migration of both H ligands to give a complex with a *trans*, edge-bridging vinyl fragment, $[Re_2W(CO)_8(O)(\mu\text{-}CH{=}CHPh)(Cp^*)]$.[31] The net result resembles the formal addition of H_2 to C≡CPh. However the isolation and characterization of complexes **1** and **4** represents the first sequential addition of hydrogen atoms across an alkynyl triple bond in a mixed-metal oxo cluster. Furthermore the photo-induced transfer of a single hydride from the metal framework to a bridging vinylidene resulting in the formation of a bridging vinyl ligand is unprecedented in cluster chemistry.

Finally, complex **4** is electron precise with an overall 64 cluster valence electrons as expected for a spiked triangular metal framework (three osmium atoms provided 24 electrons; one tungsten atom, 6 electrons; ten terminal carbonyl ligands, 20 electrons; one

Cp* ligand; 5 electrons, one μ-η^1,η^2-CH=CHPh ligand, 3 electrons; one μ-O, 4 electrons and one terminal oxo, 2 electrons).

2.2.6 Deuterium labeling experiments

This proposed sequential addition of H_2 was further supported by D_2 labeling experiments. Treatment of $[W(C{\equiv}CPh)(O)_2(Cp^*)]$ with $[D_2Os_3(CO)_{10}]$ in the dark afforded both of the labeled complexes $[Os_3W(\mu\text{-}D)(\mu\text{-}\eta^1\text{-}C{=}CDPh)(CO)_{10}(O)(\mu\text{-}O)(Cp^*)]$ (**1d**) (24%) and $[Os_3W(CO)_{10}(O)(\mu\text{-}\eta^1,\eta^2\text{-}CD{=}CDPh\{W\text{-}Os\})(\mu\text{-}O)(Cp^*)]$ (**4d**) (27%). The appearance of both the vinylidene and the vinyl complexes as products of the thermolysis was surprising, considering the specificity previously observed for the non-deuterated complex. This chemical behavior may be due to the inverse isotope effect (either kinetic or equilibrium) which should favor the C-D vs Os-D-Os bonds relatively more than C-H vs Os-H-Os bonds.[32]

2.2.6.1 Spectroscopic features of 1d and 4d

The ^2H NMR spectrum of complex **1d** gave two resonances at δ 9.32 and –18.03 which were very similar to observed chemical shifts in the ^1H NMR spectrum of complex **1** (Table 2.6). The ^1H NMR spectrum of **1d** showed the additional expected resonances for the Cp* and Ph ligands. Thus, this experiment suggested the incorporation of deuterium atoms in both the hydride site and the hydrogen site of the vinylidene ligand of complex **1d**. Similarly, the ^2H NMR spectrum of complex **4d** exhibited two peaks with chemical shifts comparable to those present in the ^1H NMR spectrum of complex **4** (Table 2.6), but broadened by nuclear quadrupole effects due to the moderate quadrupole moment of deuterium atoms (I = 1). The remaining resonances for the Cp* and Ph ligands were located in the ^1H NMR spectrum of complex **4d**. Hence, the spectroscopic data indicated the presence of two deuterium atoms on the vinyl ligand of complex **4d**.

Table 2.6 Comparison of the ^1H and ^2H chemical shifts for complexes **1** and **4**.

Complex	Non-deuterated	Deuterated
1	9.27 (1H, s)	9.32 (1H, s)
	-18.01 (1H, s)	-18.03 (1H, s)
4	8.49 (1H, d, J_{H-H} = 12 Hz)	8.56 (1H, s)
	3.47 (1H, d, J_{H-H} = 12 Hz)	3.49 (1H, s)

The above observations imply that 1) the first deuterium atom is transferred from $[D_2Os_3(CO)_{10}]$ to the acetylide ligand resulting in the formation of a bridging vinylidene ligand in complex **1d** and 2) the remaining deuterium atom present on the metal cluster of complex **1d** is transferred to the vinylidene ligand resulting in the formation of a vinyl ligand in complex **4d**. Hence, we conclude that the metal cluster acts as the source of hydrogen atoms in the described transformations.

2.3 Conclusions

The reaction of the electronically unsaturated hydride $[H_2Os_3(CO)_{10}]$ with $[W(C{\equiv}CPh)(O)_2(Cp^*)]$ has provided a μ-oxo, μ-hydrido, μ-vinylidene cluster **1** via a process involving acetylide and oxide coordination to the Os_3 framework and transfer of a hydride ligand to the unsaturated hydrocarbyl. Cluster **1** underwent remarkably selective transformation under photolytic and thermal conditions to afford the first example of both a triply oxo-bridged tungsten-osmium μ-vinylidene complex **2** and an oxo-bridged tungsten-osmium μ-η^1,η^2-vinyl complex **4**.

Intramolecular hydrogen transfer from the low oxidation state metal cluster framework to the hydrocarbyl fragment was observed. The isolation of both the μ-vinylidene **1** and the μ-vinyl **4**, represented the first structurally characterized step-wise transfer of hydride from $[H_2Os_3(CO)_{10}]$ to a metal substituted acetylene. The ability of photons to selectively induce hydrogen transfer from a metal cluster to a vinylidene ligand was also notable. There was no discernible evidence in these experiments that hydrogen transfer from

a bridging site between two late metals onto an oxygen bridge was an intermediate step in such a hydrogenation process. Thus if the mixed metal oxo cluster is a model for hydrogenation on an oxide supported late metal catalyst, the results here suggest that the oxide ligands play an innocent role in the process.

Furthermore, this reaction demonstrated the ability of the oxide group to coordinate to a low oxidation state osmium center as a μ-O (WOs) (4 electron) or μ_3-O (WOs_2) (6 electron) ligand. This property could be viewed as an activating step in a hydrogenation sequence on a supported cluster. Hence, the oxide ligand may be capable of providing an additional lone pair to the metal framework in order to compensate for the loss of a two electron ligand which in this case was a carbonyl ligand.

Finally, this reaction provided new examples of early-late oxide bridged organometallic clusters. It also granted further evidence of the efficiency of metal oxo acetylides as precursors to form new oxo bridged mixed metal cluster complexes.

2.4 Experimental section

2.4.1 Reaction of $[H_2Os_3(CO)_{10}]$ with $[W(C{\equiv}CPh)(O)_2(Cp^*)]$ in the absence of light

The cluster $[H_2Os_3(CO)_{10}]$ (200 mg, 0.23 mmol) and $[W(C{\equiv}CPh)(O)_2(Cp^*)]$ (125 mg, 0.28 mmol) were placed into a three-neck flask equipped with a water cooled condenser and dissolved in dry dichloromethane (50 mL) in the dark. The solution was heated at 38°C for four days over which time the solution turned to an orange color. The solvent was dried *in vacuo* in the dark and the red solid residue dissolved in the minimum amount of CH_2Cl_2. One major compound was separated via thin layer chromatography in air in the dark by first eluting the starting material with pure hexane and the compound **1** with a mixture of 71/25/4 hexane/THF/CH_2Cl_2. The compounds were, in order of elution $[H_2Os_3(CO)_{10}]$ (16 mg, 0.035 mmol, 5%) and $[Os_3W(\mu\text{-}H)(\mu\text{-}\eta^1\text{-}C{=}CHPh)(CO)_{10}(O)(\mu\text{-}O)(Cp^*)]$ **1** (218 mg, 0.17 mmol, 67%). Spectral data for $[Os_3W(\mu\text{-}H)(\mu\text{-}\eta^1\text{-}C{=}CHPh)(CO)_{10}(O)(\mu\text{-}O)(Cp^*)]$ **1**: IR (hexane):

ν(CO) 2132 (w); 2078 (vs); 2060 (s); 2049 (vs); 2029 (m); 2018 (m); 2005 (m); 1998 (m); 1982 (w); 1944 (w). ^{1}H NMR ($CDCl_3$) δ: 9.27 (1H, s); 7.74 (2H, d, J_{H-H} = 7.47 Hz); 7.42 (2H, dd, J_{H-H} = 7.47 Hz, J_{H-H} = 7.22 Hz); 7.33 (1H, d, J_{H-H} = 7.22 Hz); 1.90 (15H, s); -18.01 (1H, s). ^{13}C {^{1}H} NMR ($CDCl_3$) δ: 148.0 (1C, s, C=*C*HPh); 144.2 (1C, s, *C*=CHPh); 128.8 (3C, s, Ph); 128.5 (2C, s, Ph); 127.5 (1C, s, Ph); 116.7 (5C, s, C_5Me_5); 11.2 (5C, s, C_5Me_5). FAB-MS (*m/z*): 1305, $[M]^+$; 1277-1025, $[M-nCO]^+$ (n = 1-10). Anal. Calcd. for **1**: C, 25.77; H, 1.70. Found C, 25.87; H, 1.71%.

2.4.2 Thermolysis of $[Os_3W(\mu\text{-}H)(\mu\text{-}\eta^1\text{-}C{=}CHPh)(CO)_{10}(O)(\mu\text{-}O)(Cp^*)]$ 1

A sample (35 mg, 0.027 mmol) of **1** was dissolved in dry heptane (50 mL) and heated at 100°C in the dark. The reaction progressed with a color change from orange to red. After seven hours of heating, the solution was cooled and the solvent removed *in vacuo*. Separation of the reaction mixture was carried out via thin layer chromatography (eluant: CH_2Cl_2/hexane, 50/50). The first band was identified as $[Os_3W(\mu\text{-}H)(\textit{trans}\text{-}\mu\text{-}\eta^1\text{-}C{=}CHPh)(CO)_9(O)(Cp^*)(\mu_3\text{-}O)]$ **2** (27 mg, 0.020 mmol, 74%). This was followed by $[Os_3W(\mu\text{-}H)(\textit{cis}\text{-}\mu\text{-}\eta^1\text{-}C{=}CHPh)(CO)_9(O)(Cp^*)(\mu_3\text{-}O)]$ **3** (4 mg, 0.003 mmol, 11%) and, finally unreacted $[Os_3W(\mu\text{-}H)(\mu\text{-}\eta^1\text{-}C{=}CHPh)(CO)_{10}(O)(\mu\text{-}O)(Cp^*)]$ **1** (7 mg, 0.005 mmol, 14%). Spectral data for **2**: IR (hexane): υ(CO) 2093 (m); 2056 (vs); 2031 (w); 2017 (vs); 2012 (s); 2005 (m); 1997 (m); 1980 (w); 1959 (w). ^{1}H NMR ($CDCl_3$) δ: 9.60 (1H, s); 7.63 (2H, d, J_{H-H} = 7.43 Hz); 7.42 (2H, m); 7.36 (1H, m); 1.94 (15H, s); -13.65 (1H, s). ^{13}C {^{1}H} NMR ($CDCl_3$) δ: 242.6 (1C, s, CO); 187.9 (1C, s, CO); 185.9 (1C, s, CO); 182.6 (1C, s, CO); 179.4 (1C, s, CO); 176.5 (1C, s, CO); 176.1 (1C, s, CO); 174.7 (1C, s, CO); 174.6 (1C, s, CO); 146.8 (1C, s, C=*C*HPh); 143.7 (1C, s, *C*=CHPh); 129.0 (3C, s, Ph); 128.7 (2C, s, Ph); 127.8 (1C, s, Ph); 117.9 (5C, s, C_5Me_5); 11.3 (5C, s, C_5Me_5). FAB-MS (*m/z*): 1277, $[M]^+$; 1221-1053, $[M-nCO]^+$ (n = 2-8). Anal. Calcd. for **2**: C, 25.40; H, 1.74. Found: C, 25.11; H, 1.46%. Spectral data for **3**: IR (hexane): υ(CO) 2094 (m); 2057 (vs); 2022 (s); 2013 (m); 2006 (m); 1998 (m); 1980 (w); 1959 (w). ^{1}H NMR ($CDCl_3$) δ: 9.66 (1H, s); 7.65 (2H, d, J_{H-H} = 7.49 Hz); 7.50 (2H, m); 7.40 (1H, m); 2.14 (15H, s); -14.11 (1H, s). ^{13}C {^{1}H} NMR ($CDCl_3$) δ: 185.7 (1C, s, CO); 184.6 (1C, s, CO); 182.4 (1C, s, CO); 179.3 (1C, s, CO); 176.1 (1C, s, CO); 175.9 (1C, s, CO); 175.5 (1C, s, CO); 175.1 (1C, s, CO); 174.8 (1C, s, CO);

145.8 (1C, s, C=*C*HPh); 143.5 (1C, s, *C*=CHPh); 128.9 (3C, s, Ph); 128.8 (2C, s, Ph); 128.0 (1C, s, Ph); 116.4 (5C, s, C_5Me_5); 10.8 (5C, s, C_5Me_5). FAB-MS (*m/z*): 1277, $[M]^+$; 1221-1053, $[M\text{-}nCO]^+$ (n = 2-8). Anal. Calcd. for **3**: C, 25.11; H, 1.46. Found: C, 25.29; H, 1.79%.

2.4.3 Photolysis of $[Os_3W(\mu\text{-}H)(trans\text{-}\mu\text{-}\eta^1\text{-}C{=}CHPh)(CO)_9(O)(Cp^*)(\mu_3\text{-}O)]$ 2

A sample of **2** (30 mg, 0.023 mmol) was dissolved in dry dichloromethane (15 mL). The reaction vessel was placed in the presence of a 60 W incandescent light source for 15 hours. The solvent was removed under reduced pressure and the red residue dissolved in CH_2Cl_2 and separated by thin layer chromatography (eluant: CH_2Cl_2/hexane, 50/50). The first band isolated was unreacted **2** (8 mg, 0.006 mmol, 26%) and the second fraction was identified as **3** (20 mg, 0.016 mmol, 70%).

2.4.4 Photolysis of $[Os_3W(\mu\text{-}H)(\mu\text{-}\eta^1\text{-}C{=}CHPh)(CO)_{10}(O)(\mu\text{-}O)(Cp^*)]$ 1

A solution of **1** (23 mg, 0.018 mmol) in CH_2Cl_2 (15 mL) was placed in the presence of a 60 W tungsten incandescent light source for 12 hours. The solvent was removed under reduced pressure, yielding a red residue. This residue was dissolved in the minimum of dichloromethane, and purified by chromatography on silica gel plates eluting with hexane/THF/CH_2Cl_2 (71/25/4). The first band was unreacted **1** (2 mg, 0.002 mmol, 8.7%). The following fraction was identified as $[Os_3W(CO)_{10}(O)(\mu\text{-}\eta^1,\eta^2\text{-}CH{=}CHPh\{W\text{-}Os\})(\mu\text{-}O)(Cp^*)]$ **4** (20 mg, 0.018 mmol, 87%). Spectral data for $[Os_3W(CO)_{10}(O)(\mu\text{-}\eta^1,\eta^2\text{-}CH{=}CHPh\{W\text{-}Os\})(\mu\text{-}O)(Cp^*)]$ **4**: IR (hexane): ν(CO) 2112 (m); 2064 (m); 2036 (vs); 2013 (m); 2003 (w); 1983 (vw); 1971 (vw); 1943 (vw). ^1H NMR ($CDCl_3$) δ: 8.49 (1H, d, $J_{H\text{-}H}$ = 12 Hz); 7.27 (4H, m); 7.09 (1H, m); 3.47 (1H, d, $J_{H\text{-}H}$ = 12 Hz); 2.09 (15H, s). $^{13}C\ \{^1H\}$ NMR ($CDCl_3$) δ: 143.5 (1C, s, C=C); 128.2 (2C, s, Ph); 126.5 (2C, s, Ph); 126.1 (1C, s, Ph); 122.2 (1C,s, Ph); 118.0 (5C, s, C_5Me_5), 46.2 (1C, s, C=C); 11.0 (5C, s, C_5Me_5). FAB-MS (*m/z*): 1305, $[M]^+$; 1277-1025, $[M\text{-}nCO]^+$ (n = 1-10). Anal. Calcd. for **4**: C, 25.77; H, 1.70. Found C, 25.97; H, 1.6%.

2.4.5 Reaction of $[D_2Os_3(CO)_{10}]$ with $[W(C{\equiv}CPh)(O)_2(Cp^*)]$ with no light

A sample (100 mg, 0.117 mmol) of $[D_2Os_3(CO)_{10}]$ was dissolved in dry dichloromethane (50 mL) with $[W(C{\equiv}CPh)(O)_2(Cp^*)]$ (63 mg, 0.14 mmol) and heated at 30°C in the dark. After five days, the solvent was removed *in vacuo* in the dark and the residue dissolved in the minimum of dichloromethane. Two compounds were separated via thin layer chromatography in air in the dark by first eluting the starting material with pure hexane and the compounds **1d** and **4d** with a mixture of 71/25/4 hexane/THF/CH_2Cl_2. The compounds were in order of elution $[D_2Os_3(CO)_{10}]$ (20 mg, 0.023 mmol, 20%) , $[Os_3W(\mu\text{-}D)(\mu\text{-}\eta^1\text{-}C{=}CDPh)(CO)_{10}(O)(\mu\text{-}O)(Cp^*)]$ **1d** (24 mg, 0.018 mmol, 24%) and $[Os_3W(CO)_{10}(O)(\mu\text{-}\eta^1,\eta^2\text{-}CD{=}CDPh\{W\text{-}Os\})(\mu\text{-}O)(Cp^*)]$ **4d** (27 mg, 0.021 mmol, 27%). Spectral data for $[Os_3W(\mu\text{-}D)(\mu\text{-}\eta^1\text{-}C{=}CDPh)(CO)_{10}(O)(\mu\text{-}O)(Cp^*)]$ **1d**: IR (hexane): ν(CO) 2132 (w); 2078 (vs); 2060 (s); 2049 (vs); 2027 (m); 2018 (m); 2004 (m); 1997 (m); 1981 (w); 1943 (w). ^{1}H NMR ($CDCl_3$) δ: 9.30 (0.1H, s); 7.76 (2H, d, J = 7.43 Hz); 7.46 (2H, m), 7.37 (1H, m); 1.99 (15H, s); -17.99 (0.1H, s). ^{2}H NMR ($CHCl_3$) δ: 9.32 (1H, s); -18.03 (1H, s). Anal. Calcd. for **1d**: C, 25.73; H, 1.85. Found C, 25.78; H, 1.67%. **4d**: IR (hexane) ν(CO) 2112 (m); 2064 (m); 2035 (vs); 2013 (m); 2003 (w); 1983 (vw); 1970 (vw); 1944 (vw). ^{1}H NMR ($CDCl_3$) δ: 8.51 (0.05H, s); 7.29 (4H, m); 7.11 (1H, m); 3.50 (0.05H, s); 2.12 (15H, s). ^{2}H NMR ($CHCl_3$) δ: 8.56 (1H, s); 3.49 (1H, s). Anal. Calcd. for **4d**: C, 25.73; H, 1.85. Found C, 26.15; H, 1.82%.

2.4.6 X-ray structural analysis of 1

Single crystals of **1** were grown from the slow evaporation of CH_2Cl_2/hexane solutions at room temperature. A deep orange prism of dimensions 0.06 x 0.1 x 0.12 mm was selected and mounted on a glass fiber. Crystals of **1** are monoclinic, space group *P*21/*c*, with Z= 4. The Patterson map was solved for the four heavy metal atoms using 6403 [I > 2.5 σ(I)] independent data. The structure was refined by full-matrix least-squares techniques. The lighter non-hydrogen atoms were located in subsequent difference Fourier maps. The following hydrogen atoms were also found in final difference Fourier maps and refined isotropically (H1, H2, H4, H5, H6, H7 and H8). The remaining hydrogen atoms were

included in calculated positions and not refined. The structure was refined to $R_F = 0.029$ and $R_W = 0.025$. Full details are contained in Appendix A.1.

2.4.7 X-ray structural analysis of 2

Orange crystals of **2** suitable for X-ray analysis were obtained from the slow evaporation of CH_2Cl_2/hexane at room temperature. A red rectangular prism of dimensions 0.4 x 0.1 x 0.12 mm was chosen. Compound **2** crystallizes in the triclinic space group *P*-1 with $Z = 2$. Data were collected at −100°C. The generated Patterson map was solved for the four heavy metal atoms using 6046 observed [$I > 2.5\sigma(I)$] independent data. All the non-hydrogen atoms were found in subsequent difference Fourier map and refined anisotropically. The hydrogen atoms H(2) was located in the final difference Fourier maps and refined isotropically. The remaining hydrogen atoms, except H(1) were generated and their calculated positions were included with fixed isotropic thermal parameters. The position of H(1) was obtained using the XHYDEX software package and included as an exact position with a fixed isotropic thermal parameters. Refinement converged at $R = 0.035$ and $R_W = 0.035$. Full crystallographic details for **2** can be found in Appendix A.2

2.4.8 X-ray structural analysis of 3

Single crystals of **3** suitable for X-ray analysis were grown at room temperature from the slow evaporation of CH_2Cl_2/hexane solutions. An orange prism of approximate dimensions 0.2 x 0.1 x 0.15 mm was chosen and mounted. Crystals of **3** are trigonal, crystallizing in the space group *R*-3. Data were collected at −100°C. Generation of the Patterson map using 4140 observed [$I > 2.5\sigma(I)$] data enabled the location of the heavy metal atoms to be determined. The remaining non-hydrogen atoms were later located in other difference Fourier maps. The hydrogen atom positions were generated with the exception of H(1) and their calculated positions were included with fixed isotropic thermal parameters. The hydrogen atom H(1) was located using the XHYDEX program and its positional parameters included with fixed isotropic thermal parameters. The non-hydrogen atoms were refined anisotropically. Final R and R_W values were 0.043 and 0.043 respectively. Full details of the data collection can be found in Appendix A.3.

2.4.9 X-ray structural analysis of 4

Suitable crystals of **4** were obtained from the slow evaporation of CH_2Cl_2/hexane solutions at room temperature. A red prism of dimensions 0.1 x 0.15 x 0.2 mm was selected and mounted on a glass fiber. Crystals of **4** crystallize in the monoclinic space group *P*21/*n*, with Z= 4. Data were collected at –100°C. A total of 8235 unique reflections were collected of which 6927 were considered as being observed [$I > 2.5\ \sigma(I)$]. Patterson methods were used to locate the metal atoms and difference Fourier maps provided the location of the remaining non-hydrogen atoms. All non-hydrogen atoms were refined anisotropically. Hydrogen atoms were generated in ideal positions and not refined to the exception of H(1) and H(2). Both positional and isotropic thermal parameters for H(1) and H(2) were refined. Final R and R_W were 0.041 and 0.045 respectively. Full details are listed in Appendix A.4.

2.5 References

1. (a) Horton, A.D.; Kemball, A.C.; Mays, M.J. *J. Chem. Soc., Dalton Trans.* **1988**, 2953. (b) Montlo, D.; Suades, J.; Dahan, F.; Mathieu, R. *Organometallics* **1990**, 9, 2933. (c) Yánez, R.; Ros, J.; Mathieu, R.; Solans, X. Font-Bardia, M. *J. Organomet. Chem.* **1990**, 389, 219. (d) Conole, G.; Henrick, K.; McPartlin, M.; Horton, A.D.; Mays, M.J. *New. J. Chem.* **1988**, 12, 559. (e) Deeming, A.J.; Hasso, S.; Underhill, M. *J. Chem. Soc., Dalton Trans.* **1975**, 1614.

2. (a) Blenkiron, P.; Carty, A.J.; Peng, S.-M.; Lee, G.-H.; Su, C.-J.; Shiu, C.-W.; Chi, Y. *Organometallics* **1997**, 16, 519. (b) Shiu, C.-W.; Chi, Y.; Carty, A.J.; Peng, S.-M.; Lee, G.-H. *Organometallics* **1997**, 16, 5368.

3. (a) Shapley, J.R.; Keister, J.B.; Churchill, M.R.; de Boer, B.G. *J. Am. Chem. Soc.* **1975**, 97, 4145. (b) Churchill, M.R.; de Boer, B.G. *Inorg. Chem.* **1977**, 16, 878. (c) *ibid.*, **1977**, 16, 2397. (d) Keister, J.B.; Shapley, J.R. *Inorg. Chem.* **1982**, 21, 3304.

4. (a) Tachikawa, M.; Shapley, J.R.; Pierpont, C.G. *J. Am. Chem. Soc.* **1975**, 97, 7172. (b) Clauss, A.D.; Tachikawa, M.; Shapley, J.R.; Pierpont, C.G. *Inorg. Chem.* **1981**, 20, 1528. (c) Pierpont, C.G. *Inorg. Chem.* **1977**, 16, 636. (d) Jackson, W.G.; Johnson, B.F.G.; Kelland, J.W.; Lewis, J.; Schorpp, K.T. *J. Organomet. Chem.* **1975**, 87, C27.

5. Laing, M.; Sommerville, P.; Dawoodi, Z.; Mays, M.J.; Wheatley, P.J. *J. Chem. Soc., Chem. Commun.* **1978**, 1035.

6. Farrugia, L.J.; Howard, J.A.K.; Mitrprachachon, P.; Stone, F.G.A.; Woodward, P. *J. Chem. Soc., Dalton Trans.* **1981**, 155.

7. Churchill, M.R.; Bueno, C.; Kennedy, S.; Bricker, J.C.; Plotkin, J.S.; Shore, S.G. *Inorg. Chem.* **1982**, 21, 627.

8. Deeming, A.J.; Hasso, S.J. *J. Organomet. Chem.* **1976**, 114, 313.

9. Dawoodi, Z.; Henrick, K.; Mays, M.J. *J. Chem. Soc., Chem. Commun.* **1982**, 696.

10. Knox, S.A.R.; Koepke, J.W.; Andrews, M.A.; Kaesz, H.D. *J. Am. Chem. Soc.* **1975**, 97, 3942.

11. Mirza, H.A.; Vittal, J.J.; Puddephatt, R.J. *Inorg. Chem.* **1995**, 34, 4239.

12. Ceriotti, A.; Resconi, L.; Demartin, F.; Longoni, G.; Manassero, M.; Sansonni, M. *J. Organomet. Chem.* **1983**, 249, C35.

13. Goudsmit, R.J.; Johnson, B.F.G.; Lewis, J.; Raithby, P.R.; Whitmire, K.H. *J. Chem. Soc., Chem. Commun.* **1983**, 246.

14. Xiao, J.; Vittal, J.J.; Puddephatt, R.J.: Manojlovic-Muir, L.; Muir, K.W. *J. Am. Chem. Soc.* **1993**, 115, 7882.

15. Gibson, C.P.; Huang, J.-S., Dahl, L.F. *Organometallics* **1986**, 5, 1676.

16 Song, L.-C.; Fan, H.-T.; Hu, Q.-M; Qin, X.-D.; Zhu, W.-F.; Chen, Y.; Sun, J. *Organometallics* **1998**, 17, 3454.

17. Chi, Y.; Chen, B-F.; Wang, S-L.; Chiang, R-K.; Hwang, L-S. *J. Organomet. Chem.* **1989**, 377, C59.

18. (a) Churchill, M.R.; de Boer, B.G.: Rotella, F.J. *Inorg. Chem.* **1976**, 15, 1843. (b) Churchill, M.R. *Adv. Chem. Series* **1978**, 167, 36. (c) Teller, R.G.: Bau, R. *Structure and Bonding* **1981**, 44, 1.

19. Antonova, A.B.; Kovalenko, S.V.; Korniyets, E.D.; Johansson, A.A.; Struchkov, Y.T.; Yanovsky, A.I. *J. Organomet. Chem.* **1984**, 267, 299.

20. Churchill, M.R.; Li, Y-J. *J. Organomet. Chem.* **1985**, 294, 367.

21. (a) Batchelor, R.J.; Einstein, F.W.B.; Pomeroy, R.K.; Shipley, J.A. *Inorg. Chem.* **1992**, 31, 3155. (b) Batchelor, R.J.; Davis, H.B.; Einstein, F.W.B.; Pomeroy, R.K. *J. Am. Chem. Soc.* **1990**, 112. 2036.

22. Chi, Y.; Shapley, J.R.; Ziller, J.W.; Churchill, M.R. *Organometallics* **1987**, 6, 301.

23. Chi, Y.; Hwang, L.-S.; Lee, G.-H.; Peng, S.-M. *J. Chem. Soc., Chem. Commun.* **1988**, 1456.

24. Churchill, M.R.; Bueno, C.; Park, J.T.; Shapley, J.R. *Inorg. Chem.* **1984**, 23, 1017.

25. (a) Churchill, M.R.; Ziller, J.W.; Beanan, L.R. *J. Organomet. Chem.* **1985**, 287, 235. (b) Shapley, J.R.; Park, J.T.; Churchill, M.R.; Ziller, J.W.; Beanan, L.R. *J. Am. Chem. Soc.* **1984**, 106, 1144.

26. Churchill, M.R.; Ziller, J.W.; Freudenberger, J.H.; Schrock, R.R. *Organometallics* **1984**, 3, 1554.

27. Freudenberger, J.H.; Schrock, R.R.; Churchill, M.R.; Rheingold, A.L.; Ziller, J.W. *Organometallics* **1984**, 3, 1563.

28. Churchill, M.R.; Ziller, J.W. *J. Organomet. Chem.* **1985**, 286, 27.

29. Orpen, A.G. *J. Chem. Soc. Dalton Trans.* **1980**, 2509.

30. Cotton, F.A.; Wilkinson, G. In *Advanced Inorganic Chemistry (Fifth Edition)*; John Wiley & Sons: New York, 1988; pp 71-74.

31. Chi, Y.; Cheng, P-S.; Wu, H-L.; Hwang, D-K; Su, P-C.; Peng, S-M.; Lee, G-H. *J. Chem. Soc., Chem. Commun.* **1994**, 1839.

32. (a) Chi, Y.; Shapley, J.R.; Churchill, M.R.; Li, Y.-J. *Inorg. Chem.* **1986**, 25, 4165. (b) Calvert, R.B.; Shapley, J.R.; Schultz, A.J.; Williams, J.M.; Suib, S.L.; Stucky, G.D. *J. Am. Chem. Soc.* **1978**, 100, 6240. (c) Calvert, R.B.; Shapley, J.R. *J. Am. Chem. Soc.* **1978**, 100, 7727.

Chapter Three

Hydrogenation of $[Os_3W(CO)_{10}(O)(\mu\text{-}\eta^1,\eta^2\text{-}CH{=}CHPh\{W\text{-}Os\})(\mu\text{-}O)(Cp^*)]$ 4

3.1 Introduction

The interest in the structure and reactivity of transition metal complexes containing both oxo and hydrocarbyl ligands arises from the potential of these species to model the reactions that occur on the surface of heterogeneous catalysts.[1] One of the reactions of interest is the hydrogenation of a hydrocarbyl fragment. In transition metal cluster chemistry, hydrogenation of π-bound alkyne ligands can be achieved by either: (*i*) hydride migration from a cluster bound hydrogen to a coordinated alkyne ligand or (*ii*) hydrogenation of a cluster complex containing a pre-coordinated alkyne unit.[2] Reactions of the first type have been described in Chapter Two of this thesis.

Chi and co-workers discovered that the oxo ligand of $[Re_2W(CO)_8(O)(CCPh)(Cp^*)]$ (**A**) mediates a sequential conversion of the acetylide ligand to an alkenyl and finally to an alkylidene ligand upon treatment with dihydrogen. Hydrogenation of compound **A** in refluxing heptane produced $[WRe_2(\mu\text{-}H)_2(CO)_6(\mu\text{-}O)(CCPh)(Cp^*)]$ (**B**) (dark red, 50%).[1,3] The oxo ligand was converted from a terminal oxo ligand in cluster **A** to a W=O:→Re interaction in **B**, which is related to the W=O:→Os bridging oxo ligand of cluster compounds having the $WOs_3(\mu\text{-}O)$ core arrangement.[3a] The addition of two CO ligands to **B** afforded $[WRe_2(CO)_8(O)(\mu\text{-}\eta^1,\eta^2\text{-}CHCHPh)(Cp^*)]$ (**C**) (orange, 28%). The generation of **C** involves the migration of two hydrogen atoms from the cluster to the acetylide moiety to yield a *trans*, edge bridging vinyl fragment. The oxo ligand shifted from a bridging bonding mode to a terminal mode. Complex **C** was further hydrogenated to form complex $[WRe_2(\mu\text{-}H)(CO)_8(\mu\text{-}\eta^1\text{-}CHCH_2Ph)(O)(Cp^*)]$ (**D**) (yellow, 5%) where the hydrocarbyl ligand is a bridging alkylidene and the metal framework bears one

bridging hydride. The oxo ligand of complex **D** maintained a terminal bonding mode (Scheme 3.1).[3a]

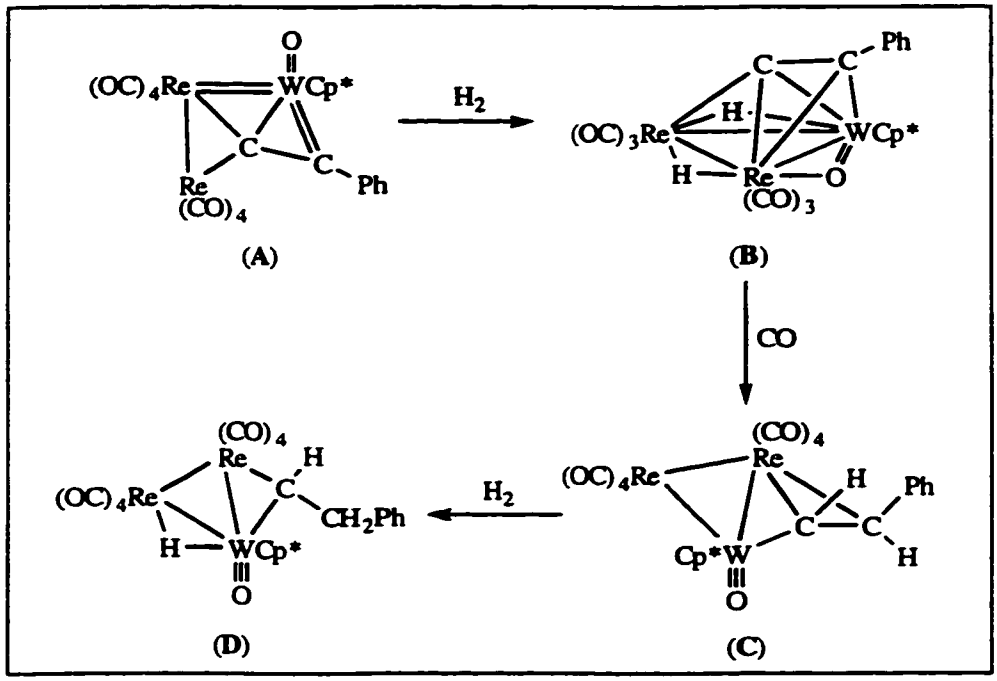

Scheme 3.1 Reactivity of $[Re_2W(CO)_8(O)(CCPh)(Cp^*)]$ with dihydrogen.

The oxo ligand plays a role in the conversion of **B** → **C** → **D**. The oxo ligand in these complexes adopts either the terminal or the asymmetrical doubly-bridging mode. It was found that the above reactivity scheme was inhibited in the absence of the oxo ligand. Thus the reaction of the acetylide cluster $[WRe_2(\mu\text{-}H)_2(CO)_8(CCPh)(Cp^*)]$ with CO produced only elimination of H_2. The complex **B** is related to $[WRe_2(\mu\text{-}H)_2(CO)_8(CCPh)(Cp^*)]$ by formally replacing an oxo ligand with two CO ligands. The authors suggested that the high electronegativity of the oxo ligand together with its capability to serve as both a four and six-electron donor by adopting various bonding modes might favor the transfer of hydrides.[3]

Work carried out on the μ_3-alkylidyne hydrocarbyl ligand of $[Os_3W(CO)_6(\mu\text{-}O)(\mu_3\text{-}C\text{-}CH_2Tol)(Cp)]$ (**E**) also led to an analogous ligand transformation. Bubbling H_2 through a solution of **E** yielded $[Os_3W(\mu\text{-}H)(\mu\text{-}\eta^1\text{-}CHCH_2Tol)(CO)_9(\mu\text{-}O)(Cp)]$ (**F**) quantitatively (Scheme 3.2).[4] Hence, the alkylidyne ligand of **E** was hydrogenated resulting in the

formation of an alkylidene ligand in **F**. The oxo ligand retained the W=O:→Os coordination mode in the process and is counted as a four-electron donor (neutral atom counting scheme). The precise role of the oxo ligand in mediating the ligand transformation was not resolved in this study. The site of unsaturation needed for the oxidative addition of a C-H or an H-H bond is not provided by the loss of a ligand (i.e., CO) in the conversion of **E** to **F**. However, the authors suggested that the μ-oxo ligand moves reversibly from a bridging (four electron donor) to a terminal (two electron donor) position generating in the process an unsaturated intermediate.[4]

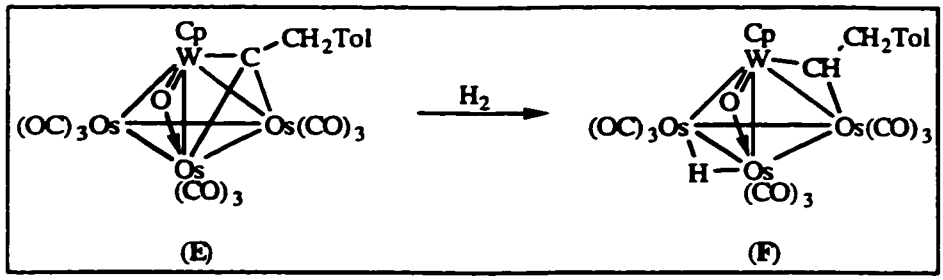

Scheme 3.2 Reactivity of $[Os_3W(CO)_6(\mu\text{-}O)(\mu_3\text{-}C\text{-}CH_2Tol)(Cp)]$ with dihydrogen.

While none of these complexes has been demonstrated to be part of a catalytic cycle, they provide a variety of structural types from which potential intermediates for hydrogenation catalytic cycles may be proposed. It was of particular interest to extend this chemistry to the hydrogenation of a vinyl ligand on a $WOs_3(\mu\text{-}O)$ framework in complex **2**. Such studies would also provide additional information as to the mediating role of the oxo ligand in allowing ligand transformations.

3.2 Results and discussion

3.2.1 Summary

The photolytic reaction of **4** with dihydrogen gas at room temperature and atmospheric pressure, afforded the related complexes $[Os_3W(\mu\text{-}H)(\textit{anti}\text{-}\mu\text{-}\eta^1\text{-}CHCH_2Ph)(CO)_9(O)(Cp^*)(\mu_3\text{-}O)]$ (**5**), $[Os_3W(\mu\text{-}H)(\textit{gauche}\text{-}\mu\text{-}\eta^1\text{-}CHCH_2Ph)(CO)_9(O)(Cp^*)$

(μ_3-O)] (**6**) and [$Os_3W(CO)_9(\mu\text{-}O)_2(\mu\text{-}\eta^1,\eta^2\text{-}CH{=}CHPh\{W\text{-}Os\})(Cp^*)$] (**7**) (Scheme 3.3). Complex **7** was also obtained using a different reaction route and will be discussed in detail in Chapter Four of this thesis. The isolation of the two isomers **5** and **6** demonstrated the non-regioselectivity of the hydrogenation process. Complexes **5** and **6** were fully characterized by IR, ^1H and ^{13}C spectroscopies. Satisfactory elemental analyses were obtained in each case. The structures of both **5** and **6** were determined by single X-ray analyses, and revealed the presence of a μ_3-oxo ligand bonded to the WOs_3 metal framework.

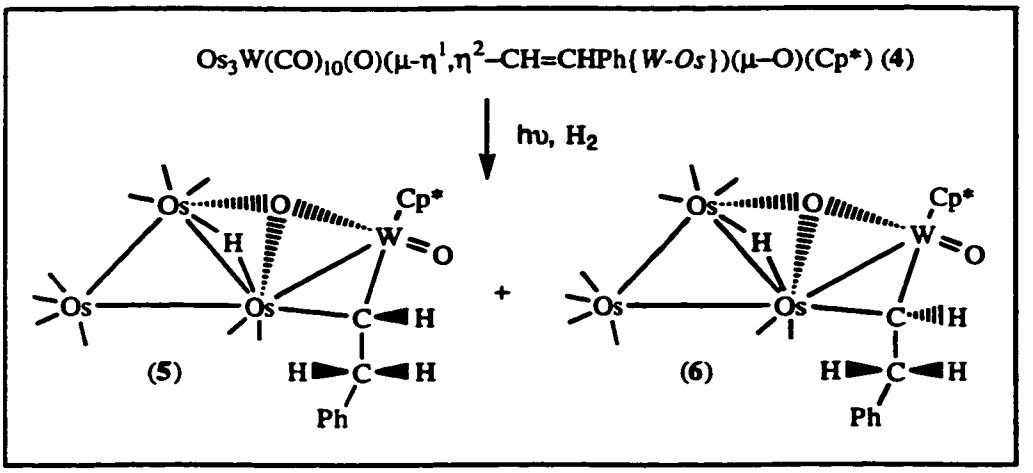

Scheme 3.3 Synthesis of [$Os_3W(\mu\text{-}H)(anti\text{-}\mu\text{-}\eta^1\text{-}CHCH_2Ph)(CO)_9(O)(Cp^*)(\mu_3\text{-}O)$] **5** and [$Os_3W(\mu\text{-}H)(gauche\text{-}\mu\text{-}\eta^1\text{-}CHCH_2Ph)(CO)_9(O)(Cp^*)(\mu_3\text{-}O)$] **6**.

Hydrogen atoms are specifically added to 1) the metal framework in order to generate a bridging hydride, and 2) the vinyl group resulting in the formation of an alkylidene ligand. A related vinyl to alkylidene transformation was observed during the hydrogenation of the heterometallic cluster [$Re_2W(CO)_8(O)(\mu\text{-}\eta^2\text{-}CH{=}CHPh)(Cp^*)$].[1] The reaction of **4** with dihydrogen provided further evidence of the ability of the $WOs_3(\mu\text{-}O)$ core to promote interesting ligand transformation.

Finally, deuterium labeling studies were conducted to further our understanding of the hydrogenation process. The reaction of **4** with D_2 gas afforded the deuterated complexes [$Os_3W(\mu\text{-}D)(anti\text{-}\mu\text{-}\eta^1\text{-}CHCHDPh)(CO)_9(O)(Cp^*)(\mu_3\text{-}O)$] (**5d**) and [$Os_3W(\mu\text{-}D)(gauche\text{-}\mu$-

η^1-CHCHDPh)(CO)$_9$(O)(Cp*)(μ_3-O)] (**6d**). The compounds **5d** and **6d** were characterized by IR, ^{1}H, ^{2}H spectroscopies and elemental analysis.

3.2.2 Study of [$Os_3W(\mu$-H)(*anti*-μ-η^1-$CHCH_2Ph)(CO)_9(O)(Cp^*)(\mu_3$-O)] **5**

3.2.2.1 Spectroscopic features of 5

The infrared spectrum of **5** showed terminal carbonyl stretching bands at 2093 (m), 2055 (vs), 2019 (s), 2014 (s), 2004 (m), 1995 (m), 1978 (w) and 1947 (vw) cm^{-1}. The ^{1}H NMR spectrum of **5** showed, in addition to the expected resonances for the Cp* and Ph ligands, a doublet at δ -13.57 in the hydride region. The ^{1}H NMR spectrum exhibited three signals at δ 8.95 (1H), 5.31 (1H) and 4.53 (1H) split in an ABX pattern, in a manner similar to that observed for the alkylidene complex [$Os_3W(\mu$-Cl)(μ-η^1-$CHCH_2$Tol)(CO)$_9$(μ-O)(Cp)].[5] The lowest field resonance was assigned to the α-hydrogen due to the presence of vicinal couplings to the two benzylic β-hydrogen atoms at higher field. The ^{13}C NMR spectrum obtained showed nine signals between δ 186.9 and 174.8 in the region expected for carbonyl ligands together with the expected resonances for the Cp* and Ph ligands. Two signals at δ 139.1 and 51.8 were also present arising from the hydrocarbyl fragment. The FAB mass spectrum was characterized by a [M]$^+$ ion at *m/z* 1279, which fragmented by loss of CO ligands to give [M-nCO]$^+$ (n = 1-5).

3.2.2.2 X-ray structure of 5

An ORTEP plot of complex **5** is shown in Figure 3.1 and selected bond lengths and angles are summarized in Table 3.1. The skeletal framework of complex **5** consists of a closed triangle of osmium atoms with a single tungsten atom spiked at Os(1) as previously observed for clusters **1**, **2**, **3** and **4**. Nonetheless, the Os-Os bond lengths (Os(1)-Os(2) = 2.8255(5) Å, Os(1)-Os(3) = 2.8038(5) Å and Os(2)-Os(3) = 2.8372(5) Å) indicated stronger similarities with the metal framework of **2** and **3**. Cluster **5** possesses a total of nine terminal carbonyl groups distributed on Os(1), Os(2) and Os(3) in the usual distorted octahedral conformation (C(22)-Os(2)-C(23) = 91.3(4)°, C(20)-Os(2)-C(23) = 94.9(4)°, C(21)-Os(2)-C(22) = 93.8(4)°, C(20)-Os(2)-C(21) = 94.9(4)° and C(31)-Os(3)-C(32) = 91.0(4), C(30)-

Os(3)-C(31) = 93.5(5)°, C(30)-Os(3)-C(32) = 92.5(4)°, O(1)-Os(3)-C(31) = 97.0(4)°, O(1)-Os(3)-C(30) = 96.3(3). The parameters associated with the carbonyl ligands (Os-CO = 1.86(1) – 1.96(1) Å; C-O =1.14(1) – 1.16(1) Å and Os-C-O = 172(1)-179.0(9)°) are within the expected ranges.[6] The CO distribution about Os(3) is significantly distorted by the presence of a μ_3-O ligand on **5**. Compared to the CO ligands of Os(2), the CO groups on Os(3) are rotated by an average of –42.6(6)° (C(23)-Os(2)-Os(3)-O(1) = -46.9(5)°, C(21)-Os(2)-Os(3)-C(32) = -41.0(7)° and C(22)-Os(2)-Os(3)-C(31) = -38.7(7)°) resulting in a staggered conformation.

The alkylidene ligand (μ-C(1)HC(2)H_2Ph) of **5** bridges W and Os(1) in a μ-η^1 fashion (W-C(1) = 2.064(9), Os(1)-C(1) = 2.27(1) Å; Os(1)-C(1)-W = 77.1(3)°). The μ-η^1 alkylidene ligand spans the W-Os(1) vector in such a way that C(1) lies closer to W than Os(1). Similar bonding modes have been observed for other WOs_3 oxo-alkylidene clusters, [$Os_3W(\mu$-Cl)(μ-η^1-CHCH_2Tol)(CO)$_9$(μ-O)(Cp)][5] (W-C = 2.06(1) Å and Os-C = 2.20(1) Å) and [$Os_3W(\mu$-H)(μ-η^1-CHCH_2Tol)(CO)$_9$(μ-O)(Cp)][7] (W-C = 2.07(3) Å and Os-C = 2.28(3) Å). The C(1)-C(2) bond distance of 1.52(1) Å is now characteristic of a single bond. This allows for free rotation about the C(1)-C(2) bond. The conformation adopted by the μ-alkylidene ligand (W-C(1)-C(2)-C(3) = 179(2)°) places the phenyl group *anti* to the bulky WCp* moiety. This specific conformation was also found for the alkylidene ligand of [$Os_3W(\mu$-Cl)(μ-η^1-CHCH_2Tol)(CO)$_9$(μ-O)(Cp)][5].

The oxo ligand of **5** links the Os(1), Os(2) and W atoms. The triply bridging bonding arrangement of the oxo ligand of **5** resembles the one encountered in complexes **2** and **3**. The W-O bond length (W-O(1) = 1.957(6) Å) is within the range expected for a double bond,[8] while the Os-O bond distances (Os(1)-O(1) = 2.099(6) Å and Os(3)-O(1) = 2.168(6) Å) are indicative of the donation of lone pairs of electrons from the oxygen atom to the osmium atoms. Thus, O(1) acts as a six electron donor. As found previously (Chapter Two), the

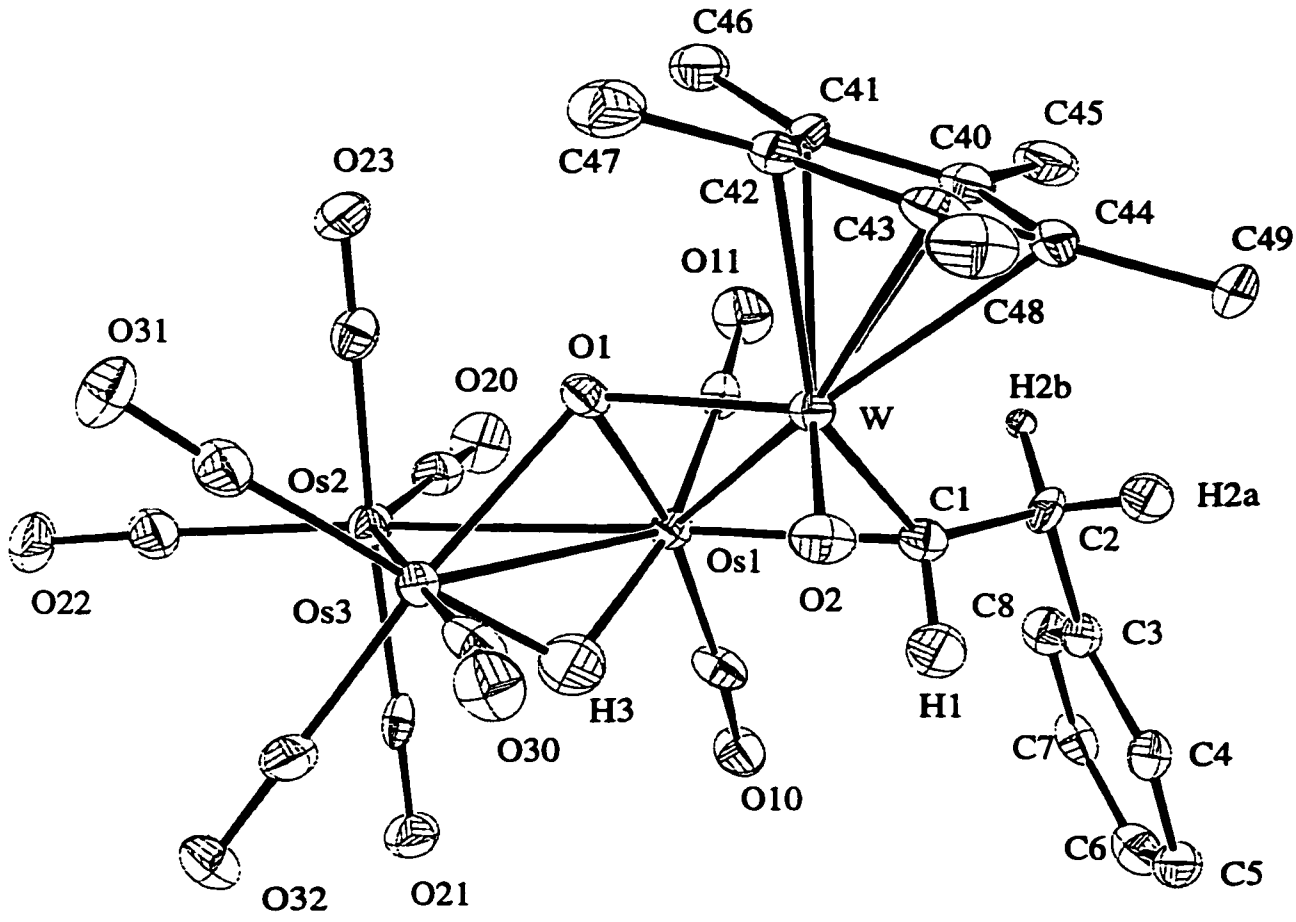

Figure 3.1 The molecular structure of $[Os_3W(\mu\text{-}H)(\textit{anti}\text{-}\mu\text{-}\eta^1\text{-}CHCH_2Ph)(CO)_9(O)(Cp^*)(\mu_3\text{-}O)]$ **5**.

Table 3.1 Selected bond lengths (Å) and angles (deg) for **5**.

		Lengths	
Os(2)-Os(3)	2.8372(5)	W-O(2)	1.704(7)
Os(2)-Os(1)	2.8255(5)	W-O(1)	1.957(6)
Os(3)-Os(1)	2.8038(5)	W-C(1)	2.064(9)
W-Os(1)	2.7090(5)	Os(1)-C(1)	2.27(1)
Os(1)-O(1)	2.099(6)	C(1)-C(2)	1.52(1)
Os(3)-O(1)	2.168(6)		
		Angles	
Os(2)-Os(1)-Os(3)	60.53(1)	Os(1)-C(1)-W	77.1(3)
Os(1)-Os(2)-Os(3)	59.36(1)	W-C(1)-C(2)	133.7(7)
Os(1)-Os(3)-Os(2)	60.12(1)	Os(1)-C(1)-C(2)	117.4(7)
Os(2)-Os(1)-W	130.59(2)	C(1)-C(2)-C(3)	113.9(8)
Os(3)-Os(1)-W	80.49(1)	Os(2)-Os(1)-O(1)	84.8(2)
Os(1)-O(1)-W	83.7(3)	Os(3)-Os(1)-O(1)	50.0(2)
O(1)-W-O(2)	108.0(3)	Os(1)-Os(3)-O(1)	47.9(2)
		Os(2)-Os(3)-O(1)	83.3(2)

presence of a μ_3-O ligand leads to a contraction of the bridged M-M bonds. Hence, the μ_3-O ligand spans the shortest Os-Os bond (Os(1)-Os(2) = 2.8255(5) Å, Os(1)-Os(3) = 2.8038(5) Å and Os(2)-Os(3) = 2.8372(5) Å).

The presence of a bridging hydride on **5** was suggested by both ^{1}H NMR spectroscopy and cluster electron count. Unfortunately, the precise position of the bridging hydride could not be located in a difference Fourier map. The XHYDEX program[9] was thus used to infer the most favored position of a bridging hydride on **5**. The hydride ligand was calculated to lie in an asymmetric fashion on the Os(1)-Os(3) vector. The bond lengths obtained (Os(1)-H(3) = 1.85(4) Å and Os(3)-H(3) = 1.61(4) Å) are similar to those found from a difference map in **1** (Os(1)-H(1) = 1.84(6) Å and Os(2)-H(1) = 1.62(7) Å). A study of the Os-Os-C(O) angles agreed with the presence of a hydride on the Os(1)-Os(3) bond as indicated by the enlargement of the Os-Os-C(O) angles on this vector (Os(1)-Os(3)-C(30) = 115.7(3)°, Os(3)-Os(2)-C(22) = 106.2(3)° and Os(1)-Os(2)-C(20) = 92.4(3)°.

The tungsten atom and the three osmium atoms define a spiked triangular core of metals which is associated with the expected 64 outer valence electrons. With all metal atoms and ligands treated as formally neutral we have three d^8 Os^0 atoms, one d^6 W^0 atom, 18 electrons for the nine terminal carbonyl ligands, 5 electrons from the Cp* ligand, 2 electrons from the μ-CH-CH_2Ph ligand, 6 electrons from the μ_3-O ligand, 2 electrons from the terminal oxo ligand and 1 electron from the μ-hydride ligand.

3.2.3 Study of [$Os_3W(\mu$-H)(*gauche*-μ-η^1-CHCH$_2$Ph)(CO)$_9$(O)(Cp*)(μ_3-O)] **6**

3.2.3.1 Spectroscopic features of 6

The spectroscopic data of **6** closely resembled the corresponding data for **5**. The infrared spectrum of complex **6** showed terminal stretching bands at 2093 (m), 2055 (s), 2014 (vs), 2003 (m), 1995 (m), 1978 (w) and 1949 (vw). The ^{1}H NMR spectrum showed a resonance at δ -13.75 in the hydride region as well as appropriate resonances for the Ph and Cp* ligands. The ^{1}H NMR spectrum had three signals at δ 8.16, 5.72 and 4.27 with an ABX

splitting pattern similar to that of the alkylidene complex **5**. The ^{13}C NMR spectrum exhibited nine carbonyl signals in addition to the Ph and Cp* resonances. Two signals at δ 150.6 (J_{W-C} = 67.7 Hz) and 60.7 were observed in the ^{13}C NMR arising from the hydrocarbyl fragment. The resonance at δ 150.56 was flanked by ^{183}W satellites of low intensity due to the low probability of finding a ^{13}C (1.108 % natural abundance) nucleus next to a ^{183}W (14.4 % natural abundance) nucleus. A molecular ion at *m/z* 1279 in the FAB mass spectrum was observed, indicating that both complexes **5** and **6** had the same molecular weight.

3.2.3.2 X-ray structure of 6

An ORTEP plot of $[Os_3W(\mu\text{-}H)(\textit{gauche}\text{-}\mu\text{-}\eta^1\text{-}CHCH_2Ph)(CO)_9(O)(Cp^*)(\mu_3\text{-}O)]$ **6** is shown in Figure 3.2. Selected bond lengths are summarized in Table 3.2. Figure 3.2 indicates that the metal framework of **6** is essentially identical to that of **5**, consisting of a triangle of osmium atoms spiked by a tungsten atom at Os(1). The Os-Os bond distances (Os(1)-Os(2) = 2.8160(5) Å, Os(1)-Os(3) = 2.8078(5) Å and Os(2)-Os(3) = 2.8331(5) Å) and the carbonyl distribution are essentially identical to **5**. The μ_3-O ligand of **6** also forces a rotation of the carbonyl ligands surrounding Os(3) resulting in a staggered conformation relative to the carbonyl ligands on Os(2). The following dihedral angles C(23)-Os(2)-Os(3)-O(1) = -39.5(5)°, C(21)-Os(2)-Os(3)-C(30) = -35.3(6)° and C(20)-Os(2)-Os(3)-C(31) = -40.8(6)° suggest that the carbonyl ligands on Os(3) are shifted from their corresponding positions on Os(2) by an average of -38.5(6)°, which strongly resembles the one obtained for complex **5** (–42.2(6)°). The bonding parameters associated with the alkylidene ligand of complex **6**, which bridges the W-Os(1) vector are (W-C(1) = 2.055(9) Å, Os(1)-C(1) = 2.222(8) Å and C(1)-C(2) = 1.55(1) Å; Os(1)-C(1)-W = 77.9(3)°), closely related to those observed for **5**.

The oxo ligand adopts a triply bridging bonding mode, linking Os(1), Os(3) and the tungsten atoms. Again the μ_3-O ligand bridges the two osmium atoms (Os(1)-Os(3)) with the smallest bond length. The geometry associated with this ligand is strongly similar to the one present in complex **5** as suggested by the distances and angles (W-O(1) = 1.953(5) Å, Os(1)-

O(1) = 2.090(5) Å and Os(3)-O(1) = 2.180(5) Å; Os(1)-O(1)-W = 83.4(2)° and Os(3)-O(1)-W = 117.1(2)°).

The location of the bridging hydride was once again obtained from the XHYDEX program created by Orpen.[9] The location of the bridging hydride was on the shortest Os-Os bond, more specifically the Os(1)-Os(3) bond as previously determined for complex **5**. The bond distances obtained resemble those of complex **5** (Os(1)-H(3) = 1.8545(3) Å and Os(3)-H(3) = 1.6079(4) Å) and suggest once more an asymmetrical bonding mode. The enlargement of the Os-Os-C(O) angles on the Os(1)-Os(3) vector also supports this position (Os(1)-Os(3)-C(32) = 118.5(3)°, Os(3)-Os(2)-C(21) = 97.5(3)° and Os(1)-Os(2)-C(22) = 103.1(3)°).

The major difference between complexes **5** and **6** lies in the stereochemistry of the hydrocarbyl fragment. The isomers **5** and **6** are distinguished by their respective W-C(1)-C(2)-C(3) dihedral angle. A comparison of the W-C(1)-C(2)-C(3) dihedral angles allowed us to distinguish and describe the difference between the two isomers. In **6**, the bulky WCp* moiety is *gauche* to the phenyl group and is characterized by a W-C(1)-C(2)-C(3) dihedral angle of –84.4(9)°. This conformation contrasts with the stereochemistry described for **5** where the phenyl group was located *anti* to the WCp* fragment. The Fischer representation of both isomers is sketched in Scheme 3.4.

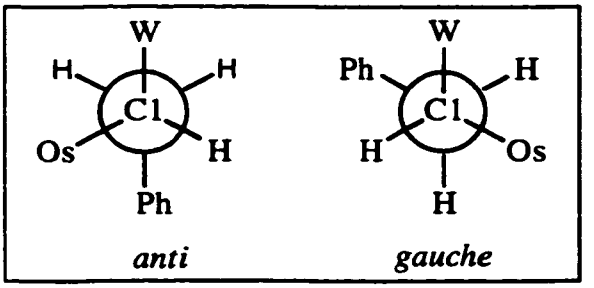

Scheme 3.4 Fischer representation of the μ-η^1-alkylidene ligand of **5** and **6**.

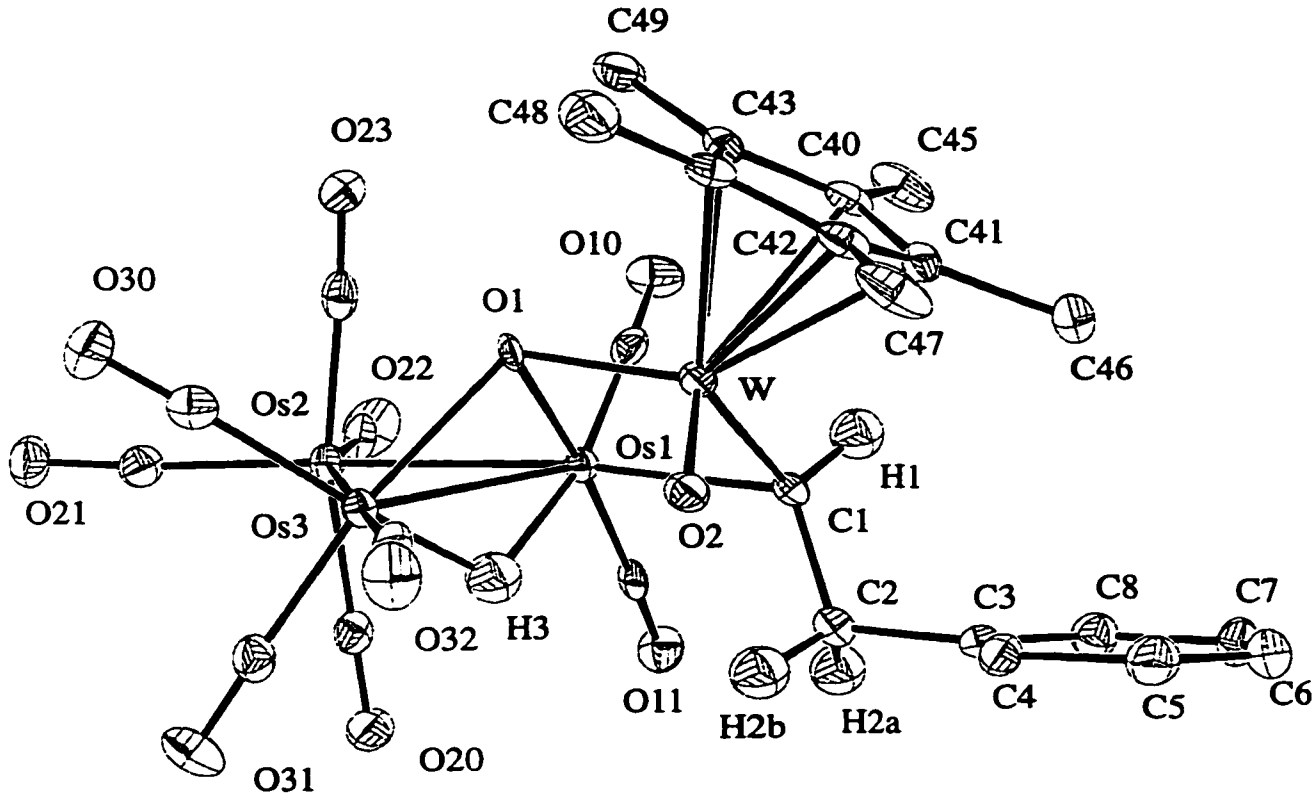

Figure 3.2 The structure of $[Os_3W(\mu\text{-}H)(\textit{gauche}\text{-}\mu\text{-}\eta^1\text{-}CHCH_2Ph)(CO)_9(O)(Cp^*)(\mu_3\text{-}O)]$ **6**.

Table 3.2 Selected bond lengths (Å) and angles (deg) for **6**.

		Lengths	
Os(2)-Os(3)	2.8331(5)	W-O(2)	1.703(5)
Os(2)-Os(1)	2.8160(5)	W-O(1)	1.953(5)
Os(3)-Os(1)	2.8078(5)	W-C(1)	2.055(9)
W-Os(1)	2.6911(4)	Os(1)-C(1)	2.222(8)
Os(1)-O(1)	2.090(5)	C(1)-C(2)	1.55(1)
Os(3)-O(1)	2.180(5)		
		Angles	
Os(2)-Os(1)-Os(3)	60.50(1)	O(2)-W-O(1)	107.1(3)
Os(1)-Os(2)-Os(3)	59.61(1)	Os(1)-C(1)-W	77.9(3)
Os(1)-Os(3)-Os(2)	59.90(1)	W-C(1)-C(2)	119.6(6)
Os(2)-Os(1)-W	132.24(2)	Os(1)-C(1)-C(2)	115.3(5)
Os(3)-Os(1)-W	79.76(1)	C(1)-C(2)-C(3)	113.0(6)
Os(1)-O(1)-W	83.4(2)	Os(2)-Os(1)-O(1)	86.6(1)
Os(3)-O(1)-W	117.1(2)	Os(3)-Os(1)-O(1)	50.3(1)

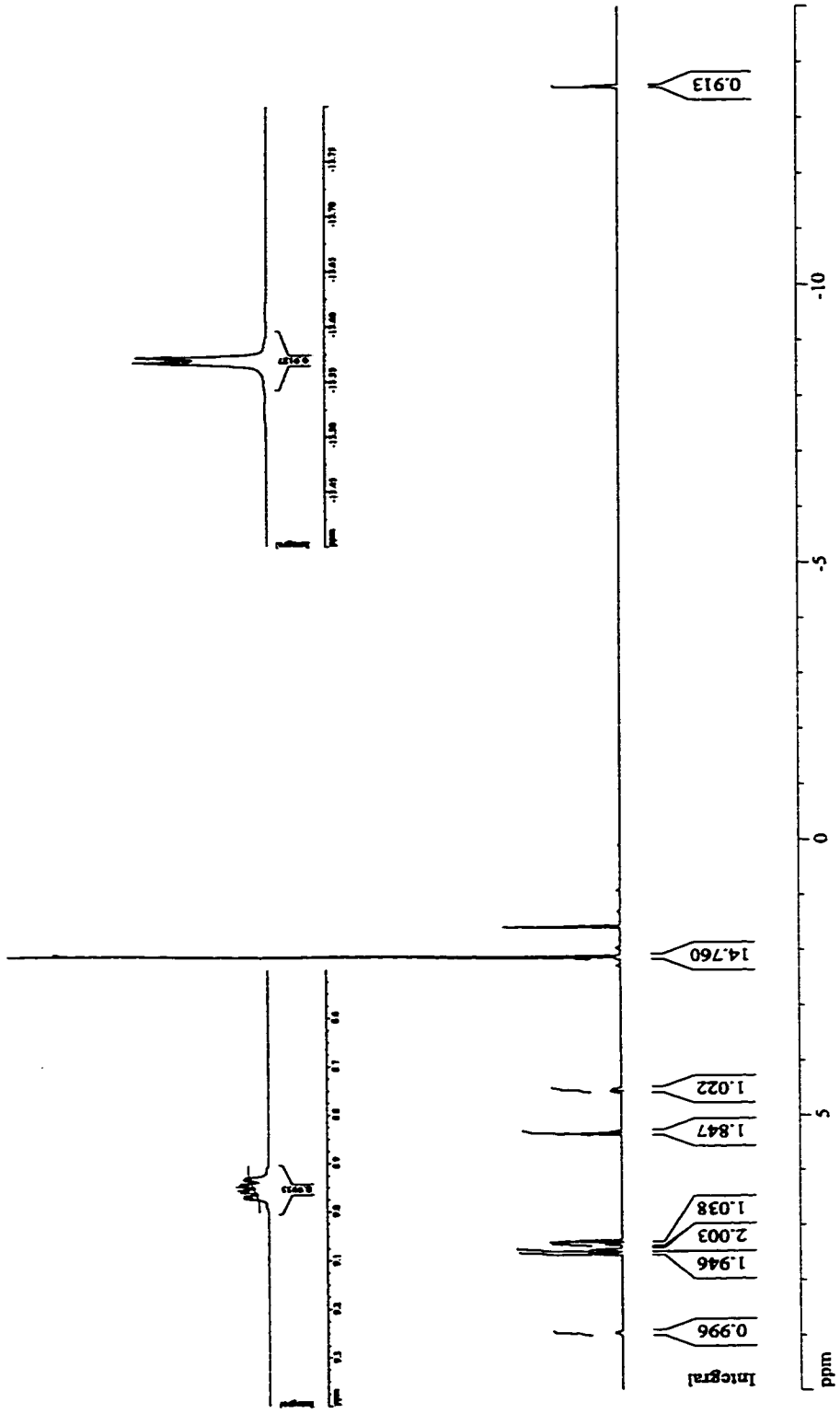

Figure 3.3 ^{1}H NMR spectrum of **5** illustrating the $J^{3}_{H\text{-}H}$ coupling.

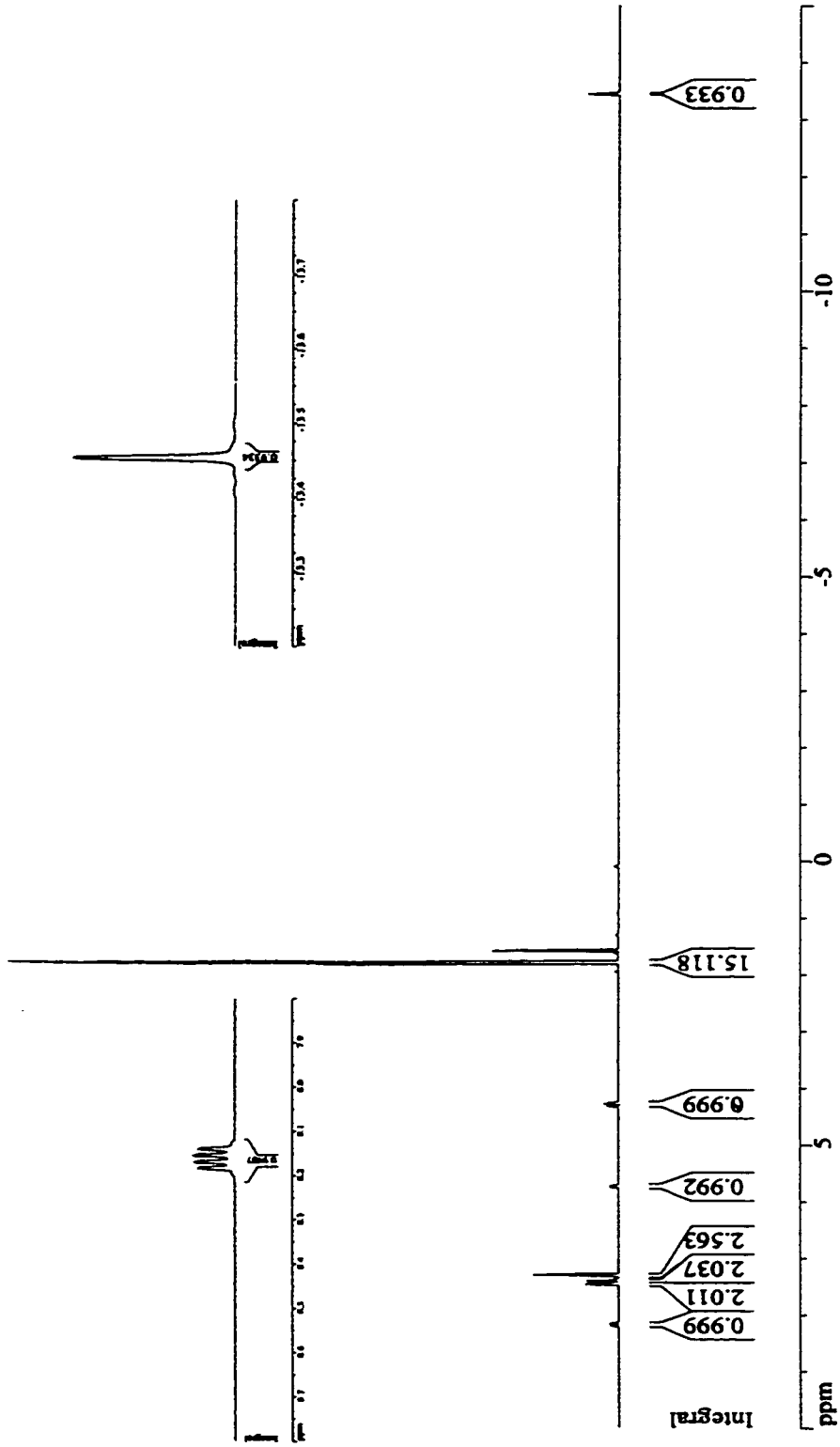

Figure 3.4 ^{1}H NMR spectrum of **6** illustrating the absence of $J^{3}_{H\text{-}H}$ coupling.

3.2.4 Comparative ^{1}H NMR study of 5 and 6

The ^{1}H NMR spectra of compounds **5** and **6** fully established them as alkylidene complexes and also provided a clear distinction between the two isomers (Figure 3.3 and 3.4). Similar ABX patterns (^{1}H NMR) have been observed previously for the two isomeric forms of $[Os_3W(\mu\text{-}Cl)(\mu\text{-}\eta^1\text{-}CHCH_2Tol)(CO)_9(\mu\text{-}O)(Cp)]$.[5] This set of isomers was separated by thin layer chromatography but even though reasonably pure compounds were obtained, only one of the two isomers in the study was characterized by single X-ray crystallography.

The ^{1}H NMR spectrum of complex **5** showed the presence of a doublet at δ -13.57 with a coupling constant of 1.79 Hz as mentioned in Section 3.2.2.1. The signal corresponding to the α-hydrogen of the alkylidene ligand (δ 8.95) also had the same coupling constant. This suggested a J^3 coupling between the hydride localized on the Os(1)-Os(3) bond and the α-hydrogen of the alkylidene ligand. The same coupling was not observed for the *gauche* isomer **6**. The ^{1}H NMR spectrum of **6** revealed the presence of only a singlet at δ -13.75. Hence, the *anti* isomer probably has the appropriate bond orientation (**5**: H(3)-Os(1)-C(1)-H(1) = 22.0(8)°; **6**: H(3)-Os(1)-C(1)-H(1) = 178(1)°) for appreciable coupling whereas the *gauche* isomer has a coupling too small to be distinguished.

3.2.5 Deuterium labeling experiments

Treatment of $[Os_3W(CO)_{10}(O)(\mu\text{-}\eta^1,\eta^2\text{-}CH{=}CHPh)(\mu\text{-}O)(Cp^*)]$ **4** with D_2 gas at room temperature and atmospheric pressure under UV, afforded the labeled complexes $[Os_3W(\mu\text{-}D)(\textit{anti}\text{-}\mu\text{-}\eta^1\text{-}CHCHDPh)(CO)_9(O)(Cp^*)(\mu_3\text{-}O)]$ **5d** and $[Os_3W(\mu\text{-}D)(\textit{gauche}\text{-}\mu\text{-}\eta^1\text{-}CHCHDPh)(CO)_9(O)(Cp^*)(\mu_3\text{-}O)]$ **6d**.

3.2.5.1 Spectroscopic features of 5d and 6d

The ^{2}H NMR spectrum of complex **5d** contained two resonances at δ 4.34 and –13.73 which strongly resemble the chemical shifts obtained from the ^{1}H NMR spectrum of complex **5** (Table 3.3), but broadened by nuclear quadrupole effects. The ^{1}H NMR spectrum of complex **5d** showed the expected resonances for the Cp* and Ph ligands. Similarly, the ^{2}H NMR spectrum of complex **6d** exhibited two peaks with chemical shifts similar to the one

observed in the ^1H NMR of complex **6** (Table 3.3). The expected resonances for the Cp* and Ph ligands were located in the ^1H NMR spectrum of complex **6d**. Thus, the experiment suggested that hydrogen atoms are selectively added to the hydride site and to the C(2) of the vinyl ligand of complex **4**, resulting in the formation of an alkylidene ligand. Chi and co-workers found a similar deuterium addition for the hydrogenation of a vinyl ligand present on a WRe_2 framework.[1]

Table 3.3 Comparison of the ^1H and ^2H chemical shifts for complexes **5** and **6**.

Complex	Non-deuterated	Deuterated
5	4.53 (1H, dd)	4.34 (1H, s)
	-13.57 (1H, d)	-13.73 (1H, s)
6	5.72 (1H, dd)	5.54 (1H, s)
	-13.75 (1H, s)	-13.61 (1H, s)

3.3 Conclusions

Cluster **4** reacted under photolytic conditions with H_2 gas in a non-regioselective manner to produce two novel isomeric clusters (**5-6**) bearing a triply bridging oxide ligand and a μ-η^1-alkylidene organic fragment. Deuterium labeling studies have shown that the hydrogen atoms were added to complex **4** in both a hydride site and to the C(2) of the precursor vinyl ligand.

This reaction provided further evidence of the ability of the doubly bridging oxo ligand to provide an additional lone pair to compensate for the loss of a two electron ligand resulting in the formation of a triply bridging oxo ligand. Hence, the capability of the oxide group to coordinate to a low oxidation state osmium center as a μ-O (WOs) (4 electron) or μ_3-O (WOs_2) (6 electron) ligand was demonstrated further by this reaction. Nonetheless, the exact contribution of the oxo ligand to promote such ligand transformation remains unknown.

Table 3.4 Geometry associated with the μ_3-O ligand of complexes **2**, **3**, **5** and **6**.

Complex	W-O(1) (Å)	Os(1)-O(1) (Å)	Os(3)-O(1) (Å)	W-Os(1) (Å)	Os(1)-Os(3) (Å)	Avg. < (deg)
2	1.959(5)	2.098(5)	2.158(5)	2.7129(5)	2.8120(6)	41.5(8)
3	1.966(9)	2.113(9)	2.163(9)	2.7123(9)	2.8031(9)	40(1)
5	1.957(6)	2.099(6)	2.168(6)	2.7090(5)	2.8038(5)	–42.2(6)
6	1.953(5)	2.090(5)	2.180(5)	2.6911(4)	2.8078(5)	–38.5(6)

The isolation of four complexes containing an uncommon μ_3-O ligand on a WOs_3 metal center allowed us to describe the preferred geometry associated with this ligand. Complexes **2**, **3**, **5** and **6** possess tungsten-oxygen and osmium-oxygen bond lengths that are very similar (Table 3.4). The bond distances were characteristic of a donation of a lone pair from the oxygen to the osmium atoms and a tungsten-oxygen double bond. Many other structural characteristics prevailed throughout the series of clusters. For example, the presence of an oxo bridge induces a contraction of the Os-Os bond distance. As well, the disposition of the carbonyl ligands on Os(3) is distorted by the presence of a μ_3-O ligand. Hence, the axial carbonyl ligands are shifted from their corresponding positions on Os(2) by an average of 41.3(8)° towards the Os(1) atom. Finally, all four complexes carried a hydride ligand located on the Os(1)-Os(3) bond. The hydride positions obtained from the XHYDEX program resembled the location of the hydride of complex **1** which was found from a difference Fourier map.

3.4 Experimental section

3.4.1 Photolysis of $[Os_3W(CO)_{10}(O)(\mu\text{-}\eta^1,\eta^2\text{-}CH{=}CHPh\{W\text{-}Os\})(\mu\text{-}O)(Cp^*)]$ 4 in the presence of H_2 (g)

A sample of **4** (25 mg, 0.019 mmol) was dissolved in 1 mL of dry dichloromethane together with 100 mL of dry hexane in a three-neck 250 mL round bottom flask equipped with a water cooled condenser. The reaction vessel was placed next to a water cooled, quartz filter which housed a 450 W Hg lamp. The red solution was purged with a stream of H_2 (g) and photolyzed for 5 hours and 45 minutes. The reaction proceeded with a color change of the solution from red to purple. The solvent was removed *in vacuo*, and the products were separated from the reaction mixture via thin layer chromatography [eluant: hexane/CH_2Cl_2, 50/50]. This yielded 2 mg of $[Os_3W(\mu\text{-}H)(\textit{gauche}\text{-}\mu\text{-}\eta^1\text{-}CHCH_2Ph)(CO)_9(O)(Cp^*)(\mu_3\text{-}O)]$ **6** (0.002 mmol, 10%), 2 mg of $[Os_3W(\mu\text{-}H)(\textit{anti}\text{-}\mu\text{-}\eta^1\text{-}CHCH_2Ph)(CO)_9(O)(Cp^*)(\mu_3\text{-}O)]$ **5** (0.002 mmol, 10%), 8 mg of $[Os_3W(CO)_9(\mu\text{-}O)_2(\mu\text{-}\eta^1,\eta^2\text{-}CH{=}CHPh\{W\text{-}Os\})(Cp^*)]$ **7** (0.006 mmol, 32%) and 10 mg of starting material (0.008 mmol, 42%). Spectral data for **6**: IR

(hexane): ν(CO) 2093 (m); 2055 (s); 2014 (vs); 2003 (m); 1995 (m); 1978 (w); 1949 (vw). ^{1}H NMR ($CDCl_3$) δ: 8.16 (1H, dd, J^3_{H-H} = 5.66 Hz, J^3_{H-H} = 11.53 Hz); 7.43 (2H, d, J^3_{H-H} = 7.23 Hz); 7.39 (2H, dd, J^3_{H-H} = 7.23 Hz, J^3_{H-H} = 7.28 Hz); 7.31 (1H, d, J^3_{H-H} = 7.28 Hz); 5.72 (1H, dd, J^3_{H-H} = 5.66 Hz, J^2_{H-H} = 12.94 Hz); 4.27 (1H, dd, J^2_{H-H} = 12.94 Hz, J^3_{H-H} = 11.53 Hz); 1.78 (15H, s); -13.75 (1H, s). $^{13}C\{^1H\}$ NMR ($CDCl_3$) δ: 188.7 (1C, s, CO); 185.8 (1C, s, CO); 183.0 (1C, s, CO); 179.4 (1C, s, CO); 176.9 (1C, s, CO); 176.2 (1C, s, CO); 176.0 (1C, s, CO); 175.5 (1C, s, CO); 174.8 (1C, s, CO); 150.6 (1C, t, *C*HCH$_2$Ph, J_{W-C} = 67.7 Hz); 145.06 (1C, s, Ph); 129.5 (2C, s, Ph); 129.8 (2C, s. Ph); 126.7 (1C, s, Ph); 116.0 (5C, s, *C*$_5$Me$_5$); 60.7 (1C, s, CH*C*H$_2$Ph); 10.4 (5C, s, C$_5$*Me*$_5$). FAB-MS (*m/z*): 1279, $[M]^+$; 1279-1139, $[M-nCO]^+$ (n = 1-5). Anal. Calcd. For **6**: C, 25.36; H, 1.89. Found: C, 25.48; H, 1.78%. Spectral data for **5**: IR (hexane): ν(CO) 2093 (m); 2055 (vs); 2019(s); 2014 (s); 2004 (m); 1995(m); 1978 (w); 1947 (vw). ^{1}H NMR ($CDCl_3$) δ: 8.95 (1H, ddd, J^3_{H-H} = 1.79 Hz, J^3_{H-H} = 10.01 Hz, J^3_{H-H} = 5.16 Hz); 7.51 (2H, d, J^3_{H-H} = 7.41 Hz); 7.45 (2H, dd, J^3_{H-H} = 7.41 Hz, J^3_{H-H} = 7.25 Hz); 7.35 (1H, d, J^3_{H-H} = 7.25 Hz); 5.31 (1H, dd, J^2_{H-H} = 14.7 Hz, J^3_{H-H} = 5.16 Hz); 4.53 (1H, dd, J^2_{H-H} = 14.7 Hz, J^3_{H-H} = 10.01 Hz); 2.12 (15H, s); -13.57 (1H, d, J^3_{H-H} = 1.79 Hz). $^{13}C\{^1H\}$ NMR ($CDCl_3$) δ: 186.9 (1C, s, CO); 185.9 (1C, s, CO); 182.9 (1C, s, CO); 179.2 (1C, s, CO); 177.2 (1C, s, CO); 176.2 (1C, s, CO); 176.0 (1C, s, CO); 175.9 (1C, s, CO); 174.8 (1C, s, CO); 146.3 (1C, s, Ph); 139.1 (1C, s, *C*HCH$_2$Ph); 129.1 (2C, s, Ph); 128.3 (2C, s, Ph); 127.0 (1C, s, Ph); 116.8 (5C, s, *C*$_5$Me$_5$); 51.8 (1C, s, CH*C*H$_2$Ph); 10.9 (5C, s, C$_5$*Me*$_5$). FAB-MS (*m/z*): 1279, $[M]^+$; 1279-1139, $[M-nCO]^+$ (n = 1-5). Anal. Calcd. For **5**: C, 25.36; H, 1.89. Found: C, 25.07; H, 1.81%.

3.4.2 Photolysis of [Os$_3$W(CO)$_{10}$(O)(μ-η^1,η^2-CH=CHPh{*W-Os*})(μ-O)(Cp*)] 4 in the presence of D$_2$ (g)

A 50 mg sample of **4** (0.038 mmol) was introduced in a 250 mL three-necked flask equipped with a water cooled condenser and dissolved in 2 mL of dry CH_2Cl_2 and 200 mL of dry hexane. The reaction vessel was placed next to a water cooled, quartz filter which housed a 450 W Hg lamp. A slow purge of D_2 (g) was bubbled through the red solution. After 5 hours and 30 minutes, the D_2 (g) was removed and the solvent removed *in vacuo*. The red/purple residue was dissolved in CH_2Cl_2 and absorbed onto a silica gel TLC plate.

Elution with hexane/CH_2Cl_2 (50/50) yielded 3 mg of [$Os_3W(\mu$-D)(*gauche*-μ-η^1-CHCHDPh)$(CO)_9$(O)(Cp*)(μ_3-O)] **6d** (0.002 mmol, 5.3%), 3mg of [$Os_3W(\mu$-D)(*anti*-μ-η^1-CHCHDPh)$(CO)_9$(O)(Cp*)(μ_3-O)] **5d** (0.002 mmol, 5.3%), 15 mg of [$Os_3W(CO)_9(\mu$-O$)_2(\mu$-η^1,η^2-CH=CHPh{*W-Os*})(Cp*)] **7** (0.012 mmol, 31.6%) and 25 mg of starting material (0.019 mmol, 50%). Spectroscopic analyses were performed on compounds **5d** and **6d**. Spectral data for **6d**: IR (hexane): ν(CO) 2093 (m); 2054 (s); 2014 (vs); 2003 (m); 1995 (m); 1978 (w); 1949 (vw). ^{1}H NMR ($CDCl_3$) δ: 8.15 (1H, d, $J^3_{H\text{-}H}$ = 11.67 Hz); 7.45 (2H, d, $J_{H\text{-}H}$ = 6.99 Hz); 7.39 (2H, dd, $J_{H\text{-}H}$ = 6.99 Hz, $J_{H\text{-}H}$ = 7.32 Hz); 7.31 (1H, d, $J_{H\text{-}H}$ = 7.32 Hz); 4.25 (1H, d, $J^3_{H\text{-}H}$ = 11.67 Hz); 1.78 (15H, s). ^{2}H NMR ($CHCl_3$) δ: 5.54 (1H, s); -13.61 (1H, s). Anal. Calcd. for **6d**: C, 25.41; H, 1.66. Found C, 25.30; H, 1.71%. Spectral data for **5d**: IR (hexane): ν(CO) 2093 (m); 2054 (vs); 2019(s); 2013 (s); 2004 (m); 1994(m); 1978 (w); 1947 (vw). . ^{1}H NMR ($CDCl_3$) δ: 8.94 (1H, dd, $J^3_{H\text{-}H}$ = 5.05 Hz); 7.51 (2H, d, $J^3_{H\text{-}H}$ = 7.44 Hz); 7.44 (2H, dd, $J^3_{H\text{-}H}$ = 7.44 Hz, $J^3_{H\text{-}H}$ = 7.27 Hz); 7.35 (1H, d, $J^3_{H\text{-}H}$ = 7.27 Hz); 5.31 (1H, d, $J^3_{H\text{-}H}$ = 5.05 Hz); 2.12 (15H, s). ^{2}H NMR ($CHCl_3$) δ: 4.34 (1H, s); -13.73 (1H, s). Anal. Calcd. for **5d**: C, 25.41; H, 1.66. Found C, 25.32; H, 1.60%.

3.4.3 X-ray structural analysis of 5 and 6

Single crystals of **5** were grown from concentrated CH_2Cl_2/hexane solutions at −15°C. A yellow crystal of approximate dimensions 0.10 x 0.18 x 0.22 mm was chosen and mounted on a glass fiber. Cluster **5** crystallizes in the monoclinic space group *P*21/*a* and contains 1 equivalent of a disordered CH_2Cl_2 solvent molecule per unit cell. A half-occupied molecule was located and a second half occupied molecule was symmetry generated. Data were collected at −100°C. Of the unique 8231 unique reflections collected, 6714 reflections with I > 2.5σ(I) were used for the refinement. The Patterson map provided the location of the four metal atoms. Difference Fourier maps provided the location of all remaining atoms, except the hydrogen atoms. The hydrogen atoms were generated, except for the bridging hydride H(3) for which the position was obtained from the XHYDEX program. Anisotropic refinement was performed for the non-hydrogen atoms. The H(1), H(2a) and H(2b) atoms were refined both positionally and thermally in a isotropic manner. All the other hydrogen

atoms were not refined. The refinement yielded $R = 0.041$ and $R_W = 0.052$. Full details are located in Appendix A.5.

Yellow prisms of **6** were obtained in a similar manner as described for complex **5**. A crystal of dimensions 0.21 x 0.1 x 0.25 mm was mounted on a glass fiber. Compound **6** crystallizes in the monoclinic space group $P21/n$ with $Z = 4$. Diffraction data were collected at −100°C. A total of 8117 independent data were collected of which 6301 were considered as being observed. The heavy atom positions were obtained from a Patterson map with the lighter elements being located in subsequent difference Fourier maps. All non-hydrogen atoms were refined anisotropically. Hydrogen atoms were included in calculated positions with fixed isotropic thermal parameters. The location of H(3) specifically was found using the XHYDEX software. Final R and R_W values were 0.035 and 0.037 respectively. Complete crystallographic details are included in Appendix A.6.

3.5 References

1. Chi, Y.; Wu, H.-L; Chen, C.-C.; Su, C.-J.; Peng, S.-M; Lee, G.-H. *Organometallics* **1997**, 16, 2434.

2. (a) Sappa, E.; Tiripicchio, A.; Braunstein, P. *Chem. Rev.* **1983**, 83, 203. (b) Raithby, P.R.; Rosales, M.J. *Adv. Inorg. Chem. Radiochem.* **1985**, 29, 169. (c) Jeannin, Y. *Transition Met. Chem.* **1993**, 18, 122.

3. (a) Chi, Y; Cheng, P.-S.; Wu, H.-L.; Hwang, D.-K.; Su, P.-C., Peng, S.-M.; Lee, G.-H. *J. Chem. Soc., Chem. Commun.*, **1994**, 1839.

4. Shapley, J.R.; Park, J.T. *J. Am. Chem. Soc.* **1984**, 106, 1144.

5. Chi, Y.; Shapley, J.R.; Ziller, J.W.; Churchill, M.R. *Organometallics* **1987**, 6, 301.

6. Churchill, M.R.; Li, Y.-J. *J. Organomet. Chem.* **1985**, 294, 367.

7. Churchill, M.R.; Li, Y.C. *J. Organomet. Chem.* **1985**, 291, 61.

8. (a) Churchill, M.R.; Ziller, J.W.; Freudenberger, J.H.; Schrock, R.R. *Organometallics* **1984**, 3, 1554. (b) Freudenberger, J.H.; Schrock, R.R.; Churchill, M.R.; Rheingold, A.L.; Ziller, J.W. *Organometallics* **1984**, 3, 1563. (c) Churchill, M.R.; Ziller, J.W. *J. Organomet. Chem.* **1985**, 286, 27.

9. Orpen, A.G. *J. Chem. Soc. Dalton Trans.* **1980**, 2509.

Chapter Four

Thermolysis of $[Os_3W(CO)_{10}(O)(\mu\text{-}\eta^1,\eta^2\text{-}CH{=}CHPh\{W\text{-}Os\})(\mu\text{-}O)(Cp^*)]$ 4

4.1 Introduction

The potential for transition metal clusters and cluster bound ligands to model the reaction mechanisms by which small organic fragments react on the surface of heterogeneous catalysts has resulted in a great deal of interest in these systems.[1]

The cluster-surface analogy arises from the structural similarities between metal crystallites and metal clusters.[1a] Metal surfaces display faces based on deltahedra or square arrays. The deltahedral unit is the most commonly encountered skeletal feature in metal clusters.[1a,2] In contrast, the square metal array is only occasionally found but still well characterized.[3] Metal clusters can only approximate the electronic complexity of a surface.[4] Nonetheless it is believed that the directed bonding theorems of chemistry can successfully describe the behavior of surface bound ligands.[5]

Major differences exist between clusters and surfaces.[1a] The difference in connectivity between surface and cluster metal atoms is reflected in the bulk electronic properties of the metal unit.[4] Furthermore, intermetallic distances in bulk metals are shorter than those present in small metal arrays. For example, bond lengths in Ru metal are evaluated at 2.68 Å,[6] compared with an average of 2.80 Å in ruthenium clusters. Nonetheless, absorption on a surface results in the elongation of the underlying metal-metal bonds as observed for a nickel surface (~ 8.5% for the adsorption of carbon atoms).[7] Conversely, metal cluster M-M bond lengths decrease with increasing nuclearity as cluster size approaches that of a metal crystallite.

Much interest has focussed on hydrocarbyl ligands and their interactions with surfaces, in terms of both bonding and reactivity.[1a] The class of hydrocarbyl ligands of interest includes acetylenic, olefinic, and alkyl groups, and their derivatives. Since this

section of the thesis focuses on the bonding of vinyl ligands on oxo-bridged mixed-metal clusters, discussion has focussed on the reactivity of vinyl ligands attached to a metal array. The fundamental reactions of surface bound vinyl groups are listed below:[8,9,10,11,12,13,14,15,16,17,18,19,20,21,22]

1) Hydrogenation of acetylene; $H + HC{\equiv}CR \rightarrow CH{=}CHR$
2) Coupling reaction; $2HC{=}CH_2 \rightarrow C_4H_4 + H_2$
3) Vinylidene formation; $HC{=}CH_2 \rightarrow H + C{=}CH_2$
4) Acetylene formation; $HC{=}CH_2 \rightarrow H_2 + HC{\equiv}CH$
5) Ethylene formation; $HC{=}CH_2 + H \rightarrow H_2C{=}CH_2$
6) Carbon-carbon bond scission; $HC{=}CH_2 \rightarrow CH + CH_2$

The bonding and reactivity of vinyl fragments on surfaces is largely dependent on the metal, the crystal face, and the surface coverage. On Ni(100),[15-19] Pt(111)[8,20,21] and Ag(111)[12-14], the surface $CHCH_2$ species have been classified as η^1-vinyls where the hydrogen-deficient carbon atom is σ bonded to the metal surface. Conversely, Pd(100)[22] and Ru(001)[11] features side-on (η^2) coordination of the vinyl groups to the metal through the π bond.

In these systems, the reactivity of surface vinyls is as follows: on Ag(111), vinyls couple to produce butadiene at 250-260 K; on Pt(111), vinyls disproportionate to form ethylidyne ($C\text{-}CH_3$), but only by going through a series of transformations that involve the formation of both vinylidene ($C{=}CH_2$) and acetylene ($HC{\equiv}CH$);[8] on Ni(100) vinyls decompose to acetylene ($HC{\equiv}CH$) at 230 K; on Ru(001), vinyls are further hydrogenated and ethylene desorbs between 150 and 250 K; and on Pd(100), the carbon-carbon bond of the vinyl specie is broken resulting in the formation of methylidyne (CH) and methylidene (CH_2) at 275 K. Thus, three different reaction pathways are observed for η^1-vinyls: coupling on Ag(111), α-C—H bond scission on Pt(111), and β-C—H bond scission on Ni(100) and Pt(111). Conversely, two reaction pathways are available for η^2-vinyls: C-H bond formation on Ru(001) and C-C bond scission on Pd(100).

The behavior of vinyl ligands in cluster chemistry fully supports most of these results. Conversions have been reported for vinyl to vinylidene[23,24] and to acetylene[23] and for acetylene to vinyl.[25] Examples are illustrated in Figure 4.1.

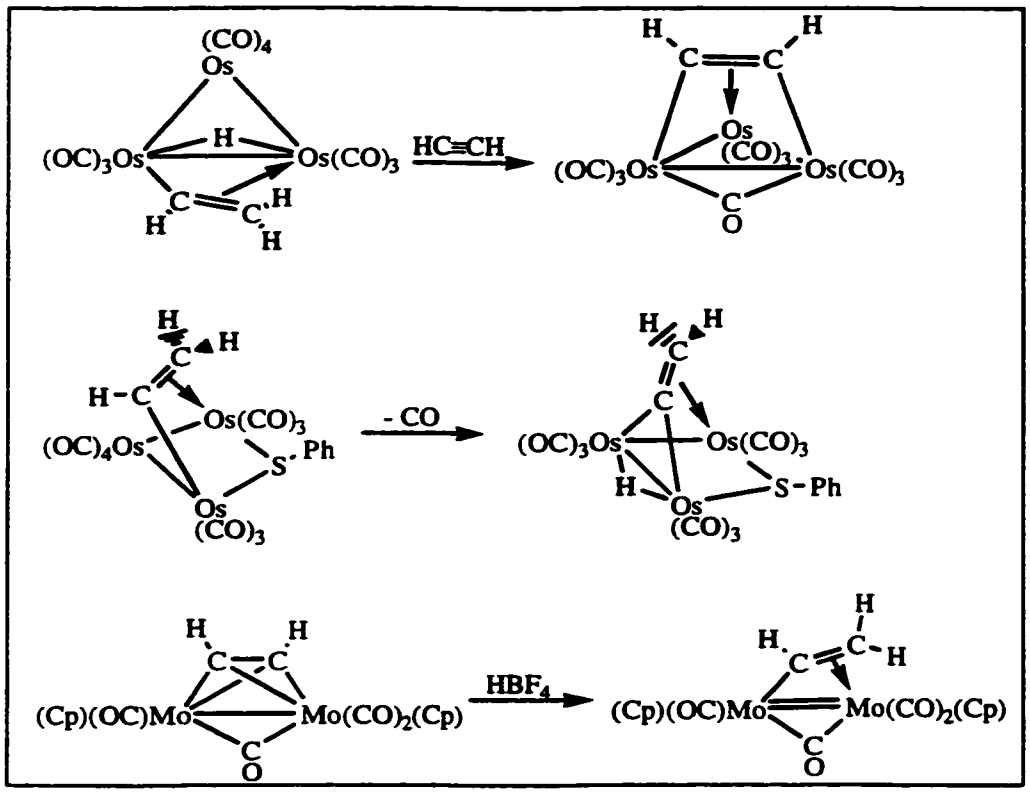

Figure 4.1 Reaction of vinyl ligands when bound to metal clusters.

It is widely accepted that chemisorbed species must be mobile in order to account for reactions catalyzed by surface metal atoms.[1a] A similar behavior is also encountered in cluster chemistry which further reinforces the cluster-surface analogy. Hence, the study of ligand dynamics, metal fragment mobility, metal framework rearrangements and/or metal fragment lability in organometallic complexes may provide further insights on the migration of chemisorbed molecules on metal surfaces.[26] For example, the free rotation of metal coordinated olefins,[27] the fluxionality of the bonding of π-allyl species,[28] and the shift of the σ-bonding around the carbon atoms of the ring in σ-metal cyclopentadienyl or aryl species[29] suggest that chemisorption species may undergo similar movements on covered surfaces.

Since chemical transformations occurring on metal surfaces proceed from reactants to products via several intermediate species, organometallic clusters may also provide models of organic fragments in unusual bonding arrangements from which potential intermediates may be proposed. In fact, due to the difficulties of characterizing absorbate interactions on metal surfaces, the cluster-surface analogy has been most successful in defining modes of metal-ligand bonding in discrete molecular clusters as models for metal-ligand binding on surfaces. Available crystallographic and spectroscopic (mainly IR) data for molecular clusters containing carbonyl, alkyne, vinylidene and benzene ligands helps surface scientists define the binding modes of these ligands on metal surfaces.[1d]

4.2 Results and discussion

4.2.1 Summary and synthesis

The pyrolysis of **4** in heptane at 100°C resulted in a color change of the solution from orange to dark red. Thin layer chromatography indicated that six complexes were formed. Monitoring the reaction via infrared spectroscopy and TLC analysis suggests the reaction sequence illustrated in Scheme 4.1. This scheme is closely related to a sequence of reactions observed by Chi and co-workers during the thermolysis of $[Os_3(CO)_{10}(NCMe)_2]$ with $[W(C{\equiv}CPh)(O)_2(Cp^*)]$.[30]

The initial product formed upon pyrolysis of **4** is the strikingly purple colored complex $[Os_3W(CO)_9(\mu\text{-}O)_2(\mu\text{-}\eta^1,\eta^2\text{-}CH{=}CHPh\{W\text{-}Os\})(Cp^*)]$ (**7**), following decarbonylation and skeletal rearrangement of the precursor. Cluster **7** consists of a butterfly arrangement of metal atoms with the terminal oxo ligand originally present in **4** now shifted to a bridging position in **7**.

Cluster **7** isomerizes to $[Os_3W(CO)_9(\mu\text{-}O)_2(\mu\text{-}\eta^1,\eta^2\text{-}CH{=}CHPh\{Os\cdots Os\})(Cp^*)]$ (**8**) upon further thermal treatment. The isomerization involves the breakage of an Os-Os bond and the formation of an additional W-Os bond. The vinyl ligand of **7** positioned on a W-Os vector has shifted and is now linking the two non-bonding osmium atoms of complex **8**.

Complex **8** is structurally related to the previously characterized $[Os_3W(CO)_9(\mu\text{-}\eta^1,\eta^2\text{-}C{\equiv}CPh)(\mu\text{-}O)_2(Cp^*)]$[30] which was obtained after the addition of $[W(C{\equiv}CPh)(O)_2(Cp^*)]$ to $[Os_3(CO)_{10}(NCMe)_2]$.

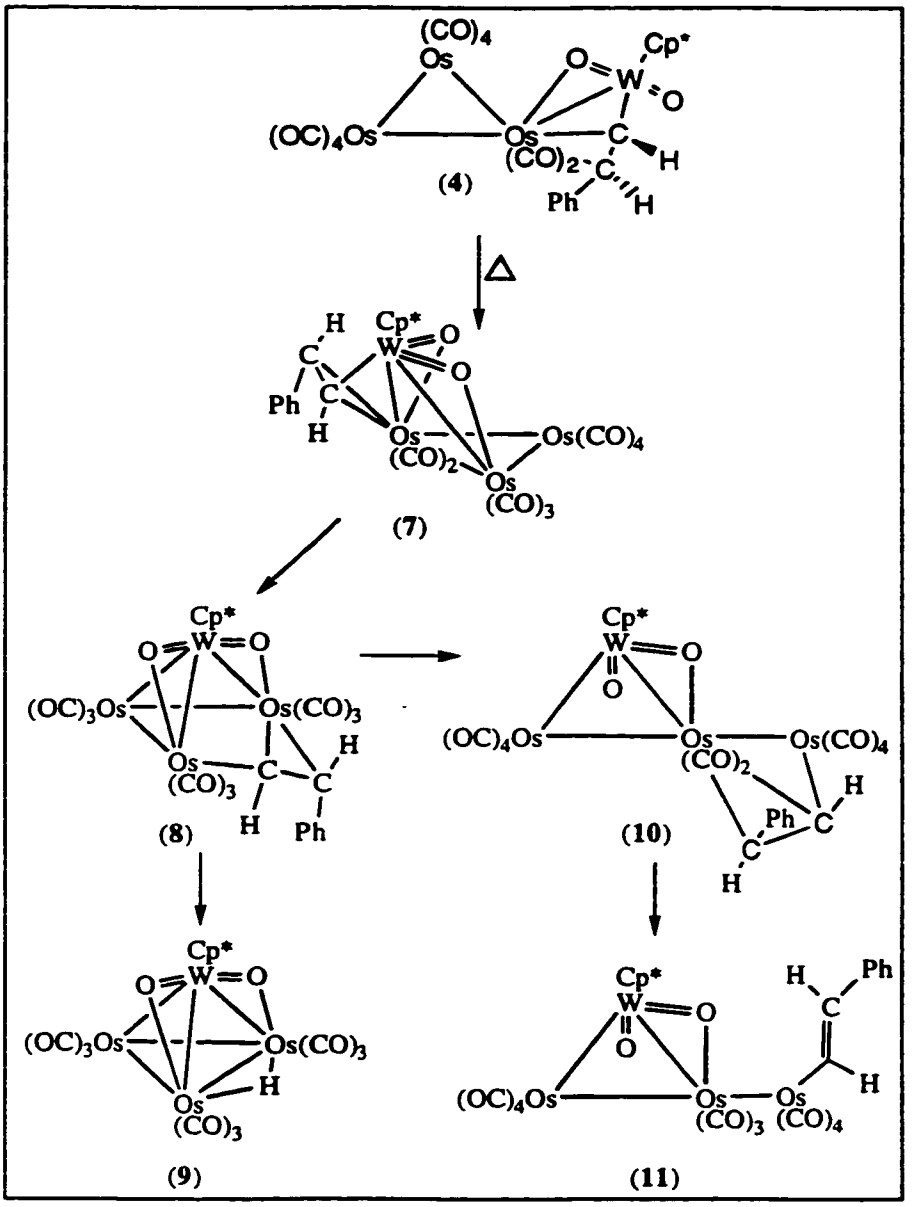

Scheme 4.1 Proposed reaction pathway.

Complex **8** reacts with carbon monoxide liberated during previous reaction steps or abstracted from other metals to produce $[Os_3W(CO)_{10}(O)(\mu\text{-}\eta^1,\eta^2\text{-}CH{=}CHPh\{Os\text{-}Os\})(\mu\text{-}O)(Cp^*)]$ (**10**). Cluster **10** consists of a spiked triangular array of metal atoms. The key

features involved in its formation are the shifting of one edge-bridging oxo ligand in **8** to the terminal mode and the breakage of a W-Os bond resulting in the opening of the butterfly framework of the precursor and the formation of a 4 metal-metal bond spiked triangular structure. Furthermore, complex **10** is related to complex **4** via a metal vertex isomerization. The $W(O)_2(Cp^*)$ apex and one of the $Os(CO)_4$ centers are interchanged in the conversion of **4** to **10** via a series of intermediates.

Complex **10** undergoes addition of one carbon monoxide molecule which is accompanied by the release of the μ-η^1,η^2-vinyl ligand to the terminal mode resulting in the formation of $[Os_3W(\eta^1\text{-}CH{=}CHPh)(CO)_{11}(O)(\mu\text{-}O)(Cp^*)]$ (**11**) (Scheme 4.1). Complex **11** is closely related to a structurally characterized acetylide complex $[Os_3W(\eta^1\text{-}C{\equiv}CPh)(CO)_{11}(O)(\mu\text{-}O)(Cp^*)]$ which was obtained from the treatment of $[Os_3W(CO)_9(\mu\text{-}\eta^1,\eta^2\text{-}C{\equiv}CPh)(\mu\text{-}O)_2(Cp^*)]$ with carbon monoxide.[30]

Two complexes devoid of a hydrocarbyl fragment were also isolated from the reaction mixture. The first of these complexes was $[Os_3W(\mu\text{-}H)(CO)_9(\mu\text{-}O)_2(Cp^*)]$ (**9**) which was previously obtained from the treatment of $[Os_3W(CO)_9(\mu\text{-}\eta^1,\eta^2\text{-}C{\equiv}CPh)(\mu\text{-}O)_2(Cp^*)]$ with dihydrogen.[30] The structural similarities between **8** and $[Os_3W(CO)_9(\mu\text{-}\eta^1,\eta^2\text{-}C{\equiv}CPh)(\mu\text{-}O)_2(Cp^*)]$, together with comparable reaction conditions (heating at 100°C for two hours) suggested that **8** may be an intermediate in the transformation of $[Os_3W(CO)_9(\mu\text{-}\eta^1,\eta^2\text{-}C{\equiv}CPh)(\mu\text{-}O)_2(Cp^*)]$ to **9** via treatment with dihydrogen. Hence, it is likely that **8** is the precursor to **9**.

The second hydrocarbyl-free complex produced during the pyrolysis of **4** is $[Os_3W(CO)_8(\mu\text{-}O)_2(Cp^*)]_2$ (**12**). The metal framework of **12** consists of an Os_6 rhombic raft where the two outer most triangles are capped by $[W(\mu\text{-}O)_2(Cp^*)]$ fragments. While hexaosmium raft complexes have been synthesized previously,[31] the metal framework of most of these complexes consists of three fused outer triangles (triangular raft) as illustrated in Figure 4.2. For example, the reaction between $[Os_6(CO)_{20}]$ and dioxygen and $P(OMe_3)$ afforded $[Os_6(CO)_{18}(\mu_3\text{-}CO)(\mu_3\text{-}O)]$ and $[Os_6(CO)_{17}\{P(OMe)_3\}_4]$, respectively.

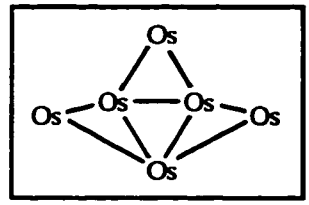

Figure 4.2 Metal framework of $[Os_6(CO)_{18}(\mu_3\text{-}CO)(\mu_3\text{-}O)]$ and $[Os_6(CO)_{17}\{P(OMe)_3\}_4]$.

A rare example of an Os_6 rhombic raft is $[Os_6(CO)_{20}\{C{=}C(H)R\}]$ (R = Me, Ph) which was obtained on addition of excess of HC≡CR (R = Me, Ph) to a solution of $[Os_6(CO)_{20}(MeCN)]$. Much of the interest in these complexes arises from the structural analogy between the Os_6 planar framework and the exposed (111) plane of metal surfaces.[31,32] Hence, the interaction of simple, unsaturated organic molecules with these "raft" complexes may provide metal-ligand bonding modes which may be of relevance to the organic/metal surface interaction. Molecular orbital calculations have shown the presence of an empty low lying molecular orbital in the Os_6 raft systems which indicates that they may be susceptible to nucleophilic addition reactions.[33]

It is possible that **12** is formed by dimerization of **10**, accompanied by the reductive elimination of a 1,4-diphenyl buta 1,3-diene molecule together with the elimination of four CO molecules. Such speculation is encouraged by the requirement for carbon monoxide to complete the sequence **8** → **10** → **11**.

4.2.2 Spectroscopic features of $[Os_3W(CO)_9(\mu\text{-}O)_2(\mu\text{-}\eta^1,\eta^2\text{-}CH{=}CHPh\{W\text{-}Os\})(Cp^*)]$ 7

The infrared spectrum of this purple crystalline complex showed characteristic stretching bands arising from terminal carbonyl ligands. The ^1H and ^{13}C NMR spectra contained the anticipated resonances for the Cp* and Ph ligands. In addition, two ^1H resonances were observed at δ 9.50 and 4.01 with a $J_{H\text{-}H}$ of 13 Hz similar to the parent compound **4** and characteristic of a *trans* substituted vinyl ligand. The ^{13}C NMR spectrum contained signals at δ 143.3 and 74.4, which may be attributed to the hydrocarbyl fragment. The FAB mass spectrum contained a molecular ion at *m/z* 1277, which fragmented by loss of up to four CO ligands. All the spectroscopic data (IR, ^1H NMR and ^{13}C NMR) for this

complex and the others to follow are included in Table 4.1 located in the experimental section.

4.2.2.1 X-ray structure of 7

An ORTEP plot of $[Os_3W(CO)_9(\mu\text{-}O)_2(\mu\text{-}\eta^1,\eta^2\text{-}CH{=}CHPh\{W\text{-}Os\})(Cp^*)]$ (**7**) is shown in Figure 4.3 and selected bond distances and angles are given in Table 4.2. The molecular structure of **7** consists of a WOs_3 butterfly core with the W and Os(3) atoms occupying wing-tip positions. A total of nine terminal carbonyl ligands are distributed on Os(1), Os(2) and Os(3) in the usual distorted octahedral conformation. The dihedral angle between the W-Os(1)-Os(2) and Os(1)-Os(2)-Os(3) planes is 116.89(4)°. The Os-Os distances observed (Os(1)-Os(2) = 2.8476(6), Os(1)-Os(3) = 2.8394(6), Os(3)-Os(2) = 2.8563(6) Å) are in the range expected for Os-Os single bonds.[34] The W-Os(2) bond length separation (W-Os(2) = 2.9219(6) Å) is similar to that observed in $[Os_3W(CO)_9(\mu\text{-}\eta^1,\eta^2\text{-}C{\equiv}CPh)(\mu\text{-}O)_2(Cp^*)]$ (avg. W-Os = 2.998 Å).[30] The W-Os(1) bond distance (W-Os(1) = 2.7281(6) Å) is significantly shorter. The W-Os(1) bond is bridged, by both a μ-O ligand and $\mu\text{-}\eta^1,\eta^2$-CH=CHPh fragment. Hence, the presence of a second bridging ligand on W-Os(1) may favor the contraction of the M-M bond length.

The vinyl ligand is linked to the W and Os(1) atoms in a $\mu\text{-}\eta^1,\eta^2$ fashion (W-C(1) = 2.135(9), Os(1)-C(1) = 2.197(9), Os(1)-C(2) = 2.32(1) Å, C(1)-C(2) = 1.39(2) Å). The vinyl ligand features a phenyl substituent *trans* to the W atom with a dihedral angle W-C(1)-C(2)-C(3) = -178(2)°. The C(1)-C(2) axis is perpendicular to the W-Os(1) vector with a torsion angle of −178(1)° for Os(2)-Os(1)-C(1)-C(2). A measure of the degree of interaction between Os(1) and the vinyl fragment was obtained from the "bent-back" angles at C(1) and C(2) (Chapter 2). The coordination is best described as a simple π donation from C(1) and C(2) to the Os(1) atom [W-C(1)-C(2) = 116.4(7)° and C(1)-C(2)-C(3) = 125.0(9)°]. The overall coordination mode of the vinyl ligand of complex **7** was observed in complex **4**.

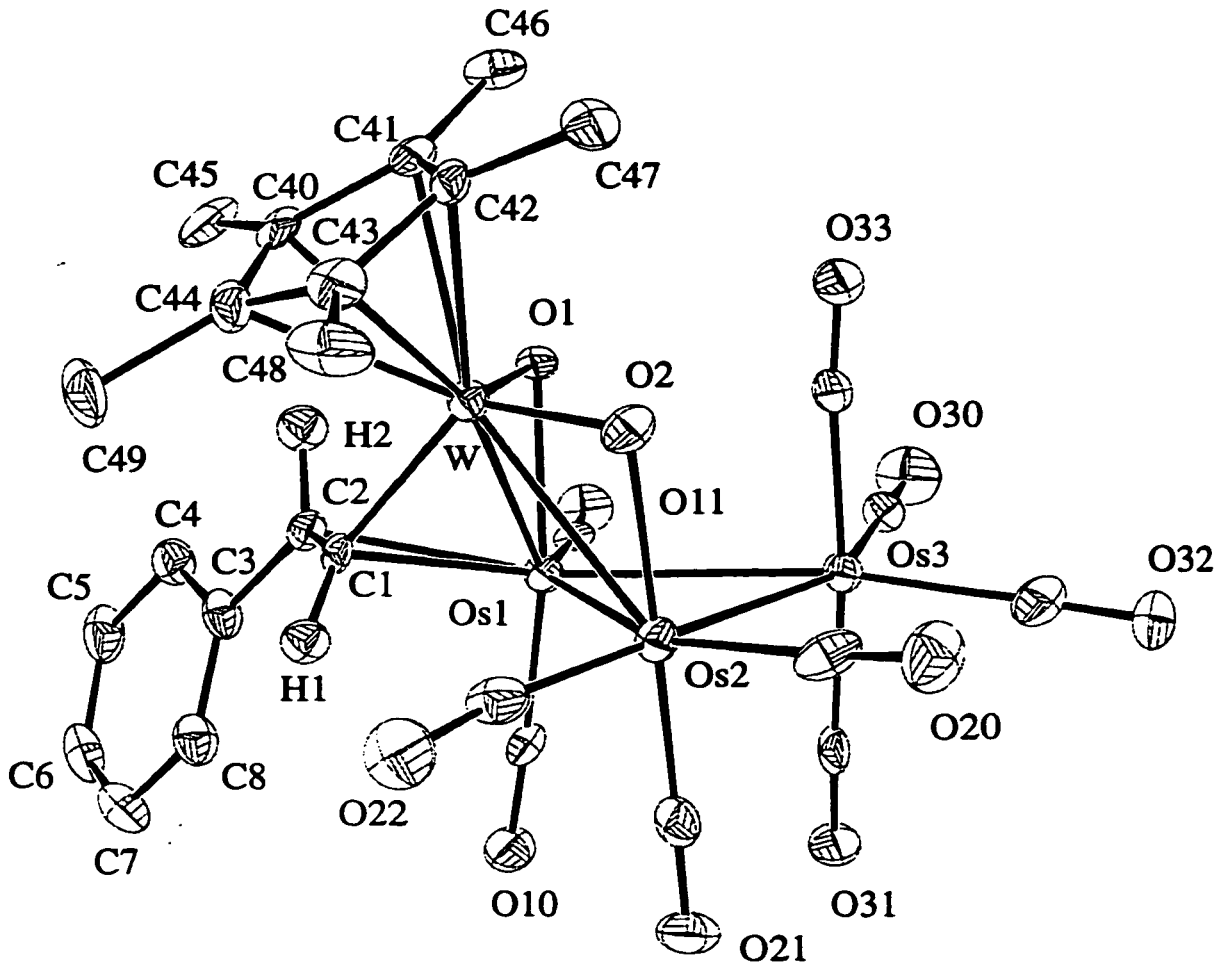

Figure 4.3 The molecular structure of $[Os_3W(CO)_9(\mu\text{-}O)_2(\mu\text{-}\eta^1,\eta^2\text{-}CH{=}CHPh\{W\text{-}Os\})(Cp^*)]$ **7**.

Table 4.2 Selected bond lengths (Å) and angles (deg) for **7**.

		Lengths	
Os(1)-Os(2)	2.8476(6)	W-O(1)	1.773(7)
Os(1)-Os(3)	2.8394(6)	W-O(2)	1.825(7)
Os(2)-Os(3)	2.8563(6)	W-C(1)	2.135(9)
Os(1)-W	2.7281(6)	Os(1)-C(1)	2.197(9)
Os(2)-W	2.9219(6)	Os(1)-C(2)	2.32(1)
Os(1)-O(1)	2.199(6)	C(1)-C(2)	1.39(2)
Os(2)-O(2)	2.087(7)		
		Angles	
Os(2)-Os(1)-Os(3)	60.30(2)	Os(2)-O(2)-W	96.4(3)
Os(1)-Os(2)-Os(3)	59.71(2)	O(1)-W-O(2)	107.7(3)
Os(1)-Os(3)-Os(2)	59.99(2)	Os(1)-C(1)-W	78.0(3)
Os(2)-Os(1)-W	63.16(2)	W-C(1)-C(2)	116.4(7)
Os(3)-Os(1)-W	97.29(2)	Os(1)-C(1)-C(2)	76.8(6)
Os(1)-Os(2)-W	56.42(2)	C(1)-C(2)-C(3)	125.0(9)
Os(3)-Os(2)-W	92.66(2)	Os(2)-Os(1)-O(1)	92.5(2)
Os(1)-O(1)-W	86.1(3)	Os(3)-Os(1)-O(1)	89.6(2)

An interesting feature of complex **7** was the presence of two bridging oxo ligands on adjacent W-Os vectors. The bond lengths to the oxo ligands (W-O(1) = 1.773(7), O(1)-Os(1) = 2.199(6), W-O(2) = 1.825(7), O(2)-Os(2) = 2.087(7) Å; Os(1)-O(1)-W = 86.1(3)°, Os(2)-O(2)-W = 96.4(3)°) are similar to the distances observed in $[Os_3W(\mu\text{-}H)(CO)_9(\mu\text{-}O)_2(Cp^*)]$.[30] The authors explained the bonding mode of the oxo ligands observed in the latter by utilizing the concept of electron counting and concluded that the oxygen atoms contribute three electrons each to the metal framework. The donor ability of the oxo ligand (as a three electron donor) is clearly different from that of the previously described W=O:→Os oxo ligand (as a four electron donor). This observation is explained in terms of the resonance of the trivalent W=O:→Os and the divalent W-O-Os bonding forms (Figure 4.4).[35] Using the same logic, we propose that the two bridging oxo ligands combined act as a six electron donor. By treating all metal atoms and ligands as formally neutral, cluster **7** is electron precise with a total of 62 cluster valence electrons as expected for a 5 M-M bond butterfly cluster.

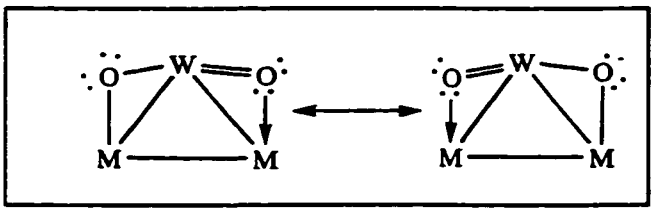

Figure 4.4 Resonance of the trivalent and the divalent bonding forms.

4.2.3 Spectroscopic features of $[Os_3W(CO)_9(\mu\text{-}O)_2(\mu\text{-}\eta^1,\eta^2\text{-}CH{=}CHPh\{Os\cdots Os\})(Cp^*)]$ 8

The infrared spectrum of the yellow complex **8** showed the presence of only terminal carbonyl groups. The ^1H and ^{13}C NMR spectra showed the anticipated resonances for the Cp* and Ph ligands. Two additional broader ^1H resonances were located at δ 5.51 and 3.85 with a $J_{H\text{-}H}$ = 18 Hz characteristics of *trans* substituted vinyl ligand. The ^{13}C NMR spectrum showed two peaks at δ 101.7 and 66.3 attributed to the hydrocarbyl fragment. In addition, five resonances between δ 186.9 and 171.9 corresponding to CO groups were present and suggested that **8** was fluxional (Section 4.2.3.2). The FAB mass spectrum was characterized

by an $[M]^+$ ion at *m/z* 1277, which fragmented by loss of CO ligands to give $[M\text{-}nCO]^+$ (n = 1-9) daughter ions.

4.2.3.1 X-ray structure of 8

As illustrated by the ORTEP plot in Figure 4.5, **8** was identified as $[Os_3W(CO)_9(\mu\text{-}O)_2(\mu\text{-}\eta^1,\eta^2\text{-}CH{=}CHPh\{Os\cdots Os\})(Cp^*)]$. Pertinent bond lengths and angles are summarized in Table 4.3. The metal framework consists of a WOs_3 butterfly core with a W-Os(3) hinge and a dihedral angle between the Os(2)-W-Os(3) and Os(1)-W-Os(3) wings of the butterfly of –92.06(6)°. The metal framework includes three W-Os bonds, of which two are linked by μ-oxo ligands. Within the metal core, the Os(1)-Os(3) (2.888(1) Å) and the Os(2)-Os(3) (2.946(1) Å) bond lengths are in the range expected for Os-Os single bonds. The Os(1)···Os(2) separation of 3.817(1) Å clearly indicates that there is no direct Os(1)···Os(2) bonding interaction. The coordination geometry about each osmium center is completed by three terminal carbonyl ligands, giving rise to octahedral geometry in each case. The tungsten center is seven coordinated, which is a common coordination environment for this metal.

The two W-Os bonds supporting oxo ligands are of equal length (W-Os(1) = 2.985(1), W-Os(2) = 2.999(1) Å) within error and are similar to the oxo bridged W-Os bond in **7**. Conversely, the unsupported W-Os(3) hinge (2.602(1) Å) is significantly shorter and is in fact one of the shortest W-Os single bonds to have been observed in W-Os oxo-carbonyl cluster complexes to date. The isostructural complex $[Os_3W(CO)_9(\mu\text{-}\eta^1,\eta^2\text{-}C{\equiv}CPh)(\mu\text{-}O)_2(Cp^*)]$[30] also features two oxo-bridged W-Os bonds which are substantially longer than the unbridged hinged vector. The bridging oxo ligand imposes certain geometric constraints on the length of the bridged bond (Figure 4.6). It has been suggested that the unusual short hinges in these complexes is due to the combined effect of the contraction of the atomic radius for the tungsten atom due to the greater formal nuclear charge and the lack of bridging oxo ligand.[30]

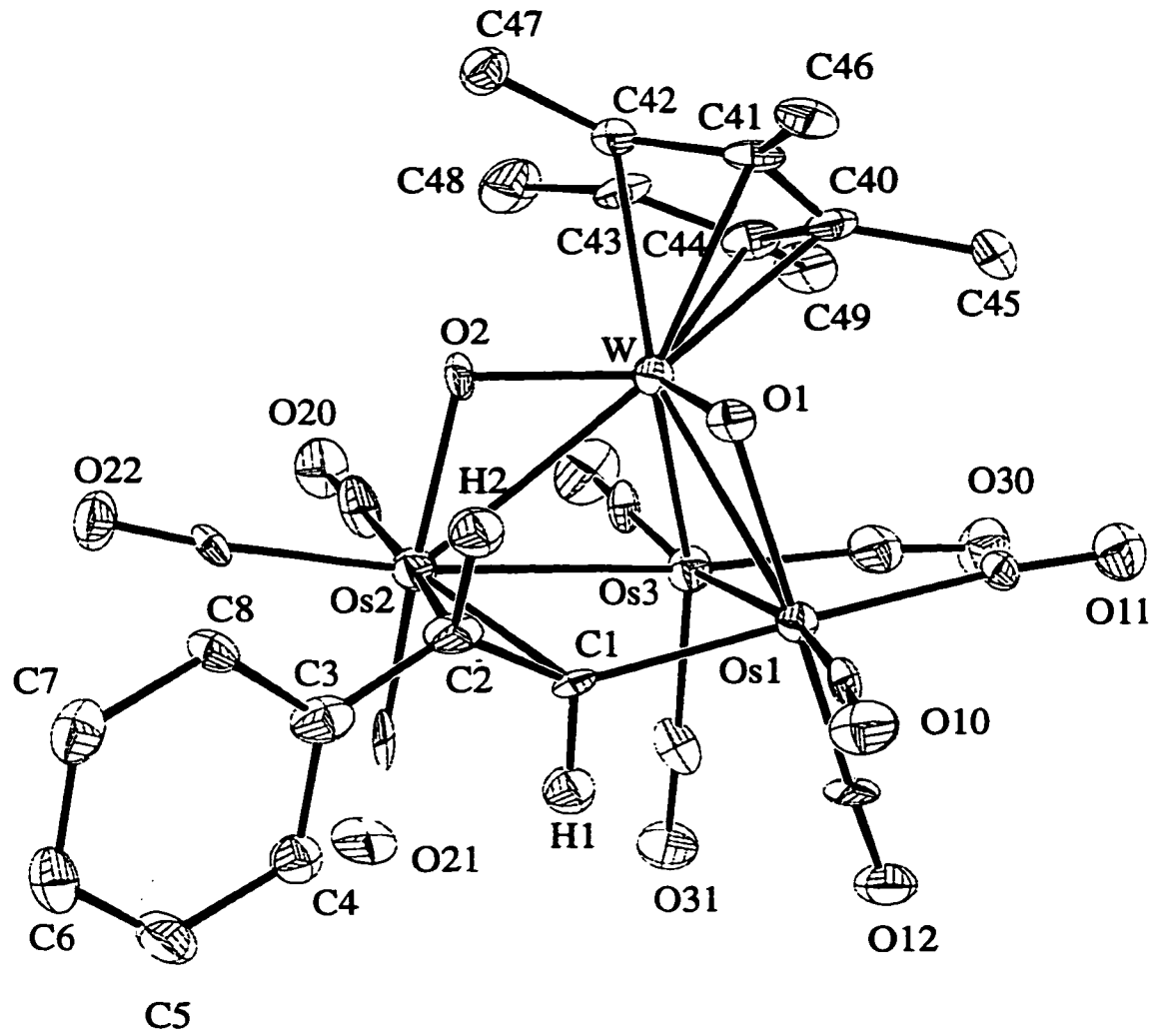

Figure 4.5 The molecular structure of $[Os_3W(CO)_9(\mu\text{-}O)_2(\mu\text{-}\eta^1,\eta^2\text{-}CH{=}CHPh\{Os{\cdots}Os\})(Cp^*)]$ **8**.

Table 4.3 Selected bond lengths (Å) and angles (deg) for **8**.

		Lengths	
Os(1)-Os(3)	2.888(1)	W-O(1)	1.79(1)
Os(2)-Os(3)	2.946(1)	W-O(2)	1.83(1)
Os(1)-W	2.985(1)	Os(1)-C(1)	2.14(2)
Os(2)-W	2.999(1)	Os(2)-C(1)	2.41(2)
Os(3)-W	2.602(1)	Os(2)-C(2)	2.40(2)
Os(1)-O(1)	2.13(1)	C(1)-C(2)	1.39(3)
Os(2)-O(2)	2.09(1)		
		Angles	
Os(1)-Os(3)-Os(2)	81.72(3)	Os(1)-C(1)-Os(2)	114.1(8)
Os(1)-Os(3)-W	65.64(3)	Os(1)-C(1)-C(2)	132(1)
Os(2)-Os(3)-W	65.10(3)	Os(2)-C(1)-C(2)	73(1)
Os(1)-O(1)-W	99.0(5)	C(1)-C(2)-C(3)	126(2)
Os(2)-O(2)-W	99.8(6)	Os(3)-Os(1)-O(1)	88.8(3)
O(1)-W-O(2)	102.4(6)	Os(3)-Os(2)-O(2)	87.2(4)

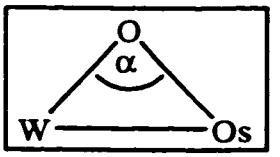

Figure 4.6 Geometric constraints imposed by bridging oxo ligands.

The bond lengths associated with the oxo ligands (W-O(1) = 1.79(1), O(1)-Os(1) = 2.13(1), W-O(2) = 1.83(1), O(2)-Os(2) = 2.09(1) Å; Os(1)-O(1)-W = 99.0(5)°, Os(2)-O(2)-W = 99.8(6)°) resemble those observed in complex **7** and suggested the resonance of the trivalent W=O:→Os and the divalent W-O-Os bonding forms. Hence the two bridging oxo ligands combined serve as a six electron donor in an electron precise, 62 electron butterfly cluster.

The other notable feature of **8** is the presence of a μ-η^1,η^2 vinyl ligand between the two osmium atoms occupying the wingtip positions of the butterfly. Thus this cluster is an unusual example of a molecule containing a μ-η^1,η^2-vinyl ligand bridging two non-bonded metal centers. The π-bonding distances are nearly identical but very long (Os(2)-C(1) = 2.41(2), Os(2)-C(2) = 2.40(2) Å) which parallels the bonding parameters of the acetylide ligand in the related complex $[Os_3W(CO)_9(\mu\text{-}\eta^1,\eta^2\text{-}C{\equiv}CPh)(\mu\text{-}O)_2(Cp^*)]$.[30] The phenyl substituent of the vinyl ligand is located *trans* to Os(1) as indicated by the Os(1)-C(1)-C(2)-C(3) dihedral angle [-144.0(3)°]. The geometry about both the C(1) and C(2) atoms suggests the retention of the C(1)=C(2) double bond (Os(1)-C(1)-C(2) = 132(1)°, C(1)-C(2)-C(3) = 126(2)°; C(1)=C(2) = 1.39(3) Å) and the coordination is again best described as a simple π donation from C(1) and C(2) to the Os(1) atom.

4.2.3.2 NMR studies of 8

The observation of only five resonances (δ 186.9, 186.4, 178.1, 175.6, 171.9) in the room temperature (298 K) $^{13}C\{^1H\}$ spectrum of a nonacarbonyl complex indicates the presence of a dynamic mirror bisecting the molecule along the W-Os(3) hinge vector. This observation is consistent with a fluxional edge-bridging alkenyl ligand undergoing $\sigma\rightarrow\pi$, $\pi\rightarrow\sigma$ exchange between the Os(1)-Os(2) metal sites (Figure 4.7). Similar results have been

obtained for the related complex $[Os_3W(CO)_9(\mu\text{-}C{\equiv}CPh)(\mu\text{-}O)_2(Cp^*)]$.[30] It was estimated from the obtained coalescence temperature of 198 K for the carbonyl ligands that the activation energy barrier for the acetylide $\sigma\rightarrow\pi$, $\pi\rightarrow\sigma$ exchange in $[Os_3W(CO)_9(\mu\text{-}\eta^1,\eta^2\text{-}C{\equiv}CPh)(\mu\text{-}O)_2(Cp^*)]$ was 9 kcal/mol.[30] A number of other bridging vinyl complexes with similar σ,π-vinyl flip mechanisms have been reported.[30,36] It was a matter of some interest to compare this fluxional behavior of the C≡CPh and CH=CHPh ligands when bound to identical metal frameworks. The technical difficulties encountered in the recording of the ^{13}C NMR spectra (long relaxation time of the carbon nucleus) and the small quantities of material available (low yield) rendered the study of this dynamic behavior via a ^{13}C NMR variable temperature study impractical. No pertinent information could be obtained from a ^1H NMR variable temperature study due to the chemical equivalence of both sites. Hence the precise fluxional behavior and activation energy of the fluxional process could not be resolved.

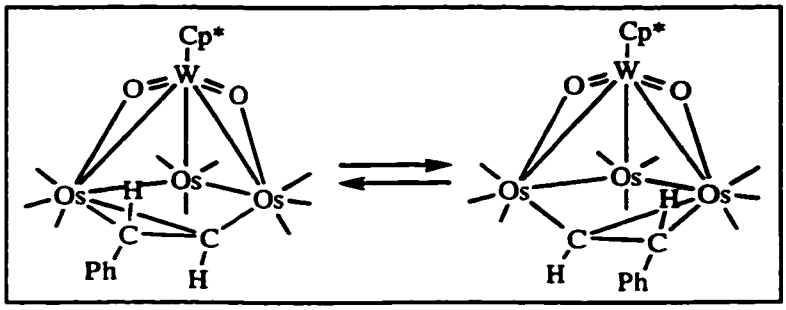

Figure 4.7 Proposed $\sigma\rightarrow\pi$, $\pi\rightarrow\sigma$ exchange of **8**.

4.2.4 Spectroscopic features of $[Os_3W(\mu\text{-}H)(CO)_9(\mu\text{-}O)_2(Cp^*)]$ 9

The infrared spectra of yellow crystalline material of **9** confirmed the presence of terminal carbonyl ligands. The ^1H NMR spectrum indicated the absence of an hydrocarbyl fragment on **9** and the presence of hydride and Cp* ligands. The FAB mass spectrum was consistent with this observation by the presence of a molecular ion at *m/z* 1075. These spectroscopic data were identical to those obtained for the previously synthesized $[Os_3W(\mu\text{-}H)(CO)_9(\mu\text{-}O)_2(Cp^*)]$.[30] The structure of the latter was proposed based on the previously structurally characterized Cp derivative, $[Os_3W(\mu\text{-}H)(CO)_9(\mu\text{-}O)_2(Cp)]$.[35] The yellow

crystals of **9** were analyzed crystallographically to confirm the suggestions previously made about this complex.

4.2.4.1 X-ray structure of 9

The molecular structure of **9** is illustrated in Figure 4.8 and selected bond lengths and angles tabulated in Table 4.4. The skeletal framework contains a tetrahedral arrangement of metal atoms. The three osmium atoms each possess three terminal carbonyl ligands completing the usual octahedral geometry about each metals. Within the structure, two of the Os-Os edges (Os(1)-Os(3) = 2.8525(8) Å and Os(2)-Os(3) = 2.854(2) Å) are of identical lengths while the Os(1)-Os(2) bond is considerably longer (Os(1)-Os(2) = 2.979(3) Å). Three W-Os bonds completed the tetrahedral structure. The position of the bridging hydride could not be obtained from a difference Fourier map and was instead inferred by the bond lengths and the Os-Os-C(O) angles. The presence of a bridging hydride ligand on a metal-metal bond usually results in the lengthening of the bond relative to non-bridged analogues and the enlargement of the Os-Os-C(O) angles, as previously discuss in Chapter Two of this thesis. The larger Os-Os-C(O) angles of the equatorial carbonyl ligands associated with the Os(1)-Os(2) edge (Os(1)-Os(2)-C(21) = 118.31(5) and Os(2)-Os(1)-C(11) = 115.4(4)°) and the greater bond length of the same bond suggested the presence of a bridging hydride on the Os(1)-Os(2) bond.

Two oxo bridged W-Os(1,2) bonds are nearly of equal length, while the non-bridged W-Os(3) bond is relatively shorter [Os(1)-W = 2.909(1) Å, Os(2)-W = 2.9104(9) Å and Os(3)-W = 2.632(1) Å]. A similar arrangement of two longer and one shorter W-Os bonding distances was encountered in **8**. It has been suggested that the notably shorter W-Os distance results from the contraction of the atomic radium for tungsten atom and the lack of bridging oxo ligand (vide supra).

The lengths associated with the oxygen centers [W-O(1) = 1.841(8) Å, Os(1)-O(1) = 2.139(8) Å; W-O(2) = 1.785(8) Å, Os(2)-O(2) = 2.137(8) Å] are similar to that found in **8** and others.[30,35] This data is in agreement with a resonance between the trivalent W=O:→Os

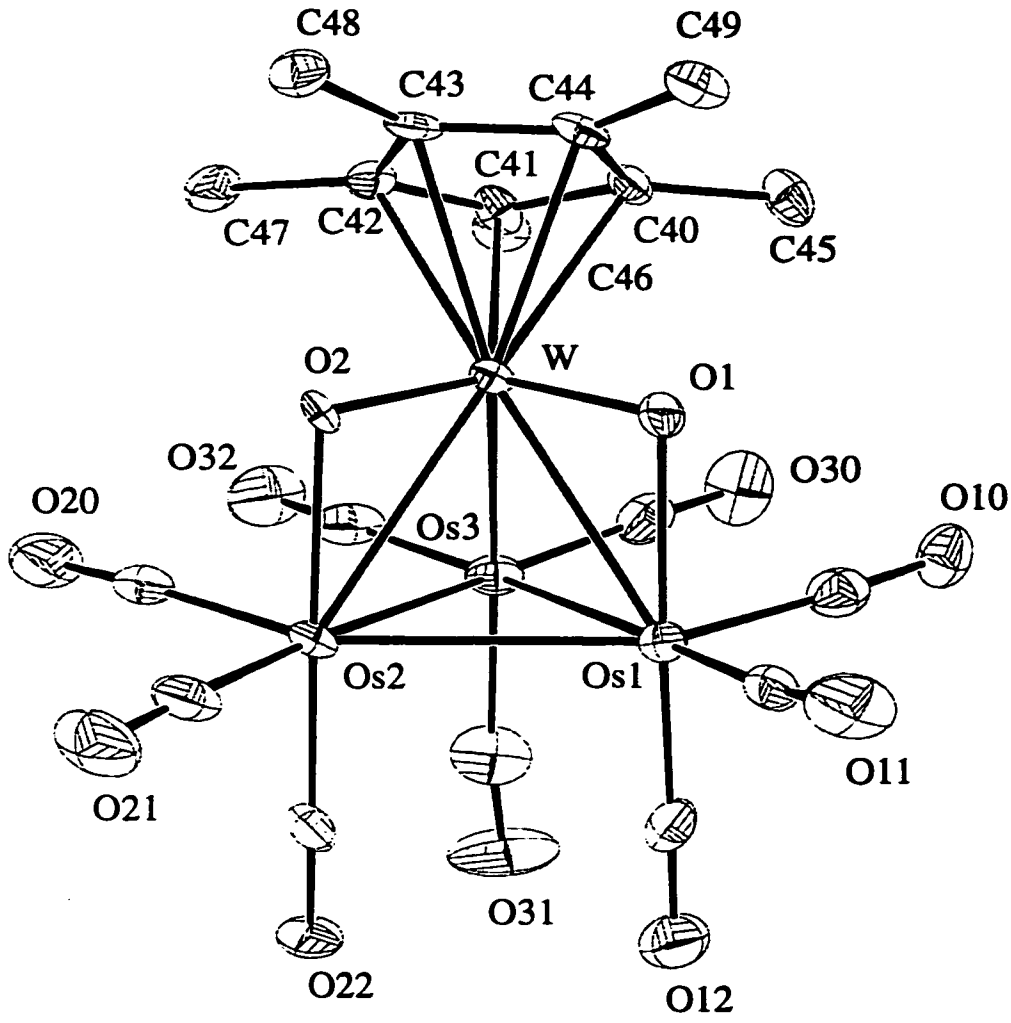

Figure 4.8 The molecular structure of $[Os_3W(\mu\text{-}H)(CO)_9(\mu\text{-}O)_2(Cp^*)]$ **9**.

Table 4.4 Selected bond lengths (Å) and angles (deg) for **9**.

Lengths			
Os(1)-Os(3)	2.8525(8)	Os(3)-W	2.632(1)
Os(1)-Os(2)	2.979(3)	Os(1)-O(1)	2.139(8)
Os(2)-Os(3)	2.854(2)	Os(2)-O(2)	2.137(8)
Os(1)-W	2.909(1)	W-O(1)	1.841(8)
Os(2)-W	2.9104(9)	W-O(2)	1.785(8)
Angles			
Os(2)-Os(1)-Os(3)	58.56(3)	Os(3)-Os(2)-W	54.32(4)
Os(1)-Os(2)-Os(3)	58.50(5)	Os(2)-Os(3)-W	63.93(4)
Os(1)-Os(3)-Os(2)	62.94(4)	Os(1)-Os(3)-W	63.93(2)
Os(2)-Os(1)-W	59.23(4)	Os(1)-O(1)-W	93.6(3)
Os(1)-Os(2)-W	59.19(4)	Os(2)-O(2)-W	95.4(4)
Os(3)-Os(1)-W	54.35(2)	O(1)-W-O(2)	103.9(4)

and divalent W-O-Os bonding forms. Thus, the two oxo ligands combined act as a six electron donor. With all metal atoms and ligands treated as formally neutral, **9** is electron precise with an overall 60 cluster valence electrons as expected for a 5 M-M bond tetrahedral structure.

4.2.5 Spectroscopic features of $[Os_3W(CO)_{10}(O)(\mu\text{-}\eta^1,\eta^2\text{-}CH{=}CHPh\{Os\text{-}Os\})(\mu\text{-}O)(Cp^*)]$ 10

Complex **10** is yellow in color. The infrared spectrum of **10** indicated the presence of terminal carbonyl groups. A room temperature ^1H NMR spectrum suggested that **10** was fluxional (Section 4.2.5.2). A room temperature ^{13}C NMR spectra showed the presence of three Cp* ligand (C_5Me_5 = 117.2, 116.7, 116.5; $C_5\mathit{Me}_5$ = 12.22, 12.18, 12.12), but the poor signal to noise ratio coupled with the fluxionality of the compound resulted in low intensity signals for the remaining peaks. A strong molecular ion in the FAB mass spectrum was located at *m/z* 1305. Since the spectral data could not provide unambiguous structural identity, an X-ray crystal structure study was undertaken.

4.2.5.1 X-ray structure of 10

An ORTEP plot of $[Os_3W(CO)_{10}(O)(\mu\text{-}\eta^1,\eta^2\text{-}CH{=}CHPh\{Os\text{-}Os\})(\mu\text{-}O)(Cp^*)]$ (**10**) is shown in Figure 4.9 with important structural parameters listed in Table 4.5. The metal framework of **10** consists of a WOs_2 triangle spiked at Os(1) by Os(3). The Os-Os bond distances (Os(1)-Os(2) = 2.9465(4) Å and Os(1)-Os(3) = 2.8155(4) Å) are in the range expected for Os-Os single bonds. Both Os(2) and Os(3) carries four terminal CO ligands while Os(1) has two CO ligands in the usual octahedral conformation.

Two W-Os bonds are also included in the metal structure. The unbridged W-Os(2) vector (2.7075(4) Å) is much shorter than the oxo bridged W-Os(1) bond (W-Os(1) = 2.8945(4) Å). It was suggested that the absence of a bridging oxo ligand together with the smaller atomic radius for the tungsten atom favor shorter bond distances.[30] The related complex $[WOs_3(\eta^1\text{-}C{\equiv}CPh)(CO)_{11}(O)(\mu\text{-}O)(Cp^*)]$[30] also features an unbridged W-Os bond which is considerably shorter then the oxo bridged vector. Similar short W-Os bond distances were also encountered for complexes **8** and **9** (vide supra).

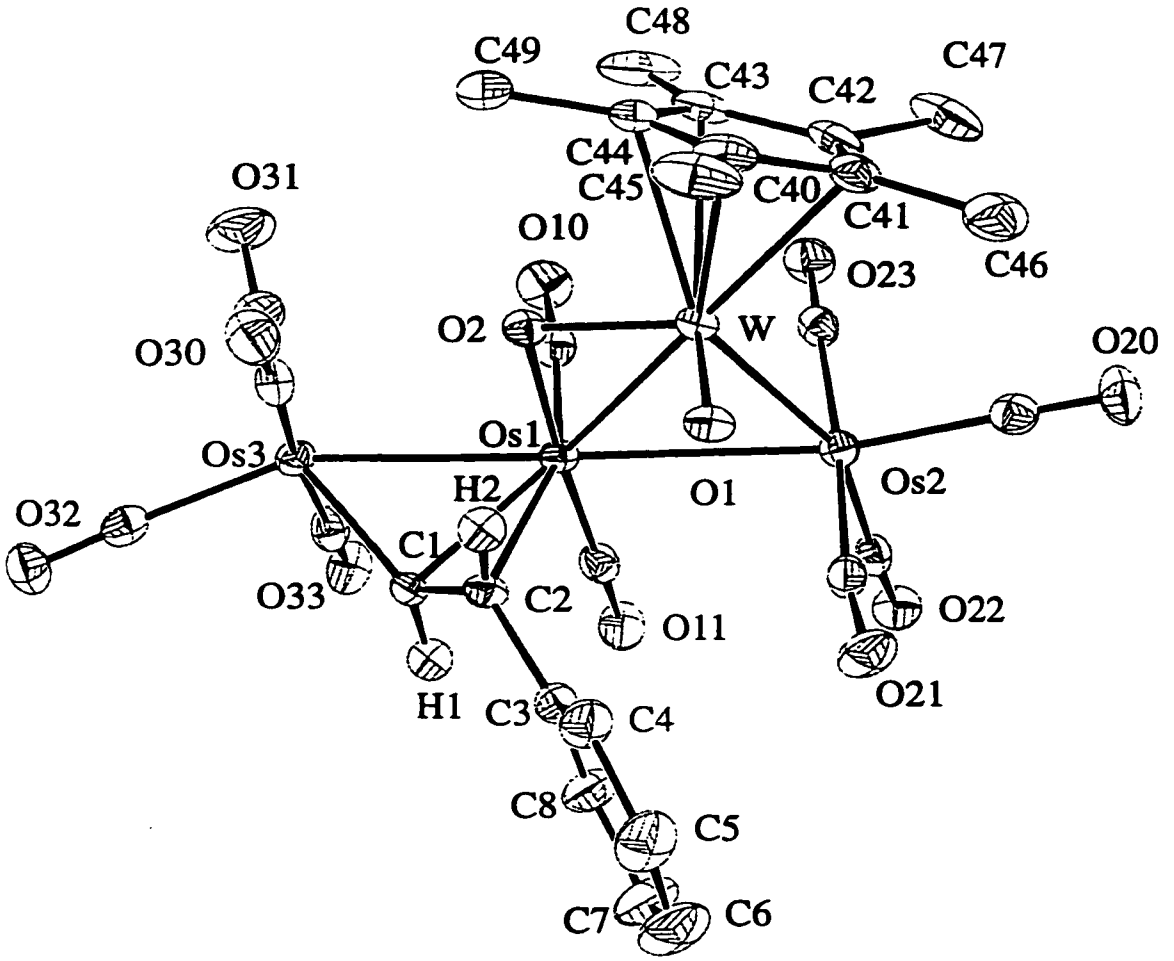

Figure 4.9 The molecular structure of $[Os_3W(CO)_{10}(O)(\mu\text{-}\eta^1,\eta^2\text{-}CH{=}CHPh\{Os\text{-}Os\})(\mu\text{-}O)(Cp^*)]$ **10**.

Table 4.5 Selected bond lengths (Å) and angles (deg) for **10**.

		Lengths	
Os(1)-Os(2)	2.9465(4)	Os(1)-O(2)	2.113(4)
Os(1)-Os(3)	2.8155(4)	Os(3)-C(1)	2.087(6)
Os(1)-W	2.8945(4)	Os(1)-C(1)	2.261(6)
Os(2)-W	2.7075(4)	Os(1)-C(2)	2.402(6)
W-O(1)	1.718(4)	C(1)-C(2)	1.381(9)
W-O(2)	1.826(4)		
		Angles	
Os(2)-Os(1)-W	55.221(9)	Os(1)-C(1)-C(2)	78.4(4)
Os(1)-Os(2)-W	61.42(1)	Os(3)-C(1)-C(2)	130.7(5)
Os(1)-W-Os(2)	63.36(1)	C(1)-C(2)-C(3)	122.5(6)
Os(1)-O(2)-W	94.3(2)	Os(2)-Os(1)-O(2)	93.7(1)
O(1)-W-O(2)	105.7(2)	Os(3)-Os(1)-O(2)	83.1(1)
Os(1)-C(1)-Os(3)	80.6(2)		

The W-O(2)-Os(1) bridge contains a short tungsten-oxygen bond length of W-O(2) = 1.826(4) Å and a relatively longer osmium-oxygen bond length of Os(1)-O(2) = 2.113(4) Å; the angle is Os(1)-O(2)-W = 94.3(2)°. These bond lengths are characteristic of a W=O:→Os interaction in which the neutral μ-O ligand acts as a four electron donor. Such a bonding interaction for the oxo ligand of a WOs_3 framework has been found for complexes **1** and **4** discussed in Chapter 2.

The vinyl ligand bridges the Os(3) and Os(1) atoms in the typical μ-η^1,η^2 fashion (Os(3)-C(1) = 2.087(6), Os(1)-C(1) = 2.261(6), Os(1)-C(2) = 2.402(6) Å). The phenyl substituent was located *trans* to the Os(3) atom with a Os(3)-C(1)-C(2)-C(3) dihedral angle of 173(1)°. Furthermore, the vinyl fragment and terminal oxo ligand are located on the same side of the WOs_2 triangular plane as indicated by the dihedral angle C(2)-Os(1)-W-O(1) = 17.5(4)°. Finally, the geometry about C(1) and C(2) [C(1)-C(2)-C(3) = 122.5(6)° and Os(3)-C(1)-C(2) = 130.7(5)°] suggests once again the simple σ-π coordination of the vinyl ligand onto the metal framework.

Complex **10** possesses 64 cluster valence electrons as anticipated for a 4 M-M bond spiked triangular structure (three osmium atoms provided 24 electrons; one tungsten atom, 6 electrons; ten terminal carbonyl ligands, 20 electrons; one Cp* ligand, 5 electrons; one μ-η^1,η^2-CH=CHPh ligand, 3 electrons; one μ-O, 4 electrons and one terminal oxo, 2 electrons).

4.2.5.2 ^{1}H NMR study of 10

A room temperature ^{1}H NMR spectrum of crystalline compound **10** in CD_2Cl_2 suggested that the latter was highly fluxional, as evidenced by the presence of three Cp* signals (δ 2.30, 2.27, 2.21). Other ^{1}H resonances include δ 8.46-8.11 (CH=CHPh), 7.64-7.06 (Ph) and 5.13-4.84 (CH=CHPh). Even upon descending to the lowest temperature accessible (208 K), the dynamic process could not be frozen out.

A room temperature ^{1}H NMR spectrum obtained in benzene was similar to the one described previously, accounting for solvent effects. Again, three Cp* signals (δ 1.99, 1.90, 1.89) were observed. ^{1}H resonances corresponding to the CH=CHPh (δ 8.59-7.87), Ph (δ

7.47-6.85) and CH=CHPh (δ 5.15-4.91) moieties were present. The NMR sample was recrystallized affording pure **10** as supported by both infrared spectroscopy and thin layer chromatography. This suggested that the NMR sample was not contaminated and that the process observed was due to dynamic instead of chemical effects.

4.2.6 Spectroscopic features of $[Os_3W(\eta^1\text{-}CH{=}CHPh)(CO)_{11}(O)(\mu\text{-}O)(Cp^*)]$ 11

The infrared spectrum of yellow crystalline **11** showed terminal carbonyl stretching bands. The ^1H and ^{13}C NMR spectra showed the anticipated resonances for both the Cp* and Ph ligands. Two additional signals were observed in the ^1H NMR spectrum at δ 7.71 and 7.09 with a $J_{H\text{-}H}$ = 18 Hz characteristic of a *trans* substituted vinyl ligand. The ^{13}C NMR spectrum of **11** was characterized by two resonances at δ 145.5 and 111.3, attributed to the hydrocarbyl fragment. The FAB mass spectrum was characterized by a $[M]^+$ at *m/z* 1333, which fragmented by loss of eleven CO.

4.2.6.1 X-ray structure of 11

Structural details of complex **11** were determined by an X-ray crystal structure study. An ORTEP plot (Figure 4.10) identifies **11** as $[Os_3W(\eta^1\text{-}CH{=}CHPh)(CO)_{11}(O)(\mu\text{-}O)(Cp^*)]$. Important bond lengths and angles are summarized in Table 4.6. The skeletal framework of **11** consists of a WOs_2 triangle with the Os(3) atom linked to Os(1). The two Os-Os bonds (Os(1)-Os(3) = 2.893(2) Å and Os(1)-Os(2) = 2.938(2) Å) present in the skeletal framework are of typical length for Os-Os single bonds. The Os(2) and Os(3) atoms carry four carbonyl groups while Os(1) has three CO groups in the usual octahedral conformation. Two W-Os bonds complete the molecular geometry of **11**. Clearly the metal disposition of **11** resembles that of **10**, but in contrast to **10** there are eleven terminal carbonyl groups.

A bridging oxo ligand links the W and Os(1) atoms. The W-Os(1) bond distance (2.937(2) Å) is much longer than the unbridged W-Os(2) length (2.722(2) Å). Similar bond distances for the W-Os bonds of a WOs_2 triangle were previously observed in **10** (vide supra). The bridging mode of the oxo ligand (W-O(2) = 1.82(2) Å, Os(1)-O(2) = 2.10(2) Å; Os(1)-O(2)-W = 97(1)°) is very similar to that in complex **10** and is best described as a W=O:→Os interaction.

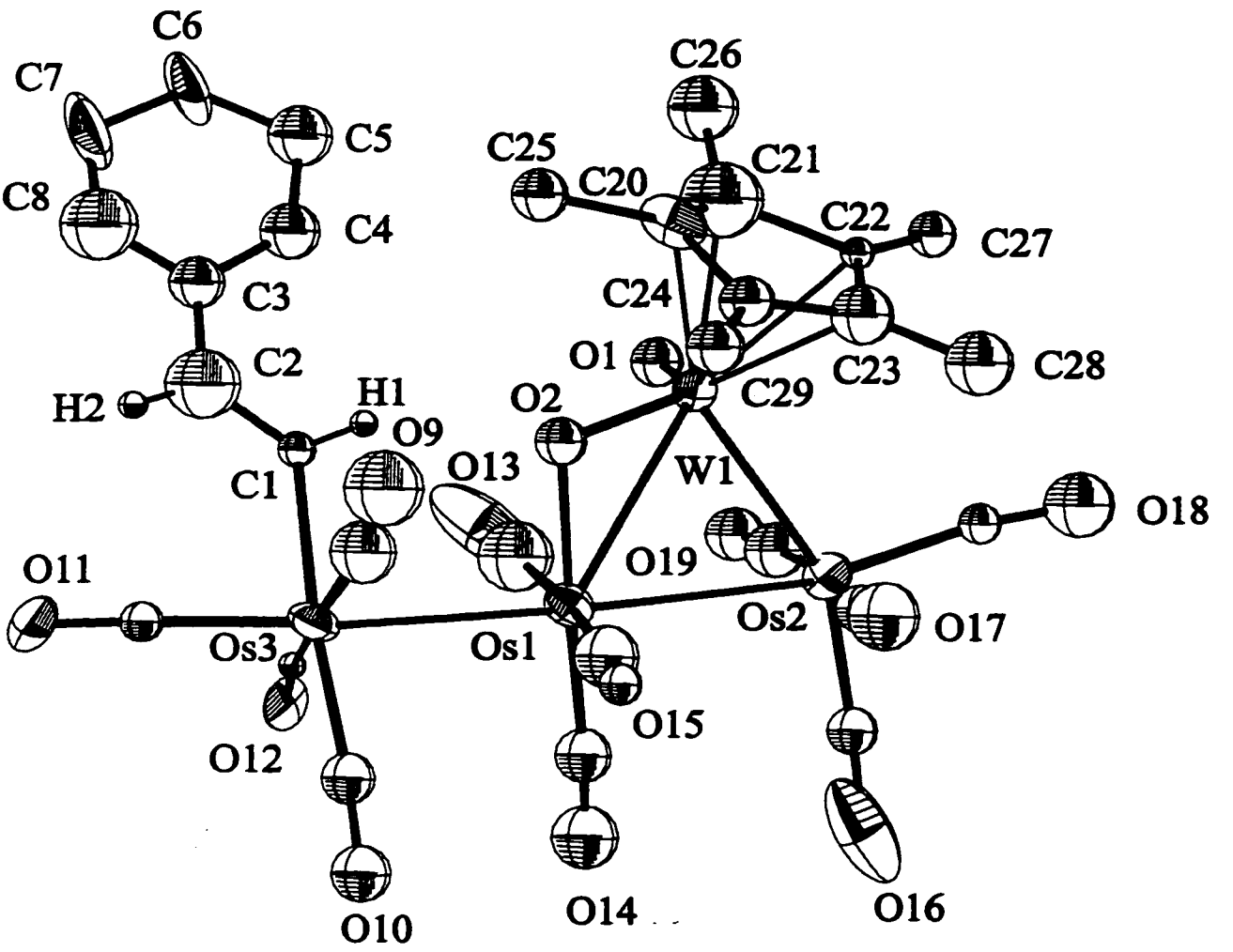

Figure 4.10 The molecular structure of $[Os_3W(\eta^1\text{-}CH{=}CHPh)(CO)_{11}(O)(\mu\text{-}O)(Cp^*)]$ **11**.

Table 4.6 Selected bond lengths (Å) and angles (deg) for **11**.

		Lengths	
Os(1)-Os(2)	2.938(2)	W-O(2)	1.82(2)
Os(1)-Os(3)	2.893(2)	Os(1)-O(2)	2.10(2)
Os(1)-W	2.937(2)	Os(3)-C(1)	2.25(3)
Os(2)-W	2.722(2)	C(1)-C(2)	1.30(4)
W-O(1)	1.66(2)		
		Angles	
Os(2)-Os(1)-W	55.20(5)	O(1)-W-O(2)	107(1)
Os(1)-Os(2)-W	62.39(5)	Os(3)-C(1)-C(2)	128(2)
Os(1)-W-Os(2)	62.41(6)	C(1)-C(2)-C(3)	123(3)
Os(1)-O(2)-W	97(1)	Os(3)-Os(1)-Os(2)	175.78(9)

A terminal vinyl ligand is attached to Os(3). The vinyl ligand features a phenyl substituent *trans* to Os(3) and dihedral angle of Os(3)-C(1)-C(2)-C(3) = -173.9°. The C(1)-C(2) bond distance (1.30(4) Å) is characteristic of carbon-carbon double bonds.

Complex **11** is electron precise with an overall 64 cluster valence electrons (24 electrons from the three osmium atoms, 6 electrons from the tungsten atom, 22 electrons from the eleven terminal carbonyl ligands, 5 electrons from the Cp* ligand, 1 electron from the η^1-CH=CHPh ligand, 4 electrons from the μ-O ligand and 2 electrons from the terminal oxo ligand).

4.2.7 Spectroscopic features of $[Os_3W(CO)_8(\mu\text{-}O)_2(Cp^*)]_2$ 12

The infrared spectrum of the green complex **12** shows stretching bands in the terminal carbonyl region. The ^1H and ^{13}C NMR spectra suggest the absence of a hydrocarbyl fragment as they contained only the anticipated resonances for the Cp* (δ_H 2.15, δ_C 117.8, 12.1) ligand. FAB-MS gave $(M\text{-}CO)^+$ as the highest molecular weight ion. Fragment ions consistent with the loss of a further eight CO ligands were also observed.

4.2.7.1 X-ray structure of 12

An X-ray crystal structure analysis identified complex **12** as $[Os_3W(CO)_8(\mu\text{-}O)_2(Cp^*)]_2$. Figure 4.11 illustrates the molecular structure of **12** as an ORTEP plot. A summary of selected bond lengths and angles is listed in Table 4.7. The molecule contains a crystallographic center of inversion which results in half of the molecule being symmetry generated. The metal framework of **12** consists of a chain of four osmium triangles sharing three common edges. The two outer triangles are capped on opposite sides of the plane by a $W(\mu\text{-}O)_2(Cp^*)$ fragment. The Os-Os distances present in **12** vary between 2.7759(5) and 2.8668(5) Å as expected for a single bond between osmium atoms. The Os(2) and Os(3) atoms each have three terminal carbonyls bonded to them while Os(1) has two. The stereochemistry at Os(1), Os(2) and Os(3) consists of a distorted octahedral.

Each of the symmetry equivalent halves of the complex contains a $W(\mu\text{-}O)_2(Cp^*)$ fragment which is linked to the Os_6 plane via three W-Os bonds. Two of the W-Os bonds

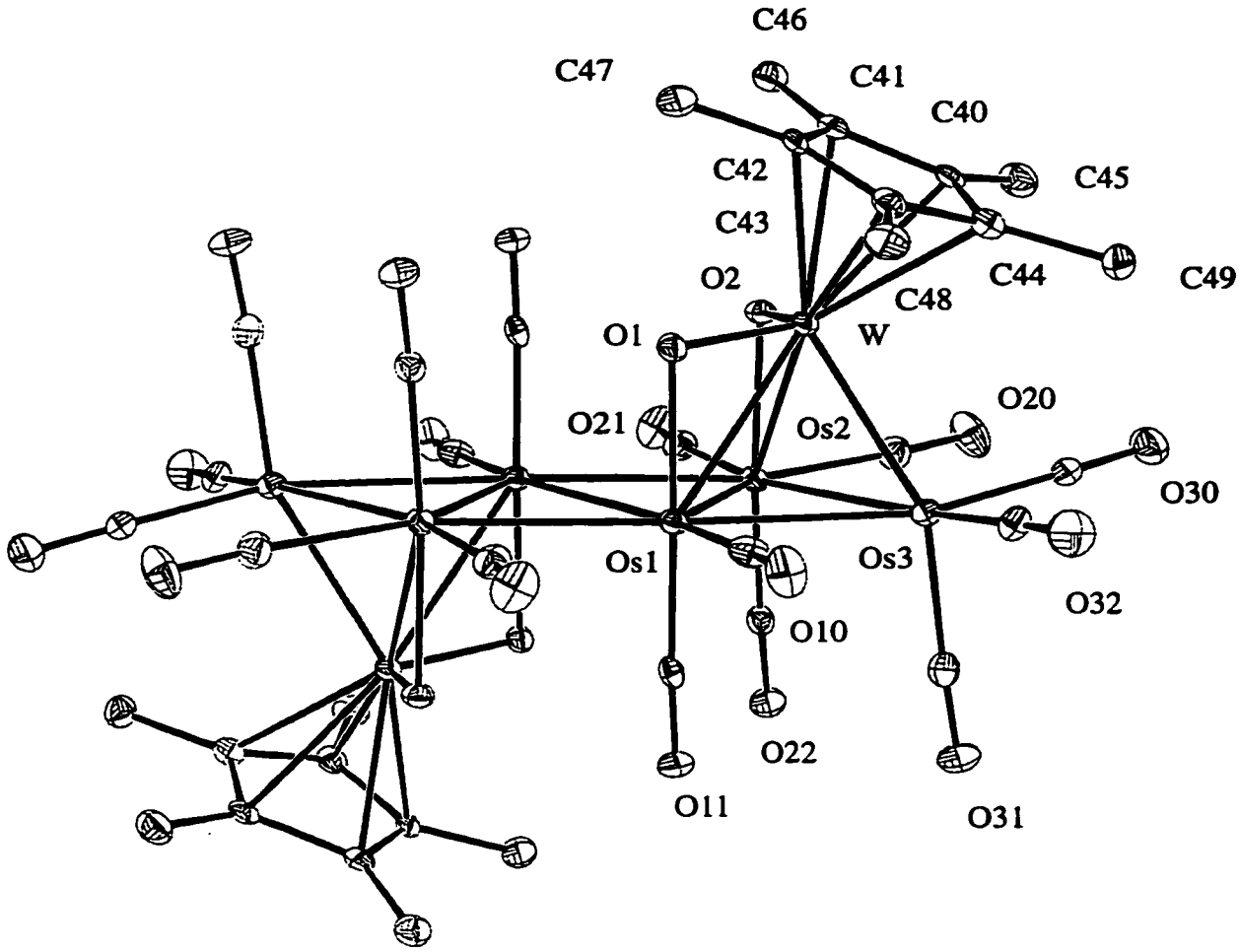

Figure 4.11 The molecular structure of $[Os_3W(CO)_8(\mu\text{-}O)_2(Cp^*)]_2$ **12**.

Table 4.7 Selected bond lengths (Å) and angles (deg) for **12**.

		Lengths	
Os(1)-Os(2)	2.7759(5)	Os(2)-W	2.9468(4)
Os(1)-Os(3)	2.8668(5)	Os(3)-W	2.6634(5)
Os(2)-Os(3)	2.8585(5)	Os(1)-O(1)	2.144(5)
Os(1)-Os(1)a	2.7982(6)	Os(2)-O(2)	2.170(5)
Os(1)-Os(2)a	2.8184(5)	W-O(1)	1.805(5)
Os(2)-Os(1)a	2.8184(5)	W-O(2)	1.781(5)
Os(1)-W	2.8586(5)		
		Angles	
Os(2)-Os(1)-Os(3)	60.85(1)	Os(3)-Os(2)-W	54.59(1)
Os(1)-Os(2)-Os(3)	61.15(1)	Os(2)-Os(3)-W	64.39(1)
Os(1)-Os(3)-Os(2)	58.00(1)	Os(1)-Os(3)-W	62.12(1)
Os(2)-Os(1)-W	63.05(1)	Os(1)-O(1)-W	92.4(2)
Os(1)-Os(2)-W	59.85(1)	Os(2)-O(2)-W	96.0(2)
Os(3)-Os(1)-W	55.45(1)	O(1)-W-O(2)	106.4(2)

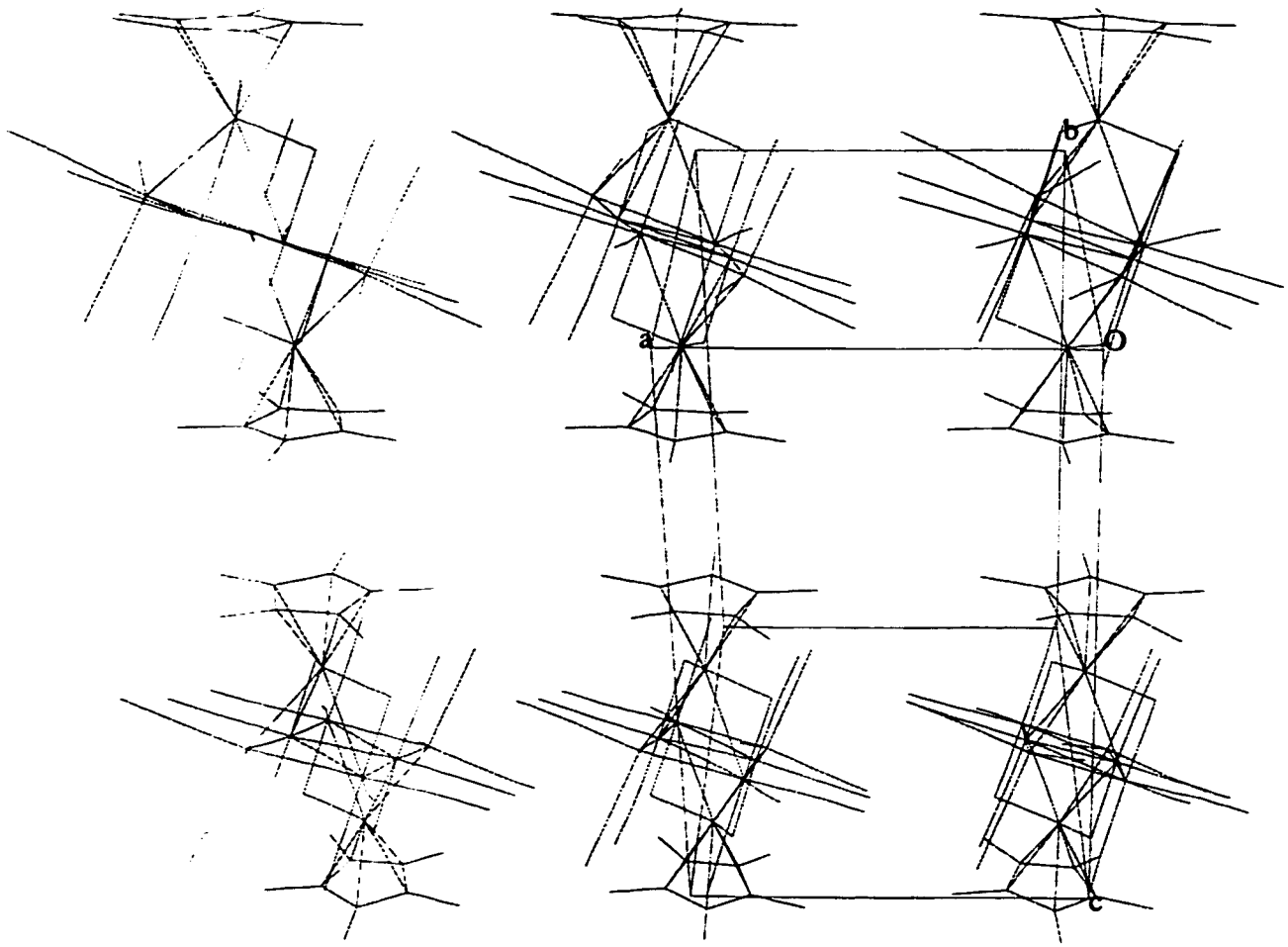

Figure 4.12 Packing diagram of $[Os_3W(CO)_8(\mu\text{-}O)_2(Cp^*)]_2$ **12**.

support oxo ligands (W-Os(1) = 2.8586(5), W-Os(2) = 2.9468(4) Å). These bond distances are significantly longer than the unsupported W-Os(3) distance (2.6634(5) Å). Hence **12** provides another example of a complex where the greater formal nuclear charge of the tungsten atom and the absence of a bridging oxo ligand result in a shorter W-Os distance. This situation was previously encountered for complexes **8** to **11** (vide supra).

The bond lengths and angles associated with the bridging oxo ligands of **12** (W-O(1) = 1.805(5), O(1)-Os(1) = 2.144(5), W-O(2) = 1.781(5), O(2)-Os(2) = 2.170(5) Å; W-O(1)-Os(1) = 92.4(2), W-O(2)-Os(2) = 96.0(2)°) strongly resemble those of complexes **7-9**. Hence the resonance of the trivalent W=O:→Os and the divalent W-O-Os bonding forms prevails which indicates that each bridging oxo ligand acts as a three electron donor. Complex **12** possesses a total of 114 cluster valence electrons as expected for a 15 M-M bond Os_6W_2 metal framework.

Furthermore a packing diagram of **12** suggests the presence of a layered $W(O)_2|Os_6|W(O)_2$ lattice (Figure 4.12). The distance between the Os_6 planes is evaluated at 13.82(1) Å. Hence **12** may mimic the interaction occurring on the surfaces of late metal oxide catalysts.

4.3 Conclusions

The thermolysis of **4** has provided six clusters which offered various bonding modes for both the [W(O)$_2$(Cp*)] fragment and the hydrocarbyl ligand on Os_3. Structural evidence for the effect of the oxo ligand on the W-Os bond distance was provided by complexes **8-12**. Bridging oxo ligands impose a geometric constraint which results in the lengthening of the supported W-Os bond. Conversely, the absence of an oxo ligand and the smaller atomic radius for the tungsten atom lead to a shortening of the W-Os bond.

This reaction provided further evidence of the ability of the oxo ligand to move reversibly from a bridging (4-electron donor) to a terminal (2-electron donor) bonding mode. For example, the transformation of **4** to **7** involves the shifting of the terminal oxo group to

the bridging mode while the transformation of **8** to **10** demonstrates the shifting of one bridging oxo ligand to the terminal mode. This property of the oxo ligand may allow for ligand migration on supported clusters. The reaction scheme illustrates the migration of the vinyl ligand from a bridging position on a W-Os vector to a terminal position on a Os atom via intermediates where the vinyl ligand bridges two Os atoms.

Cluster **11** represents an unusual example of a cluster with a σ-vinyl ligand in which the additional unsaturation in the hydrocarbyl is not used in intramolecular coordination. It is to our knowledge, the first example of an $Os(CO)_4(\eta^1\text{-}CH{=}CHPh)$ fragment attached to an Os_2W core via a single unsupported Os-Os bond.

Finally, this reaction provided a rare example of an Os_6 rhombic raft exhibiting $W(O)_2|Os_6|W(O)_2$ layering properties. Complex **12** could possibly serve as a template for reactions occurring on oxide supported late metal catalysts.

4.4 Experimental section

4.4.1 The thermolysis of $[Os_3W(CO)_{10}(O)(\mu\text{-}\eta^1,\eta^2\text{-}CH{=}CHPh\{W\text{-}Os\})(\mu\text{-}O)(Cp^*)]$ 4

Heating a n-heptane solution (50 mL) of **4** (100 mg, 0.0766 mmol) at 100°C for 2 hours resulted in a gradual color change from orange to dark red. The solvent was then removed *in vacuo* and the residue separated via thin layer chromatography (CH_2Cl_2/hexane, 50/50) Six compounds were isolated. In order of elution, they were 4 mg $[Os_3W(CO)_8(\mu\text{-}O)_2(Cp^*)]_2$ **12** (0.001745 mmol, 2.28%), 12 mg $[Os_3W(CO)_9(\mu\text{-}O)_2(\mu\text{-}\eta^1,\eta^2\text{-}CH{=}CHPh\{W\text{-}Os\})(Cp^*)]$ **7** (0.009397 mmol, 12.3%), 5 mg $[Os_3W(\mu\text{-}H)(CO)_9(\mu\text{-}O)_2(Cp^*)]$ **9** (0.004256 mmol, 5.56%), 18 mg $[Os_3W(CO)_9(\mu\text{-}O)_2(\mu\text{-}\eta^1,\eta^2\text{-}CH{=}CHPh\{Os\cdots Os\})(Cp^*)]$ **8** (0.014029 mmol, 18.3%), 8 mg $[Os_3W(CO)_{10}(O)(\mu\text{-}\eta^1,\eta^2\text{-}CH{=}CHPh\{Os\text{-}Os\})(\mu\text{-}O)(Cp^*)]$ **10** (0.006102 mmol. 7.97%), 8 mg $[Os_3W(\eta^1\text{-}CH{=}CHPh)(CO)_{11}(O)(\mu\text{-}O)(Cp^*)]$ **11** (0.006002 mmol, 7.84%) and 20 mg of baseline decomposition.

Table 4.1 Spectroscopic data for complexes **7-12.**

COMPOUND	IR (hexane) ν(CO) (cm^{-1})	^1H NMR ($CDCl_3$) (ppm)	$^{13}C\{^1H\}$ NMR ($CDCl_3$) (ppm)
7	2096 (m); 2042 (vs); 2022 (vs); 2008 (w); 1986 (vw); 1977 (vw); 1950 (vw); 1945 (w)	9.50 (1H, d, J_{H-H} = 13 Hz); 7.38 (4H, m); 7.16 (1H, m); 4.01 (1H, d, J_{H-H} = 13 Hz); 2.06 (15H, s)	143.3 (1C, s, C=C); 128.8 (2C, s, Ph); 126.8 (1C, s, Ph); 126.8 (1C, s, Ph); 126.7 (2C, s, Ph); 119.0 (5C, s, C_5Me_5); 74.4 (1C, s, C=C), 11.0 (5C, s, C_5Me_5)
8	2085 (m), 2066 (vs), 2026 (vs), 2000 (s), 1992 (w), 1981 (w), 1954 (w), 1938 (w)	7.34 (2H, m); 7.12 (3H, m); 5.51 (1H, d, J_{H-H} = 18 Hz); 3.85 (1H, d, J_{H-H} = 18 Hz); 2.13 (15H, s)	186.9 (1C, s, CO); 186.4 (2C, s, CO); 178.1 (2C, s, CO); 175.6 (2C, s, CO); 171.9 (2C, s, CO); 129.0 (3C, s, Ph); 128.1 (1C, s, Ph); 125,5 (2C, s, Ph); 116.2 (5C, s, C_5Me_5); 101.7 (1, s, CHCHPh); 66.3 (1C, s, CHCHPh); 12.7 (5C, s, C_5Me_5)
9	2094 (m), 2069(s), 2056 (vw), 2024(vs), 2013 (s), 2005 (m), 1987 (w), 1958 (m), 1936 (m)	2.07 (15H, s); -15.71 (1H,s)	192.6 (1C, s, CO); 184.0 (2C, s, CO); 174.7 (2C, s, CO); 172.0 (2C, s, CO); 169.1 (2C, s, CO); 116.5 (5C, s, C_5Me_5); 11.8 (5C, s, C_5Me_5);
10	2118 (w), 2095 (w), 2089 (m), 2046 (vs), 2037 (s), 2015 (s), 2004 (w), 1986 (m), 1924 (w)	See Section 4.2.5.2	See Section 4.2.5.2

Table 4.1 (continued)

11	2118 (w), 2090 (s), 2041 (vs) 2036 (s, sh), 2024 (m, sh), 2014 (s), 2006 (m, sh), 1990 (s), 1976 (vw), 1960 (vw), 1937 (vw)	7.71 (1H, d, J_{H-H} = 18 Hz); 7.25 (4H, m); 7.10-7.09 (1H, m); 7.09 (1H, d, J_{H-H} = 18 Hz); 2.15 (15H, s);	195.1 (1C, s, CO); 190.2 (1C, s, CO); 187.4 (1C, s, CO); 184.1 (1C, s, CO); 181.8 (1C, s, CO); 181.3 (1C, s, CO); 180.3 (1C, s, CO); 178.2 (1C, s, CO); 175.2 (1C, s, CO); 173.7 (1C, s, CO); 167.3 (1C, s, CO); 145.5 (1C, s, CHCHPh); 142.5 (1C, s, Ph); 128.6 (2C, s, Ph); 126.1 (1C, s, Ph); 125.5 (2C, s, Ph); 117.6 (5C, s, C_5Me_5); 111.3 (1C, s, CHCHPh); 12.2 (5C, s, C_5Me_5)
12	2092 (w), 2074 (s), 2028 (vs), 2003 (m), 1998 (s), 1985 (w), 1954 (vw), 1941 (w)	2.15 (15H, s)	177.8 (C_5Me_5); 12.1 (C_5Me_5)

Spectral data for $[Os_3W(CO)_9(\mu\text{-}O)_2(\mu\text{-}\eta^1\text{-}\eta^2\text{-}CH{=}CHPh\{W\text{-}Os\})(Cp^*)]$ **7**: FAB-MS (*m/z*): 1277, $[M]^+$; 1249-1165, $[M\text{-}nCO]^+$ (n = 1-4). Anal. Calcd. For **7**: C, 25.40; H, 1.74. Found: C, 25.42: H, 1.71%.

Spectral data for $[Os_3W(CO)_9(\mu\text{-}O)_2(\mu\text{-}\eta^1,\eta^2\text{-}CH{=}CHPh\{Os\cdots Os\})(Cp^*)]$ **8**: FAB-MS (*m/z*): 1277, $[M]^+$; 1249-1025, $[M\text{-}nCO]^+$ (n = 1-9). Anal. Calcd. For **8**: C, 25.40; H, 1.74. Found: C. 24.59; H, 1.69%.

Spectral data for $[Os_3W(\mu\text{-}H)(CO)_9(\mu\text{-}O)_2(Cp^*)]$ **9**: FAB-MS (*m/z*): 1075, $[M]^+$.

Spectral data for $[Os_3W(CO)_{10}(O)(\mu\text{-}\eta^1,\eta^2\text{-}CH{=}CHPh\{Os\text{-}Os\})(\mu\text{-}O)(Cp^*)]$ **10**: FAB-MS (*m/z*): 1305, $[M]^+$; 1249-1025, $[M\text{-}nCO]^+$ (n = 2-10). Anal. Calcd. For **10**: C, 25.77; H, 1.70. Found: C, 26.07; H, 1.70%.

Spectral data for $[Os_3W(\eta^1\text{-}CH{=}CHPh)(CO)_{11}(O)(\mu\text{-}O)(Cp^*)]$ **11**: FAB-MS (*m/z*): 1333, $[M]^+$; 1305-1025, $[M\text{-}nCO]^+$ (n = 1-11).

Spectral data for $[Os_3W(CO)_8(\mu\text{-}O)_2(Cp^*)]_2$ **12**: FAB-MS (*m/z*): 2264-2040, $[M\text{-}nCO]^+$ (n = 1-9).

4.4.2 X-ray structural analysis of 7

Single crystals of **7** were grown from concentrated CH_2Cl_2/hexane solutions at −15°C. A purple prism of dimensions 0.175 x 0.075 x 0.05 mm was selected and mounted. Cluster **7** crystallized in the monoclinic space group *P21/n* with $Z = 4$. A total of 34555 (5213 observed) reflections were collected at −100 °C. The structure was solved by Patterson and Fourier techniques and refined by full-matrix least-squares with all non-hydrogen atoms anisotropic. Hydrogen atoms were included in calculated positions with fixed isotropic thermal parameters. Refinement converged at $R = 0.039$ and $R_w = 0.031$. Full details are contained in Appendix A.7.

4.4.3 X-ray structural analysis of 8

Crystals suitable for an X-ray diffraction study were obtained from CH_2Cl_2/hexane solutions at −15 °C. A yellow prism of approximate dimensions 0.1 x 0.08 x 0.2 mm was selected and mounted on a glass fibre. Crystals of **8** are monoclinic, space group *P21/n* with $Z = 4$. A total of 4607 observed [with $I > 2.5\ \sigma(I)$] data were collected and the structure was solved via Patterson and Fourier techniques. Hydrogen atoms were generated with fixed isotropic thermal parameters. All remaining atoms were refined anisotropicaly and refinement was reached at $R = 0.055$ and $R_w = 0.059$. Full details are listed in Appendix A.8.

4.4.4 X-ray structural analysis of 9

Suitable crystals of **9** were obtained from concentrated hexane/CH_2Cl_2 solutions at −15°C. A yellow prism of dimensions 0.2 x 0.2 x 0.1 mm was selected and mounted on a glass fibre. Compound **9** crystallizes in the monoclinic space group *P21/n* with $Z = 4$. Diffraction data were collected at −100 °C. A total of 6282 independent data were collected of which 4726 were considered as being observed. The heavy atom positions were obtained from a Patterson map with the lighter elements being located in subsequent difference Fourier maps. All non-hydrogen atoms were refined anisotropically. Hydrogen atoms were included in calculated positions with fixed isotropic thermal parameters. Final R and R_w values were 0.040 and 0.050 respectively. Full details are located in Appendix A.9.

4.4.5 X-ray structural analysis of 10

Orange prisms of **10** were obtained from an ether solution at −15°C. Cluster **10** crystallises in the monoclinic space group *P21/n* with $Z = 4$. A total of 8245 unique reflections were collected of which 6350 were considered observed [with $I > 2.5\ \sigma(I)$]. Solution (Patterson/Fourier) and refinement of the structure gave $R = 0.028$ and $R_w = 0.026$ with all non-hydrogen atoms anisotropic and hydrogen atoms in fixed positions with fixed isotropic thermal parameters. Full details are listed in Appendix A.10.

4.4.6 X-ray structural analysis of 11

Computations for **11** were performed using the SHELXTL suite of programs.[37] Single crystals of **11** suitable for X-ray analysis were obtained from an ether solution at

–15°C. A fragment of approximate dimensions 0.2 x 0.2 x 0.3 mm was cut and mounted into a glass capillary. Compound **11** crystallises in the triclinic space group *P*-1 and with $Z = 12$, contains six independent molecules per asymmetric unit. There are also twelve equivalents of diethyl ether solvent molecules per unit cell. A total of 101818 independent data were collected of which 40160 were considered as being unique. The structure of **11** was solved using the direct method. All non-hydrogen atoms were refined with anisotropic thermal parameters. Hydrogen atoms were put in calculated positions and treated as riding on the attached atoms. All six independent molecules are the same within the experimental errors. Final R and R_w values were 0.0587 and 0.1196 respectively. Complete crystallographic details are included in Appendix A.11.

4.4.7 X-ray structural analysis of 12

Deep green needles of **12** were grown from a CH_2Cl_2/hexane solution at –15°C. A crystal of approximate dimensions 0.2 x 0.05 x 0.08 mm was selected and mounted on a glass fiber. Cluster **12** crystallises in the triclinic space group *P-1* with $Z = 1$. The molecule lies across an inversion center and contains symmetry related atoms. There are also two equivalents of dichloromethane solvent molecules per unit cell. A total of 6421 unique reflections (5443 observed) were collected at –100°C. Patterson methods were used to locate the metal atoms and difference Fourier maps provided the location of the remaining non-hydrogen atoms. All non-hydrogen atoms were refined anisotropically. Hydrogen atoms were include in fixed positions with fixed isotropic thermal parameters. Refinement converged at $R = 0.033$ and $R_w = 0.038$. Complete details are contained in Appendix A.12.

4.5 References

1. a) Muetterties, E.L. *Science* **1977**, 196, 839. b) Ugo, R *Catal. Rev.-Sci. Eng.* **1975**, 11(2), 725. c) Kaesz, H.D.; Shriver, D.F. In *The Chemistry of Metal Cluster Complexes*; Shriver, D.F., Kaesz, H.D., Adams, R.D., Eds.; VCH: New York, 1990; pp 1-10. d) *The Synergy Between Dynamics and Reactivity at Clusters and Surfaces, NATO ASI Series C: Mathematical and Physical Sciences - Advanced Study Institute;*

Farrugia, L.J., Ed.; Kluwer Academic Publishers: Netherlands, 1995; Volume 465, 368 p.

2. Chini, P.; Longini, G; Albano, V.G. *Adv. Organometal. Chem.* **1976**, 14, 285.

3. Johnson, B.F.G.; Lewis, J. *Adv. Inorg. Chem. Radiochem.* **1981**, 24, 225.

4. Baetzold, R.C. *Inorg. Chem.* **1981**, 20, 118.

5. a) Muetterties, E.L. *Bull. Soc. Chim. Belg.* **1976**, 85, 451. b) Lauher, J.W. *J. Amer. Chem. Soc.* **1979**, 101, 2604. c) Shustorovich, E.; Baetzold, R.C. *J. Amer. Chem. Soc.* **1980**, 102, 5989.

6. *Chem. Soc. Spec. Publ. No. 18 "Tables of Interactomic Distances and Configurations in Molecules and Ions: supplement 1956-1959";* Sutton, L.E., McConnell, A.A., Gwladys, M.L., Mitchell, A.D., Eds.; Chemical Society: London, 1975.

7. Muetterties, E.L. *Bull. Soc. Chim. Belg.* **1975**, 84, 959.

8. Zaera, F.; Bernstein, N. *J. Am. Chem. Soc.* **1994**, 116, 4881.

9. Yang, M.X.; Eng Jr., J.; Kash, P.W.; Flynn, G.W.; Bent, B.E.; Holbrook, M.T.; Bare, S.R.; Gland, J.L.; Fischer, D.A. *J. Phys. Chem.* **1996**, 100, 12431.

10. Lehwald, S.; Ibach, H. *Surface Sci.* **1979**, 89, 425.

11. Parmeter, J.E.; Hills, M.M.; Weinberg, W.H. *J. Am Chem. Soc.* **1987**, 109, 72.

12. Zhou, X.-L.; White, J.M. *J. Phys. Chem.* **1991**, 95, 5575.

13. Zhou, X.-L.; Schwaner, A.L.; White, J.M. *J. Am. Chem. Soc.* **1993**, 115, 4309.

14. Zhou, X.-L.; White, J.M. *J. Phys. Chem.* **1992**, 96, 7703.

15. Zaera, F.; Fischer, D.A.; Carr, R.G.; Gland, J.L. *J. Chem. Phys* **1988**, 89, 5335.

16. Zaera, F.; Hall, R.B. *J. Phys. Chem.* **1987**, 91, 4318.

17. Zaera, F.; Hall, R.B. *Surface Sci.* **1987**, 180, 1.

18. Hall, R.B.; Bares, S.J.; DeSantolo, A.M.; Zaera, F. *J. Vac. Sci. Technol. A* **1986**, 4, 1493.

19. Zhu, X.-Y.; Castro, M.E.; Akhter, S.; White, J.M.; Houston, J.E. *Surface Sci.* **1988**, 207, 1.

20. Liu, Z.; Zhou, X.-L.; Buchanan, D.A.; Kiss, J.; White, J.M. *J. Am. Chem. Soc.* **1992**, 114, 2031.

21. Zhou, X.-L.; Liu, Z.-M.; White, J.M. *Chem. Phys. Lett.* **1992**, 195, 618.

22. Stuve, E.M.; Brundle, C.R. *Surface Sci.* **1985**, 152/153, 532.

23. Deeming, A.J.; Hasso, S.; Underhill, M. *J. Organomet. Chem.* **1974**, 80, C53.

24. a) Cooksey, C.J.; Deeming, A.J.; Rothwell, I.P. *J. Chem. Soc., Dalton Trans.* **1981**, 1718. b) Deeming, A.J.; Hasso, S.; Underhill, M. *J. Chem. Soc., Dalton Trans.* **1975**, 1614. c) Bryan, E.G.; Jackson, W.G.; Johnson, B.F.G.; Keland, J.W.; Lewis, J.; Schorpp, K.T. *J. Organomet. Chem.* **1976**, 108, 385. d) Keister, J.B.; Shapley, J.R. *J.*

Organomet. Chem. **1975**, 85, C29. e) Boyar, E.; Deeming, A.J.; Henrick, K.; McPartlin, M.; Scott, A. *J. Chem. Soc., Dalton Trans.* **1986**, 1431.

25. a) Beck, J.A.; Knox, S.A.R.; Riding, G.H.; Taylor, G.E.; Winter, M.J. *J. Organomet. Chem.* **1980**, 202, C49. b) Ahmed, K.J.; Chisholm, M.H.; Folting, K.; Huffman, J.C. *J. Am. Chem. Soc.* **1986**, 108, 989.

26. Beringhelli, T.; Alfonso, G.D.; Minoja, A.P.; Mynott, R. In *The Synergy Between Dynamics and Reactivity at Clusters and Surfaces, NATO ASI Series C: Mathematical and Physical Sciences - Advanced Study Institute;* Farrugia, L.J., Ed.; Kluwer Academic Publishers: Netherlands, 1995; Volume 465, pp 193-202.

27. Cramer, R. *J. Amer. Chem. Soc.* **1964**, 86, 217.

28. a) Powell, J.; Shaw, B.L. *J. Chem. Soc., A* **1967**, 1839. b) Vrieze, K.; Volger, H.C.; van Leeuwen, P.W.N.M. *Inorg. Chim. Acta Rev.* **1969**, 3, 109.

29. a) Bennet, M.J.; Cotton, F.A.; Davison, A.; Faller, J.W.; Lippard, S.J.; Morehouse, S.M. *J. Amer. Chem. Soc.* **1966**, 88, 4371. b) Whitesides, G.M.; Fleming, J.S. *J. Amer. Chem. Soc.* **1967**, 89, 2855.

30. Shiu, C.-W.; Chi, Y.; Carty, A.J.; Peng, S.-M.; Lee, G.-H. *Organometallics* **1997**, 16, 5368.

31. (a) Goudsmit, R.J.; Johnson, B.F.G.; Lewis, J.; Raithby, P.R.; Whitmire, K.H. *J. Chem. Soc., Chem. Commun.*, **1982**, 640. (b) Goudsmit, R.J.; Johnson, B.F.G.; Lewis, J.; Raithby, P.R.; Whitmire, K.H. *J. Chem. Soc., Chem. Commun.*, **1983**, 246.

32. Jeffrey, J. G.; Johnson, B. F. G.; Lewis, J.; Raithby, P. R.; Welch, D. A. *J. Chem. Soc., Chem. Commun.* **1986**, 318.

33. Evans, D.G.; Mingos, D.M.P. *Organometallics* **1983**, 2, 435.

34. Churchill, M.R.; de Boer, B.G. *Inorg. Chem.* **1977**, 16, 878.

35. Chi, Y.; Hwang, L.-S.; Lee, G.-H.; Peng, S.-M. *J. Chem. Soc., Chem. Commun.*, **1988**, 1456.

36. a) Koike, M, Hamilton, D.H., Wilson, S.R., Shapley, J.R. *Organometallics* **1996**, 15, 4930 and references therein. b) Farrugia, L.J.; Chi, Y.; Tu, W.-C. *Organometallics* **1993**, 12, 1616.

37. a) Sheldrick, G.M. *Acta Crystallogr.* **1990**, A46, 467. b) Sheldrick, G.M. *Acta Crystallogr.* **1993**, A49 (Suppl.), C53.

Appendix A.1

Structure Determination Summary for

$[Os_3W(\mu\text{-}H)(\mu\text{-}\eta^1\text{-}C{=}CHPh)(CO)_{10}(O)(\mu\text{-}O)(Cp^*)]$ 1

Empirical Formula	$Os_3WO_{12}C_{28}H_{22}$	
Crystal size (mm)	0.06 x 0.1 x 0.12	
Crystal System	Monoclinic	
Space Group	*P*21/c	
Unit Cell Dimensions	a = 14.2388(6) Å	$\alpha = 90$
	b = 13.8555(6) Å	$\beta = 91.16(1)$
	c = 16.1666(7) Å	$\gamma = 90$
Volume $(Å)^3$	3188.79(24)	
Z	4	
Formula Weight	1304.91	
Density (calc.) $(g\ cm^{-3})$	2.718	
Absorption Coefficient (mm^{-1})	15.57	
λ(Mo-Kα)	0.7107 Å	
Temperature (°C)	-100	
2θ Range (deg)	57.5	
Index Ranges	$-19 \le 19, 0 \le 18, 0 \le 21$	
Reflections Collected	36628	
Independent Reflections	8268	
Observed Reflections [$I > 2.5\ \sigma(I)$]	6403	
Weighting Scheme	$\omega^{-1} = \sigma^2(F_o) + 0.0001\ F_o^2$	
Number of Parameters Refined	425	
Final *R* Indices (obs. data)	$R = 0.029$; $R_W = 0.025$	
Final *R* Indices (all data)	$R = 0.029$; $R_W = 0.026$	
Goodness of Fit	1.53	
Largest and Mean Δ/σ	0.000	
Largest Difference Peak/Hole $(e/Å^3)$	-0.940/1.520	

Bond lengths (Å) for 1

Os(1)-Os(2)	2.9995(4)	C(6)-H(5)	1.98(6)
Os(1)-Os(3)	2.8529(4)	C(6)-H(6)	0.90(7)
Os(1)-W	2.7586(3)	C(6)-H(7)	1.91(6)
Os(1)-O(1)	2.110(4)	C(7)-C(8)	1.379(10)
Os(1)-C(1)	2.200(6)	C(7)-H(6)	1.99(6)
Os(1)-C(10)	1.855(7)	C(7)-H(7)	0.87(7)
Os(1)-C(11)	1.877(8)	C(8)-H(7)	1.99(7)
Os(1)-H(1)	1.84(6)	C(8)-H(8)	0.98(5)
Os(2)-Os(3)	2.9025(4)	C(40)-C(41)	1.423(9)
Os(2)-C(20)	1.990(8)	C(40)-C(44)	1.415(8)
Os(2)-C(21)	1.929(7)	C(40)-C(45)	1.510(9)
Os(2)-C(22)	1.942(8)	C(41)-C(42)	1.402(9)
Os(2)-C(23)	1.960(7)	C(41)-C(46)	1.506(9)
Os(2)-H(1)	1.62(7)	C(42)-C(43)	1.442(9)
Os(3)-C(30)	1.967(7)	C(42)-C(47)	1.482(9)
Os(3)-C(31)	1.910(8)	C(43)-C(44)	1.414(9)
Os(3)-C(32)	1.924(8)	C(43)-C(48)	1.515(9)
Os(3)-C(33)	1.931(7)	C(44)-C(49)	1.510(9)
W-O(1)	1.844(4)	C(45)-H(45a)	1.063(7)
W-O(2)	1.711(4)	C(45)-H(45b)	1.083(7)
W-C(1)	2.031(6)	C(45)-H(45c)	1.087(7)
W-C(40)	2.447(6)	C(46)-H(46a)	1.077(7)
W-C(41)	2.497(6)	C(46)-H(46b)	1.090(8)
W-C(42)	2.462(6)	C(46)-H(46c)	1.066(8)
W-C(43)	2.325(6)	C(47)-H(47a)	1.081(7)
W-C(44)	2.363(6)	C(47)-H(47b)	1.073(7)
O(10)-C(10)	1.157(8)	C(47)-H(47c)	1.088(7)
O(11)-C(11)	1.153(9)	C(48)-H(48a)	1.076(7)
O(20)-C(20)	1.121(9)	C(48)-H(48b)	1.077(8)
O(21)-C(21)	1.123(8)	C(48)-H(48c)	1.073(7)
O(22)-C(22)	1.129(9)	C(49)-H(49a)	1.085(7)
O(23)-C(23)	1.124(9)	C(49)-H(49b)	1.076(7)
O(30)-C(30)	1.135(9)	C(49)-H(49c)	1.071(7)
O(31)-C(31)	1.140(9)	H(45a)-H(45b)	1.76366(7)
O(32)-C(32)	1.138(9)	H(45a)-H(45c)	1.76366(5)
O(33)-C(33)	1.146(9)	H(45b)-H(45c)	1.76358(5)
C(1)-C(2)	1.319(9)	H(46a)-H(46b)	1.76366(6)
C(2)-C(3)	1.484(9)	H(46a)-H(46c)	1.76366(5)
C(2)-H(2)	1.12(6)	H(46b)-H(46c)	1.76358(6)
C(3)-C(4)	1.393(9)	H(47a)-H(47b)	1.76366(5)
C(3)-C(8)	1.385(10)	H(47a)-H(47c)	1.76366(6)
C(3)-H(4)	1.99(5)	H(47b)-H(47c)	1.76358(7)
C(4)-C(5)	1.396(11)	H(48a)-H(48b)	1.76366(5)
C(4)-H(4)	0.91(5)	H(48a)-H(48c)	1.76366(7)
C(4)-H(5)	1.95(6)	H(48b)-H(48c)	1.76358(7)

C(5)-C(6)	1.366(13)	H(49a)-H(49b)	1.76366(5)
C(5)-H(5)	0.88(6)	H(49a)-H(49c)	1.76366(6)
C(5)-H(6)	1.97(7)	H(49b)-H(49c)	1.76358(7)
C(6)-C(7)	1.368(12)		

Bond angles (deg) for 1

Os(2)-Os(1)-Os(3)	59.402(8)	C(6)-C(7)-H(7)	115(4)
Os(2)-Os(1)-W	98.037(10)	C(8)-C(7)-H(6)	143.8(20)
Os(2)-Os(1)-O(1)	82.54(11)	C(8)-C(7)-H(7)	123(4)
Os(2)-Os(1)-C(1)	112.65(14)	H(6)-C(7)-H(7)	92(5)
Os(2)-Os(1)-C(10)	95.82(20)	C(3)-C(8)-C(7)	120.7(7)
Os(2)-Os(1)-C(11)	149.19(22)	C(3)-C(8)-H(7)	142.0(19)
Os(2)-Os(1)-H(1)	28.0(20)	C(3)-C(8)-H(8)	120(3)
Os(3)-Os(1)-W	132.896(12)	C(7)-C(8)-H(7)	21.3(18)
Os(3)-Os(1)-O(1)	91.81(11)	C(7)-C(8)-H(8)	119(3)
Os(3)-Os(1)-C(1)	171.88(15)	H(7)-C(8)-H(8)	97(3)
Os(3)-Os(1)-C(10)	92.26(20)	Os(1)-C(10)-O(10)	177.6(6)
Os(3)-Os(1)-C(11)	90.05(22)	Os(1)-C(11)-O(11)	176.5(6)
Os(3)-Os(1)-H(1)	87.3(20)	Os(2)-C(20)-O(20)	174.3(6)
W-Os(1)-O(1)	41.93(11)	Os(2)-C(21)-O(21)	176.3(5)
W-Os(1)-C(1)	46.70(15)	Os(2)-C(22)-O(22)	179.3(6)
W-Os(1)-C(10)	133.18(20)	Os(2)-C(23)-O(23)	175.7(6)
W-Os(1)-C(11)	100.79(21)	Os(3)-C(30)-O(30)	173.5(5)
W-Os(1)-H(1)	78.7(19)	Os(3)-C(31)-O(31)	177.2(6)
O(1)-Os(1)-C(1)	88.59(19)	Os(3)-C(32)-O(32)	175.9(7)
O(1)-Os(1)-C(10)	174.06(23)	Os(3)-C(33)-O(33)	177.0(6)
O(1)-Os(1)-C(11)	95.5(3)	W-C(40)-C(41)	75.2(3)
O(1)-Os(1)-H(1)	81.4(20)	W-C(40)-C(44)	69.7(3)
C(1)-Os(1)-C(10)	86.77(25)	W-C(40)-C(45)	130.8(4)
C(1)-Os(1)-C(11)	98.0(3)	C(41)-C(40)-C(44)	107.9(5)
C(1)-Os(1)-H(1)	84.7(20)	C(41)-C(40)-C(45)	123.4(5)
C(10)-Os(1)-C(11)	88.8(3)	C(44)-C(40)-C(45)	127.4(6)
C(10)-Os(1)-H(1)	94.5(20)	W-C(41)-C(40)	71.4(3)
C(11)-Os(1)-H(1)	175.8(20)	W-C(41)-C(42)	72.2(3)
Os(1)-Os(2)-Os(3)	57.785(8)	W-C(41)-C(46)	127.5(4)
Os(1)-Os(2)-C(20)	88.06(18)	C(40)-C(41)-C(42)	109.3(5)
Os(1)-Os(2)-C(21)	118.11(19)	C(40)-C(41)-C(46)	124.0(6)
Os(1)-Os(2)-C(22)	144.69(21)	C(42)-C(41)-C(46)	126.5(6)
Os(1)-Os(2)-C(23)	86.53(18)	W-C(42)-C(41)	75.0(4)
Os(1)-Os(2)-H(1)	32.1(22)	W-C(42)-C(43)	67.3(3)
Os(3)-Os(2)-C(20)	84.85(18)	W-C(42)-C(47)	120.1(4)
Os(3)-Os(2)-C(21)	172.91(19)	C(41)-C(42)-C(43)	106.5(5)
Os(3)-Os(2)-C(22)	86.97(22)	C(41)-C(42)-C(47)	127.9(6)
Os(3)-Os(2)-C(23)	92.91(18)	C(43)-C(42)-C(47)	125.6(6)
Os(3)-Os(2)-H(1)	89.8(22)	W-C(43)-C(42)	77.7(3)
C(20)-Os(2)-C(21)	89.3(3)	W-C(43)-C(44)	73.9(4)
C(20)-Os(2)-C(22)	91.1(3)	W-C(43)-C(48)	118.4(4)
C(20)-Os(2)-C(23)	174.5(3)	C(42)-C(43)-C(44)	108.7(5)
C(20)-Os(2)-H(1)	92.1(22)	C(42)-C(43)-C(48)	124.8(6)
C(21)-Os(2)-C(22)	97.2(3)	C(44)-C(43)-C(48)	126.3(6)
C(21)-Os(2)-C(23)	92.6(3)	W-C(44)-C(40)	76.2(3)

C(21)-Os(2)-H(1)	86.4(21)	W-C(44)-C(43)	71.0(3)
C(22)-Os(2)-C(23)	93.7(3)	W-C(44)-C(49)	121.8(4)
C(22)-Os(2)-H(1)	175.3(21)	C(40)-C(44)-C(43)	107.5(5)
C(23)-Os(2)-H(1)	82.9(22)	C(40)-C(44)-C(49)	126.0(6)
Os(1)-Os(3)-Os(2)	62.813(9)	C(43)-C(44)-C(49)	126.4(5)
Os(1)-Os(3)-C(30)	81.37(17)	C(40)-C(45)-H(45a)	110.0(6)
Os(1)-Os(3)-C(31)	95.56(22)	C(40)-C(45)-H(45b)	108.7(5)
Os(1)-Os(3)-C(32)	161.46(22)	C(40)-C(45)-H(45c)	108.5(6)
Os(1)-Os(3)-C(33)	92.64(20)	H(45a)-C(45)-H(45b)	110.5(6)
Os(2)-Os(3)-C(30)	93.29(17)	H(45a)-C(45)-H(45c)	110.3(6)
Os(2)-Os(3)-C(31)	157.30(22)	H(45b)-C(45)-H(45c)	108.7(6)
Os(2)-Os(3)-C(32)	100.44(23)	C(41)-C(46)-H(46a)	109.1(6)
Os(2)-Os(3)-C(33)	84.91(19)	C(41)-C(46)-H(46b)	108.2(6)
C(30)-Os(3)-C(31)	89.9(3)	C(41)-C(46)-H(46c)	109.8(6)
C(30)-Os(3)-C(32)	92.4(3)	H(46a)-C(46)-H(46b)	109.0(6)
C(30)-Os(3)-C(33)	173.9(3)	H(46a)-C(46)-H(46c)	110.8(6)
C(31)-Os(3)-C(32)	101.9(3)	H(46b)-C(46)-H(46c)	109.8(6)
C(31)-Os(3)-C(33)	89.6(3)	C(42)-C(47)-H(47a)	109.4(6)
C(32)-Os(3)-C(33)	93.7(3)	C(42)-C(47)-H(47b)	110.1(6)
Os(1)-W-O(1)	49.85(12)	C(42)-C(47)-H(47c)	109.1(6)
Os(1)-W-O(2)	110.84(14)	H(47a)-C(47)-H(47b)	110.0(6)
Os(1)-W-C(1)	52.03(16)	H(47a)-C(47)-H(47c)	108.8(7)
Os(1)-W-C(40)	124.96(14)	H(47b)-C(47)-H(47c)	109.4(6)
Os(1)-W-C(41)	102.37(13)	C(43)-C(48)-H(48a)	108.7(6)
Os(1)-W-C(42)	108.29(14)	C(43)-C(48)-H(48b)	108.7(6)
Os(1)-W-C(43)	140.18(16)	C(43)-C(48)-H(48c)	108.9(6)
Os(1)-W-C(44)	158.05(14)	H(48a)-C(48)-H(48b)	110.0(7)
O(1)-W-O(2)	106.23(20)	H(48a)-C(48)-H(48c)	110.3(6)
O(1)-W-C(1)	101.83(20)	H(48b)-C(48)-H(48c)	110.2(6)
O(1)-W-C(40)	132.71(20)	C(44)-C(49)-H(49a)	108.6(6)
O(1)-W-C(41)	99.67(20)	C(44)-C(49)-H(49b)	109.1(6)
O(1)-W-C(42)	79.97(19)	C(44)-C(49)-H(49c)	109.5(5)
O(1)-W-C(43)	97.21(20)	H(49a)-C(49)-H(49b)	109.4(6)
O(1)-W-C(44)	132.11(20)	H(49a)-C(49)-H(49c)	109.8(6)
O(2)-W-C(1)	101.86(21)	H(49b)-C(49)-H(49c)	110.4(6)
O(2)-W-C(40)	115.75(21)	Os(1)-H(1)-Os(2)	119(4)
O(2)-W-C(41)	146.21(19)	C(3)-H(4)-C(4)	38.5(22)
O(2)-W-C(42)	132.63(20)	C(4)-H(5)-C(5)	39(3)
O(2)-W-C(43)	98.61(20)	C(4)-H(5)-C(6)	75.6(20)
O(2)-W-C(44)	90.05(20)	C(5)-H(5)-C(6)	35(3)
C(1)-W-C(40)	90.30(22)	C(5)-H(6)-C(6)	36(3)
C(1)-W-C(41)	93.51(21)	C(5)-H(6)-C(7)	72.8(23)
C(1)-W-C(42)	123.21(22)	C(6)-H(6)-C(7)	35(3)
C(1)-W-C(43)	146.74(22)	C(6)-H(7)-C(7)	40(3)
C(1)-W-C(44)	118.76(22)	C(6)-H(7)-C(8)	75.7(25)
C(40)-W-C(41)	33.44(21)	C(7)-H(7)-C(8)	35(3)

C(40)-W-C(42)	55.97(21)	C(45)-H(45a)-H(45b)	35.1(4)
C(40)-W-C(43)	57.06(21)	C(45)-H(45a)-H(45c)	35.3(4)
C(40)-W-C(44)	34.15(20)	H(45b)-H(45a)-H(45c)	60.0
C(41)-W-C(42)	32.83(21)	C(45)-H(45b)-H(45a)	34.4(4)
C(41)-W-C(43)	56.27(20)	C(45)-H(45b)-H(45c)	35.7(4)
C(41)-W-C(44)	56.27(20)	H(45a)-H(45b)-H(45c)	60.0
C(42)-W-C(43)	34.91(21)	C(45)-H(45c)-H(45a)	34.4(3)
C(42)-W-C(44)	57.46(21)	C(45)-H(45c)-H(45b)	35.6(4)
C(43)-W-C(44)	35.10(22)	H(45a)-H(45c)-H(45b)	60.0
Os(1)-O(1)-W	88.22(17)	C(46)-H(46a)-H(46b)	35.7(4)
Os(1)-C(1)-W	81.27(22)	C(46)-H(46a)-H(46c)	34.4(4)
Os(1)-C(1)-C(2)	128.9(4)	H(46b)-H(46a)-H(46c)	60.0
W-C(1)-C(2)	148.6(5)	C(46)-H(46b)-H(46a)	35.3(4)
C(1)-C(2)-C(3)	126.8(6)	C(46)-H(46b)-H(46c)	34.6(4)
C(1)-C(2)-H(2)	119(3)	H(46a)-H(46b)-H(46c)	60.0
C(3)-C(2)-H(2)	113(3)	C(46)-H(46c)-H(46a)	34.8(4)
C(2)-C(3)-C(4)	122.0(6)	C(46)-H(46c)-H(46b)	35.5(4)
C(2)-C(3)-C(8)	119.7(6)	H(46a)-H(46c)-H(46b)	60.0
C(2)-C(3)-H(4)	98.0(16)	C(47)-H(47a)-H(47b)	34.9(4)
C(4)-C(3)-C(8)	118.3(6)	C(47)-H(47a)-H(47c)	35.7(4)
C(4)-C(3)-H(4)	24.0(15)	H(47b)-H(47a)-H(47c)	60.0
C(8)-C(3)-H(4)	142.3(16)	C(47)-H(47b)-H(47a)	35.2(4)
C(3)-C(4)-C(5)	119.4(7)	C(47)-H(47b)-H(47c)	35.6(4)
C(3)-C(4)-H(4)	117(3)	H(47a)-H(47b)-H(47c)	60.0
C(3)-C(4)-H(5)	143.1(18)	C(47)-H(47c)-H(47a)	35.5(4)
C(5)-C(4)-H(4)	122(3)	C(47)-H(47c)-H(47b)	35.0(4)
C(5)-C(4)-H(5)	23.8(17)	H(47a)-H(47c)-H(47b)	60.0
H(4)-C(4)-H(5)	98(3)	C(48)-H(48a)-H(48b)	35.0(4)
C(4)-C(5)-C(6)	121.5(7)	C(48)-H(48a)-H(48c)	34.8(4)
C(4)-C(5)-H(5)	116(4)	H(48b)-H(48a)-H(48c)	60.0
C(4)-C(5)-H(6)	144.8(19)	C(48)-H(48b)-H(48a)	35.0(4)
C(6)-C(5)-H(5)	121(4)	C(48)-H(48b)-H(48c)	34.8(4)
C(6)-C(5)-H(6)	23.3(18)	H(48a)-H(48b)-H(48c)	60.0
H(5)-C(5)-H(6)	98(4)	C(48)-H(48c)-H(48a)	34.9(4)
C(5)-C(6)-C(7)	118.6(7)	C(48)-H(48c)-H(48b)	35.0(4)
C(5)-C(6)-H(5)	22.2(17)	H(48a)-H(48c)-H(48b)	60.0
C(5)-C(6)-H(6)	119(4)	C(49)-H(49a)-H(49b)	35.1(4)
C(5)-C(6)-H(7)	142.7(21)	C(49)-H(49a)-H(49c)	34.9(4)
C(7)-C(6)-H(5)	140.8(17)	H(49b)-H(49a)-H(49c)	60.0
C(7)-C(6)-H(6)	121(4)	C(49)-H(49b)-H(49a)	35.5(4)
C(7)-C(6)-H(7)	24.2(20)	C(49)-H(49b)-H(49c)	34.7(4)
H(5)-C(6)-H(6)	97(4)	H(49a)-H(49b)-H(49c)	60.0
H(5)-C(6)-H(7)	164(3)	C(49)-H(49c)-H(49a)	35.4(4)
H(6)-C(6)-H(7)	97(5)	C(49)-H(49c)-H(49b)	34.9(4)
C(6)-C(7)-C(8)	121.2(8)	H(49a)-H(49c)-H(49b)	60.0
C(6)-C(7)-H(6)	22.6(20)		

Atomic Coordinates and equivalent isotropic displacement coefficients ($Å^2 \times 10^3$) for 1.

	x	y	z	U(eq)
Os1	0.716211(16)	0.570443(18)	0.239178(14)	1.810(9)
Os2	0.692510(17)	0.732443(18)	0.117462(15)	1.972(9)
Os3	0.533455(17)	0.629436(19)	0.184081(16)	2.245(10)
W	0.860569(17)	0.474921(18)	0.162663(14)	1.834(10)
O1	0.7363(3)	0.4890(3)	0.13070(24)	2.33(17)
O2	0.9229(3)	0.5522(3)	0.1022(3)	2.79(20)
O10	0.7105(4)	0.6934(4)	0.3926(3)	3.80(23)
O11	0.6260(4)	0.4095(4)	0.3364(4)	6.0(3)
O20	0.6850(4)	0.5843(4)	-0.0268(3)	3.64(24)
O21	0.8672(3)	0.8139(4)	0.0365(3)	3.27(21)
O22	0.5490(4)	0.8592(5)	0.0237(3)	5.6(3)
O23	0.7121(4)	0.8666(3)	0.2689(3)	3.53(22)
O30	0.5501(3)	0.4522(3)	0.0686(3)	3.09(20)
O31	0.4282(4)	0.5039(4)	0.3063(4)	5.2(3)
O32	0.3714(4)	0.7070(4)	0.0761(3)	4.9(3)
O33	0.5244(3)	0.7933(4)	0.3121(3)	4.32(25)
C1	0.8643(4)	0.5439(4)	0.2735(4)	1.93(23)
C2	0.9146(4)	0.5811(5)	0.3351(4)	2.3(3)
C3	1.0177(4)	0.5725(4)	0.3484(4)	2.3(3)
C4	1.0791(5)	0.5650(5)	0.2827(5)	2.8(3)
C5	1.1748(5)	0.5516(5)	0.2990(6)	3.5(3)
C6	1.2101(5)	0.5467(5)	0.3781(6)	3.5(4)
C7	1.1500(5)	0.5593(5)	0.4422(5)	3.4(3)
C8	1.0552(5)	0.5734(5)	0.4281(4)	2.7(3)
C10	0.7110(4)	0.6472(5)	0.3330(4)	2.5(3)
C11	0.6630(5)	0.4692(6)	0.2996(5)	3.5(3)
C20	0.6865(5)	0.6339(5)	0.0280(4)	2.7(3)
C21	0.8037(5)	0.7855(5)	0.0687(4)	2.4(3)
C22	0.6017(5)	0.8129(5)	0.0586(4)	3.5(3)
C23	0.7017(4)	0.8195(5)	0.2129(4)	2.6(3)
C30	0.5495(4)	0.5184(5)	0.1099(4)	2.4(3)
C31	0.4668(5)	0.5494(5)	0.2591(5)	3.3(3)
C32	0.4330(5)	0.6816(6)	0.1164(5)	3.5(3)
C33	0.5295(4)	0.7337(5)	0.2632(4)	3.0(3)
C40	0.9496(4)	0.3401(4)	0.2227(4)	2.19(25)
C41	0.8539(4)	0.3112(4)	0.2269(4)	2.18(25)
C42	0.8156(4)	0.3043(4)	0.1465(4)	2.3(3)
C43	0.8889(5)	0.3326(4)	0.0912(4)	2.2(3)
C44	0.9715(4)	0.3518(4)	0.1383(4)	2.10(24)
C45	1.0173(5)	0.3364(5)	0.2957(4)	3.0(3)
C46	0.8065(5)	0.2830(5)	0.3057(4)	3.4(3)
C47	0.7181(5)	0.2784(5)	0.1214(5)	3.4(3)
C48	0.8794(5)	0.3337(5)	-0.0023(4)	3.4(3)

C49	1.0674(5)	0.3736(5)	0.1049(4)	3.2(3)
H1	0.763(4)	0.667(5)	0.173(4)	4.0(16)
H2	0.879(4)	0.626(5)	0.383(4)	3.4(15)
H4	1.053(4)	0.561(4)	0.231(3)	0.5(11)
H5	1.210(4)	0.542(4)	0.256(4)	1.6(13)
H6	1.271(5)	0.535(5)	0.387(4)	2.9(15)
H7	1.176(5)	0.560(5)	0.491(4)	2.9(16)
H8	1.014(3)	0.584(3)	0.476(3)	0.6(10)
H45a	1.043	0.265	0.304	4.3
H45b	1.075	0.386	0.285	4.3
H45c	0.981	0.360	0.350	4.3
H46a	0.817	0.207	0.317	4.3
H46b	0.839	0.324	0.356	4.3
H46c	0.733	0.300	0.301	4.3
H47a	0.712	0.201	0.117	4.3
H47b	0.670	0.306	0.166	4.3
H47c	0.702	0.310	0.061	4.3
H48a	0.895	0.263	-0.025	4.3
H48b	0.808	0.354	-0.019	4.3
H48c	0.928	0.385	-0.026	4.3
H49a	1.106	0.306	0.099	4.3
H49b	1.059	0.407	0.045	4.3
H49c	1.105	0.421	0.147	4.3

Appendix A.2

Structure Determination Summary for

$[Os_3W(\mu\text{-}H)(trans\text{-}\mu\text{-}\eta^1\text{-}C{=}CHPh)(CO)_9(O)(Cp^*)(\mu_3\text{-}O)]$ 2

Empirical Formula	$Os_3WO_{11}C_{27}H_{22}$	
Crystal size (mm)	0.4 x 0.1 x 0.12	
Crystal System	Triclinic	
Space Group	*P*-1	
Unit Cell Dimensions	a = 7.7765(3) Å	α = 74.20(1)
	b = 13.1192(6) Å	β = 76.19(1)
	c = 15.9504(7) Å	γ = 84.08(1)
Volume $(Å)^3$	1519.21(11)	
Z	2	
Formula Weight	1276.90	
Density (calc.) $(g\ cm^{-3})$	2.791	
Absorption Coefficient (mm^{-1})	16.33	
λ(Mo-Kα)	0.70930 Å	
Temperature (°C)	-100	
2θ Range (deg)	57.4	
Index Ranges	$-10 \le 10, 0 \le 17, -20 \le 21$	
Reflections Collected	17858	
Independent Reflections	7796	
Observed Reflections [I > 2.5 σ(I)]	6046	
Weighting Scheme	$\omega^{-1} = \sigma^2(F_o) + 0.0001\ F_o^2$	
Number of Parameters Refined	383	
Final *R* Indices (obs. data)	R = 0.035; R_W = 0.035	
Final *R* Indices (all data)	R = 0.035; R_W = 0.035	
Goodness of Fit	1.43	
Largest and Mean Δ/σ	0.000	
Largest Difference Peak/Hole $(e/Å^3)$	-1.770/2.430	

Bond lengths (Å) for 2

Os(1)-Os(2)	2.8139(5)	C(2)-H(2)	0.87(7)
Os(1)-Os(3)	2.8120(6)	C(3)-C(4)	1.383(12)
Os(1)-W	2.7129(5)	C(3)-C(8)	1.403(12)
Os(1)-O(1)	2.098(5)	C(4)-C(5)	1.407(13)
Os(1)-C(1)	2.194(8)	C(4)-H(4)	1.079(9)
Os(1)-C(10)	1.884(9)	C(5)-C(6)	1.400(14)
Os(1)-C(11)	1.881(9)	C(5)-H(5)	1.064(9)
Os(1)-H(1)	1.8548(4)	C(6)-C(7)	1.353(15)
Os(2)-Os(3)	2.8373(6)	C(6)-H(6)	1.102(9)
Os(2)-C(20)	1.925(10)	C(7)-C(8)	1.391(14)
Os(2)-C(21)	1.962(10)	C(7)-H(7)	1.076(9)
Os(2)-C(22)	1.901(10)	C(8)-H(8)	1.069(9)
Os(2)-C(23)	1.946(10)	C(40)-C(41)	1.428(12)
Os(3)-O(1)	2.158(5)	C(40)-C(44)	1.425(13)
Os(3)-C(30)	1.939(10)	C(40)-C(45)	1.517(13)
Os(3)-C(31)	1.905(9)	C(41)-C(42)	1.416(12)
Os(3)-C(32)	1.882(8)	C(41)-C(46)	1.489(12)
Os(3)-H(1)	1.6082(4)	C(42)-C(43)	1.475(12)
W-O(1)	1.959(5)	C(42)-C(47)	1.509(12)
W-O(2)	1.721(5)	C(43)-C(44)	1.394(12)
W-C(1)	2.024(8)	C(43)-C(48)	1.495(13)
W-C(40)	2.366(8)	C(44)-C(49)	1.505(12)
W-C(41)	2.454(7)	C(45)-H(45a)	1.063(9)
W-C(42)	2.452(7)	C(45)-H(45b)	1.122(11)
W-C(43)	2.381(8)	C(45)-H(45c)	1.056(11)
W-C(44)	2.358(8)	C(46)-H(46a)	1.068(8)
O(10)-C(10)	1.147(11)	C(46)-H(46b)	1.054(10)
O(11)-C(11)	1.134(11)	C(46)-H(46c)	1.125(11)
O(20)-C(20)	1.143(13)	C(47)-H(47a)	1.060(8)
O(21)-C(21)	1.124(12)	C(47)-H(47b)	1.087(9)
O(22)-C(22)	1.142(12)	C(47)-H(47c)	1.086(9)
O(23)-C(23)	1.133(13)	C(48)-H(48a)	1.086(9)
O(30)-C(30)	1.127(11)	C(48)-H(48b)	1.090(10)
O(31)-C(31)	1.137(11)	C(48)-H(48c)	1.086(9)
O(32)-C(32)	1.152(10)	C(49)-H(49a)	1.060(9)
C(1)-C(2)	1.331(11)	C(49)-H(49b)	1.103(10)
C(1)-H(2)	1.86(7)	C(49)-H(49c)	1.093(10)
C(2)-C(3)	1.474(12)		

Bond angles (deg) for 2

Os(2)-Os(1)-Os(3)	60.574(14)	Os(1)-O(1)-W	83.86(20)
Os(2)-Os(1)-W	131.323(17)	Os(3)-O(1)-W	118.78(23)
Os(2)-Os(1)-O(1)	85.71(15)	Os(1)-C(1)-W	80.0(3)
Os(2)-Os(1)-C(1)	178.35(19)	Os(1)-C(1)-C(2)	129.3(6)
Os(2)-Os(1)-C(10)	88.9(3)	Os(1)-C(1)-H(2)	104.2(22)
Os(2)-Os(1)-C(11)	95.3(3)	W-C(1)-C(2)	150.6(6)
Os(2)-Os(1)-H(1)	76.616(15)	W-C(1)-H(2)	174.9(21)
Os(3)-Os(1)-W	79.796(13)	C(2)-C(1)-H(2)	25.6(21)
Os(3)-Os(1)-O(1)	49.58(14)	C(1)-C(2)-C(3)	127.3(8)
Os(3)-Os(1)-C(1)	117.80(19)	C(1)-C(2)-H(2)	113(4)
Os(3)-Os(1)-C(10)	137.3(3)	C(3)-C(2)-H(2)	119(4)
Os(3)-Os(1)-C(11)	120.4(3)	C(2)-C(3)-C(4)	121.9(7)
Os(3)-Os(1)-H(1)	32.871(10)	C(2)-C(3)-C(8)	119.1(7)
W-Os(1)-O(1)	45.87(15)	C(4)-C(3)-C(8)	118.8(8)
W-Os(1)-C(1)	47.26(20)	C(3)-C(4)-C(5)	120.3(8)
W-Os(1)-C(10)	104.7(3)	C(3)-C(4)-H(4)	119.8(8)
W-Os(1)-C(11)	130.6(3)	C(5)-C(4)-H(4)	119.8(8)
W-Os(1)-H(1)	85.090(15)	C(4)-C(5)-C(6)	119.6(9)
O(1)-Os(1)-C(1)	92.96(25)	C(4)-C(5)-H(5)	120.2(9)
O(1)-Os(1)-C(10)	103.4(3)	C(6)-C(5)-H(5)	120.2(9)
O(1)-Os(1)-C(11)	167.4(3)	C(5)-C(6)-C(7)	119.9(9)
O(1)-Os(1)-H(1)	75.65(13)	C(5)-C(6)-H(6)	119.9(9)
C(1)-Os(1)-C(10)	92.4(3)	C(7)-C(6)-H(6)	120.2(9)
C(1)-Os(1)-C(11)	85.8(3)	C(6)-C(7)-C(8)	121.1(9)
C(1)-Os(1)-H(1)	102.13(18)	C(6)-C(7)-H(7)	119.4(9)
C(10)-Os(1)-C(11)	89.3(4)	C(8)-C(7)-H(7)	119.5(9)
C(10)-Os(1)-H(1)	165.5(3)	C(3)-C(8)-C(7)	120.2(8)
C(11)-Os(1)-H(1)	92.3(3)	C(3)-C(8)-H(8)	120.2(8)
Os(1)-Os(2)-Os(3)	59.680(15)	C(7)-C(8)-H(8)	119.6(8)
Os(1)-Os(2)-C(20)	104.0(3)	Os(1)-C(10)-O(10)	176.7(8)
Os(1)-Os(2)-C(21)	84.3(3)	Os(1)-C(11)-O(11)	175.8(8)
Os(1)-Os(2)-C(22)	157.8(3)	Os(2)-C(20)-O(20)	179.7(9)
Os(1)-Os(2)-C(23)	82.4(3)	Os(2)-C(21)-O(21)	177.9(8)
Os(3)-Os(2)-C(20)	163.7(3)	Os(2)-C(22)-O(22)	176.8(10)
Os(3)-Os(2)-C(21)	87.7(3)	Os(2)-C(23)-O(23)	178.7(8)
Os(3)-Os(2)-C(22)	98.1(3)	Os(3)-C(30)-O(30)	171.6(8)
Os(3)-Os(2)-C(23)	81.8(3)	Os(3)-C(31)-O(31)	178.1(8)
C(20)-Os(2)-C(21)	91.2(4)	Os(3)-C(32)-O(32)	179.0(7)
C(20)-Os(2)-C(22)	98.2(5)	W-C(40)-C(41)	76.2(4)
C(20)-Os(2)-C(23)	96.4(4)	W-C(40)-C(44)	72.1(4)
C(21)-Os(2)-C(22)	95.5(4)	W-C(40)-C(45)	121.4(6)
C(21)-Os(2)-C(23)	166.0(4)	C(41)-C(40)-C(44)	108.6(7)
C(22)-Os(2)-C(23)	95.1(4)	C(41)-C(40)-C(45)	125.5(8)
Os(1)-Os(3)-Os(2)	59.746(13)	C(44)-C(40)-C(45)	125.8(8)
Os(1)-Os(3)-O(1)	47.74(14)	W-C(41)-C(40)	69.4(4)

Os(1)-Os(3)-C(30)	117.22(25)	W-C(41)-C(42)	73.1(4)
Os(1)-Os(3)-C(31)	131.01(25)	W-C(41)-C(46)	125.3(6)
Os(1)-Os(3)-C(32)	121.6(3)	C(40)-C(41)-C(42)	108.3(7)
Os(1)-Os(3)-H(1)	38.752(11)	C(40)-C(41)-C(46)	123.9(8)
Os(2)-Os(3)-O(1)	84.04(14)	C(42)-C(41)-C(46)	127.7(8)
Os(2)-Os(3)-C(30)	175.9(3)	W-C(42)-C(41)	73.3(4)
Os(2)-Os(3)-C(31)	88.2(3)	W-C(42)-C(43)	69.7(4)
Os(2)-Os(3)-C(32)	88.6(3)	W-C(42)-C(47)	126.4(5)
Os(2)-Os(3)-H(1)	79.298(16)	C(41)-C(42)-C(43)	106.4(7)
O(1)-Os(3)-C(30)	95.7(3)	C(41)-C(42)-C(47)	126.6(8)
O(1)-Os(3)-C(31)	97.1(3)	C(43)-C(42)-C(47)	126.8(8)
O(1)-Os(3)-C(32)	169.2(3)	W-C(43)-C(42)	74.8(4)
O(1)-Os(3)-H(1)	78.95(14)	W-C(43)-C(44)	72.0(5)
C(30)-Os(3)-C(31)	95.9(4)	W-C(43)-C(48)	126.8(5)
C(30)-Os(3)-C(32)	91.1(4)	C(42)-C(43)-C(44)	108.4(7)
C(30)-Os(3)-H(1)	96.6(3)	C(42)-C(43)-C(48)	125.1(8)
C(31)-Os(3)-C(32)	90.4(4)	C(44)-C(43)-C(48)	125.7(8)
C(31)-Os(3)-H(1)	167.2(3)	W-C(44)-C(40)	72.7(5)
C(32)-Os(3)-H(1)	92.02(25)	W-C(44)-C(43)	73.8(5)
Os(1)-W-O(1)	50.27(15)	W-C(44)-C(49)	120.1(5)
Os(1)-W-O(2)	112.37(19)	C(40)-C(44)-C(43)	108.2(7)
Os(1)-W-C(1)	52.78(22)	C(40)-C(44)-C(49)	126.4(8)
Os(1)-W-C(40)	121.32(22)	C(43)-C(44)-C(49)	125.4(8)
Os(1)-W-C(41)	100.85(20)	C(40)-C(45)-H(45a)	110.4(8)
Os(1)-W-C(42)	110.69(21)	C(40)-C(45)-H(45b)	107.1(8)
Os(1)-W-C(43)	144.69(21)	C(40)-C(45)-H(45c)	110.8(8)
Os(1)-W-C(44)	156.20(21)	H(45a)-C(45)-H(45b)	107.6(9)
O(1)-W-O(2)	109.18(24)	H(45a)-C(45)-H(45c)	112.6(9)
O(1)-W-C(1)	102.8(3)	H(45b)-C(45)-H(45c)	108.1(8)
O(1)-W-C(40)	81.9(3)	C(41)-C(46)-H(46a)	110.4(8)
O(1)-W-C(41)	84.84(24)	C(41)-C(46)-H(46b)	111.3(8)
O(1)-W-C(42)	116.06(25)	C(41)-C(46)-H(46c)	107.4(8)
O(1)-W-C(43)	138.47(24)	H(46a)-C(46)-H(46b)	112.5(9)
O(1)-W-C(44)	112.9(3)	H(46a)-C(46)-H(46c)	107.0(8)
O(2)-W-C(1)	102.8(3)	H(46b)-C(46)-H(46c)	108.0(8)
O(2)-W-C(40)	114.5(3)	C(42)-C(47)-H(47a)	110.1(7)
O(2)-W-C(41)	145.6(3)	C(42)-C(47)-H(47b)	108.6(7)
O(2)-W-C(42)	130.9(3)	C(42)-C(47)-H(47c)	108.6(7)
O(2)-W-C(43)	96.5(3)	H(47a)-C(47)-H(47b)	110.4(7)
O(2)-W-C(44)	88.1(3)	H(47a)-C(47)-H(47c)	110.5(8)
C(1)-W-C(40)	138.6(3)	H(47b)-C(47)-H(47c)	108.5(7)
C(1)-W-C(41)	104.4(3)	C(43)-C(48)-H(48a)	110.6(7)
C(1)-W-C(42)	85.2(3)	C(43)-C(48)-H(48b)	110.4(8)
C(1)-W-C(43)	102.5(3)	C(43)-C(48)-H(48c)	110.7(8)
C(1)-W-C(44)	136.7(3)	H(48a)-C(48)-H(48b)	108.3(8)
C(40)-W-C(41)	34.4(3)	H(48a)-C(48)-H(48c)	108.6(8)

C(40)-W-C(42)	57.2(3)	H(48b)-C(48)-H(48c)	108.2(8)
C(40)-W-C(43)	57.5(3)	C(44)-C(49)-H(49a)	111.8(7)
C(40)-W-C(44)	35.1(3)	C(44)-C(49)-H(49b)	109.0(8)
C(41)-W-C(42)	33.6(3)	C(44)-C(49)-H(49c)	109.8(8)
C(41)-W-C(43)	57.2(3)	H(49a)-C(49)-H(49b)	109.2(9)
C(41)-W-C(44)	57.5(3)	H(49a)-C(49)-H(49c)	110.0(8)
C(42)-W-C(43)	35.5(3)	H(49b)-C(49)-H(49c)	106.9(7)
C(42)-W-C(44)	57.9(3)	Os(1)-H(1)-Os(3)	108.378(16)
C(43)-W-C(44)	34.2(3)	C(1)-H(2)-C(2)	41(3)
Os(1)-O(1)-Os(3)	82.68(18)		

Atomic Coordinates and equivalent isotropic displacement coefficients ($Å^2$ x 10^3) for 2.

	x	Y	z	U(eq)
Os1	0.76355(4)	0.810939(25)	0.185377(21)	1.648(13)
Os2	0.86753(4)	0.60343(3)	0.170863(24)	2.346(15)
Os3	0.67190(4)	0.63906(3)	0.335602(22)	1.808(13)
W	0.75433(4)	0.905674(25)	0.317921(21)	1.497(13)
O1	0.8516(6)	0.7655(4)	0.3053(3)	1.82(23)
O2	0.5551(7)	0.8916(4)	0.3946(4)	2.22(24)
O10	1.0918(9)	0.8876(6)	0.0434(4)	4.0(4)
O11	0.5533(10)	0.8677(6)	0.0419(5)	4.3(4)
O20	1.0708(11)	0.6335(7)	-0.0238(6)	6.0(5)
O21	0.5122(9)	0.6070(5)	0.1159(5)	3.6(3)
O22	0.9076(10)	0.3632(6)	0.2336(6)	5.7(5)
O23	1.1814(9)	0.6406(6)	0.2441(5)	4.4(4)
O30	0.4407(8)	0.6762(5)	0.5097(4)	3.3(3)
O31	0.9024(9)	0.4656(6)	0.4303(5)	4.3(4)
O32	0.4107(9)	0.4790(5)	0.3422(5)	3.7(3)
C1	0.6801(9)	0.9709(6)	0.2009(5)	1.6(3)
C2	0.6098(10)	1.0515(6)	0.1467(5)	1.7(3)
C3	0.5302(10)	1.1518(6)	0.1660(6)	2.0(3)
C4	0.4282(11)	1.1556(7)	0.2490(6)	2.5(4)
C5	0.3462(13)	1.2520(8)	0.2636(6)	3.4(5)
C6	0.3709(13)	1.3445(7)	0.1938(7)	3.2(5)
C7	0.4695(14)	1.3403(8)	0.1124(7)	3.5(5)
C8	0.5472(12)	1.2451(7)	0.0964(6)	2.6(4)
C10	0.9694(13)	0.8597(7)	0.0989(6)	2.8(4)
C11	0.6357(12)	0.8434(7)	0.0945(6)	2.7(4)
C20	0.9951(14)	0.6226(8)	0.0487(7)	3.7(5)
C21	0.6407(12)	0.6075(7)	0.1362(6)	2.8(4)
C22	0.8907(13)	0.4531(8)	0.2080(7)	3.7(5)
C23	1.0654(12)	0.6282(8)	0.2169(6)	2.9(4)
C30	0.5275(12)	0.6707(7)	0.4434(6)	2.5(4)
C31	0.8150(11)	0.5292(7)	0.3945(6)	2.6(4)
C32	0.5111(11)	0.5390(6)	0.3397(6)	2.3(4)
C40	1.0044(10)	0.8990(7)	0.3798(6)	2.3(4)
C41	1.0655(10)	0.9508(7)	0.2876(6)	2.2(4)
C42	0.9661(10)	1.0476(7)	0.2678(6)	2.3(4)
C43	0.8430(10)	1.0553(7)	0.3521(6)	2.2(4)
C44	0.8706(11)	0.9655(7)	0.4189(5)	2.2(4)
C45	1.0797(13)	0.7948(8)	0.4291(7)	3.8(5)
C46	1.2151(11)	0.9090(8)	0.2266(7)	3.4(5)
C47	0.9934(11)	1.1311(7)	0.1799(6)	2.5(4)
C48	0.7304(11)	1.1513(8)	0.3662(7)	3.2(5)
C49	0.7764(12)	0.9442(8)	0.5157(6)	3.3(5)
H1	0.584	0.730	0.266	4.7

H2	0.619(8)	1.042(5)	0.094(4)	0.3(14)
H4	0.412	1.084	0.303	3.4
H5	0.268	1.255	0.328	4.7
H6	0.311	1.421	0.205	4.7
H7	0.488	1.412	0.059	4.7
H8	0.620	1.243	0.031	4.7
H45a	1.188	0.808	0.454	4.7
H45b	0.973	0.760	0.488	4.7
H45c	1.113	0.741	0.388	4.7
H46a	1.336	0.943	0.223	4.7
H46b	1.224	0.825	0.245	4.7
H46c	1.187	0.935	0.158	4.7
H47a	1.094	1.182	0.176	4.7
H47b	1.031	1.092	0.126	4.7
H47c	0.869	1.176	0.175	4.7
H48a	0.806	1.207	0.381	4.7
H48b	0.681	1.191	0.306	4.7
H48c	0.617	1.129	0.421	4.7
H49a	0.843	0.976	0.553	4.7
H49b	0.641	0.980	0.520	4.7
H49c	0.764	0.859	0.544	4.7

Appendix A.3

Structure Determination Summary for

$[Os_3W(\mu\text{-}H)(cis\text{-}\mu\text{-}\eta^1\text{-}C{=}CHPh)(CO)_9(O)(Cp^*)(\mu_3\text{-}O)]$ 3

Empirical Formula	$Os_3WO_{11}C_{27}H_{22}$	
Crystal size (mm)	0.2 x 0.1 x 0.15	
Crystal System	Trigonal	
Space Group	R-3	
Unit Cell Dimensions	$a = 42.6555(22)$ Å	$\alpha = 90$
	$b = 42.6555(22)$ Å	$\beta = 90$
	$c = 9.3793(5)$ Å	$\gamma = 120$
Volume (Å)^3	14779.2(11)	
Z	18	
Formula Weight	1276.90	
Density (calc.) (g cm^{-3})	2.582	
Absorption Coefficient (mm^{-1})	15.11	
λ(Mo-Kα)	0.70930 Å	
Temperature (°C)	-100	
2θ Range (deg)	57.4	
Index Ranges	$-48 \leq 49, 0 \leq 57, 0 \leq 7$	
Reflections Collected	16743	
Independent Reflections	6428	
Observed Reflections [I > 2.5 σ(I)]	4140	
Weighting Scheme	$\omega^{-1} = \sigma^2(F_o) + 0.0001\ F_o^2$	
Number of Parameters Refined	379	
Final *R* Indices (obs. data)	$R = 0.043$; $R_W = 0.043$	
Final *R* Indices (all data)	$R = 0.043$; $R_W = 0.043$	
Goodness of Fit	1.60	
Largest and Mean Δ/σ	0.000	
Largest Difference Peak/Hole (e/Å^3)	-1.300/3.400	

Bond lengths (Å) for 3

Os(1)-Os(2)	2.8296(8)	C(2)-H(2)	1.112(16)
Os(1)-Os(3)	2.8031(9)	C(3)-C(4)	1.401(24)
Os(1)-W	2.7123(9)	C(3)-C(8)	1.41(3)
Os(1)-O(1)	2.113(9)	C(4)-C(5)	1.43(3)
Os(1)-C(1)	2.158(14)	C(4)-H(4)	1.095(18)
Os(1)-C(10)	1.894(19)	C(5)-C(6)	1.36(3)
Os(1)-C(11)	1.884(17)	C(5)-H(5)	1.107(17)
Os(1)-H(1)	1.8535(6)	C(6)-C(7)	1.39(3)
Os(2)-Os(3)	2.8322(9)	C(6)-H(6)	1.103(16)
Os(2)-C(20)	1.929(18)	C(7)-C(8)	1.40(3)
Os(2)-C(21)	1.939(18)	C(7)-H(7)	1.121(20)
Os(2)-C(22)	1.953(17)	C(8)-H(8)	1.114(17)
Os(2)-C(23)	1.855(22)	C(40)-C(41)	1.434(24)
Os(3)-O(1)	2.163(9)	C(40)-C(44)	1.43(3)
Os(3)-C(30)	1.902(22)	C(40)-C(45)	1.49(3)
Os(3)-C(31)	1.916(18)	C(41)-C(42)	1.44(3)
Os(3)-C(32)	1.866(16)	C(41)-C(46)	1.49(3)
Os(3)-H(1)	1.6082(6)	C(42)-C(43)	1.42(3)
W-O(1)	1.966(9)	C(42)-C(47)	1.51(3)
W-O(2)	1.704(11)	C(43)-C(44)	1.40(3)
W-C(1)	2.050(15)	C(43)-C(48)	1.52(3)
W-C(40)	2.325(14)	C(44)-C(49)	1.52(3)
W-C(41)	2.373(15)	C(45)-H(45a)	1.077(19)
W-C(42)	2.394(16)	C(45)-H(45b)	1.136(22)
W-C(43)	2.470(17)	C(45)-H(45c)	1.089(21)
W-C(44)	2.443(15)	C(46)-H(46a)	1.106(19)
O(10)-C(10)	1.140(22)	C(46)-H(46b)	1.072(20)
O(11)-C(11)	1.133(19)	C(46)-H(46c)	1.124(24)
O(20)-C(20)	1.171(21)	C(47)-H(47a)	1.083(18)
O(21)-C(21)	1.119(22)	C(47)-H(47b)	1.091(20)
O(22)-C(22)	1.145(21)	C(47)-H(47c)	1.100(23)
O(23)-C(23)	1.17(3)	C(48)-H(48a)	1.080(19)
O(30)-C(30)	1.16(3)	C(48)-H(48b)	1.111(25)
O(31)-C(31)	1.144(21)	C(48)-H(48c)	1.096(23)
O(32)-C(32)	1.148(20)	C(49)-H(49a)	1.071(18)
C(1)-C(2)	1.289(21)	C(49)-H(49b)	1.127(23)
C(2)-C(3)	1.479(24)	C(49)-H(49c)	1.075(20)

Bond angles (deg) for 3

Os(2)-Os(1)-Os(3)	60.370(22)	C(43)-W-C(44)	33.2(6)
Os(2)-Os(1)-W	130.13(3)	Os(1)-O(1)-Os(3)	81.9(3)
Os(2)-Os(1)-O(1)	84.31(24)	Os(1)-O(1)-W	83.3(3)
Os(2)-Os(1)-C(1)	176.4(4)	Os(3)-O(1)-W	117.6(4)
Os(2)-Os(1)-C(10)	89.1(5)	Os(1)-C(1)-W	80.2(5)
Os(2)-Os(1)-C(11)	91.3(4)	Os(1)-C(1)-C(2)	140.3(12)
Os(2)-Os(1)-H(1)	77.901(23)	W-C(1)-C(2)	138.6(12)
Os(3)-Os(1)-W	79.66(3)	C(1)-C(2)-C(3)	128.7(15)
Os(3)-Os(1)-O(1)	49.81(24)	C(1)-C(2)-H(2)	115.7(14)
Os(3)-Os(1)-C(1)	116.2(4)	C(3)-C(2)-H(2)	115.6(13)
Os(3)-Os(1)-C(10)	137.7(5)	C(2)-C(3)-C(4)	119.2(17)
Os(3)-Os(1)-C(11)	117.2(4)	C(2)-C(3)-C(8)	121.1(15)
Os(3)-Os(1)-H(1)	33.084(16)	C(4)-C(3)-C(8)	119.6(17)
W-Os(1)-O(1)	46.04(24)	C(3)-C(4)-C(5)	117.5(17)
W-Os(1)-C(1)	48.1(4)	C(3)-C(4)-H(4)	120.8(17)
W-Os(1)-C(10)	104.2(5)	C(5)-C(4)-H(4)	121.7(16)
W-Os(1)-C(11)	135.5(4)	C(4)-C(5)-C(6)	122.4(16)
W-Os(1)-H(1)	84.29(3)	C(4)-C(5)-H(5)	118.5(19)
O(1)-Os(1)-C(1)	94.1(5)	C(6)-C(5)-H(5)	119.1(18)
O(1)-Os(1)-C(10)	102.8(6)	C(5)-C(6)-C(7)	119.9(16)
O(1)-Os(1)-C(11)	166.6(5)	C(5)-C(6)-H(6)	120.0(16)
O(1)-Os(1)-H(1)	75.80(24)	C(7)-C(6)-H(6)	120.0(17)
C(1)-Os(1)-C(10)	94.5(6)	C(6)-C(7)-C(8)	119.5(18)
C(1)-Os(1)-C(11)	89.4(6)	C(6)-C(7)-H(7)	119.1(17)
C(1)-Os(1)-H(1)	98.5(4)	C(8)-C(7)-H(7)	121.4(17)
C(10)-Os(1)-C(11)	89.8(7)	C(3)-C(8)-C(7)	121.0(16)
C(10)-Os(1)-H(1)	167.0(5)	C(3)-C(8)-H(8)	119.7(16)
C(11)-Os(1)-H(1)	90.9(5)	C(7)-C(8)-H(8)	119.4(18)
Os(1)-Os(2)-Os(3)	59.351(22)	Os(1)-C(10)-O(10)	177.1(14)
Os(1)-Os(2)-C(20)	86.1(4)	Os(1)-C(11)-O(11)	173.4(13)
Os(1)-Os(2)-C(21)	164.0(5)	Os(2)-C(20)-O(20)	178.4(14)
Os(1)-Os(2)-C(22)	85.5(4)	Os(2)-C(21)-O(21)	177.9(17)
Os(1)-Os(2)-C(23)	97.6(5)	Os(2)-C(22)-O(22)	179.3(14)
Os(3)-Os(2)-C(20)	82.6(5)	Os(2)-C(23)-O(23)	179.1(14)
Os(3)-Os(2)-C(21)	104.7(5)	Os(3)-C(30)-O(30)	171.2(14)
Os(3)-Os(2)-C(22)	86.9(5)	Os(3)-C(31)-O(31)	176.7(14)
Os(3)-Os(2)-C(23)	156.9(5)	Os(3)-C(32)-O(32)	175.8(14)
C(20)-Os(2)-C(21)	92.5(7)	W-C(40)-C(41)	74.1(8)
C(20)-Os(2)-C(22)	168.9(7)	W-C(40)-C(44)	77.2(9)
C(20)-Os(2)-C(23)	94.2(7)	W-C(40)-C(45)	120.1(11)
C(21)-Os(2)-C(22)	93.6(6)	C(41)-C(40)-C(44)	109.7(15)
C(21)-Os(2)-C(23)	98.3(7)	C(41)-C(40)-C(45)	125.4(17)
C(22)-Os(2)-C(23)	94.0(7)	C(44)-C(40)-C(45)	124.6(16)
Os(1)-Os(3)-Os(2)	60.279(23)	W-C(41)-C(40)	70.4(8)
Os(1)-Os(3)-O(1)	48.28(24)	W-C(41)-C(42)	73.2(9)

Os(1)-Os(3)-C(30)	117.0(5)	W-C(41)-C(46)	120.7(11)
Os(1)-Os(3)-C(31)	134.2(5)	C(40)-C(41)-C(42)	104.3(16)
Os(1)-Os(3)-C(32)	120.6(5)	C(40)-C(41)-C(46)	126.5(17)
Os(1)-Os(3)-H(1)	38.987(19)	C(42)-C(41)-C(46)	129.2(17)
Os(2)-Os(3)-O(1)	83.39(24)	W-C(42)-C(41)	71.6(9)
Os(2)-Os(3)-C(30)	177.1(5)	W-C(42)-C(43)	76.0(9)
Os(2)-Os(3)-C(31)	87.8(5)	W-C(42)-C(47)	125.2(11)
Os(2)-Os(3)-C(32)	90.1(5)	C(41)-C(42)-C(43)	110.5(16)
Os(2)-Os(3)-H(1)	81.39(3)	C(41)-C(42)-C(47)	123.4(19)
O(1)-Os(3)-C(30)	93.9(5)	C(43)-C(42)-C(47)	125.7(20)
O(1)-Os(3)-C(31)	100.2(6)	W-C(43)-C(42)	70.1(10)
O(1)-Os(3)-C(32)	168.8(6)	W-C(43)-C(44)	72.3(9)
O(1)-Os(3)-H(1)	79.36(24)	W-C(43)-C(48)	127.0(12)
C(30)-Os(3)-C(31)	93.8(7)	C(42)-C(43)-C(44)	107.3(19)
C(30)-Os(3)-C(32)	92.4(7)	C(42)-C(43)-C(48)	127.4(19)
C(30)-Os(3)-H(1)	97.1(5)	C(44)-C(43)-C(48)	125.1(20)
C(31)-Os(3)-C(32)	88.6(7)	W-C(44)-C(40)	68.1(8)
C(31)-Os(3)-H(1)	169.1(5)	W-C(44)-C(43)	74.4(10)
C(32)-Os(3)-H(1)	90.7(5)	W-C(44)-C(49)	123.4(10)
Os(1)-W-O(1)	50.7(3)	C(40)-C(44)-C(43)	108.0(17)
Os(1)-W-O(2)	114.2(3)	C(40)-C(44)-C(49)	125.5(17)
Os(1)-W-C(1)	51.6(4)	C(43)-C(44)-C(49)	126.4(19)
Os(1)-W-C(40)	132.0(4)	C(40)-C(45)-H(45a)	113.4(16)
Os(1)-W-C(41)	161.1(4)	C(40)-C(45)-H(45b)	110.4(16)
Os(1)-W-C(42)	131.9(6)	C(40)-C(45)-H(45c)	112.8(17)
Os(1)-W-C(43)	104.1(5)	H(45a)-C(45)-H(45b)	105.7(17)
Os(1)-W-C(44)	104.0(4)	H(45a)-C(45)-H(45c)	109.1(17)
O(1)-W-O(2)	107.9(4)	H(45b)-C(45)-H(45c)	104.9(17)
O(1)-W-C(1)	102.3(5)	C(41)-C(46)-H(46a)	111.9(17)
O(1)-W-C(40)	92.4(5)	C(41)-C(46)-H(46b)	113.6(19)
O(1)-W-C(41)	126.7(5)	C(41)-C(46)-H(46c)	111.2(16)
O(1)-W-C(42)	141.7(5)	H(46a)-C(46)-H(46b)	108.1(16)
O(1)-W-C(43)	111.5(6)	H(46a)-C(46)-H(46c)	104.5(19)
O(1)-W-C(44)	85.6(5)	H(46b)-C(46)-H(46c)	106.9(18)
O(2)-W-C(1)	103.7(5)	C(42)-C(47)-H(47a)	111.8(16)
O(2)-W-C(40)	105.3(6)	C(42)-C(47)-H(47b)	110.8(18)
O(2)-W-C(41)	84.7(5)	C(42)-C(47)-H(47c)	110.7(17)
O(2)-W-C(42)	103.0(6)	H(47a)-C(47)-H(47b)	108.4(17)
O(2)-W-C(43)	136.9(6)	H(47a)-C(47)-H(47c)	107.8(18)
O(2)-W-C(44)	139.6(6)	H(47b)-C(47)-H(47c)	107.2(16)
C(1)-W-C(40)	141.4(6)	C(43)-C(48)-H(48a)	112.9(16)
C(1)-W-C(41)	125.3(6)	C(43)-C(48)-H(48b)	110.4(17)
C(1)-W-C(42)	91.5(6)	C(43)-C(48)-H(48c)	111.8(19)
C(1)-W-C(43)	84.4(6)	H(48a)-C(48)-H(48b)	107.2(20)
C(1)-W-C(44)	110.4(6)	H(48a)-C(48)-H(48c)	108.3(18)
C(40)-W-C(41)	35.5(6)	H(48b)-C(48)-H(48c)	106.1(16)

C(40)-W-C(42)	57.5(6)	C(44)-C(49)-H(49a)	112.1(16)
C(40)-W-C(43)	57.0(6)	C(44)-C(49)-H(49b)	109.3(16)
C(40)-W-C(44)	34.7(6)	C(44)-C(49)-H(49c)	111.5(18)
C(41)-W-C(42)	35.1(7)	H(49a)-C(49)-H(49b)	106.7(18)
C(41)-W-C(43)	58.0(7)	H(49a)-C(49)-H(49c)	110.6(17)
C(41)-W-C(44)	58.1(6)	H(49b)-C(49)-H(49c)	106.4(16)
C(42)-W-C(43)	33.9(7)	Os(1)-H(1)-Os(3)	107.93(3)
C(42)-W-C(44)	56.1(6)		

Atomic Coordinates and equivalent isotropic displacement coefficients ($Å^2 \times 10^3$) for 3.

	x	Y	z	U(eq)
Os1	0.059302(15)	0.231821(15)	0.24325(7)	2.50(3)
Os2	0.043502(17)	0.288225(16)	0.28351(8)	2.89(4)
Os3	0.036607(16)	0.256839(16)	0.01093(7)	2.70(4)
W	0.094911(16)	0.220427(17)	0.02802(8)	2.84(4)
O1	0.08848(24)	0.26229(24)	0.0634(10)	2.3(5)
O2	0.0681(3)	0.1969(3)	-0.1124(11)	3.5(6)
O10	0.1146(3)	0.2650(4)	0.4809(13)	5.0(8)
O11	0.0001(3)	0.1846(3)	0.4490(12)	3.9(6)
O20	0.1216(3)	0.3395(3)	0.1760(12)	4.5(7)
O21	0.0205(4)	0.3448(3)	0.2364(15)	6.4(9)
O22	-0.0350(3)	0.2268(3)	0.3399(15)	5.5(8)
O23	0.0634(4)	0.3018(3)	0.5956(16)	5.2(9)
O30	0.0289(4)	0.2233(4)	-0.2832(16)	5.6(9)
O31	0.0616(4)	0.3323(3)	-0.1104(13)	5.1(9)
O32	-0.0407(3)	0.2399(3)	-0.0154(13)	5.0(8)
C1	0.0694(4)	0.1879(4)	0.2001(16)	2.7(8)
C2	0.0597(4)	0.1557(4)	0.2437(18)	3.5(9)
C3	0.0387(4)	0.1367(4)	0.3722(22)	3.8(11)
C4	0.0095(5)	0.1013(5)	0.3591(20)	4.1(10)
C5	-0.0094(5)	0.0834(5)	0.4863(24)	4.6(12)
C6	-0.0004(4)	0.0997(5)	0.6162(20)	3.6(10)
C7	0.0290(5)	0.1346(5)	0.6293(22)	5.2(12)
C8	0.0485(5)	0.1529(4)	0.5078(21)	3.9(11)
C10	0.0940(5)	0.2518(4)	0.3915(21)	3.6(10)
C11	0.0238(4)	0.2024(4)	0.3774(18)	2.9(9)
C20	0.0922(5)	0.3203(4)	0.2187(18)	3.6(10)
C21	0.0294(5)	0.3245(5)	0.2553(19)	4.3(11)
C22	-0.0060(5)	0.2496(4)	0.3200(17)	3.2(10)
C23	0.0555(5)	0.2966(4)	0.4753(24)	3.7(11)
C30	0.0337(4)	0.2351(5)	-0.1692(24)	4.1(12)
C31	0.0520(5)	0.3037(5)	-0.0691(19)	4.1(11)
C32	-0.0111(5)	0.2472(4)	-0.0010(17)	3.2(9)
C40	0.1522(4)	0.2565(4)	-0.0684(20)	2.9(9)
C41	0.1419(4)	0.2201(5)	-0.1061(20)	3.3(10)
C42	0.1402(4)	0.2029(5)	0.0280(25)	4.6(12)
C43	0.1506(4)	0.2282(5)	0.141(3)	5.1(14)
C44	0.1587(4)	0.2616(5)	0.0814(21)	3.6(1)
C45	0.1588(5)	0.2859(5)	-0.1712(23)	6.1(14)
C46	0.1349(5)	0.2046(6)	-0.2522(24)	6.4(13)
C47	0.1328(5)	0.1644(5)	0.0405(24)	6.6(14)
C48	0.1558(5)	0.2222(7)	0.2974(22)	7.0(18)
C49	0.1723(5)	0.2971(6)	0.1604(22)	6.2(13)

H1	0.024	0.221	0.106	5.5
H2	0.068	0.140	0.175	5.5
H4	0.002	0.088	0.255	5.5
H5	-0.032	0.055	0.478	5.5
H6	-0.016	0.085	0.711	5.5
H7	0.037	0.147	0.738	5.5
H8	0.073	0.181	0.519	5.5
H45a	0.186	0.300	-0.211	5.5
H45b	0.141	0.274	-0.269	5.5
H45c	0.152	0.305	-0.128	5.5
H46a	0.160	0.207	-0.302	5.5
H46b	0.114	0.177	-0.257	5.5
H46c	0.126	0.220	-0.326	5.5
H47a	0.158	0.163	0.037	5.5
H47b	0.119	0.152	0.140	5.5
H47c	0.115	0.148	-0.047	5.5
H48a	0.183	0.227	0.321	5.5
H48b	0.151	0.240	0.367	5.5
H48c	0.137	0.194	0.332	5.5
H49a	0.201	0.312	0.170	5.5
H49b	0.165	0.315	0.099	5.5
H49c	0.160	0.293	0.264	5.5

Appendix A.4

Structure Determination Summary for

$[Os_3W(CO)_{10}(O)(\mu\text{-}\eta^1,\eta^2\text{-}CH{=}CHPh\{W\text{-}Os\})(\mu\text{-}O)(Cp^*)]$ 4

Empirical Formula	$Os_3WO_{12}C_{28}H_{22}$	
Crystal size (mm)	0.1 x 0.15 x 0.2	
Crystal System	Monoclinic	
Space Group	*P*21/*n*	
Unit Cell Dimensions	*a* = 13.0041(6) Å	α = 90
	b = 17.9262(8) Å	β = 112.23(1)
	c = 14.7546(7) Å	γ = 90
Volume (Å)^3	3183.9(3)	
Z	4	
Formula Weight	1304.91	
Density (calc.) (g cm^{-3})	2.722	
Absorption Coefficient (mm^{-1})	15.59	
λ(Mo-Kα)	0.70930 Å	
Temperature (°C)	-100	
2θ Range (deg)	57.3	
Index Ranges	$-17 \le 16, 0 \le 24, 0 \le 19$	
Reflections Collected	36307	
Independent Reflections	8235	
Observed Reflections [I > 2.5 σ(I)]	6927	
Weighting Scheme	$\omega^{-1} = \sigma^2(F_o) + 0.0001\ F_o^2$	
Number of Parameters Refined	406	
Final *R* Indices (obs. data)	$R = 0.041$; $R_W = 0.045$	
Final *R* Indices (all data)	$R = 0.041$; $R_W = 0.045$	
Goodness of Fit	2.90	
Largest and Mean Δ/σ	0.000	
Largest Difference Peak/Hole (e/Å^3)	-4.940/5.060	

Bond lengths (Å) for 4

Os(1)-Os(2)	2.8529(5)	C(2)-H(2)	1.00(11)
Os(1)-Os(3)	2.8660(5)	C(3)-C(4)	1.410(13)
Os(1)-W	2.8257(4)	C(3)-C(8)	1.383(12)
Os(1)-O(1)	2.167(5)	C(4)-C(5)	1.363(13)
Os(1)-C(1)	2.217(8)	C(4)-H(4)	1.077(9)
Os(1)-C(2)	2.302(9)	C(5)-C(6)	1.362(15)
Os(1)-C(10)	1.844(9)	C(5)-H(5)	1.079(10)
Os(1)-C(11)	1.910(10)	C(6)-C(7)	1.356(16)
Os(2)-Os(3)	2.8664(7)	C(6)-H(6)	1.078(10)
Os(2)-C(20)	1.956(10)	C(7)-C(8)	1.413(15)
Os(2)-C(21)	1.834(15)	C(7)-H(7)	1.081(10)
Os(2)-C(22)	1.909(12)	C(8)-H(8)	1.078(10)
Os(2)-C(23)	1.968(12)	C(40)-C(41)	1.419(13)
Os(3)-C(30)	1.942(10)	C(40)-C(44)	1.437(14)
Os(3)-C(31)	1.942(12)	C(40)-C(45)	1.487(14)
Os(3)-C(32)	1.964(16)	C(41)-C(42)	1.405(14)
Os(3)-C(33)	1.952(10)	C(41)-C(46)	1.512(14)
W-O(1)	1.817(5)	C(42)-C(43)	1.419(13)
W-O(2)	1.714(6)	C(42)-C(47)	1.520(13)
W-C(1)	2.053(8)	C(43)-C(44)	1.387(13)
W-C(40)	2.378(9)	C(43)-C(48)	1.485(14)
W-C(41)	2.407(9)	C(44)-C(49)	1.510(13)
W-C(42)	2.444(9)	C(45)-H(45a)	1.082(10)
W-C(43)	2.390(8)	C(45)-H(45b)	1.080(13)
W-C(44)	2.376(8)	C(45)-H(45c)	1.077(13)
O(10)-C(10)	1.156(11)	C(46)-H(46a)	1.069(10)
O(11)-C(11)	1.144(13)	C(46)-H(46b)	1.072(12)
O(20)-C(20)	1.143(12)	C(46)-H(46c)	1.103(12)
O(21)-C(21)	1.156(19)	C(47)-H(47a)	1.081(9)
O(22)-C(22)	1.144(15)	C(47)-H(47b)	1.091(11)
O(23)-C(23)	1.133(14)	C(47)-H(47c)	1.073(12)
O(30)-C(30)	1.102(13)	C(48)-H(48a)	1.081(10)
O(31)-C(31)	1.127(15)	C(48)-H(48b)	1.075(11)
O(32)-C(32)	1.118(19)	C(48)-H(48c)	1.077(11)
O(33)-C(33)	1.123(13)	C(49)-H(49a)	1.077(10)
C(1)-C(2)	1.448(12)	C(49)-H(49b)	1.082(13)
C(1)-H(1)	1.12(8)	C(49)-H(49c)	1.079(12)
C(2)-C(3)	1.468(12)		

Bond angles (deg) for 4

Os(2)-Os(1)-Os(3)	60.160(15)	W-C(1)-C(2)	116.3(6)
Os(2)-Os(1)-W	114.939(15)	W-C(1)-H(1)	126(4)
Os(2)-Os(1)-O(1)	84.38(15)	C(2)-C(1)-H(1)	114(4)
Os(2)-Os(1)-C(1)	160.70(22)	Os(1)-C(2)-C(1)	68.1(5)
Os(2)-Os(1)-C(2)	152.36(22)	Os(1)-C(2)-C(3)	124.4(6)
Os(2)-Os(1)-C(10)	99.6(3)	Os(1)-C(2)-H(2)	109(6)
Os(2)-Os(1)-C(11)	73.5(3)	C(1)-C(2)-C(3)	123.8(8)
Os(3)-Os(1)-W	128.185(16)	C(1)-C(2)-H(2)	123(6)
Os(3)-Os(1)-O(1)	91.27(15)	C(3)-C(2)-H(2)	104(6)
Os(3)-Os(1)-C(1)	131.19(21)	C(2)-C(3)-C(4)	124.1(8)
Os(3)-Os(1)-C(2)	94.51(22)	C(2)-C(3)-C(8)	117.6(8)
Os(3)-Os(1)-C(10)	87.71(25)	C(4)-C(3)-C(8)	118.2(8)
Os(3)-Os(1)-C(11)	131.5(3)	C(3)-C(4)-C(5)	120.4(9)
W-Os(1)-O(1)	40.02(14)	C(3)-C(4)-H(4)	119.8(8)
W-Os(1)-C(1)	46.11(22)	C(5)-C(4)-H(4)	119.8(9)
W-Os(1)-C(2)	70.52(21)	C(4)-C(5)-C(6)	121.0(9)
W-Os(1)-C(10)	138.8(3)	C(4)-C(5)-H(5)	119.3(9)
W-Os(1)-C(11)	82.68(25)	C(6)-C(5)-H(5)	119.7(9)
O(1)-Os(1)-C(1)	80.1(3)	C(5)-C(6)-C(7)	120.6(9)
O(1)-Os(1)-C(2)	85.4(3)	C(5)-C(6)-H(6)	119.7(10)
O(1)-Os(1)-C(10)	174.7(3)	C(7)-C(6)-H(6)	119.7(10)
O(1)-Os(1)-C(11)	98.0(3)	C(6)-C(7)-C(8)	119.9(9)
C(1)-Os(1)-C(2)	37.3(3)	C(6)-C(7)-H(7)	120.3(10)
C(1)-Os(1)-C(10)	96.7(3)	C(8)-C(7)-H(7)	119.8(11)
C(1)-Os(1)-C(11)	97.3(3)	C(3)-C(8)-C(7)	119.8(9)
C(2)-Os(1)-C(10)	89.4(4)	C(3)-C(8)-H(8)	120.0(9)
C(2)-Os(1)-C(11)	133.5(4)	C(7)-C(8)-H(8)	120.2(9)
C(10)-Os(1)-C(11)	86.6(4)	Os(1)-C(10)-O(10)	176.1(7)
Os(1)-Os(2)-Os(3)	60.147(13)	Os(1)-C(11)-O(11)	169.3(9)
Os(1)-Os(2)-C(20)	88.1(3)	Os(2)-C(20)-O(20)	171.5(8)
Os(1)-Os(2)-C(21)	107.3(4)	Os(2)-C(21)-O(21)	174.5(12)
Os(1)-Os(2)-C(22)	155.3(5)	Os(2)-C(22)-O(22)	176.4(15)
Os(1)-Os(2)-C(23)	87.9(3)	Os(2)-C(23)-O(23)	176.0(13)
Os(3)-Os(2)-C(20)	85.6(3)	Os(3)-C(30)-O(30)	177.3(11)
Os(3)-Os(2)-C(21)	167.1(4)	Os(3)-C(31)-O(31)	173.8(14)
Os(3)-Os(2)-C(22)	95.2(5)	Os(3)-C(32)-O(32)	175.1(13)
Os(3)-Os(2)-C(23)	91.6(4)	Os(3)-C(33)-O(33)	172.4(9)
C(20)-Os(2)-C(21)	91.1(5)	W-C(40)-C(41)	73.9(5)
C(20)-Os(2)-C(22)	90.4(4)	W-C(40)-C(44)	72.3(5)
C(20)-Os(2)-C(23)	175.9(4)	W-C(40)-C(45)	119.0(6)
C(21)-Os(2)-C(22)	97.4(7)	C(41)-C(40)-C(44)	106.9(8)
C(21)-Os(2)-C(23)	91.0(6)	C(41)-C(40)-C(45)	125.8(10)
C(22)-Os(2)-C(23)	92.8(4)	C(44)-C(40)-C(45)	127.3(9)
Os(1)-Os(3)-Os(2)	59.693(13)	W-C(41)-C(40)	71.6(5)
Os(1)-Os(3)-C(30)	154.5(4)	W-C(41)-C(42)	74.6(5)

Os(1)-Os(3)-C(31)	91.3(3)	W-C(41)-C(46)	120.6(6)
Os(1)-Os(3)-C(32)	106.8(3)	C(40)-C(41)-C(42)	107.4(8)
Os(1)-Os(3)-C(33)	83.2(3)	C(40)-C(41)-C(46)	124.6(9)
Os(2)-Os(3)-C(30)	95.5(4)	C(42)-C(41)-C(46)	128.0(9)
Os(2)-Os(3)-C(31)	86.4(4)	W-C(42)-C(41)	71.8(5)
Os(2)-Os(3)-C(32)	165.7(3)	W-C(42)-C(43)	70.9(5)
Os(2)-Os(3)-C(33)	93.0(3)	W-C(42)-C(47)	124.6(6)
C(30)-Os(3)-C(31)	92.8(5)	C(41)-C(42)-C(43)	109.4(8)
C(30)-Os(3)-C(32)	98.4(5)	C(41)-C(42)-C(47)	123.0(9)
C(30)-Os(3)-C(33)	93.2(4)	C(43)-C(42)-C(47)	127.6(9)
C(31)-Os(3)-C(32)	89.5(7)	W-C(43)-C(42)	75.0(5)
C(31)-Os(3)-C(33)	174.0(4)	W-C(43)-C(44)	72.6(5)
C(32)-Os(3)-C(33)	89.7(6)	W-C(43)-C(48)	125.4(6)
Os(1)-W-O(1)	50.08(17)	C(42)-C(43)-C(44)	107.0(8)
Os(1)-W-O(2)	97.69(19)	C(42)-C(43)-C(48)	125.4(8)
Os(1)-W-C(1)	51.10(21)	C(44)-C(43)-C(48)	126.9(9)
Os(1)-W-C(40)	160.44(24)	W-C(44)-C(40)	72.5(5)
Os(1)-W-C(41)	130.25(22)	W-C(44)-C(43)	73.6(5)
Os(1)-W-C(42)	119.51(20)	W-C(44)-C(49)	121.0(6)
Os(1)-W-C(43)	131.63(21)	C(40)-C(44)-C(43)	109.1(8)
Os(1)-W-C(44)	162.2(3)	C(40)-C(44)-C(49)	123.6(9)
O(1)-W-O(2)	115.0(3)	C(43)-C(44)-C(49)	127.3(10)
O(1)-W-C(1)	93.4(3)	C(40)-C(45)-H(45a)	109.3(9)
O(1)-W-C(40)	110.4(3)	C(40)-C(45)-H(45b)	109.5(10)
O(1)-W-C(41)	83.8(3)	C(40)-C(45)-H(45c)	109.5(9)
O(1)-W-C(42)	92.5(3)	H(45a)-C(45)-H(45b)	109.3(10)
O(1)-W-C(43)	125.5(3)	H(45a)-C(45)-H(45c)	109.5(11)
O(1)-W-C(44)	141.1(3)	H(45b)-C(45)-H(45c)	109.7(10)
O(2)-W-C(1)	105.0(3)	C(41)-C(46)-H(46a)	110.4(9)
O(2)-W-C(40)	89.4(3)	C(41)-C(46)-H(46b)	110.2(9)
O(2)-W-C(41)	121.1(3)	C(41)-C(46)-H(46c)	108.3(9)
O(2)-W-C(42)	142.7(3)	H(46a)-C(46)-H(46b)	111.0(10)
O(2)-W-C(43)	117.6(3)	H(46a)-C(46)-H(46c)	108.6(10)
O(2)-W-C(44)	88.2(3)	H(46b)-C(46)-H(46c)	108.3(9)
C(1)-W-C(40)	144.0(3)	C(42)-C(47)-H(47a)	109.8(9)
C(1)-W-C(41)	130.4(3)	C(42)-C(47)-H(47b)	109.2(9)
C(1)-W-C(42)	97.6(3)	C(42)-C(47)-H(47c)	110.1(8)
C(1)-W-C(43)	86.6(3)	H(47a)-C(47)-H(47b)	108.6(9)
C(1)-W-C(44)	111.2(3)	H(47a)-C(47)-H(47c)	109.9(10)
C(40)-W-C(41)	34.5(3)	H(47b)-C(47)-H(47c)	109.2(9)
C(40)-W-C(42)	56.3(3)	C(43)-C(48)-H(48a)	108.9(9)
C(40)-W-C(43)	57.7(3)	C(43)-C(48)-H(48b)	109.3(8)
C(40)-W-C(44)	35.2(3)	C(43)-C(48)-H(48c)	109.1(9)
C(41)-W-C(42)	33.7(3)	H(48a)-C(48)-H(48b)	109.8(9)
C(41)-W-C(43)	57.4(3)	H(48a)-C(48)-H(48c)	109.6(9)
C(41)-W-C(44)	57.3(3)	H(48b)-C(48)-H(48c)	110.1(10)

C(42)-W-C(43)	34.1(3)	C(44)-C(49)-H(49a)	109.6(8)
C(42)-W-C(44)	55.8(3)	C(44)-C(49)-H(49b)	109.3(9)
C(43)-W-C(44)	33.8(3)	C(44)-C(49)-H(49c)	109.4(9)
Os(1)-O(1)-W	89.90(23)	H(49a)-C(49)-H(49b)	109.5(10)
Os(1)-C(1)-W	82.8(3)	H(49a)-C(49)-H(49c)	109.7(10)
Os(1)-C(1)-C(2)	74.5(5)	H(49b)-C(49)-H(49c)	109.3(9)
Os(1)-C(1)-H(1)	123(4)		

Atomic Coordinates and equivalent isotropic displacement coefficients ($Å^2 \times 10^3$) for 4

	x	Y	z	U(eq)
Os1	0.17195(3)	0.207537(18)	0.004483(23)	2.090(14)
Os2	0.23912(4)	0.056274(21)	0.00218(3)	3.883(21)
Os3	0.40315(3)	0.16958(3)	0.08657(3)	3.803(20)
W	0.02665(3)	0.232060(19)	0.103468(24)	2.156(14)
O1	0.1516(5)	0.1755(3)	0.1383(4)	2.5(3)
O2	-0.0897(5)	0.1923(4)	0.0183(5)	3.5(3)
O10	0.2030(6)	0.2661(4)	-0.1739(5)	3.9(3)
O11	-0.0305(6)	0.1346(4)	-0.1488(5)	4.5(4)
O20	0.2398(7)	0.0297(4)	0.2095(6)	5.4(5)
O21	0.0308(10)	-0.0323(5)	-0.0899(8)	8.5(8)
O22	0.4097(11)	-0.0691(6)	0.0454(8)	11.0(9)
O23	0.2338(9)	0.0839(5)	-0.2069(6)	7.7(6)
O30	0.6000(7)	0.0638(6)	0.1677(6)	7.5(6)
O31	0.4262(8)	0.1856(7)	-0.1117(7)	9.3(7)
O32	0.5380(8)	0.3152(6)	0.1438(10)	9.4(8)
O33	0.3770(6)	0.1729(5)	0.2847(6)	5.5(5)
C1	0.0814(7)	0.3065(4)	0.0259(6)	2.2(3)
C2	0.1979(7)	0.3263(5)	0.0686(7)	2.6(4)
C3	0.2474(7)	0.3879(5)	0.0333(7)	2.8(4)
C4	0.2053(8)	0.4144(5)	-0.0639(7)	3.2(4)
C5	0.2566(8)	0.4717(5)	-0.0908(8)	3.6(5)
C6	0.3498(9)	0.5040(6)	-0.0251(8)	4.0(5)
C7	0.3935(8)	0.4800(6)	0.0690(9)	4.4(6)
C8	0.3416(8)	0.4213(5)	0.0997(7)	3.6(4)
C10	0.1949(7)	0.2430(5)	-0.1037(6)	2.6(4)
C11	0.0464(8)	0.1559(5)	-0.0857(7)	3.4(5)
C20	0.2382(9)	0.0453(5)	0.1338(8)	4.0(5)
C21	0.1124(14)	0.0000(6)	-0.0500(10)	6.3(9)
C22	0.3434(14)	-0.0235(7)	0.0267(9)	7.0(9)
C23	0.2394(11)	0.0751(6)	-0.1291(9)	5.4(7)
C30	0.5280(9)	0.1013(8)	0.1362(8)	5.5(7)
C31	0.4138(9)	0.1764(9)	-0.0410(10)	6.0(7)
C32	0.4857(10)	0.2637(9)	0.1245(12)	6.5(8)
C33	0.3792(8)	0.1699(6)	0.2095(8)	3.7(5)
C40	-0.0554(8)	0.2215(5)	0.2222(7)	3.2(4)
C41	0.0608(8)	0.2269(5)	0.2755(6)	3.1(4)
C42	0.0939(7)	0.2987(5)	0.2596(7)	3.0(4)
C43	0.0012(7)	0.3373(5)	0.1922(6)	2.8(4)
C44	-0.0906(7)	0.2913(6)	0.1722(7)	3.2(4)
C45	-0.1257(10)	0.1554(7)	0.2193(9)	5.2(7)
C46	0.1319(10)	0.1656(6)	0.3391(8)	4.7(6)
C47	0.2116(9)	0.3277(6)	0.3106(7)	4.3(5)

C48	0.0009(9)	0.4165(6)	0.1625(8)	4.3(5)
C49	-0.2099(8)	0.3094(7)	0.1101(8)	4.6(5)
H1	0.029(6)	0.343(4)	-0.035(6)	2.0(16)
H2	0.243(8)	0.324(6)	0.141(8)	5.(3)
H4	0.132	0.389	-0.117	5.4
H5	0.223	0.491	-0.165	5.4
H6	0.389	0.549	-0.048	5.4
H7	0.468	0.505	0.120	5.4
H8	0.375	0.403	0.175	5.4
H45a	-0.156	0.160	0.278	5.4
H45b	-0.195	0.154	0.150	5.4
H45c	-0.077	0.105	0.228	5.4
H46a	0.139	0.173	0.413	5.4
H46b	0.098	0.112	0.311	5.4
H46c	0.216	0.169	0.337	5.4
H47a	0.220	0.355	0.379	5.4
H47b	0.270	0.281	0.327	5.4
H47c	0.231	0.366	0.264	5.4
H48a	-0.012	0.452	0.217	5.4
H48b	0.080	0.430	0.158	5.4
H48c	-0.065	0.425	0.092	5.4
H49a	-0.249	0.336	0.155	5.4
H49b	-0.213	0.347	0.051	5.4
H49c	-0.254	0.259	0.079	5.4

AppendixA.5

Structure Determination Summary for

$[Os_3W(\mu\text{-}H)(anti\text{-}\mu\text{-}\eta^1\text{-}CHCH_2Ph)(CO)_9(O)(Cp^*)(\mu_3\text{-}O)]$ 5

Empirical Formula	$Os_3WO_{11}C_{27}H_{24}$	
Crystal Size(mm)	0.10 x 0.18 x 0.22	
Crystal System	Monoclinic	
Space Group	*P*21/*a*	
Unit Cell Dimensions	*a* = 10.2809(5) Å	α = 90
	b = 30.6303(14) Å	β=115.70(1)
	c = 11.2528(5) Å	γ=90
Volume $(Å)^3$	3192.9(3)	
Z	4	
Formula Weight	1278.92	
Density (calc.) (gcm^{-3})	2.747	
Absorption Coefficient (mm^{-1})	15.63	
λ (Mo-Kα)	0.70930 Å	
Temperature (°C)	-100	
2θ Range (deg)	57.3	
Index Ranges	$-13 \le 12, 0 \le 41, 0 \le 15$	
Reflections Collected	29063	
Independent Reflections	8231	
Observed Reflections [$I > 2.5\ \sigma(I)$]	6714	
Weighting Scheme	$\omega^{-1} = \sigma^2(F_o) + 0.0001\ F_o^2$	
Number of Parameters Refined	391	
Final *R* Indices (obs. data)	$R = 0.041$; $R_w = 0.052$	
Final *R* Indices (all data)	$R = 0.041$; $R_w = 0.052$	
Goodness of Fit	1.78	
Largest and Mean Δ/σ	0.000	
Largest Difference Peak/Hole $(e/Å^3)$	-2.210/2.980	

Bond lengths (Å) for 5

Os(1)-Os(2)	2.8255(5)	C(40)-C(44)	1.474(15)
Os(1)-Os(3)	2.8038(5)	C(40)-C(45)	1.484(16)
Os(1)-W	2.7090(5)	C(41)-C(42)	1.414(14)
Os(1)-O(1)	2.099(6)	C(41)-C(46)	1.484(15)
Os(1)-C(1)	2.274(10)	C(42)-C(43)	1.437(15)
Os(1)-C(10)	1.886(10)	C(42)-C(47)	1.486(16)
Os(1)-C(11)	1.861(10)	C(43)-C(44)	1.432(17)
Os(1)-H(3)	1.8533(4)	C(43)-C(48)	1.511(15)
Os(2)-Os(3)	2.8372(5)	C(44)-C(49)	1.483(15)
Os(2)-C(20)	1.919(11)	C(45)-H(45a)	0.998(10)
Os(2)-C(21)	1.957(11)	C(45)-H(45b)	1.001(13)
Os(2)-C(22)	1.913(11)	C(45)-H(45c)	1.004(13)
Os(2)-C(23)	1.934(11)	C(46)-H(46a)	1.001(10)
Os(3)-O(1)	2.168(6)	C(46)-H(46b)	1.002(10)
Os(3)-C(30)	1.936(11)	C(46)-H(46c)	0.999(12)
Os(3)-C(31)	1.895(12)	C(47)-H(47a)	1.000(11)
Os(3)-C(32)	1.881(11)	C(47)-H(47b)	1.000(12)
Os(3)-H(3)	1.6088(4)	C(47)-H(47c)	0.999(12)
W-O(1)	1.957(6)	C(48)-H(48a)	1.001(11)
W-O(2)	1.704(7)	C(48)-H(48b)	1.001(14)
W-C(1)	2.064(9)	C(48)-H(48c)	1.001(13)
W-C(40)	2.496(10)	C(49)-H(49a)	1.006(11)
W-C(41)	2.469(9)	C(49)-H(49b)	1.000(13)
W-C(42)	2.350(9)	C(49)-H(49c)	0.993(13)
W-C(43)	2.350(9)	H(2a)-H(2b)	1.66(13)
W-C(44)	2.380(10)	H(45a)-H(45b)	1.63302(4)
O(10)-C(10)	1.146(12)	H(45a)-H(45c)	1.63301(6)
O(11)-C(11)	1.163(13)	H(45b)-H(45c)	1.63295(6)
O(20)-C(20)	1.144(13)	H(46a)-H(46b)	1.63302(6)
O(21)-C(21)	1.151(14)	H(46a)-H(46c)	1.63302(6)
O(22)-C(22)	1.142(14)	H(46b)-H(46c)	1.63294(5)
O(23)-C(23)	1.147(13)	H(47a)-H(47b)	1.63302(7)
O(30)-C(30)	1.137(13)	H(47a)-H(47c)	1.63302(6)
O(31)-C(31)	1.137(14)	H(47b)-H(47c)	1.63296(4)
O(32)-C(32)	1.136(13)	H(48a)-H(48b)	1.63301(5)
C(1)-C(2)	1.516(14)	H(48a)-H(48c)	1.63300(5)
C(1)-H(1)	1.12(11)	H(48b)-H(48c)	1.63292(7)
C(2)-C(3)	1.526(13)	H(49a)-H(49b)	1.63302(8)
C(2)-H(2a)	0.96(11)	H(49a)-H(49c)	1.63302(7)
C(2)-H(2b)	1.07(9)	H(49b)-H(49c)	1.63295(5)
C(3)-C(4)	1.386(15)	Cl(1)-Cl(1)a	2.884(21)
C(3)-C(8)	1.396(14)	Cl(1)-Cl(2)	2.865(16)
C(4)-C(5)	1.401(14)	Cl(1)-Cl(2)a	0.388(16)
C(4)-H(4)	1.004(9)	Cl(1)-C(50)	1.70(3)
C(5)-C(6)	1.387(15)	Cl(1)-C(50)a	1.55(3)

C(5)-H(5)	1.005(11)	Cl(2)-Cl(1)a	0.388(16)
C(6)-C(7)	1.344(18)	Cl(2)-Cl(2)a	2.898(25)
C(6)-H(6)	1.002(10)	Cl(2)-C(50)	1.73(3)
C(7)-C(8)	1.414(15)	Cl(2)-C(50)a	1.53(3)
C(7)-H(7)	1.002(10)	C(50)-Cl(1)a	1.55(3)
C(8)-H(8)	1.001(11)	C(50)-Cl(2)a	1.53(3)
C(40)-C(41)	1.399(15)	C(50)-C(50)a	1.50(5)

Bond angles (deg) for 5

Os(2)-Os(1)-Os(3)	60.529(13)	Os(3)-C(31)-O(31)	177.5(9)
Os(2)-Os(1)-W	130.590(17)	Os(3)-C(32)-O(32)	179.0(9)
Os(2)-Os(1)-O(1)	84.81(17)	W-C(40)-C(41)	72.6(6)
Os(2)-Os(1)-C(1)	176.5(3)	W-C(40)-C(44)	68.2(5)
Os(2)-Os(1)-C(10)	91.9(3)	W-C(40)-C(45)	131.8(7)
Os(2)-Os(1)-C(11)	90.9(3)	C(41)-C(40)-C(44)	108.7(9)
Os(2)-Os(1)-H(3)	77.194(14)	C(41)-C(40)-C(45)	126.6(10)
Os(3)-Os(1)-W	80.494(14)	C(44)-C(40)-C(45)	124.1(10)
Os(3)-Os(1)-O(1)	49.98(17)	W-C(41)-C(40)	74.7(5)
Os(3)-Os(1)-C(1)	116.2(3)	W-C(41)-C(42)	68.4(5)
Os(3)-Os(1)-C(10)	118.7(3)	W-C(41)-C(46)	126.0(6)
Os(3)-Os(1)-C(11)	137.5(3)	C(40)-C(41)-C(42)	109.5(9)
Os(3)-Os(1)-H(3)	33.081(10)	C(40)-C(41)-C(46)	124.3(9)
W-Os(1)-O(1)	45.90(17)	C(42)-C(41)-C(46)	126.1(9)
W-Os(1)-C(1)	47.97(23)	W-C(42)-C(41)	77.6(5)
W-Os(1)-C(10)	135.4(3)	W-C(42)-C(43)	72.2(5)
W-Os(1)-C(11)	100.0(3)	W-C(42)-C(47)	118.7(7)
W-Os(1)-H(3)	86.301(14)	C(41)-C(42)-C(43)	106.9(9)
O(1)-Os(1)-C(1)	93.9(3)	C(41)-C(42)-C(47)	125.3(9)
O(1)-Os(1)-C(10)	168.2(3)	C(43)-C(42)-C(47)	127.6(9)
O(1)-Os(1)-C(11)	100.6(3)	W-C(43)-C(42)	72.2(5)
O(1)-Os(1)-H(3)	76.39(17)	W-C(43)-C(44)	73.6(5)
C(1)-Os(1)-C(10)	88.8(4)	W-C(43)-C(48)	118.8(7)
C(1)-Os(1)-C(11)	92.4(4)	C(42)-C(43)-C(44)	109.7(9)
C(1)-Os(1)-H(3)	99.4(3)	C(42)-C(43)-C(48)	124.7(11)
C(10)-Os(1)-C(11)	90.8(4)	C(44)-C(43)-C(48)	125.5(11)
C(10)-Os(1)-H(3)	91.8(3)	W-C(44)-C(40)	76.8(5)
C(11)-Os(1)-H(3)	167.9(3)	W-C(44)-C(43)	71.2(5)
Os(1)-Os(2)-Os(3)	59.356(13)	W-C(44)-C(49)	126.8(7)
Os(1)-Os(2)-C(20)	92.4(3)	C(40)-C(44)-C(43)	104.7(9)
Os(1)-Os(2)-C(21)	85.9(3)	C(40)-C(44)-C(49)	126.8(11)
Os(1)-Os(2)-C(22)	165.6(3)	C(43)-C(44)-C(49)	127.1(10)
Os(1)-Os(2)-C(23)	86.4(3)	C(40)-C(45)-H(45a)	110.3(10)
Os(3)-Os(2)-C(20)	151.5(3)	C(40)-C(45)-H(45b)	109.5(11)
Os(3)-Os(2)-C(21)	87.6(3)	C(40)-C(45)-H(45c)	109.0(10)
Os(3)-Os(2)-C(22)	106.2(3)	H(45a)-C(45)-H(45b)	109.6(11)
Os(3)-Os(2)-C(23)	80.3(3)	H(45a)-C(45)-H(45c)	109.4(12)
C(20)-Os(2)-C(21)	94.9(4)	H(45b)-C(45)-H(45c)	109.1(10)
C(20)-Os(2)-C(22)	102.0(4)	C(41)-C(46)-H(46a)	109.4(9)
C(20)-Os(2)-C(23)	94.9(4)	C(41)-C(46)-H(46b)	109.5(10)
C(21)-Os(2)-C(22)	93.8(4)	C(41)-C(46)-H(46c)	109.7(10)
C(21)-Os(2)-C(23)	167.8(4)	H(46a)-C(46)-H(46b)	109.3(11)
C(22)-Os(2)-C(23)	91.3(4)	H(46a)-C(46)-H(46c)	109.5(10)
Os(1)-Os(3)-Os(2)	60.115(13)	H(46b)-C(46)-H(46c)	109.4(10)
Os(1)-Os(3)-O(1)	47.88(16)	C(42)-C(47)-H(47a)	109.8(10)

Os(1)-Os(3)-C(30)	115.7(3)	C(42)-C(47)-H(47b)	109.5(9)
Os(1)-Os(3)-C(31)	134.0(3)	C(42)-C(47)-H(47c)	109.0(11)
Os(1)-Os(3)-C(32)	120.3(3)	H(47a)-C(47)-H(47b)	109.5(12)
Os(1)-Os(3)-H(3)	38.961(11)	H(47a)-C(47)-H(47c)	109.5(10)
Os(2)-Os(3)-O(1)	83.32(16)	H(47b)-C(47)-H(47c)	109.5(12)
Os(2)-Os(3)-C(30)	174.5(3)	C(43)-C(48)-H(48a)	109.7(10)
Os(2)-Os(3)-C(31)	91.9(3)	C(43)-C(48)-H(48b)	109.1(10)
Os(2)-Os(3)-C(32)	87.1(3)	C(43)-C(48)-H(48c)	110.2(11)
Os(2)-Os(3)-H(3)	80.282(15)	H(48a)-C(48)-H(48b)	109.3(12)
O(1)-Os(3)-C(30)	96.3(3)	H(48a)-C(48)-H(48c)	109.3(11)
O(1)-Os(3)-C(31)	97.0(4)	H(48b)-C(48)-H(48c)	109.3(11)
O(1)-Os(3)-C(32)	167.7(3)	C(44)-C(49)-H(49a)	109.2(9)
O(1)-Os(3)-H(3)	79.46(17)	C(44)-C(49)-H(49b)	109.7(11)
C(30)-Os(3)-C(31)	93.5(5)	C(44)-C(49)-H(49c)	109.4(10)
C(30)-Os(3)-C(32)	92.5(4)	H(49a)-C(49)-H(49b)	109.0(10)
C(30)-Os(3)-H(3)	94.3(3)	H(49a)-C(49)-H(49c)	109.5(12)
C(31)-Os(3)-C(32)	91.0(4)	H(49b)-C(49)-H(49c)	110.0(10)
C(31)-Os(3)-H(3)	171.7(3)	C(2)-H(2a)-H(2b)	37(5)
C(32)-Os(3)-H(3)	91.4(3)	C(2)-H(2b)-H(2a)	33(4)
Os(1)-W-O(1)	50.39(17)	Os(1)-H(3)-Os(3)	107.957(17)
Os(1)-W-O(2)	112.09(21)	C(45)-H(45a)-H(45b)	35.3(7)
Os(1)-W-C(1)	54.9(3)	C(45)-H(45a)-H(45c)	35.4(8)
Os(1)-W-C(40)	108.00(22)	H(45b)-H(45a)-H(45c)	60.0
Os(1)-W-C(41)	104.26(21)	C(45)-H(45b)-H(45a)	35.1(6)
Os(1)-W-C(42)	128.30(24)	C(45)-H(45b)-H(45c)	35.5(7)
Os(1)-W-C(43)	160.9(3)	H(45a)-H(45b)-H(45c)	60.0
Os(1)-W-C(44)	137.5(3)	C(45)-H(45c)-H(45a)	35.2(6)
O(1)-W-O(2)	108.0(3)	C(45)-H(45c)-H(45b)	35.4(7)
O(1)-W-C(1)	105.3(3)	H(45a)-H(45c)-H(45b)	60.0
O(1)-W-C(40)	109.3(3)	C(46)-H(46a)-H(46b)	35.4(6)
O(1)-W-C(41)	82.0(3)	C(46)-H(46a)-H(46c)	35.2(7)
O(1)-W-C(42)	85.9(3)	H(46b)-H(46a)-H(46c)	60.0
O(1)-W-C(43)	120.3(3)	C(46)-H(46b)-H(46a)	35.3(6)
O(1)-W-C(44)	139.5(3)	C(46)-H(46b)-H(46c)	35.3(7)
O(2)-W-C(1)	98.8(4)	H(46a)-H(46b)-H(46c)	60.0
O(2)-W-C(40)	136.9(3)	C(46)-H(46c)-H(46a)	35.3(6)
O(2)-W-C(41)	139.7(3)	C(46)-H(46c)-H(46b)	35.3(6)
O(2)-W-C(42)	106.3(3)	H(46a)-H(46c)-H(46b)	60.0
O(2)-W-C(43)	86.2(3)	C(47)-H(47a)-H(47b)	35.3(7)
O(2)-W-C(44)	102.0(3)	C(47)-H(47a)-H(47c)	35.2(7)
C(1)-W-C(40)	91.4(4)	H(47b)-H(47a)-H(47c)	60.0
C(1)-W-C(41)	116.5(4)	C(47)-H(47b)-H(47a)	35.3(7)
C(1)-W-C(42)	147.9(4)	C(47)-H(47b)-H(47c)	35.2(7)
C(1)-W-C(43)	130.2(4)	H(47a)-H(47b)-H(47c)	60.0
C(1)-W-C(44)	96.3(4)	C(47)-H(47c)-H(47a)	35.2(6)
C(40)-W-C(41)	32.7(3)	C(47)-H(47c)-H(47b)	35.3(7)

C(40)-W-C(42)	56.5(3)	H(47a)-H(47c)-H(47b)	60.0
C(40)-W-C(43)	56.6(3)	C(48)-H(48a)-H(48b)	35.4(8)
C(40)-W-C(44)	35.1(3)	C(48)-H(48a)-H(48c)	35.4(8)
C(41)-W-C(42)	34.0(3)	H(48b)-H(48a)-H(48c)	60.0
C(41)-W-C(43)	56.7(3)	C(48)-H(48b)-H(48a)	35.4(6)
C(41)-W-C(44)	57.5(3)	C(48)-H(48b)-H(48c)	35.4(7)
C(42)-W-C(43)	35.6(4)	H(48a)-H(48b)-H(48c)	60.0
C(42)-W-C(44)	59.4(4)	C(48)-H(48c)-H(48a)	35.4(6)
C(43)-W-C(44)	35.2(4)	C(48)-H(48c)-H(48b)	35.4(8)
Os(1)-O(1)-Os(3)	82.14(20)	H(48a)-H(48c)-H(48b)	60.0
Os(1)-O(1)-W	83.7(3)	C(49)-H(49a)-H(49b)	35.4(7)
Os(3)-O(1)-W	119.4(3)	C(49)-H(49a)-H(49c)	35.0(7)
Os(1)-C(1)-W	77.1(3)	H(49b)-H(49a)-H(49c)	60.0
Os(1)-C(1)-C(2)	117.4(7)	C(49)-H(49b)-H(49a)	35.6(6)
Os(1)-C(1)-H(1)	105(5)	C(49)-H(49b)-H(49c)	34.9(7)
W-C(1)-C(2)	133.7(7)	H(49a)-H(49b)-H(49c)	60.0
W-C(1)-H(1)	101(5)	C(49)-H(49c)-H(49a)	35.5(7)
C(2)-C(1)-H(1)	114(5)	C(49)-H(49c)-H(49b)	35.1(7)
C(1)-C(2)-C(3)	113.9(8)	H(49a)-H(49c)-H(49b)	60.0
C(1)-C(2)-H(2a)	109(6)	Cl(1)a-Cl(1)-Cl(2)	7.7(3)
C(1)-C(2)-H(2b)	115(4)	Cl(1)a-Cl(1)-Cl(2)a	83.3(24)
C(3)-C(2)-H(2a)	98(6)	Cl(1)a-Cl(1)-C(50)	26.0(10)
C(3)-C(2)-H(2b)	109(4)	Cl(1)a-Cl(1)-C(50)a	28.7(10)
H(2a)-C(2)-H(2b)	109(7)	Cl(2)-Cl(1)-Cl(2)a	91.0(24)
C(2)-C(3)-C(4)	120.2(9)	Cl(2)-Cl(1)-C(50)	33.6(10)
C(2)-C(3)-C(8)	120.8(9)	Cl(2)-Cl(1)-C(50)a	21.2(10)
C(4)-C(3)-C(8)	119.0(9)	Cl(2)a-Cl(1)-C(50)	58(3)
C(3)-C(4)-C(5)	120.4(9)	Cl(2)a-Cl(1)-C(50)a	111(3)
C(3)-C(4)-H(4)	119.5(9)	C(50)-Cl(1)-C(50)a	54.7(13)
C(5)-C(4)-H(4)	120.0(10)	Cl(1)-Cl(2)-Cl(1)a	89.0(24)
C(4)-C(5)-C(6)	119.8(10)	Cl(1)-Cl(2)-Cl(2)a	7.7(3)
C(4)-C(5)-H(5)	120.2(10)	Cl(1)-Cl(2)-C(50)	32.8(9)
C(6)-C(5)-H(5)	120.0(10)	Cl(1)-Cl(2)-C(50)a	21.6(10)
C(5)-C(6)-C(7)	120.4(9)	Cl(1)a-Cl(2)-Cl(2)a	81.3(24)
C(5)-C(6)-H(6)	120.1(12)	Cl(1)a-Cl(2)-C(50)	56.8(24)
C(7)-C(6)-H(6)	119.5(11)	Cl(1)a-Cl(2)-C(50)a	109(3)
C(6)-C(7)-C(8)	120.9(9)	Cl(2)a-Cl(2)-C(50)	25.3(9)
C(6)-C(7)-H(7)	119.2(10)	Cl(2)a-Cl(2)-C(50)a	29.0(10)
C(8)-C(7)-H(7)	119.9(11)	C(50)-Cl(2)-C(50)a	54.3(14)
C(3)-C(8)-C(7)	119.5(10)	Cl(1)-C(50)-Cl(1)a	125.3(17)
C(3)-C(8)-H(8)	120.0(10)	Cl(1)-C(50)-Cl(2)	113.6(15)
C(7)-C(8)-H(8)	120.5(9)	Cl(1)-C(50)-Cl(2)a	12.5(6)
Os(1)-C(10)-O(10)	175.6(9)	Cl(1)-C(50)-C(50)a	57.8(15)
Os(1)-C(11)-O(11)	177.2(9)	Cl(1)a-C(50)-Cl(2)	12.1(6)
Os(2)-C(20)-O(20)	176.4(9)	Cl(1)a-C(50)-Cl(2)a	137.2(18)
Os(2)-C(21)-O(21)	178.9(8)	Cl(1)a-C(50)-C(50)a	67.6(16)

Os(2)-C(22)-O(22)	175.6(9)	Cl(2)-C(50)-Cl(2)a	125.7(17)
Os(2)-C(23)-O(23)	178.7(9)	Cl(2)-C(50)-C(50)a	55.9(15)
Os(3)-C(30)-O(30)	171.3(10)	Cl(2)a-C(50)-C(50)a	69.8(16)

Atomic Coordinates and equivalent isotropic displacement coefficients ($Å^2 \times 10^3$) for 5

	x	Y	z	U(eq)
Os1	0.39661(4)	0.357917(12)	0.13713(3)	1.925(15)
Os2	0.31462(4)	0.437568(13)	-0.00253(3)	2.317(18)
Os3	0.18661(4)	0.410167(13)	0.16332(3)	2.099(15)
W	0.45050(4)	0.338196(13)	0.38893(3)	2.015(16)
O1	0.4074(7)	0.39467(22)	0.2986(5)	2.2(3)
O2	0.2994(7)	0.32091(25)	0.4015(6)	2.8(3)
O10	0.3060(8)	0.3079(3)	-0.1188(6)	3.3(3)
O11	0.7007(8)	0.3701(3)	0.1661(8)	3.9(4)
O20	0.5456(10)	0.4268(3)	-0.1033(8)	4.3(5)
O21	0.0794(9)	0.3838(3)	-0.2276(7)	3.8(4)
O22	0.1743(10)	0.5241(3)	-0.1276(8)	4.3(5)
O23	0.5206(9)	0.4827(3)	0.2556(7)	3.6(4)
O30	0.0355(8)	0.3762(3)	0.3274(7)	3.5(4)
O31	0.1884(10)	0.5022(3)	0.2632(8)	4.3(5)
O32	-0.1012(8)	0.4242(3)	-0.0703(7)	3.8(4)
C1	0.4497(11)	0.2939(3)	0.2505(9)	2.5(4)
C2	0.5646(11)	0.2653(3)	0.2400(10)	2.5(5)
C3	0.5085(11)	0.2361(3)	0.1179(9)	2.4(4)
C4	0.4076(11)	0.2039(3)	0.1019(9)	2.6(4)
C5	0.3545(11)	0.1774(3)	-0.0108(10)	2.8(5)
C6	0.4031(13)	0.1835(4)	-0.1069(10)	3.4(5)
C7	0.5016(12)	0.2144(4)	-0.0922(9)	2.9(5)
C8	0.5574(11)	0.2415(4)	0.0209(10)	2.9(5)
C10	0.3454(11)	0.3259(4)	-0.0200(9)	2.9(5)
C11	0.5845(11)	0.3643(3)	0.1557(9)	2.4(4)
C20	0.4566(12)	0.4316(4)	-0.0693(9)	2.9(5)
C21	0.1671(12)	0.4033(3)	-0.1435(10)	2.8(5)
C22	0.2272(12)	0.4923(4)	-0.0760(10)	3.1(5)
C23	0.4440(12)	0.4654(3)	0.1603(10)	2.8(5)
C30	0.0986(11)	0.3859(4)	0.2699(10)	3.1(5)
C31	0.1854(12)	0.4679(4)	0.2231(10)	3.2(5)
C32	0.0066(11)	0.4190(3)	0.0184(10)	2.7(5)
C40	0.7171(11)	0.3306(4)	0.5191(9)	2.7(4)
C41	0.6827(11)	0.3745(3)	0.5237(8)	2.3(4)
C42	0.5857(10)	0.3782(3)	0.5816(8)	2.4(4)
C43	0.5654(11)	0.3350(4)	0.6204(9)	3.0(5)
C44	0.6372(11)	0.3039(4)	0.5744(9)	3.0(5)
C45	0.8304(12)	0.3131(4)	0.4837(11)	3.9(5)
C46	0.7464(12)	0.4113(4)	0.4807(10)	3.2(5)
C47	0.5251(13)	0.4197(4)	0.6041(10)	3.7(6)
C48	0.4764(13)	0.3242(5)	0.6937(10)	4.2(6)
C49	0.6546(13)	0.2565(4)	0.6034(11)	3.9(6)

H1	0.343(11)	0.277(4)	0.222(9)	3.2(23)
H2a	0.592(11)	0.243(4)	0.306(9)	2.8(22)
H2b	0.659(9)	0.282(3)	0.248(7)	1.0(16)
H3	0.205	0.364	0.106	4.2
H4	0.372	0.200	0.171	4.2
H5	0.281	0.154	-0.022	4.2
H6	0.366	0.164	-0.187	4.2
H7	0.535	0.218	-0.163	4.2
H8	0.631	0.264	0.031	4.2
H45a	0.927	0.315	0.561	4.2
H45b	0.808	0.282	0.455	4.2
H45c	0.831	0.331	0.409	4.2
H46a	0.841	0.420	0.555	4.2
H46b	0.762	0.402	0.403	4.2
H46c	0.679	0.437	0.456	4.2
H47a	0.594	0.433	0.689	4.2
H47b	0.508	0.440	0.530	4.2
H47c	0.432	0.414	0.608	4.2
H48a	0.540	0.324	0.791	4.2
H48b	0.400	0.347	0.674	4.2
H48c	0.430	0.295	0.666	4.2
H49a	0.743	0.252	0.689	4.2
H49b	0.568	0.245	0.613	4.2
H49c	0.666	0.241	0.531	4.2
Cl1	0.1283(11)	0.4741(4)	0.5682(10)	8.41(24)
Cl2	-0.1129(13)	0.5326(4)	0.4643(11)	10.2(3)
C50	-0.019(3)	0.4907(10)	0.4329(24)	5.2(6)

AppendixA.6

Structure Determination Summary for

$[Os_3W(\mu\text{-}H)(gauche\text{-}\mu\text{-}\eta^1\text{-}CHCH_2Ph)(CO)_9(O)(Cp^*)(\mu_3\text{-}O)]$ 6

Empirical Formula	$Os_3WO_{11}C_{27}H_{24}$	
Crystal Size (mm)	0.21 x 0.1 x 0.25	
Crystal System	Monoclinic	
Space Group	*P21/n*	
Unit Cell Dimensions	a = 10.7162(5) Å	$\alpha = 90$
	b = 21.3049(9) Å	$\beta = 111.01(1)$
	c = 14.7394(7) Å	$\gamma = 90$
Volume $(Å)^3$	3141.48(25)	
Z	4	
Formula Weight	1278.92	
Density (calc.) (gcm^{-3})	2.704	
Absorption Coefficient (mm^{-1})	15.80	
λ (Mo-Kα)	0.70930 Å	
Temperature (°C)	-100	
2θ Range (deg)	57.3	
Index Ranges	$-14 \le 13, 0 \le 28, 0 \le 19$	
Reflections Collected	36248	
Independent Reflections	8117	
Observed Reflections [$I > 2.5\ \sigma(I)$]	6301	
Weighting Scheme	$\omega^{-1} = \sigma^2(F_o) + 0.0001\ F_o^2$	
Number of Parameters Refined	379	
Final *R* Indices (obs. data)	$R = 0.035$; $R_W = 0.037$	
Final *R* Indices (all data)	$R = 0.035$; $R_W = 0.037$	
Goodness of Fit	1.50	
Largest and Mean Δ/σ	0.000	
Largest Difference Peak/Hole $(e/Å^3)$	-2.000/1.980	

Bond lengths (Å) for 6

Os(1)-Os(2)	2.8160(5)	C(2)-H(2a)	1.086(8)
Os(1)-Os(3)	2.8078(5)	C(2)-H(2b)	1.046(9)
Os(1)-W	2.6911(4)	C(3)-C(4)	1.390(12)
Os(1)-O(1)	2.090(5)	C(3)-C(8)	1.370(14)
Os(1)-C(1)	2.222(8)	C(4)-C(5)	1.408(13)
Os(1)-C(10)	1.885(10)	C(4)-H(4)	1.082(9)
Os(1)-C(11)	1.892(9)	C(5)-C(6)	1.341(16)
Os(1)-H(3)	1.8545(3)	C(5)-H(5)	1.077(10)
Os(2)-Os(3)	2.8331(5)	C(6)-C(7)	1.391(14)
Os(2)-C(20)	1.952(10)	C(6)-H(6)	1.082(9)
Os(2)-C(21)	1.913(10)	C(7)-C(8)	1.397(13)
Os(2)-C(22)	1.931(10)	C(7)-H(7)	1.065(10)
Os(2)-C(23)	1.924(10)	C(8)-H(8)	1.076(9)
Os(3)-O(1)	2.180(5)	C(40)-C(41)	1.435(12)
Os(3)-C(30)	1.904(10)	C(40)-C(44)	1.380(14)
Os(3)-C(31)	1.877(10)	C(40)-C(45)	1.516(14)
Os(3)-C(32)	1.958(9)	C(41)-C(42)	1.411(14)
Os(3)-H(3)	1.6079(4)	C(41)-C(46)	1.522(14)
W-O(1)	1.953(5)	C(42)-C(43)	1.405(13)
W-O(2)	1.703(5)	C(42)-C(47)	1.501(12)
W-C(1)	2.055(9)	C(43)-C(44)	1.443(14)
W-C(40)	2.486(9)	C(43)-C(48)	1.484(16)
W-C(41)	2.386(9)	C(44)-C(49)	1.497(12)
W-C(42)	2.344(8)	C(45)-H(45a)	1.088(10)
W-C(43)	2.336(8)	C(45)-H(45b)	1.069(12)
W-C(44)	2.453(8)	C(45)-H(45c)	1.076(11)
O(10)-C(10)	1.152(12)	C(46)-H(46a)	1.072(10)
O(11)-C(11)	1.148(11)	C(46)-H(46b)	1.081(12)
O(20)-C(20)	1.130(12)	C(46)-H(46c)	1.077(12)
O(21)-C(21)	1.139(13)	C(47)-H(47a)	1.053(9)
O(22)-C(22)	1.139(12)	C(47)-H(47b)	1.108(12)
O(23)-C(23)	1.167(12)	C(47)-H(47c)	1.090(12)
O(30)-C(30)	1.137(12)	C(48)-H(48a)	1.098(10)
O(31)-C(31)	1.135(12)	C(48)-H(48b)	1.060(12)
O(32)-C(32)	1.118(11)	C(48)-H(48c)	1.056(12)
C(1)-C(2)	1.545(11)	C(49)-H(49a)	1.072(9)
C(1)-H(1)	1.064(9)	C(49)-H(49b)	1.064(11)
C(2)-C(3)	1.533(11)	C(49)-H(49c)	1.100(12)

Bond angles (deg) for 6

Os(2)-Os(1)-Os(3)	60.497(12)	Os(3)-O(1)-W	117.07(24)
Os(2)-Os(1)-W	132.242(17)	Os(1)-C(1)-W	77.9(3)
Os(2)-Os(1)-O(1)	86.62(14)	Os(1)-C(1)-C(2)	115.3(5)
Os(2)-Os(1)-C(1)	173.12(21)	Os(1)-C(1)-H(1)	108.7(5)
Os(2)-Os(1)-C(10)	91.7(3)	W-C(1)-C(2)	119.6(6)
Os(2)-Os(1)-C(11)	93.08(24)	W-C(1)-H(1)	109.8(5)
Os(2)-Os(1)-H(3)	76.836(13)	C(2)-C(1)-H(1)	118.5(8)
Os(3)-Os(1)-W	79.762(13)	C(1)-C(2)-C(3)	113.0(6)
Os(3)-Os(1)-O(1)	50.28(14)	C(1)-C(2)-H(2a)	106.7(6)
Os(3)-Os(1)-C(1)	115.26(23)	C(1)-C(2)-H(2b)	110.0(8)
Os(3)-Os(1)-C(10)	136.6(3)	C(3)-C(2)-H(2a)	106.8(7)
Os(3)-Os(1)-C(11)	122.24(25)	C(3)-C(2)-H(2b)	108.8(7)
Os(3)-Os(1)-H(3)	32.962(9)	H(2a)-C(2)-H(2b)	111.6(7)
W-Os(1)-O(1)	46.13(14)	C(2)-C(3)-C(4)	119.4(8)
W-Os(1)-C(1)	48.29(21)	C(2)-C(3)-C(8)	121.1(8)
W-Os(1)-C(10)	101.5(3)	C(4)-C(3)-C(8)	119.5(8)
W-Os(1)-C(11)	132.28(24)	C(3)-C(4)-C(5)	119.6(9)
W-Os(1)-H(3)	83.815(13)	C(3)-C(4)-H(4)	120.6(8)
O(1)-Os(1)-C(1)	94.4(3)	C(5)-C(4)-H(4)	119.8(8)
O(1)-Os(1)-C(10)	99.7(3)	C(4)-C(5)-C(6)	120.7(9)
O(1)-Os(1)-C(11)	171.1(3)	C(4)-C(5)-H(5)	119.9(10)
O(1)-Os(1)-H(3)	75.93(14)	C(6)-C(5)-H(5)	119.4(9)
C(1)-Os(1)-C(10)	94.9(3)	C(5)-C(6)-C(7)	120.2(9)
C(1)-Os(1)-C(11)	84.8(3)	C(5)-C(6)-H(6)	120.9(9)
C(1)-Os(1)-H(3)	96.79(22)	C(7)-C(6)-H(6)	119.0(10)
C(10)-Os(1)-C(11)	89.2(4)	C(6)-C(7)-C(8)	119.9(9)
C(10)-Os(1)-H(3)	167.8(3)	C(6)-C(7)-H(7)	120.1(9)
C(11)-Os(1)-H(3)	95.32(24)	C(8)-C(7)-H(7)	120.0(9)
Os(1)-Os(2)-Os(3)	59.608(12)	C(3)-C(8)-C(7)	120.2(8)
Os(1)-Os(2)-C(20)	83.81(25)	C(3)-C(8)-H(8)	120.9(8)
Os(1)-Os(2)-C(21)	157.1(3)	C(7)-C(8)-H(8)	118.9(9)
Os(1)-Os(2)-C(22)	103.1(3)	Os(1)-C(10)-O(10)	178.0(8)
Os(1)-Os(2)-C(23)	81.6(3)	Os(1)-C(11)-O(11)	176.8(7)
Os(3)-Os(2)-C(20)	84.14(25)	Os(2)-C(20)-O(20)	179.4(9)
Os(3)-Os(2)-C(21)	97.5(3)	Os(2)-C(21)-O(21)	176.2(8)
Os(3)-Os(2)-C(22)	162.7(3)	Os(2)-C(22)-O(22)	175.3(9)
Os(3)-Os(2)-C(23)	85.91(25)	Os(2)-C(23)-O(23)	177.5(8)
C(20)-Os(2)-C(21)	96.8(4)	Os(3)-C(30)-O(30)	177.1(8)
C(20)-Os(2)-C(22)	92.7(4)	Os(3)-C(31)-O(31)	177.6(8)
C(20)-Os(2)-C(23)	165.1(3)	Os(3)-C(32)-O(32)	170.2(8)
C(21)-Os(2)-C(22)	99.8(4)	W-C(40)-C(41)	69.1(5)
C(21)-Os(2)-C(23)	95.5(4)	W-C(40)-C(44)	72.5(5)
C(22)-Os(2)-C(23)	93.5(4)	W-C(40)-C(45)	128.2(6)
Os(1)-Os(3)-Os(2)	59.895(12)	C(41)-C(40)-C(44)	108.0(8)
Os(1)-Os(3)-O(1)	47.51(14)	C(41)-C(40)-C(45)	124.8(9)

Os(1)-Os(3)-C(30)	128.7(3)	C(44)-C(40)-C(45)	127.0(8)
Os(1)-Os(3)-C(31)	122.1(3)	W-C(41)-C(40)	76.7(5)
Os(1)-Os(3)-C(32)	118.5(3)	W-C(41)-C(42)	71.0(5)
Os(1)-Os(3)-H(3)	38.869(10)	W-C(41)-C(46)	126.6(6)
Os(2)-Os(3)-O(1)	84.55(13)	C(40)-C(41)-C(42)	108.0(8)
Os(2)-Os(3)-C(30)	83.69(24)	C(40)-C(41)-C(46)	123.4(9)
Os(2)-Os(3)-C(31)	91.2(3)	C(42)-C(41)-C(46)	127.7(8)
Os(2)-Os(3)-C(32)	178.2(3)	W-C(42)-C(41)	74.3(5)
Os(2)-Os(3)-H(3)	79.751(14)	W-C(42)-C(43)	72.2(5)
O(1)-Os(3)-C(30)	98.4(3)	W-C(42)-C(47)	119.4(6)
O(1)-Os(3)-C(31)	169.4(3)	C(41)-C(42)-C(43)	108.0(8)
O(1)-Os(3)-C(32)	94.7(3)	C(41)-C(42)-C(47)	124.1(9)
O(1)-Os(3)-H(3)	78.37(14)	C(43)-C(42)-C(47)	127.9(10)
C(30)-Os(3)-C(31)	90.7(4)	W-C(43)-C(42)	72.8(5)
C(30)-Os(3)-C(32)	98.0(4)	W-C(43)-C(44)	76.9(5)
C(30)-Os(3)-H(3)	163.36(24)	W-C(43)-C(48)	121.8(7)
C(31)-Os(3)-C(32)	89.3(4)	C(42)-C(43)-C(44)	107.5(9)
C(31)-Os(3)-H(3)	91.3(3)	C(42)-C(43)-C(48)	126.7(9)
C(32)-Os(3)-H(3)	98.5(3)	C(44)-C(43)-C(48)	125.4(9)
Os(1)-W-O(1)	50.48(16)	W-C(44)-C(40)	75.1(5)
Os(1)-W-O(2)	111.70(18)	W-C(44)-C(43)	68.1(4)
Os(1)-W-C(1)	53.84(21)	W-C(44)-C(49)	123.4(6)
Os(1)-W-C(40)	104.50(20)	C(40)-C(44)-C(43)	108.4(8)
Os(1)-W-C(41)	130.38(23)	C(40)-C(44)-C(49)	127.1(9)
Os(1)-W-C(42)	161.22(21)	C(43)-C(44)-C(49)	124.5(9)
Os(1)-W-C(43)	135.69(23)	C(40)-C(45)-H(45a)	108.2(8)
Os(1)-W-C(44)	106.50(19)	C(40)-C(45)-H(45b)	109.7(8)
O(1)-W-O(2)	107.06(25)	C(40)-C(45)-H(45c)	109.5(10)
O(1)-W-C(1)	104.3(3)	H(45a)-C(45)-H(45b)	109.6(10)
O(1)-W-C(40)	108.1(3)	H(45a)-C(45)-H(45c)	109.2(9)
O(1)-W-C(41)	140.20(24)	H(45b)-C(45)-H(45c)	110.6(9)
O(1)-W-C(42)	128.9(3)	C(41)-C(46)-H(46a)	109.1(8)
O(1)-W-C(43)	94.3(3)	C(41)-C(46)-H(46b)	108.8(10)
O(1)-W-C(44)	84.50(24)	C(41)-C(46)-H(46c)	109.0(8)
O(2)-W-C(1)	100.0(3)	H(46a)-C(46)-H(46b)	110.0(9)
O(2)-W-C(40)	140.4(3)	H(46a)-C(46)-H(46c)	110.3(11)
O(2)-W-C(41)	106.7(3)	H(46b)-C(46)-H(46c)	109.6(9)
O(2)-W-C(42)	86.8(3)	C(42)-C(47)-H(47a)	111.7(8)
O(2)-W-C(43)	103.3(3)	C(42)-C(47)-H(47b)	108.6(9)
O(2)-W-C(44)	138.2(3)	C(42)-C(47)-H(47c)	109.5(9)
C(1)-W-C(40)	88.5(3)	H(47a)-C(47)-H(47b)	109.4(10)
C(1)-W-C(41)	89.9(3)	H(47a)-C(47)-H(47c)	110.8(10)
C(1)-W-C(42)	121.8(3)	H(47b)-C(47)-H(47c)	106.8(8)
C(1)-W-C(43)	144.3(3)	C(43)-C(48)-H(48a)	106.8(9)
C(1)-W-C(44)	116.2(3)	C(43)-C(48)-H(48b)	108.6(9)
C(40)-W-C(41)	34.2(3)	C(43)-C(48)-H(48c)	108.8(9)

C(40)-W-C(42)	56.8(3)	H(48a)-C(48)-H(48b)	109.5(10)
C(40)-W-C(43)	56.6(3)	H(48a)-C(48)-H(48c)	109.9(10)
C(40)-W-C(44)	32.4(3)	H(48b)-C(48)-H(48c)	112.9(11)
C(41)-W-C(42)	34.7(3)	C(44)-C(49)-H(49a)	109.3(8)
C(41)-W-C(43)	57.7(3)	C(44)-C(49)-H(49b)	110.0(9)
C(41)-W-C(44)	56.1(3)	C(44)-C(49)-H(49c)	108.3(8)
C(42)-W-C(43)	34.9(3)	H(49a)-C(49)-H(49b)	111.3(9)
C(42)-W-C(44)	57.2(3)	H(49a)-C(49)-H(49c)	108.6(9)
C(43)-W-C(44)	35.0(3)	H(49b)-C(49)-H(49c)	109.2(8)
Os(1)-O(1)-Os(3)	82.21(18)	Os(1)-H(3)-Os(3)	108.170(15)
Os(1)-O(1)-W	83.39(20)		

Atomic Coordinates and equivalent isotropic displacement coefficients ($Å^2 \times 10^3$) for 6.

	x	y	z	U(eq)
Os1	0.45686(3)	0.915125(14)	0.179174(23)	1.786(14)
Os2	0.28734(4)	1.014693(14)	0.185503(25)	2.110(14)
Os3	0.23969(3)	0.891643(14)	0.238387(24)	1.936(14)
W	0.55045(3)	0.815218(14)	0.295469(23)	1.828(13)
O1	0.4553(5)	0.88903(23)	0.3155(4)	1.73(23)
O2	0.4393(6)	0.75466(25)	0.2660(4)	2.2(3)
O10	0.6982(7)	1.0015(3)	0.2439(5)	3.7(3)
O11	0.4150(7)	0.9389(3)	-0.0330(5)	3.1(3)
O20	0.1216(7)	0.9711(3)	-0.0223(5)	3.6(3)
O21	0.0654(8)	1.0810(3)	0.2324(5)	4.1(4)
O22	0.3950(9)	1.1287(3)	0.1095(6)	5.0(4)
O23	0.4891(7)	1.0272(3)	0.3958(5)	3.3(3)
O30	0.1584(8)	0.9609(3)	0.3888(5)	3.6(3)
O31	-0.0445(7)	0.8943(3)	0.0969(5)	4.4(4)
O32	0.1757(7)	0.7594(3)	0.2913(5)	3.8(4)
C1	0.5686(8)	0.8306(4)	0.1631(6)	2.0(3)
C2	0.4932(9)	0.7876(4)	0.0762(6)	2.2(4)
C3	0.5692(9)	0.7270(4)	0.0744(6)	2.1(3)
C4	0.5410(9)	0.6728(4)	0.1159(6)	2.4(4)
C5	0.6157(11)	0.6179(4)	0.1192(7)	3.1(5)
C6	0.7131(10)	0.6173(4)	0.0820(7)	3.2(4)
C7	0.7411(10)	0.6711(4)	0.0394(7)	3.1(4)
C8	0.6684(10)	0.7260(4)	0.0361(7)	2.8(4)
C10	0.6074(10)	0.9683(4)	0.2181(6)	2.6(4)
C11	0.4344(8)	0.9308(4)	0.0479(7)	2.1(4)
C20	0.1817(10)	0.9872(4)	0.0540(7)	2.7(4)
C21	0.1452(10)	1.0557(4)	0.2118(7)	2.9(4)
C22	0.3605(10)	1.0854(4)	0.1392(7)	3.1(5)
C23	0.4149(10)	1.0215(4)	0.3159(7)	2.7(5)
C30	0.1910(9)	0.9340(4)	0.3344(7)	2.6(4)
C31	0.0621(10)	0.8945(4)	0.1512(7)	2.9(4)
C32	0.2098(10)	0.8056(4)	0.2726(7)	2.7(4)
C40	0.7943(9)	0.8352(4)	0.3739(6)	2.6(4)
C41	0.7682(9)	0.7695(4)	0.3546(6)	2.5(4)
C42	0.6957(9)	0.7480(4)	0.4117(6)	2.5(4)
C43	0.6694(10)	0.7998(4)	0.4611(6)	3.0(4)
C44	0.7345(9)	0.8537(4)	0.4383(6)	2.4(4)
C45	0.8831(10)	0.8746(5)	0.3362(8)	4.1(5)
C46	0.8321(11)	0.7304(5)	0.2966(8)	4.2(5)
C47	0.6562(11)	0.6808(4)	0.4163(8)	4.2(5)
C48	0.6019(12)	0.7987(6)	0.5331(7)	4.4(6)
C49	0.7370(10)	0.9177(4)	0.4806(7)	3.7(4)

H1	0.668	0.844	0.174	3.9
H2a	0.485	0.814	0.011	3.9
H2b	0.399	0.776	0.078	3.9
H3	0.293	0.876	0.152	3.9
H4	0.462	0.672	0.146	3.9
H5	0.595	0.576	0.152	3.9
H6	0.772	0.575	0.086	3.9
H7	0.816	0.670	0.007	3.9
H8	0.692	0.767	0.004	3.9
H45a	0.984	0.873	0.390	3.9
H45b	0.882	0.856	0.269	3.9
H45c	0.848	0.922	0.327	3.9
H46a	0.930	0.716	0.343	3.9
H46b	0.771	0.689	0.269	3.9
H46c	0.838	0.758	0.237	3.9
H47a	0.730	0.656	0.472	3.9
H47b	0.561	0.680	0.429	3.9
H47c	0.637	0.659	0.346	3.9
H48a	0.680	0.791	0.605	3.9
H48b	0.556	0.843	0.532	3.9
H48c	0.533	0.761	0.516	3.9
H49a	0.826	0.923	0.543	3.9
H49b	0.731	0.953	0.427	3.9
H49c	0.650	0.922	0.503	3.9

Appendix A.7

Structure Determination Summary for

$[Os_3W(CO)_9(\mu\text{-}O)_2(\mu\text{-}\eta^1,\eta^2\text{-}CH{=}CHPh\{W\text{-}Os\})(Cp^*)]$ 7

Empirical Formula	$Os_3WO_{11}C_{27}H_{22}$	
Crystal size (mm)	.175 x 0.075 x 0.05	
Crystal System	Monoclinic	
Space Group	*P*21/n	
Unit Cell Dimensions	a = 14.8146(9) Å	α = 90
	b = 12.5353(7) Å	β = 93.41(1)
	c = 16.2211(9) Å	γ = 90
Volume (Å)^3	3007.0(3)	
Z	4	
Formula Weight	1276.90	
Density (calc.) (g cm^{-3})	2.821	
Absorption Coefficient (mm^{-1})	16.50	
λ(Mo-Kα)	0.70930 Å	
Temperature (°C)	-100	
2θ Range (deg)	57.4	
Index Ranges	$-20 \le 20, 0 \le 16, 0 \le 21$	
Reflections Collected	34555	
Independent Reflections	7795	
Observed Reflections [I > 2.5 σ(I)]	5213	
Weighting Scheme	$\omega^{-1} = \sigma^2(F_o) + 0.0001\ F_o^2$	
Number of Parameters Refined	379	
Final *R* Indices (obs. data)	R = 0.039; R_W = 0.031	
Final *R* Indices (all data)	R = 0.039; R_W = 0.031	
Goodness of Fit	1.97	
Largest and Mean Δ/σ	0.000	
Largest Difference Peak/Hole (e/Å^3)	-1.730/3.710	

Bond lengths (Å) for 7

Os(1)-Os(3)	2.8394(6)	C(40)-C(41)	1.410(15)
Os(1)-W	2.7281(6)	C(40)-C(45)	1.471(17)
Os(1)-Os(2)	2.8476(6)	C(1)-C(2)	1.390(15)
Os(1)-C(10)	1.841(11)	C(1)-H(1)	1.101(10)
Os(1)-C(11)	1.886(13)	C(42)-C(43)	1.435(16)
Os(1)-C(1)	2.197(9)	C(42)-C(41)	1.415(17)
Os(1)-C(2)	2.316(10)	C(42)-C(47)	1.503(15)
Os(1)-O(1)	2.199(6)	C(43)-C(44)	1.437(17)
Os(3)-Os(2)	2.8563(6)	C(43)-C(48)	1.482(18)
Os(3)-C(32)	1.926(12)	C(3)-C(2)	1.499(14)
Os(3)-C(30)	1.876(14)	C(3)-C(8)	1.381(17)
Os(3)-C(31)	1.984(12)	C(2)-H(2)	1.105(10)
Os(3)-C(33)	1.961(12)	C(33)-O(33)	1.134(14)
W-Os(2)	2.9219(6)	C(44)-C(49)	1.535(16)
W-C(40)	2.415(11)	C(46)-C(41)	1.501(16)
W-C(1)	2.135(9)	C(46)-H(46a)	1.096(11)
W-C(42)	2.438(10)	C(46)-H(46b)	1.088(12)
W-C(43)	2.381(11)	C(46)-H(46c)	1.090(11)
W-C(44)	2.369(11)	C(47)-H(47a)	1.081(11)
W-C(41)	2.418(10)	C(47)-H(47b)	1.096(12)
W-O(1)	1.773(7)	C(47)-H(47c)	1.097(12)
W-O(2)	1.825(7)	C(8)-C(7)	1.375(16)
Os(2)-C(21)	1.869(13)	C(8)-H(8)	1.111(12)
Os(2)-C(22)	1.893(13)	C(5)-C(6)	1.366(20)
Os(2)-C(20)	1.901(13)	C(5)-H(5)	1.109(13)
Os(2)-O(2)	2.087(7)	C(48)-H(48a)	1.083(13)
C(10)-O(10)	1.160(13)	C(48)-H(48b)	1.091(12)
C(21)-O(21)	1.157(15)	C(48)-H(48c)	1.108(15)
C(32)-O(32)	1.113(15)	C(7)-C(6)	1.379(19)
C(30)-O(30)	1.162(17)	C(7)-H(7)	1.111(12)
C(22)-O(22)	1.154(15)	C(6)-H(6)	1.097(12)
C(11)-O(11)	1.153(15)	C(49)-H(49a)	1.089(13)
C(4)-C(3)	1.389(17)	C(49)-H(49b)	1.085(14)
C(4)-C(5)	1.399(16)	C(49)-H(49c)	1.093(16)
C(4)-H(4)	1.106(12)	C(45)-H(45a)	1.081(11)
C(20)-O(20)	1.134(16)	C(45)-H(45b)	1.102(14)
C(31)-O(31)	1.106(14)	C(45)-H(45c)	1.091(12)
C(40)-C(44)	1.414(20)		

Bond angles (deg) for 7

Os(3)-Os(1)-W	97.290(18)	C(21)-Os(2)-O(2)	178.3(4)
Os(3)-Os(1)-Os(2)	60.298(15)	C(22)-Os(2)-C(20)	96.7(5)
Os(3)-Os(1)-C(10)	97.5(3)	C(22)-Os(2)-O(2)	91.5(4)
Os(3)-Os(1)-C(11)	89.5(3)	C(20)-Os(2)-O(2)	88.9(4)
Os(3)-Os(1)-C(1)	140.7(3)	Os(1)-C(10)-O(10)	177.1(9)
Os(3)-Os(1)-C(2)	168.07(25)	Os(2)-C(21)-O(21)	178.2(10)
Os(3)-Os(1)-O(1)	89.55(17)	Os(3)-C(32)-O(32)	178.9(11)
W-Os(1)-Os(2)	63.164(16)	Os(3)-C(30)-O(30)	179.4(9)
W-Os(1)-C(10)	137.3(4)	Os(2)-C(22)-O(22)	173.3(10)
W-Os(1)-C(11)	128.9(3)	Os(1)-C(11)-O(11)	174.9(9)
W-Os(1)-C(1)	49.97(25)	C(3)-C(4)-C(5)	119.0(11)
W-Os(1)-C(2)	73.1(3)	C(3)-C(4)-H(4)	120.7(10)
W-Os(1)-O(1)	40.42(18)	C(5)-C(4)-H(4)	120.3(12)
Os(2)-Os(1)-C(10)	90.7(3)	Os(2)-C(20)-O(20)	175.9(10)
Os(2)-Os(1)-C(11)	149.7(3)	Os(3)-C(31)-O(31)	176.3(10)
Os(2)-Os(1)-C(1)	83.0(3)	W-C(40)-C(44)	71.0(6)
Os(2)-Os(1)-C(2)	118.8(3)	W-C(40)-C(41)	73.2(6)
Os(2)-Os(1)-O(1)	92.48(17)	W-C(40)-C(45)	121.9(7)
C(10)-Os(1)-C(11)	91.0(5)	C(44)-C(40)-C(41)	107.1(10)
C(10)-Os(1)-C(1)	96.5(4)	C(44)-C(40)-C(45)	126.8(11)
C(10)-Os(1)-C(2)	94.4(4)	C(41)-C(40)-C(45)	126.1(12)
C(10)-Os(1)-O(1)	173.0(4)	Os(1)-C(1)-W	78.0(3)
C(11)-Os(1)-C(1)	126.7(4)	Os(1)-C(1)-C(2)	76.8(6)
C(11)-Os(1)-C(2)	91.2(4)	Os(1)-C(1)-H(1)	113.9(6)
C(11)-Os(1)-O(1)	89.4(3)	W-C(1)-C(2)	116.4(7)
C(1)-Os(1)-C(2)	35.7(4)	W-C(1)-H(1)	114.7(7)
C(1)-Os(1)-O(1)	77.6(3)	C(2)-C(1)-H(1)	128.9(9)
C(2)-Os(1)-O(1)	78.6(3)	W-C(42)-C(43)	70.5(6)
Os(1)-Os(3)-Os(2)	59.993(15)	W-C(42)-C(41)	72.3(6)
Os(1)-Os(3)-C(32)	160.2(4)	W-C(42)-C(47)	119.9(7)
Os(1)-Os(3)-C(30)	98.2(3)	C(43)-C(42)-C(41)	108.8(9)
Os(1)-Os(3)-C(31)	85.7(3)	C(43)-C(42)-C(47)	124.1(10)
Os(1)-Os(3)-C(33)	89.2(3)	C(41)-C(42)-C(47)	126.9(10)
Os(2)-Os(3)-C(32)	100.6(4)	W-C(43)-C(42)	74.8(6)
Os(2)-Os(3)-C(30)	157.6(3)	W-C(43)-C(44)	71.9(6)
Os(2)-Os(3)-C(31)	92.7(3)	W-C(43)-C(48)	121.1(8)
Os(2)-Os(3)-C(33)	83.1(3)	C(42)-C(43)-C(44)	105.2(10)
C(32)-Os(3)-C(30)	101.5(5)	C(42)-C(43)-C(48)	126.2(11)
C(32)-Os(3)-C(31)	91.7(5)	C(44)-C(43)-C(48)	128.4(11)
C(32)-Os(3)-C(33)	92.4(5)	C(4)-C(3)-C(2)	117.8(10)
C(30)-Os(3)-C(31)	90.5(5)	C(4)-C(3)-C(8)	119.7(10)
C(30)-Os(3)-C(33)	92.1(5)	C(2)-C(3)-C(8)	122.5(10)
C(31)-Os(3)-C(33)	174.6(4)	Os(1)-C(2)-C(1)	67.5(5)
Os(1)-W-Os(2)	60.415(16)	Os(1)-C(2)-C(3)	121.1(7)
Os(1)-W-C(40)	122.9(3)	Os(1)-C(2)-H(2)	105.3(6)

Os(1)-W-C(1)	52.0(3)	C(1)-C(2)-C(3)	125.0(9)
Os(1)-W-C(42)	161.6(3)	C(1)-C(2)-H(2)	114.5(9)
Os(1)-W-C(43)	163.6(3)	C(3)-C(2)-H(2)	113.9(9)
Os(1)-W-C(44)	135.2(3)	Os(3)-C(33)-O(33)	174.2(9)
Os(1)-W-C(41)	133.9(3)	W-C(44)-C(40)	74.6(6)
Os(1)-W-O(1)	53.52(20)	W-C(44)-C(43)	72.9(6)
Os(1)-W-O(2)	98.13(22)	W-C(44)-C(49)	123.4(8)
Os(2)-W-C(40)	170.1(3)	C(40)-C(44)-C(43)	109.9(10)
Os(2)-W-C(1)	82.3(3)	C(40)-C(44)-C(49)	125.8(12)
Os(2)-W-C(42)	123.9(3)	C(43)-C(44)-C(49)	124.0(12)
Os(2)-W-C(43)	115.7(3)	C(41)-C(46)-H(46a)	110.8(10)
Os(2)-W-C(44)	136.1(3)	C(41)-C(46)-H(46b)	111.2(10)
Os(2)-W-C(41)	151.9(3)	C(41)-C(46)-H(46c)	111.1(9)
Os(2)-W-O(1)	100.04(21)	H(46a)-C(46)-H(46b)	107.7(10)
Os(2)-W-O(2)	45.22(22)	H(46a)-C(46)-H(46c)	107.6(10)
C(40)-W-C(1)	93.0(3)	H(46b)-C(46)-H(46c)	108.2(10)
C(40)-W-C(42)	56.5(3)	W-C(41)-C(40)	72.9(6)
C(40)-W-C(43)	58.2(4)	W-C(41)-C(42)	73.8(6)
C(40)-W-C(44)	34.4(5)	W-C(41)-C(46)	120.3(7)
C(40)-W-C(41)	33.9(4)	C(40)-C(41)-C(42)	108.8(10)
C(40)-W-O(1)	88.5(4)	C(40)-C(41)-C(46)	124.4(11)
C(40)-W-O(2)	136.6(3)	C(42)-C(41)-C(46)	126.8(10)
C(1)-W-C(42)	142.4(3)	C(42)-C(47)-H(47a)	111.6(10)
C(1)-W-C(43)	112.8(4)	C(42)-C(47)-H(47b)	111.2(9)
C(1)-W-C(44)	85.7(4)	C(42)-C(47)-H(47c)	110.4(9)
C(1)-W-C(41)	125.8(4)	H(47a)-C(47)-H(47b)	108.3(10)
C(1)-W-O(1)	89.1(3)	H(47a)-C(47)-H(47c)	108.1(9)
C(1)-W-O(2)	126.2(3)	H(47b)-C(47)-H(47c)	107.1(10)
C(42)-W-C(43)	34.6(4)	C(3)-C(8)-C(7)	120.4(11)
C(42)-W-C(44)	56.7(4)	C(3)-C(8)-H(8)	119.7(10)
C(42)-W-C(41)	33.9(4)	C(7)-C(8)-H(8)	119.9(11)
C(42)-W-O(1)	109.3(3)	C(4)-C(5)-C(6)	120.8(12)
C(42)-W-O(2)	80.1(3)	C(4)-C(5)-H(5)	119.6(13)
C(43)-W-C(44)	35.2(4)	C(6)-C(5)-H(5)	119.6(11)
C(43)-W-C(41)	57.7(4)	C(43)-C(48)-H(48a)	112.2(11)
C(43)-W-O(1)	139.6(4)	C(43)-C(48)-H(48b)	111.6(11)
C(43)-W-O(2)	86.8(4)	C(43)-C(48)-H(48c)	110.5(10)
C(44)-W-C(41)	56.6(4)	H(48a)-C(48)-H(48b)	108.5(10)
C(44)-W-O(1)	121.9(4)	H(48a)-C(48)-H(48c)	107.2(11)
C(44)-W-O(2)	121.5(4)	H(48b)-C(48)-H(48c)	106.6(12)
C(41)-W-O(1)	81.9(3)	C(8)-C(7)-C(6)	120.4(11)
C(41)-W-O(2)	107.2(3)	C(8)-C(7)-H(7)	119.5(12)
O(1)-W-O(2)	107.7(3)	C(6)-C(7)-H(7)	120.1(11)
Os(1)-Os(2)-Os(3)	59.709(15)	C(5)-C(6)-C(7)	119.6(11)
Os(1)-Os(2)-W	56.422(15)	C(5)-C(6)-H(6)	121.1(13)
Os(1)-Os(2)-C(21)	90.0(4)	C(7)-C(6)-H(6)	119.4(13)

Os(1)-Os(2)-C(22)	110.4(4)	C(44)-C(49)-H(49a)	110.8(11)
Os(1)-Os(2)-C(20)	152.8(4)	C(44)-C(49)-H(49b)	111.1(11)
Os(1)-Os(2)-O(2)	88.63(19)	C(44)-C(49)-H(49c)	110.5(12)
Os(3)-Os(2)-W	92.661(18)	H(49a)-C(49)-H(49b)	108.4(12)
Os(3)-Os(2)-C(21)	86.8(3)	H(49a)-C(49)-H(49c)	107.8(12)
Os(3)-Os(2)-C(22)	168.8(4)	H(49b)-C(49)-H(49c)	108.1(11)
Os(3)-Os(2)-C(20)	93.4(4)	C(40)-C(45)-H(45a)	111.8(10)
Os(3)-Os(2)-O(2)	93.31(20)	C(40)-C(45)-H(45b)	110.3(10)
W-Os(2)-C(21)	140.0(4)	C(40)-C(45)-H(45c)	111.1(11)
W-Os(2)-C(22)	84.8(4)	H(45a)-C(45)-H(45b)	107.8(11)
W-Os(2)-C(20)	127.2(3)	H(45a)-C(45)-H(45c)	108.6(10)
W-Os(2)-O(2)	38.37(19)	H(45b)-C(45)-H(45c)	107.1(10)
C(21)-Os(2)-C(22)	88.2(5)	Os(1)-O(1)-W	86.07(25)
C(21)-Os(2)-C(20)	92.8(5)	W-O(2)-Os(2)	96.4(3)

Atomic Coordinates and equivalent isotropic displacement coefficients ($Å^2$ x 10^3) for 7.

	X	y	z	U(eq)
Os1	0.50191(3)	0.34603(3)	0.16457(3)	1.969(17)
Os3	0.44714(3)	0.18945(3)	0.04538(3)	2.251(18)
W	0.47479(3)	0.22694(3)	0.30168(3)	2.098(19)
Os2	0.33005(3)	0.24592(3)	0.17209(3)	2.230(18)
C10	0.4490(7)	0.4620(9)	0.1114(7)	2.4(5)
C21	0.2795(8)	0.3469(10)	0.0982(8)	3.2(5)
C32	0.3709(8)	0.0918(10)	-0.0186(7)	3.3(6)
C30	0.5550(9)	0.1811(8)	-0.0093(8)	3.1(6)
C22	0.2638(8)	0.3094(10)	0.2554(8)	3.4(6)
C11	0.6095(8)	0.3670(8)	0.1100(7)	2.5(5)
C4	0.6631(9)	0.5975(9)	0.2825(7)	3.4(6)
C20	0.2425(8)	0.1410(10)	0.1392(7)	3.5(6)
C31	0.4063(8)	0.3115(9)	-0.0253(7)	2.7(5)
C40	0.5774(9)	0.2290(8)	0.4230(6)	3.0(5)
C1	0.4756(7)	0.3967(7)	0.2906(6)	1.7(4)
C42	0.4845(8)	0.0834(8)	0.4032(6)	2.3(5)
C43	0.4295(8)	0.1680(9)	0.4325(7)	3.1(5)
C3	0.5747(8)	0.5613(8)	0.2709(7)	2.7(5)
C2	0.5584(7)	0.4436(8)	0.2773(6)	2.2(5)
C33	0.4871(8)	0.0780(9)	0.1241(7)	2.7(5)
C44	0.4899(10)	0.2569(9)	0.4460(7)	3.5(6)
C46	0.6513(8)	0.0625(9)	0.3629(7)	3.2(5)
C41	0.5730(8)	0.1226(8)	0.3948(6)	2.6(5)
C47	0.4495(8)	-0.0257(8)	0.3802(7)	3.1(5)
C8	0.5056(8)	0.6333(8)	0.2534(8)	3.1(6)
C5	0.6804(10)	0.7067(10)	0.2751(8)	4.2(7)
C48	0.3327(9)	0.1605(10)	0.4499(8)	4.6(7)
C7	0.5241(9)	0.7403(9)	0.2461(8)	3.8(6)
C6	0.6121(10)	0.7767(9)	0.2543(8)	4.0(6)
C49	0.4637(11)	0.3620(10)	0.4868(8)	5.2(8)
C45	0.6585(9)	0.2970(10)	0.4287(7)	4.2(6)
O1	0.5699(4)	0.2212(5)	0.2405(4)	2.2(3)
O2	0.3891(5)	0.1366(6)	0.2560(4)	2.8(3)
O11	0.6787(6)	0.3789(6)	0.0823(5)	3.6(4)
O10	0.4179(6)	0.5378(6)	0.0802(5)	3.7(4)
O31	0.3859(6)	0.3772(6)	-0.0680(5)	3.6(4)
O30	0.6218(7)	0.1750(7)	-0.0431(6)	4.9(5)
O32	0.3257(6)	0.0363(6)	-0.0551(6)	4.7(4)
O33	0.5097(6)	0.0076(6)	0.1641(5)	3.5(4)
O21	0.2467(6)	0.4101(6)	0.0540(5)	3.9(4)
O20	0.1927(6)	0.0744(7)	0.1232(6)	4.6(5)
O22	0.2185(6)	0.3531(8)	0.3001(6)	5.1(5)

H1	0.409	0.435	0.296	2.6
H2	0.618	0.398	0.303	3.1
H4	0.719	0.541	0.298	4.3
H5	0.750	0.737	0.286	5.3
H6	0.626	0.861	0.244	4.8
H7	0.468	0.797	0.233	4.7
H8	0.435	0.605	0.246	4.0
H45a	0.697	0.287	0.487	5.0
H45b	0.703	0.277	0.379	5.0
H45c	0.641	0.381	0.421	5.0
H46a	0.689	0.020	0.413	4.0
H46b	0.629	0.004	0.317	4.0
H46c	0.699	0.116	0.335	4.0
H47a	0.458	-0.081	0.431	3.8
H47b	0.378	-0.023	0.360	3.8
H47c	0.486	-0.058	0.329	3.8
H48a	0.323	0.132	0.512	5.4
H48b	0.299	0.237	0.442	5.4
H48c	0.297	0.104	0.406	5.4
H49a	0.476	0.358	0.554	6.0
H49b	0.502	0.428	0.464	6.0
H49c	0.392	0.379	0.474	6.0

Appendix A.8

Structure Determination Summary for

$[Os_3W(CO)_9(\mu\text{-}O)_2(\mu\text{-}\eta^1,\eta^2\text{-}CH{=}CHPh\{Os\cdots Os\})(Cp^*)]$ 8

Empirical Formula	$Os_3WO_{11}C_{27}H_{22}$	
Crystal size (mm)	0.1 x 0.08 x 0.2	
Crystal System	Monoclinic	
Space Group	*P*21/n	
Unit Cell Dimensions	a = 13.5235(7) Å	$\alpha = 90$
	b = 11.4462(6) Å	$\beta = 105.65(1)$
	c = 20.2486(10) Å	$\gamma = 90$
Volume $(Å)^3$	3018.1(3)	
Z	4	
Formula Weight	1276.90	
Density (calc.) $(g\ cm^{-3})$	2.810	
Absorption Coefficient (mm^{-1})	16.44	
λ(Mo-Kα)	0.70930 Å	
Temperature (°C)	-100	
2θ Range (deg)	57.3	
Index Ranges	$-18 \le 17, 0 \le 15, 0 \le 27$	
Reflections Collected	34268	
Independent Reflections	7808	
Observed Reflections [I > 2.5 σ(I)]	4607	
Weighting Scheme	$\omega^{-1} = \sigma^2(F_o) + 0.0001\ F_o^2$	
Number of Parameters Refined	379	
Final *R* Indices (obs. data)	$R = 0.055$; $R_W = 0.059$	
Final *R* Indices (all data)	$R = 0.055$; $R_W = 0.059$	
Goodness of Fit	2.01	
Largest and Mean Δ/σ	0.000	
Largest Difference Peak/Hole $(e/Å^3)$	-4.020/3.820	

Bond lengths (Å) for 8

Os(1)-Os(3)	2.8875(12)	C(2)-H(2)	1.094(17)
Os(1)-W	2.9851(12)	C(3)-C(4)	1.38(3)
Os(1)-O(1)	2.128(12)	C(3)-C(8)	1.41(3)
Os(1)-C(1)	2.136(18)	C(4)-C(5)	1.37(3)
Os(1)-C(10)	1.915(24)	C(4)-H(4)	1.108(20)
Os(1)-C(11)	1.928(18)	C(5)-C(6)	1.36(3)
Os(1)-C(12)	1.903(18)	C(5)-H(5)	1.107(22)
Os(2)-Os(3)	2.9458(12)	C(6)-C(7)	1.41(3)
Os(2)-W	2.9991(12)	C(6)-H(6)	1.100(21)
Os(2)-O(2)	2.088(13)	C(7)-C(8)	1.39(3)
Os(2)-C(1)	2.408(16)	C(7)-H(7)	1.108(22)
Os(2)-C(2)	2.401(21)	C(8)-H(8)	1.101(19)
Os(2)-C(20)	1.928(21)	C(40)-C(41)	1.38(3)
Os(2)-C(21)	1.875(25)	C(40)-C(44)	1.41(3)
Os(2)-C(22)	1.990(21)	C(40)-C(45)	1.54(3)
Os(3)-W	2.6024(11)	C(41)-C(42)	1.44(3)
Os(3)-C(30)	1.92(3)	C(41)-C(46)	1.53(3)
Os(3)-C(31)	1.969(24)	C(42)-C(43)	1.40(3)
Os(3)-C(32)	1.919(24)	C(42)-C(47)	1.48(3)
W-O(1)	1.787(12)	C(43)-C(44)	1.39(3)
W-O(2)	1.827(12)	C(43)-C(48)	1.52(3)
W-C(40)	2.347(22)	C(44)-C(49)	1.45(3)
W-C(41)	2.427(19)	C(45)-H(45a)	1.086(24)
W-C(42)	2.436(19)	C(45)-H(45b)	1.11(3)
W-C(43)	2.409(21)	C(45)-H(45c)	1.080(23)
W-C(44)	2.432(22)	C(46)-H(46a)	1.080(20)
O(10)-C(10)	1.13(3)	C(46)-H(46b)	1.093(23)
O(11)-C(11)	1.157(23)	C(46)-H(46c)	1.093(22)
O(12)-C(12)	1.116(23)	C(47)-H(47a)	1.077(20)
O(20)-C(20)	1.13(3)	C(47)-H(47b)	1.094(22)
O(21)-C(21)	1.16(3)	C(47)-H(47c)	1.096(22)
O(22)-C(22)	1.08(3)	C(48)-H(48a)	1.080(25)
O(30)-C(30)	1.13(3)	C(48)-H(48b)	1.093(24)
O(31)-C(31)	1.13(3)	C(48)-H(48c)	1.10(3)
O(32)-C(32)	1.14(3)	C(49)-H(49a)	1.086(22)
C(1)-C(2)	1.39(3)	C(49)-H(49b)	1.086(24)
C(1)-H(1)	1.101(16)	C(49)-H(49c)	1.10(3)
C(2)-C(3)	1.48(3)		

Bond angles (deg) for 8

Os(3)-Os(1)-W	52.58(3)	C(41)-W-C(44)	56.5(7)
Os(3)-Os(1)-O(1)	88.8(3)	C(42)-W-C(43)	33.7(7)
Os(3)-Os(1)-C(1)	80.0(5)	C(42)-W-C(44)	56.8(7)
Os(3)-Os(1)-C(10)	169.6(6)	C(43)-W-C(44)	33.5(8)
Os(3)-Os(1)-C(11)	98.4(6)	Os(1)-O(1)-W	99.0(5)
Os(3)-Os(1)-C(12)	87.3(7)	Os(2)-O(2)-W	99.8(6)
W-Os(1)-O(1)	36.3(3)	Os(1)-C(1)-Os(2)	114.1(8)
W-Os(1)-C(1)	81.3(4)	Os(1)-C(1)-C(2)	131.5(13)
W-Os(1)-C(10)	128.8(6)	Os(1)-C(1)-H(1)	107.4(11)
W-Os(1)-C(11)	99.2(5)	Os(2)-C(1)-C(2)	72.9(11)
W-Os(1)-C(12)	139.9(7)	Os(2)-C(1)-H(1)	105.2(10)
O(1)-Os(1)-C(1)	88.0(5)	C(2)-C(1)-H(1)	117.0(17)
O(1)-Os(1)-C(10)	93.6(7)	Os(2)-C(2)-C(1)	73.5(11)
O(1)-Os(1)-C(11)	93.8(6)	Os(2)-C(2)-C(3)	114.2(13)
O(1)-Os(1)-C(12)	176.0(8)	Os(2)-C(2)-H(2)	103.8(14)
C(1)-Os(1)-C(10)	89.9(7)	C(1)-C(2)-C(3)	126.0(17)
C(1)-Os(1)-C(11)	177.7(7)	C(1)-C(2)-H(2)	114.5(19)
C(1)-Os(1)-C(12)	92.2(8)	C(3)-C(2)-H(2)	114.6(18)
C(10)-Os(1)-C(11)	91.5(8)	C(2)-C(3)-C(4)	124.3(19)
C(10)-Os(1)-C(12)	90.4(10)	C(2)-C(3)-C(8)	117.1(18)
C(11)-Os(1)-C(12)	86.0(9)	C(4)-C(3)-C(8)	118.5(21)
Os(3)-Os(2)-W	51.91(3)	C(3)-C(4)-C(5)	121.5(20)
Os(3)-Os(2)-O(2)	87.2(4)	C(3)-C(4)-H(4)	119.4(20)
Os(3)-Os(2)-C(1)	74.8(4)	C(5)-C(4)-H(4)	119.1(20)
Os(3)-Os(2)-C(2)	105.6(5)	C(4)-C(5)-C(6)	121.0(21)
Os(3)-Os(2)-C(20)	83.1(6)	C(4)-C(5)-H(5)	119.2(23)
Os(3)-Os(2)-C(21)	90.9(6)	C(6)-C(5)-H(5)	119.8(22)
Os(3)-Os(2)-C(22)	172.7(6)	C(5)-C(6)-C(7)	118.9(20)
W-Os(2)-O(2)	36.9(3)	C(5)-C(6)-H(6)	120.6(21)
W-Os(2)-C(1)	77.0(4)	C(7)-C(6)-H(6)	120.5(20)
W-Os(2)-C(2)	85.8(5)	C(6)-C(7)-C(8)	120.5(19)
W-Os(2)-C(20)	95.8(6)	C(6)-C(7)-H(7)	119.8(22)
W-Os(2)-C(21)	140.7(6)	C(8)-C(7)-H(7)	119.6(21)
W-Os(2)-C(22)	122.5(6)	C(3)-C(8)-C(7)	119.5(19)
O(2)-Os(2)-C(1)	96.0(5)	C(3)-C(8)-H(8)	120.5(19)
O(2)-Os(2)-C(2)	84.4(6)	C(7)-C(8)-H(8)	120.0(19)
O(2)-Os(2)-C(20)	90.9(8)	Os(1)-C(10)-O(10)	173.8(17)
O(2)-Os(2)-C(21)	177.2(6)	Os(1)-C(11)-O(11)	174.6(16)
O(2)-Os(2)-C(22)	86.5(7)	Os(1)-C(12)-O(12)	176.6(22)
C(1)-Os(2)-C(2)	33.6(6)	Os(2)-C(20)-O(20)	174.2(19)
C(1)-Os(2)-C(20)	156.4(8)	Os(2)-C(21)-O(21)	177.7(16)
C(1)-Os(2)-C(21)	81.6(7)	Os(2)-C(22)-O(22)	172.0(20)
C(1)-Os(2)-C(22)	109.4(8)	Os(3)-C(30)-O(30)	174.5(21)
C(2)-Os(2)-C(20)	169.8(8)	Os(3)-C(31)-O(31)	178.3(19)
C(2)-Os(2)-C(21)	94.2(7)	Os(3)-C(32)-O(32)	179.8(20)

C(2)-Os(2)-C(22)	77.4(8)	W-C(40)-C(41)	76.4(13)
C(20)-Os(2)-C(21)	90.9(9)	W-C(40)-C(44)	76.2(13)
C(20)-Os(2)-C(22)	93.4(9)	W-C(40)-C(45)	122.9(14)
C(21)-Os(2)-C(22)	95.5(8)	C(41)-C(40)-C(44)	110.7(19)
Os(1)-Os(3)-Os(2)	81.72(3)	C(41)-C(40)-C(45)	122.4(21)
Os(1)-Os(3)-W	65.64(3)	C(44)-C(40)-C(45)	126.1(21)
Os(1)-Os(3)-C(30)	88.0(7)	W-C(41)-C(40)	70.0(12)
Os(1)-Os(3)-C(31)	93.4(6)	W-C(41)-C(42)	73.1(11)
Os(1)-Os(3)-C(32)	169.1(6)	W-C(41)-C(46)	116.4(13)
Os(2)-Os(3)-W	65.10(3)	C(40)-C(41)-C(42)	107.2(20)
Os(2)-Os(3)-C(30)	166.9(6)	C(40)-C(41)-C(46)	126.4(20)
Os(2)-Os(3)-C(31)	92.9(6)	C(42)-C(41)-C(46)	125.9(20)
Os(2)-Os(3)-C(32)	95.4(6)	W-C(42)-C(41)	72.5(11)
W-Os(3)-C(30)	103.3(6)	W-C(42)-C(43)	72.1(11)
W-Os(3)-C(31)	150.7(6)	W-C(42)-C(47)	120.2(15)
W-Os(3)-C(32)	103.6(6)	C(41)-C(42)-C(43)	105.4(19)
C(30)-Os(3)-C(31)	95.7(9)	C(41)-C(42)-C(47)	127.5(20)
C(30)-Os(3)-C(32)	93.3(9)	C(43)-C(42)-C(47)	127.1(20)
C(31)-Os(3)-C(32)	97.2(9)	W-C(43)-C(42)	74.2(12)
Os(1)-W-Os(2)	79.25(3)	W-C(43)-C(44)	74.2(12)
Os(1)-W-Os(3)	61.78(3)	W-C(43)-C(48)	122.1(16)
Os(1)-W-O(1)	44.8(4)	C(42)-C(43)-C(44)	111.5(19)
Os(1)-W-O(2)	110.5(4)	C(42)-C(43)-C(48)	124.1(20)
Os(1)-W-C(40)	107.6(5)	C(44)-C(43)-C(48)	124.2(20)
Os(1)-W-C(41)	119.3(5)	W-C(44)-C(40)	69.6(12)
Os(1)-W-C(42)	152.0(5)	W-C(44)-C(43)	72.3(13)
Os(1)-W-C(43)	158.6(6)	W-C(44)-C(49)	133.6(15)
Os(1)-W-C(44)	125.2(5)	C(40)-C(44)-C(43)	104.9(18)
Os(2)-W-Os(3)	62.99(3)	C(40)-C(44)-C(49)	125.0(21)
Os(2)-W-O(1)	100.8(4)	C(43)-C(44)-C(49)	128.4(21)
Os(2)-W-O(2)	43.3(4)	C(40)-C(45)-H(45a)	111.7(20)
Os(2)-W-C(40)	164.2(6)	C(40)-C(45)-H(45b)	110.3(21)
Os(2)-W-C(41)	153.8(5)	C(40)-C(45)-H(45c)	112.2(19)
Os(2)-W-C(42)	122.5(5)	H(45a)-C(45)-H(45b)	106.5(19)
Os(2)-W-C(43)	113.7(6)	H(45a)-C(45)-H(45c)	109.0(22)
Os(2)-W-C(44)	130.3(5)	H(45b)-C(45)-H(45c)	106.9(21)
Os(3)-W-O(1)	106.5(4)	C(41)-C(46)-H(46a)	111.4(18)
Os(3)-W-O(2)	104.2(4)	C(41)-C(46)-H(46b)	110.2(19)
Os(3)-W-C(40)	107.0(5)	C(41)-C(46)-H(46c)	110.5(17)
Os(3)-W-C(41)	140.7(5)	H(46a)-C(46)-H(46b)	108.5(18)
Os(3)-W-C(42)	141.2(6)	H(46a)-C(46)-H(46c)	108.5(19)
Os(3)-W-C(43)	107.6(5)	H(46b)-C(46)-H(46c)	107.6(18)
Os(3)-W-C(44)	89.6(5)	C(42)-C(47)-H(47a)	111.3(18)
O(1)-W-O(2)	102.4(6)	C(42)-C(47)-H(47b)	110.7(17)
O(1)-W-C(40)	93.7(7)	C(42)-C(47)-H(47c)	110.3(18)
O(1)-W-C(41)	84.0(6)	H(47a)-C(47)-H(47b)	108.6(18)

O(1)-W-C(42)	109.3(7)	H(47a)-C(47)-H(47c)	108.5(18)
O(1)-W-C(43)	139.6(6)	H(47b)-C(47)-H(47c)	107.2(18)
O(1)-W-C(44)	127.5(7)	C(43)-C(48)-H(48a)	111.8(22)
O(2)-W-C(40)	138.9(6)	C(43)-C(48)-H(48b)	111.4(19)
O(2)-W-C(41)	110.5(7)	C(43)-C(48)-H(48c)	110.5(21)
O(2)-W-C(42)	82.2(6)	H(48a)-C(48)-H(48b)	108.5(22)
O(2)-W-C(43)	89.7(7)	H(48a)-C(48)-H(48c)	107.6(20)
O(2)-W-C(44)	122.0(7)	H(48b)-C(48)-H(48c)	106.7(22)
C(40)-W-C(41)	33.6(7)	C(44)-C(49)-H(49a)	111.0(20)
C(40)-W-C(42)	56.7(7)	C(44)-C(49)-H(49b)	111.4(21)
C(40)-W-C(43)	55.7(8)	C(44)-C(49)-H(49c)	110.5(19)
C(40)-W-C(44)	34.3(8)	H(49a)-C(49)-H(49b)	108.6(19)
C(41)-W-C(42)	34.4(7)	H(49a)-C(49)-H(49c)	107.6(21)
C(41)-W-C(43)	55.8(7)	H(49b)-C(49)-H(49c)	107.6(20)

Atomic Coordinates and equivalent isotropic displacement coefficients ($Å^2 \times 10^3$) for 8.

	X	y	z	U(eq)
Os1	0.40769(6)	0.26356(7)	0.03896(4)	2.29(3)
Os2	0.64837(6)	0.26798(7)	0.18986(4)	2.46(3)
Os3	0.44255(7)	0.16908(7)	0.17555(5)	2.77(4)
W	0.44912(7)	0.39605(7)	0.17058(5)	2.29(4)
O1	0.4215(9)	0.4344(10)	0.0819(6)	2.1(6)
O2	0.5857(9)	0.4306(11)	0.2020(7)	2.7(6)
O10	0.4197(12)	0.3460(12)	-0.1013(8)	3.5(7)
O11	0.1710(12)	0.2600(13)	-0.0047(8)	4.4(8)
O12	0.3846(11)	0.0136(12)	-0.0102(8)	3.7(8)
O20	0.6833(12)	0.2190(14)	0.3426(8)	4.4(9)
O21	0.7317(12)	0.0284(12)	0.1685(8)	3.8(8)
O22	0.8545(12)	0.3973(13)	0.2235(8)	3.8(8)
O30	0.2143(13)	0.1096(13)	0.1384(10)	4.6(9)
O31	0.5074(13)	-0.0747(13)	0.1349(9)	4.9(9)
O32	0.4766(16)	0.1174(15)	0.3283(10)	5.9(11)
C1	0.5715(14)	0.2539(14)	0.0681(8)	1.7(7)
C2	0.6462(17)	0.3403(15)	0.0782(11)	2.7(10)
C3	0.7462(19)	0.3312(18)	0.0615(11)	3.2(11)
C4	0.7870(16)	0.2281(17)	0.0449(10)	2.7(9)
C5	0.8806(17)	0.2253(21)	0.0307(12)	4.1(12)
C6	0.9363(16)	0.3250(20)	0.0317(11)	3.1(10)
C7	0.8961(18)	0.4316(19)	0.0472(12)	3.8(11)
C8	0.8024(15)	0.4350(17)	0.0630(11)	2.6(9)
C10	0.4099(14)	0.3183(18)	-0.0500(12)	2.6(9)
C11	0.2597(14)	0.2658(16)	0.0139(9)	2.1(8)
C12	0.3948(17)	0.1068(16)	0.0065(12)	3.4(10)
C20	0.6667(15)	0.2324(21)	0.2855(11)	3.5(11)
C21	0.6992(14)	0.1206(22)	0.1752(9)	3.0(11)
C22	0.7827(15)	0.3500(18)	0.2071(11)	2.8(10)
C30	0.2980(21)	0.1362(19)	0.1542(12)	3.7(12)
C31	0.4824(16)	0.0144(19)	0.1488(11)	3.0(10)
C32	0.4640(16)	0.1365(18)	0.2713(13)	2.9(10)
C40	0.2911(17)	0.4655(18)	0.1818(12)	3.3(11)
C41	0.3456(18)	0.5664(18)	0.1778(11)	3.1(10)
C42	0.4329(17)	0.5688(17)	0.2371(11)	3.1(10)
C43	0.4221(19)	0.4700(17)	0.2757(11)	3.2(11)
C44	0.3339(18)	0.4068(17)	0.2442(11)	3.0(11)
C45	0.1879(18)	0.4370(20)	0.1297(14)	4.5(12)
C46	0.3253(17)	0.6511(17)	0.1175(11)	3.1(10)
C47	0.5160(16)	0.6564(18)	0.2541(11)	3.0(10)
C48	0.4936(21)	0.4405(21)	0.3452(12)	4.6(13)
C49	0.2814(18)	0.3197(21)	0.2741(13)	4.3(13)

H1	0.593	0.167	0.054	3.0
H2	0.617	0.429	0.078	3.0
H4	0.743	0.146	0.043	3.9
H5	0.911	0.141	0.018	3.9
H6	1.011	0.322	0.020	3.9
H7	0.939	0.514	0.046	3.9
H8	0.773	0.519	0.077	3.9
H45a	0.124	0.479	0.143	4.7
H45b	0.187	0.471	0.078	4.7
H45c	0.174	0.344	0.125	4.7
H46a	0.279	0.724	0.125	4.7
H46b	0.398	0.685	0.111	4.7
H46c	0.286	0.607	0.070	4.7
H47a	0.497	0.727	0.284	4.7
H47b	0.588	0.616	0.283	4.7
H47c	0.529	0.692	0.207	4.7
H48a	0.470	0.482	0.386	4.7
H48b	0.498	0.346	0.354	4.7
H48c	0.573	0.470	0.349	4.7
H49a	0.236	0.360	0.305	4.7
H49b	0.231	0.266	0.235	4.7
H49c	0.337	0.261	0.308	4.7

Appendix A.9

Structure Determination Summary for $[Os_3W(\mu\text{-}H)(CO)_9(\mu\text{-}O)_2(Cp^*)]$ 9	
Empirical Formula	$Os_3WO_{11}C_{19}H_{16}$
Crystal size (mm)	0.2 x 0.2 x 0.1
Crystal System	Monoclinic
Space Group	*P*21/n
Unit Cell Dimensions	$a = 11.4845(8)$ Å $\quad \alpha = 90$
	$b = 14.1705(11)$ Å $\quad \beta = 101.79(1)$
	$c = 15.2438(11)$ Å $\quad \gamma = 90$
Volume $(Å)^3$	2428.4(3)
Z	4
Formula Weight	1173.76
Density (calc.) $(g\ cm^{-3})$	3.210
Absorption Coefficient (mm^{-1})	20.42
λ(Mo-Kα)	0.70930 Å
Temperature (°C)	-100
2θ Range (deg)	57.4
Index Ranges	$-15 \le 15, 0 \le 19, 0 \le 20$
Reflections Collected	27861
Independent Reflections	6282
Observed Reflections [$I > 2.5\ \sigma(I)$]	4726
Weighting Scheme	$\omega^{-1} = \sigma^2(F_o) + 0.0001\ F_o^2$
Number of Parameters Refined	307
Final *R* Indices (obs. data)	$R = 0.040$; $R_w = 0.050$
Final *R* Indices (all data)	$R = 0.040$; $R_w = 0.051$
Goodness of Fit	2.22
Largest and Mean Δ/σ	0.000
Largest Difference Peak/Hole $(e/Å^3)$	-2.460/3.870

Bond lengths (Å) for 9

Os(1)-Os(3)	2.8525(8)	O(30)-C(30)	1.180(22)
Os(1)-W	2.9094(11)	O(31)-C(31)	1.132(21)
Os(1)-O(1)	2.139(8)	O(32)-C(32)	1.177(20)
Os(1)-C(10)	1.915(17)	C(40)-C(41)	1.450(17)
Os(1)-C(11)	1.950(15)	C(40)-C(44)	1.435(18)
Os(1)-C(12)	1.819(15)	C(40)-C(45)	1.475(19)
Os(2)-Os(3)	2.8542(23)	C(41)-C(42)	1.376(19)
Os(2)-W	2.9104(9)	C(41)-C(46)	1.520(17)
Os(2)-O(2)	2.137(8)	C(42)-C(43)	1.467(19)
Os(2)-C(20)	1.945(19)	C(42)-C(47)	1.502(19)
Os(2)-C(21)	1.903(18)	C(43)-C(44)	1.410(19)
Os(2)-C(22)	1.879(16)	C(43)-C(48)	1.508(19)
Os(3)-W	2.6318(11)	C(44)-C(49)	1.513(18)
Os(3)-C(30)	1.838(18)	C(45)-H(45a)	1.072(14)
Os(3)-C(31)	1.964(18)	C(45)-H(45b)	1.077(15)
Os(3)-C(32)	1.864(17)	C(45)-H(45c)	1.102(15)
W-O(1)	1.841(8)	C(46)-H(46a)	1.086(12)
W-O(2)	1.785(8)	C(46)-H(46b)	1.078(15)
W-C(40)	2.406(11)	C(46)-H(46c)	1.082(13)
W-C(41)	2.434(11)	C(47)-H(47a)	1.092(13)
W-C(42)	2.404(13)	C(47)-H(47b)	1.071(14)
W-C(43)	2.413(11)	C(47)-H(47c)	1.091(16)
W-C(44)	2.400(11)	C(48)-H(48a)	1.066(13)
O(10)-C(10)	1.144(20)	C(48)-H(48b)	1.080(14)
O(11)-C(11)	1.132(18)	C(48)-H(48c)	1.102(14)
O(12)-C(12)	1.203(19)	C(49)-H(49a)	1.082(12)
O(20)-C(20)	1.151(23)	C(49)-H(49b)	1.080(14)
O(21)-C(21)	1.136(21)	C(49)-H(49c)	1.098(15)
O(22)-C(22)	1.135(18)		

Bond angles (deg) for 9

Os(3)-Os(1)-W	54.347(19)	C(40)-W-C(42)	56.8(4)
Os(3)-Os(1)-O(1)	90.70(22)	C(40)-W-C(43)	57.2(5)
Os(3)-Os(1)-C(10)	85.6(4)	C(40)-W-C(44)	34.7(4)
Os(3)-Os(1)-C(11)	173.5(4)	C(41)-W-C(42)	33.0(5)
Os(3)-Os(1)-C(12)	89.4(5)	C(41)-W-C(43)	57.1(4)
W-Os(1)-O(1)	39.17(21)	C(41)-W-C(44)	57.5(4)
W-Os(1)-C(10)	97.0(4)	C(42)-W-C(43)	35.5(4)
W-Os(1)-C(11)	121.5(4)	C(42)-W-C(44)	57.5(5)
W-Os(1)-C(12)	141.6(5)	C(43)-W-C(44)	34.1(5)
O(1)-Os(1)-C(10)	86.2(5)	Os(1)-O(1)-W	93.6(3)
O(1)-Os(1)-C(11)	86.8(4)	Os(2)-O(2)-W	95.4(4)
O(1)-Os(1)-C(12)	177.7(5)	Os(1)-C(10)-O(10)	172.6(13)
C(10)-Os(1)-C(11)	100.1(6)	Os(1)-C(11)-O(11)	174.8(11)
C(10)-Os(1)-C(12)	91.6(6)	Os(1)-C(12)-O(12)	177.7(14)
C(11)-Os(1)-C(12)	93.3(6)	Os(2)-C(20)-O(20)	176.4(13)
Os(3)-Os(2)-W	54.32(4)	Os(2)-C(21)-O(21)	175.4(15)
Os(3)-Os(2)-O(2)	89.13(21)	Os(2)-C(22)-O(22)	179.2(14)
Os(3)-Os(2)-C(20)	84.6(6)	Os(3)-C(30)-O(30)	178.0(13)
Os(3)-Os(2)-C(21)	175.9(5)	Os(3)-C(31)-O(31)	172.1(18)
Os(3)-Os(2)-C(22)	87.2(5)	Os(3)-C(32)-O(32)	176.2(15)
W-Os(2)-O(2)	37.64(21)	W-C(40)-C(41)	73.6(6)
W-Os(2)-C(20)	95.9(4)	W-C(40)-C(44)	72.4(6)
W-Os(2)-C(21)	126.8(4)	W-C(40)-C(45)	122.3(9)
W-Os(2)-C(22)	139.3(5)	C(41)-C(40)-C(44)	107.5(11)
O(2)-Os(2)-C(20)	85.9(5)	C(41)-C(40)-C(45)	129.3(12)
O(2)-Os(2)-C(21)	93.1(5)	C(44)-C(40)-C(45)	123.1(11)
O(2)-Os(2)-C(22)	176.1(5)	W-C(41)-C(40)	71.5(6)
C(20)-Os(2)-C(21)	99.1(8)	W-C(41)-C(42)	72.3(7)
C(20)-Os(2)-C(22)	92.5(6)	W-C(41)-C(46)	133.2(9)
C(21)-Os(2)-C(22)	90.6(6)	C(40)-C(41)-C(42)	108.1(11)
Os(1)-Os(3)-Os(2)	62.94(4)	C(40)-C(41)-C(46)	125.1(11)
Os(1)-Os(3)-W	63.930(21)	C(42)-C(41)-C(46)	125.2(12)
Os(1)-Os(3)-C(30)	98.2(5)	W-C(42)-C(41)	74.6(7)
Os(1)-Os(3)-C(31)	96.5(5)	W-C(42)-C(43)	72.6(7)
Os(1)-Os(3)-C(32)	161.0(6)	W-C(42)-C(47)	120.8(8)
Os(2)-Os(3)-W	63.93(4)	C(41)-C(42)-C(43)	109.2(12)
Os(2)-Os(3)-C(30)	159.1(4)	C(41)-C(42)-C(47)	127.5(13)
Os(2)-Os(3)-C(31)	95.4(5)	C(43)-C(42)-C(47)	123.3(12)
Os(2)-Os(3)-C(32)	99.2(6)	W-C(43)-C(42)	72.0(7)
W-Os(3)-C(30)	100.6(4)	W-C(43)-C(44)	72.5(7)
W-Os(3)-C(31)	156.0(5)	W-C(43)-C(48)	119.7(8)
W-Os(3)-C(32)	103.4(5)	C(42)-C(43)-C(44)	106.8(12)
C(30)-Os(3)-C(31)	95.8(7)	C(42)-C(43)-C(48)	126.1(12)
C(30)-Os(3)-C(32)	98.1(7)	C(44)-C(43)-C(48)	127.1(11)
C(31)-Os(3)-C(32)	91.5(7)	W-C(44)-C(40)	72.9(6)

Os(1)-W-Os(2)	61.58(8)	W-C(44)-C(43)	73.5(6)
Os(1)-W-Os(3)	61.72(3)	W-C(44)-C(49)	120.2(8)
Os(1)-W-O(1)	47.21(25)	C(40)-C(44)-C(43)	108.5(11)
Os(1)-W-O(2)	97.2(3)	C(40)-C(44)-C(49)	123.1(12)
Os(1)-W-C(40)	118.3(3)	C(43)-C(44)-C(49)	128.5(12)
Os(1)-W-C(41)	135.8(3)	C(40)-C(45)-H(45a)	110.2(13)
Os(1)-W-C(42)	167.2(3)	C(40)-C(45)-H(45b)	110.4(11)
Os(1)-W-C(43)	154.9(3)	C(40)-C(45)-H(45c)	109.3(11)
Os(1)-W-C(44)	126.7(3)	H(45a)-C(45)-H(45b)	110.3(12)
Os(2)-W-Os(3)	61.75(7)	H(45a)-C(45)-H(45c)	108.4(12)
Os(2)-W-O(1)	97.16(25)	H(45b)-C(45)-H(45c)	108.1(13)
Os(2)-W-O(2)	46.99(25)	C(41)-C(46)-H(46a)	109.2(11)
Os(2)-W-C(40)	168.1(3)	C(41)-C(46)-H(46b)	110.2(11)
Os(2)-W-C(41)	135.9(3)	C(41)-C(46)-H(46c)	109.8(11)
Os(2)-W-C(42)	120.4(3)	H(46a)-C(46)-H(46b)	109.2(12)
Os(2)-W-C(43)	128.5(3)	H(46a)-C(46)-H(46c)	108.9(11)
Os(2)-W-C(44)	156.1(3)	H(46b)-C(46)-H(46c)	109.5(12)
Os(3)-W-O(1)	105.2(3)	C(42)-C(47)-H(47a)	109.1(11)
Os(3)-W-O(2)	104.90(25)	C(42)-C(47)-H(47b)	111.5(12)
Os(3)-W-C(40)	107.1(3)	C(42)-C(47)-H(47c)	109.7(11)
Os(3)-W-C(41)	90.1(3)	H(47a)-C(47)-H(47b)	109.3(12)
Os(3)-W-C(42)	107.1(3)	H(47a)-C(47)-H(47c)	107.8(12)
Os(3)-W-C(43)	142.5(3)	H(47b)-C(47)-H(47c)	109.3(12)
Os(3)-W-C(44)	141.8(3)	C(43)-C(48)-H(48a)	110.6(11)
O(1)-W-O(2)	103.9(4)	C(43)-C(48)-H(48b)	109.9(11)
O(1)-W-C(40)	89.7(4)	C(43)-C(48)-H(48c)	109.0(11)
O(1)-W-C(41)	124.0(4)	H(48a)-C(48)-H(48b)	110.5(12)
O(1)-W-C(42)	138.8(4)	H(48a)-C(48)-H(48c)	108.9(11)
O(1)-W-C(43)	108.2(4)	H(48b)-C(48)-H(48c)	107.8(12)
O(1)-W-C(44)	81.4(4)	C(44)-C(49)-H(49a)	110.6(11)
O(2)-W-C(40)	140.3(4)	C(44)-C(49)-H(49b)	110.9(11)
O(2)-W-C(41)	124.0(4)	C(44)-C(49)-H(49c)	109.9(11)
O(2)-W-C(42)	91.8(4)	H(49a)-C(49)-H(49b)	109.3(12)
O(2)-W-C(43)	83.1(4)	H(49a)-C(49)-H(49c)	108.0(12)
O(2)-W-C(44)	109.9(4)	H(49b)-C(49)-H(49c)	108.1(11)
C(40)-W-C(41)	34.9(4)		

Atomic Coordinates and equivalent isotropic displacement coefficients ($Å^2 \times 10^3$) for 9.

	X	y	z	U(eq)
Os1	0.48906(4)	0.94420(4)	0.31375(3)	2.408(19)
Os2	0.29500(4)	0.84979(4)	0.18382(4)	2.617(21)
Os3	0.48405(5)	0.74440(4)	0.29052(4)	2.701(21)
W	0.53960(4)	0.84395(3)	0.15919(3)	1.783(18)
O1	0.5854(7)	0.9602(6)	0.2085(6)	2.5(3)
O2	0.4010(6)	0.8668(6)	0.0848(5)	2.1(3)
O10	0.7357(10)	0.9204(7)	0.4327(7)	4.1(5)
O11	0.4846(10)	1.1614(7)	0.3172(9)	4.9(6)
O12	0.3634(11)	0.9181(9)	0.4679(8)	5.5(6)
O20	0.2146(12)	0.6583(10)	0.0939(11)	7.4(8)
O21	0.0896(10)	0.9675(10)	0.0832(8)	6.2(7)
O22	0.1564(10)	0.8135(8)	0.3283(7)	4.8(6)
O30	0.7277(11)	0.7018(8)	0.4011(9)	5.5(6)
O31	0.3618(14)	0.6992(9)	0.4483(10)	7.6(9)
O32	0.4282(13)	0.5485(8)	0.2120(9)	6.2(7)
C10	0.6408(14)	0.9244(10)	0.3913(10)	3.4(7)
C11	0.4807(11)	1.0816(11)	0.3163(10)	3.1(6)
C12	0.4127(14)	0.9304(11)	0.4064(10)	3.7(7)
C20	0.2480(14)	0.7292(15)	0.1265(12)	5.2(9)
C21	0.1696(13)	0.9261(14)	0.1198(11)	4.5(9)
C22	0.2084(12)	0.8279(11)	0.2739(11)	3.9(7)
C30	0.6331(16)	0.7177(11)	0.3565(10)	3.8(7)
C31	0.3985(17)	0.7158(11)	0.3865(13)	5.1(9)
C32	0.4489(15)	0.6256(12)	0.2395(11)	4.3(8)
C40	0.7436(10)	0.8090(9)	0.1559(9)	2.3(5)
C41	0.6782(10)	0.7215(8)	0.1349(9)	2.4(5)
C42	0.5973(11)	0.7340(10)	0.0557(9)	2.8(6)
C43	0.6108(11)	0.8293(8)	0.0215(9)	2.5(5)
C44	0.7007(10)	0.8742(9)	0.0846(9)	2.4(5)
C45	0.8421(11)	0.8310(10)	0.2315(10)	3.5(6)
C46	0.7137(12)	0.6270(9)	0.1794(10)	2.9(6)
C47	0.5102(13)	0.6631(9)	0.0071(10)	3.3(6)
C48	0.5397(12)	0.8712(10)	-0.0638(9)	2.9(6)
C49	0.7494(12)	0.9731(9)	0.0819(10)	3.0(6)
H45a	0.925	0.809	0.217	3.9
H45b	0.844	0.905	0.246	3.9
H45c	0.828	0.793	0.292	3.9
H46a	0.780	0.594	0.148	3.9
H46b	0.751	0.637	0.250	3.9
H46c	0.637	0.581	0.172	3.9
H47a	0.554	0.621	-0.037	3.9
H47b	0.478	0.618	0.053	3.9

H47c	0.436	0.700	-0.035	3.9
H48a	0.583	0.860	-0.118	3.9
H48b	0.452	0.841	-0.078	3.9
H48c	0.530	0.948	-0.054	3.9
H49a	0.822	0.974	0.046	3.9
H49b	0.681	1.021	0.050	3.9
H49c	0.784	0.998	0.150	3.9

Appendix A.10

Structure Determination Summary for

$[Os_3W(CO)_{10}(O)(\mu\text{-}\eta^1,\eta^2\text{-}CH{=}CHPh\{Os\text{-}Os\})(\mu\text{-}O)(Cp^*)]$ 10

Empirical Formula	$Os_3WO_{12}C_{28}H_{22}$	
Crystal size (mm)	0.13 x 0.15 x 0.10	
Crystal System	Monoclinic	
Space Group	*P*21/n	
Unit Cell Dimensions	a = 10.5039(6) Å	$\alpha = 90$
	b = 11.3609(6) Å	$\beta = 81.63(1)$
	c = 27.0631(14) Å	$\gamma = 90$
Volume $(Å)^3$	3195.1(3)	
Z	4	
Formula Weight	1304.91	
Density (calc.) $(g\ cm^{-3})$	2.713	
Absorption Coefficient (mm^{-1})	15.54	
λ(Mo-Kα)	0.70930 Å	
Temperature (°C)	-100	
2θ Range (deg)	57.3	
Index Ranges	$-13 \le 14, 0 \le 15, 0 \le 36$	
Reflections Collected	36645	
Independent Reflections	8245	
Observed Reflections [$I > 2.5\ \sigma(I)$]	6350	
Weighting Scheme	$\omega^{-1} = \sigma^2(F_o) + 0.0001\ F_o^2$	
Number of Parameters Refined	397	
Final *R* Indices (obs. Data)	$R = 0.028$; $R_W = 0.026$	
Final *R* Indices (all data)	$R = 0.028$; $R_W = 0.026$	
Goodness of Fit	1.80	
Largest and Mean Δ/σ	0.000	
Largest Difference Peak/Hole $(e/Å^3)$	-1.370/1.650	

Bond lengths (Å) for 10

Os(1)-Os(2)	2.9465(4)	C(2)-H(2)	0.995(7)
Os(1)-Os(3)	2.8155(4)	C(3)-C(4)	1.392(10)
Os(1)-W	2.8945(4)	C(3)-C(8)	1.369(11)
Os(1)-O(2)	2.113(4)	C(4)-C(5)	1.405(12)
Os(1)-C(1)	2.261(6)	C(4)-H(4)	0.988(8)
Os(1)-C(2)	2.402(6)	C(5)-C(6)	1.358(16)
Os(1)-C(10)	1.853(7)	C(5)-H(5)	1.005(9)
Os(1)-C(11)	1.855(8)	C(6)-C(7)	1.364(15)
Os(2)-W	2.7075(4)	C(6)-H(6)	1.004(8)
Os(2)-C(20)	1.891(8)	C(7)-C(8)	1.395(11)
Os(2)-C(21)	1.963(8)	C(7)-H(7)	0.989(9)
Os(2)-C(22)	1.955(8)	C(8)-H(8)	0.995(8)
Os(2)-C(23)	1.946(7)	C(40)-C(41)	1.410(12)
Os(3)-C(1)	2.087(6)	C(40)-C(44)	1.405(11)
Os(3)-C(30)	1.956(9)	C(40)-C(45)	1.502(11)
Os(3)-C(31)	1.950(8)	C(41)-C(42)	1.442(11)
Os(3)-C(32)	1.908(8)	C(41)-C(46)	1.540(11)
Os(3)-C(33)	1.964(8)	C(42)-C(43)	1.399(12)
W-O(1)	1.718(4)	C(42)-C(47)	1.510(12)
W-O(2)	1.826(4)	C(43)-C(44)	1.394(13)
W-C(40)	2.391(7)	C(43)-C(48)	1.518(12)
W-C(41)	2.397(7)	C(44)-C(49)	1.490(12)
W-C(42)	2.490(7)	C(45)-H(45a)	1.075(8)
W-C(43)	2.472(7)	C(45)-H(45b)	1.047(10)
W-C(44)	2.402(7)	C(45)-H(45c)	1.124(10)
O(10)-C(10)	1.170(9)	C(46)-H(46a)	1.067(8)
O(11)-C(11)	1.152(10)	C(46)-H(46b)	1.120(11)
O(20)-C(20)	1.163(10)	C(46)-H(46c)	1.021(10)
O(21)-C(21)	1.139(9)	C(47)-H(47a)	1.055(8)
O(22)-C(22)	1.134(9)	C(47)-H(47b)	1.064(11)
O(23)-C(23)	1.128(9)	C(47)-H(47c)	1.104(10)
O(30)-C(30)	1.148(10)	C(48)-H(48a)	1.050(8)
O(31)-C(31)	1.141(10)	C(48)-H(48b)	1.121(11)
O(32)-C(32)	1.143(9)	C(48)-H(48c)	1.056(11)
O(33)-C(33)	1.131(10)	C(49)-H(49a)	1.100(8)
C(1)-C(2)	1.381(9)	C(49)-H(49b)	1.041(11)
C(1)-H(1)	0.983(6)	C(49)-H(49c)	1.116(12)
C(2)-C(3)	1.480(9)		

Bond angles (deg) for 10

Os(2)-Os(1)-Os(3)	176.460(13)	Os(3)-C(1)-C(2)	130.7(5)
Os(2)-Os(1)-W	55.221(9)	Os(3)-C(1)-H(1)	122.2(5)
Os(2)-Os(1)-O(2)	93.70(12)	C(2)-C(1)-H(1)	106.3(6)
Os(2)-Os(1)-C(1)	132.46(16)	Os(1)-C(2)-C(1)	67.3(4)
Os(2)-Os(1)-C(2)	103.87(16)	Os(1)-C(2)-C(3)	126.7(5)
Os(2)-Os(1)-C(10)	94.77(21)	Os(1)-C(2)-H(2)	95.8(4)
Os(2)-Os(1)-C(11)	82.26(21)	C(1)-C(2)-C(3)	122.5(6)
Os(3)-Os(1)-W	121.395(12)	C(1)-C(2)-H(2)	124.6(6)
Os(3)-Os(1)-O(2)	83.06(12)	C(3)-C(2)-H(2)	110.0(6)
Os(3)-Os(1)-C(1)	47.00(16)	C(2)-C(3)-C(4)	119.5(7)
Os(3)-Os(1)-C(2)	74.25(16)	C(2)-C(3)-C(8)	122.5(6)
Os(3)-Os(1)-C(10)	86.80(21)	C(4)-C(3)-C(8)	118.0(7)
Os(3)-Os(1)-C(11)	100.94(21)	C(3)-C(4)-C(5)	120.1(8)
W-Os(1)-O(2)	38.97(12)	C(3)-C(4)-H(4)	115.6(7)
W-Os(1)-C(1)	117.29(17)	C(5)-C(4)-H(4)	123.7(8)
W-Os(1)-C(2)	86.02(16)	C(4)-C(5)-C(6)	120.7(8)
W-Os(1)-C(10)	99.96(21)	C(4)-C(5)-H(5)	116.9(10)
W-Os(1)-C(11)	136.80(21)	C(6)-C(5)-H(5)	120.2(9)
O(2)-Os(1)-C(1)	97.38(21)	C(5)-C(6)-C(7)	119.6(8)
O(2)-Os(1)-C(2)	80.94(20)	C(5)-C(6)-H(6)	117.9(10)
O(2)-Os(1)-C(10)	91.94(25)	C(7)-C(6)-H(6)	122.5(11)
O(2)-Os(1)-C(11)	175.70(24)	C(6)-C(7)-C(8)	120.3(9)
C(1)-Os(1)-C(2)	34.29(23)	C(6)-C(7)-H(7)	120.1(9)
C(1)-Os(1)-C(10)	130.6(3)	C(8)-C(7)-H(7)	119.5(9)
C(1)-Os(1)-C(11)	84.4(3)	C(3)-C(8)-C(7)	121.3(8)
C(2)-Os(1)-C(10)	160.4(3)	C(3)-C(8)-H(8)	118.5(7)
C(2)-Os(1)-C(11)	98.5(3)	C(7)-C(8)-H(8)	116.6(8)
C(10)-Os(1)-C(11)	89.9(3)	Os(1)-C(10)-O(10)	174.4(6)
Os(1)-Os(2)-W	61.415(10)	Os(1)-C(11)-O(11)	179.2(6)
Os(1)-Os(2)-C(20)	165.74(22)	Os(2)-C(20)-O(20)	175.9(7)
Os(1)-Os(2)-C(21)	92.67(20)	Os(2)-C(21)-O(21)	172.3(6)
Os(1)-Os(2)-C(22)	98.08(19)	Os(2)-C(22)-O(22)	175.5(6)
Os(1)-Os(2)-C(23)	83.10(21)	Os(2)-C(23)-O(23)	178.0(6)
W-Os(2)-C(20)	104.64(22)	Os(3)-C(30)-O(30)	175.6(6)
W-Os(2)-C(21)	84.61(21)	Os(3)-C(31)-O(31)	177.0(8)
W-Os(2)-C(22)	159.03(19)	Os(3)-C(32)-O(32)	177.9(6)
W-Os(2)-C(23)	91.32(21)	Os(3)-C(33)-O(33)	179.4(6)
C(20)-Os(2)-C(21)	88.7(3)	W-C(40)-C(41)	73.1(4)
C(20)-Os(2)-C(22)	96.0(3)	W-C(40)-C(44)	73.4(4)
C(20)-Os(2)-C(23)	94.9(3)	W-C(40)-C(45)	117.9(5)
C(21)-Os(2)-C(22)	92.5(3)	C(41)-C(40)-C(44)	107.9(7)
C(21)-Os(2)-C(23)	175.2(3)	C(41)-C(40)-C(45)	124.7(7)
C(22)-Os(2)-C(23)	90.3(3)	C(44)-C(40)-C(45)	127.4(8)
Os(1)-Os(3)-C(1)	52.41(17)	W-C(41)-C(40)	72.7(4)
Os(1)-Os(3)-C(30)	89.52(21)	W-C(41)-C(42)	76.4(4)

Os(1)-Os(3)-C(31)	104.18(24)	W-C(41)-C(46)	119.7(5)
Os(1)-Os(3)-C(32)	155.08(20)	C(40)-C(41)-C(42)	107.6(6)
Os(1)-Os(3)-C(33)	85.37(20)	C(40)-C(41)-C(46)	127.7(7)
C(1)-Os(3)-C(30)	89.2(3)	C(42)-C(41)-C(46)	124.6(8)
C(1)-Os(3)-C(31)	156.6(3)	W-C(42)-C(41)	69.3(4)
C(1)-Os(3)-C(32)	102.8(3)	W-C(42)-C(43)	72.9(4)
C(1)-Os(3)-C(33)	87.2(3)	W-C(42)-C(47)	133.6(5)
C(30)-Os(3)-C(31)	90.6(3)	C(41)-C(42)-C(43)	106.6(7)
C(30)-Os(3)-C(32)	92.7(3)	C(41)-C(42)-C(47)	124.1(8)
C(30)-Os(3)-C(33)	174.8(3)	C(43)-C(42)-C(47)	127.8(8)
C(31)-Os(3)-C(32)	100.6(3)	W-C(43)-C(42)	74.4(4)
C(31)-Os(3)-C(33)	91.3(3)	W-C(43)-C(44)	70.7(4)
C(32)-Os(3)-C(33)	91.7(3)	W-C(43)-C(48)	121.6(5)
Os(1)-W-Os(2)	63.364(10)	C(42)-C(43)-C(44)	109.5(7)
Os(1)-W-O(1)	104.58(15)	C(42)-C(43)-C(48)	127.6(9)
Os(1)-W-O(2)	46.72(14)	C(44)-C(43)-C(48)	122.9(8)
Os(1)-W-C(40)	154.08(20)	W-C(44)-C(40)	72.5(4)
Os(1)-W-C(41)	159.93(19)	W-C(44)-C(43)	76.1(4)
Os(1)-W-C(42)	126.19(19)	W-C(44)-C(49)	118.0(5)
Os(1)-W-C(43)	110.70(17)	C(40)-C(44)-C(43)	108.3(7)
Os(1)-W-C(44)	121.83(19)	C(40)-C(44)-C(49)	125.4(9)
Os(2)-W-O(1)	98.62(15)	C(43)-C(44)-C(49)	126.2(8)
Os(2)-W-O(2)	109.42(14)	C(40)-C(45)-H(45a)	110.0(7)
Os(2)-W-C(40)	139.44(20)	C(40)-C(45)-H(45b)	111.5(8)
Os(2)-W-C(41)	105.23(19)	C(40)-C(45)-H(45c)	107.4(7)
Os(2)-W-C(42)	90.95(19)	H(45a)-C(45)-H(45b)	112.5(8)
Os(2)-W-C(43)	110.28(22)	H(45a)-C(45)-H(45c)	106.6(8)
Os(2)-W-C(44)	143.29(20)	H(45b)-C(45)-H(45c)	108.6(7)
O(1)-W-O(2)	105.69(20)	C(41)-C(46)-H(46a)	107.5(7)
O(1)-W-C(40)	86.00(23)	C(41)-C(46)-H(46b)	104.7(8)
O(1)-W-C(41)	93.16(23)	C(41)-C(46)-H(46c)	110.4(8)
O(1)-W-C(42)	126.56(24)	H(46a)-C(46)-H(46b)	107.5(8)
O(1)-W-C(43)	141.59(24)	H(46a)-C(46)-H(46c)	115.3(10)
O(1)-W-C(44)	112.9(3)	H(46b)-C(46)-H(46c)	110.8(8)
O(2)-W-C(40)	107.91(24)	C(42)-C(47)-H(47a)	109.6(8)
O(2)-W-C(41)	137.06(22)	C(42)-C(47)-H(47b)	109.2(8)
O(2)-W-C(42)	120.23(24)	C(42)-C(47)-H(47c)	106.8(8)
O(2)-W-C(43)	88.37(23)	H(47a)-C(47)-H(47b)	112.7(9)
O(2)-W-C(44)	80.45(23)	H(47a)-C(47)-H(47c)	109.5(8)
C(40)-W-C(41)	34.2(3)	H(47b)-C(47)-H(47c)	108.9(8)
C(40)-W-C(42)	56.2(3)	C(43)-C(48)-H(48a)	110.1(7)
C(40)-W-C(43)	55.6(3)	C(43)-C(48)-H(48b)	106.4(8)
C(40)-W-C(44)	34.1(3)	C(43)-C(48)-H(48c)	109.5(9)
C(41)-W-C(42)	34.3(3)	H(48a)-C(48)-H(48b)	108.6(10)
C(41)-W-C(43)	55.76(24)	H(48a)-C(48)-H(48c)	113.7(9)
C(41)-W-C(44)	56.6(3)	H(48b)-C(48)-H(48c)	108.2(7)

C(42)-W-C(43)	32.7(3)	C(44)-C(49)-H(49a)	109.2(7)
C(42)-W-C(44)	55.5(3)	C(44)-C(49)-H(49b)	112.9(9)
C(43)-W-C(44)	33.2(3)	C(44)-C(49)-H(49c)	108.4(8)
Os(1)-O(2)-W	94.31(19)	H(49a)-C(49)-H(49b)	110.9(9)
Os(1)-C(1)-Os(3)	80.60(21)	H(49a)-C(49)-H(49c)	105.5(9)
Os(1)-C(1)-C(2)	78.4(4)	H(49b)-C(49)-H(49c)	109.7(8)
Os(1)-C(1)-H(1)	105.6(5)		

Atomic Coordinates and equivalent isotropic displacement coefficients ($Å^2 \times 10^3$) for 10.

	X	y	z	U(eq)
Os1	0.055244(24)	0.906520(23)	0.166517(10)	2.039(10)
Os2	0.27166(3)	0.739624(25)	0.160593(10)	2.317(10)
Os3	-0.15122(3)	1.064240(24)	0.165776(11)	2.422(11)
W	0.13133(3)	0.746524(24)	0.084278(10)	2.118(11)
O1	0.2360(4)	0.8266(4)	0.04253(17)	2.55(20)
O2	-0.0088(4)	0.8409(4)	0.10134(16)	2.32(18)
O10	-0.1360(5)	0.7596(5)	0.23430(20)	4.2(3)
O11	0.1644(5)	0.9918(5)	0.25681(21)	4.1(3)
O20	0.4682(6)	0.5452(5)	0.13057(22)	4.6(3)
O21	0.4666(5)	0.8989(5)	0.09474(21)	4.1(3)
O22	0.3748(5)	0.8082(5)	0.25781(19)	3.39(24)
O23	0.0725(5)	0.5814(5)	0.22328(20)	3.89(25)
O30	-0.1629(6)	1.0092(5)	0.05423(22)	4.4(3)
O31	-0.3915(6)	0.9089(6)	0.1961(3)	6.0(3)
O32	-0.2707(5)	1.3064(5)	0.15608(21)	4.0(3)
O33	-0.1204(5)	1.1127(5)	0.27594(20)	4.0(3)
C1	0.0450(6)	1.1002(6)	0.14815(25)	2.2(3)
C2	0.1348(6)	1.0604(6)	0.10938(25)	2.3(3)
C3	0.2680(6)	1.1063(6)	0.1001(3)	2.7(3)
C4	0.3336(7)	1.1086(7)	0.0516(3)	3.4(3)
C5	0.4562(8)	1.1603(9)	0.0418(4)	4.8(4)
C6	0.5128(8)	1.2069(9)	0.0793(4)	6.0(5)
C7	0.4506(8)	1.2021(9)	0.1272(4)	5.2(5)
C8	0.3287(7)	1.1514(7)	0.1374(3)	3.8(4)
C10	-0.0587(7)	0.8113(6)	0.2072(3)	2.7(3)
C11	0.1234(7)	0.9590(6)	0.2221(3)	2.9(3)
C20	0.3915(7)	0.6168(7)	0.1436(3)	3.3(3)
C21	0.3885(7)	0.8463(6)	0.1188(3)	2.9(3)
C22	0.3378(7)	0.7877(6)	0.2214(3)	2.7(3)
C23	0.1440(7)	0.6399(6)	0.1997(3)	2.8(3)
C30	-0.1559(7)	1.0254(7)	0.0956(3)	3.2(3)
C31	-0.3039(8)	0.9683(7)	0.1860(3)	3.9(4)
C32	-0.2281(6)	1.2147(7)	0.1596(3)	3.0(3)
C33	-0.1323(7)	1.0948(7)	0.2358(3)	3.1(3)
C40	0.0946(8)	0.6306(7)	0.0140(3)	3.2(3)
C41	0.1790(7)	0.5659(6)	0.0396(3)	3.1(3)
C42	0.1074(8)	0.5284(6)	0.0865(3)	3.4(4)
C43	-0.0161(8)	0.5760(6)	0.0888(3)	3.6(3)
C44	-0.0241(7)	0.6394(6)	0.0452(3)	3.5(4)
C45	0.1303(10)	0.6828(8)	-0.0371(3)	5.2(5)
C46	0.3200(9)	0.5325(8)	0.0211(4)	5.6(5)
C47	0.1513(10)	0.4332(7)	0.1191(4)	5.8(6)

C48	-0.1284(9)	0.5634(9)	0.1306(4)	6.4(5)
C49	-0.1390(9)	0.7042(8)	0.0331(5)	6.6(6)
H1	0.094	1.141	0.171	3.2
H2	0.114	1.020	0.079	3.2
H4	0.283	1.083	0.025	5.1
H5	0.509	1.141	0.009	5.1
H6	0.600	1.244	0.070	5.1
H7	0.494	1.230	0.155	5.1
H8	0.275	1.175	0.169	5.1
H45a	0.113	0.620	-0.065	7.9
H45b	0.083	0.763	-0.041	7.9
H45c	0.237	0.700	-0.043	7.9
H46a	0.319	0.452	0.001	7.9
H46b	0.356	0.603	-0.006	7.9
H46c	0.372	0.531	0.050	7.9
H47a	0.120	0.350	0.108	7.9
H47b	0.253	0.438	0.117	7.9
H47c	0.106	0.452	0.158	7.9
H48a	-0.177	0.484	0.127	7.9
H48b	-0.086	0.560	0.166	7.9
H48c	-0.188	0.639	0.132	7.9
H49a	-0.199	0.644	0.014	7.9
H49b	-0.193	0.742	0.064	7.9
H49c	-0.106	0.774	0.005	7.9

Appendix A.11

Structure Determination Summary for

$[Os_3W(\eta^1\text{-}CH{=}CHPh)(CO)_{11}(O)(\mu\text{-}O)(Cp^*)]$ 11

Empirical Formula	$Os_3WO_{13}C_{29}H_{22}$	
Crystal size (mm)	0.2 x 0.2 x 0.3	
Crystal System	Triclinic	
Space Group	*P*-1	
Unit Cell Dimensions	a = 21.242(2) Å	α = 75.442(2)
	b = 21.309(2) Å	β = 77.720(2)
	c = 27.904(3) Å	γ = 70.785(2)
Volume (Å)^3	11427(2)	
Z	12	
Formula Weight	1333.0	
Density (calc.) (g cm^{-3})	2.457	
Absorption Coefficient (mm^{-1})	13.049	
λ(Mo-Kα)	0.71073 Å	
Temperature (°C)	-100	
2θ Range (deg)	57.3	
Index Ranges	$-25 \le 25, -25 \le 25, -33 \le 33$	
Reflections Collected	101818	
Independent Reflections	40160	
Weighting Scheme	$\omega^{-1} = \sigma^2(F_o) + 0.0001\ F_o^2$	
Number of Parameters Refined	2618	
Final *R* Indices (obs. Data)	R = 0.0587; R_W = 0.1196	
Final *R* Indices (all data)	R = 0.2164; R_W = 0.1652	
Goodness of Fit	0.770	
Largest and Mean Δ/σ	0.000	
Largest Difference Peak/Hole (e/Å^3)	3.773/-2.945	

Bond lengths (Å) for 11

Os(1E)-C(14E)	1.92(4)	O(12E)-C(12E)	1.15(4)
Os(1E)-C(13E)	1.95(4)	O(13E)-C(13E)	1.10(6)
Os(1E)-C(15E)	1.96(5)	O(14E)-C(14E)	1.10(5)
Os(1E)-O(2E)	2.10(2)	O(15E)-C(15E)	1.16(5)
Os(1E)-Os(3E)	2.893(2)	O(16E)-C(16E)	1.29(5)
Os(1E)-W(1E)	2.937(2)	O(17E)-C(17E)	1.13(5)
Os(1E)-Os(2E)	2.938(2)	O(18E)-C(18E)	1.16(3)
Os(2E)-C(18E)	1.88(2)	O(19E)-C(19E)	1.28(5)
Os(2E)-C(19E)	1.88(4)	C(1E)-C(2E)	1.30(4)
Os(2E)-C(16E)	1.93(4)	C(2E)-C(3E)	1.43(5)
Os(2E)-C(17E)	1.97(4)	C(3E)-C(4E)	1.28(6)
Os(2E)-W(1E)	2.722(2)	C(3E)-C(8E)	1.37(5)
Os(3E)-C(9E)	1.82(5)	C(4E)-C(5E)	1.27(6)
Os(3E)-C(11E)	1.895(11)	C(5E)-C(6E)	1.41(4)
Os(3E)-C(10E)	1.97(3)	C(6E)-C(7E)	1.37(6)
Os(3E)-C(12E)	2.01(2)	C(7E)-C(8E)	1.37(5)
Os(3E)-C(1E)	2.25(3)	C(20E)-C(21E)	1.23(5)
W(1E)-O(1E)	1.66(2)	C(20E)-C(24E)	1.42(5)
W(1E)-O(2E)	1.817(18)	C(20E)-C(25E)	1.57(4)
W(1E)-C(21E)	2.31(4)	C(21E)-C(26E)	1.54(6)
W(1E)-C(22E)	2.42(3)	C(21E)-C(22E)	1.59(6)
W(1E)-C(24E)	2.41(3)	C(22E)-C(23E)	1.38(5)
W(1E)-C(20E)	2.42(4)	C(22E)-C(27E)	1.45(3)
W(1E)-C(23E)	2.47(3)	C(23E)-C(24E)	1.39(4)
O(9E)-C(9E)	1.27(6)	C(23E)-C(28E)	1.49(5)
O(10E)-C(10E)	1.19(3)	C(24E)-C(29E)	1.52(4)
O(11E)-C(11E)	1.18(3)		

Bond angles (deg) for 11

C(14E)-Os(1E)-C(13E)	92(2)	C(24E)-W(1E)-C(23E)	33.1(10)
C(14E)-Os(1E)-C(15E)	89.4(14)	C(20E)-W(1E)-C(23E)	55.8(14)
C(13E)-Os(1E)-C(15E)	173.5(13)	O(1E)-W(1E)-Os(2E)	97.2(7)
C(14E)-Os(1E)-O(2E)	175.1(13)	O(2E)-W(1E)-Os(2E)	104.4(6)
C(13E)-Os(1E)-O(2E)	93.0(17)	C(21E)-W(1E)-Os(2E)	140.4(14)
C(15E)-Os(1E)-O(2E)	85.7(9)	C(22E)-W(1E)-Os(2E)	101.6(7)
C(14E)-Os(1E)-Os(3E)	95.1(8)	C(24E)-W(1E)-Os(2E)	114.0(9)
C(13E)-Os(1E)-Os(3E)	86.1(10)	C(20E)-W(1E)-Os(2E)	146.8(11)
C(15E)-Os(1E)-Os(3E)	87.4(8)	C(23E)-W(1E)-Os(2E)	91.8(9)
O(2E)-Os(1E)-Os(3E)	85.6(6)	O(1E)-W(1E)-Os(1E)	95.0(9)
C(14E)-Os(1E)-W(1E)	142.6(9)	O(2E)-W(1E)-Os(1E)	45.3(7)
C(13E)-Os(1E)-W(1E)	84.0(15)	C(21E)-W(1E)-Os(1E)	156.7(13)
C(15E)-Os(1E)-W(1E)	98.7(8)	C(22E)-W(1E)-Os(1E)	159.5(7)
O(2E)-Os(1E)-W(1E)	37.9(5)	C(24E)-W(1E)-Os(1E)	117.1(8)
Os(3E)-Os(1E)-W(1E)	121.53(7)	C(20E)-W(1E)-Os(1E)	130.6(8)
C(14E)-Os(1E)-Os(2E)	88.5(8)	C(23E)-W(1E)-Os(1E)	129.6(11)
C(13E)-Os(1E)-Os(2E)	95.9(10)	Os(2E)-W(1E)-Os(1E)	62.41(6)
C(15E)-Os(1E)-Os(2E)	90.5(8)	W(1E)-O(2E)-Os(1E)	96.8(10)
O(2E)-Os(1E)-Os(2E)	90.6(6)	C(2E)-C(1E)-Os(3E)	128(2)
Os(3E)-Os(1E)-Os(2E)	175.78(9)	C(1E)-C(2E)-C(3E)	123(3)
W(1E)-Os(1E)-Os(2E)	55.20(5)	C(4E)-C(3E)-C(8E)	114(4)
C(18E)-Os(2E)-C(19E)	94.2(15)	C(4E)-C(3E)-C(2E)	118(4)
C(18E)-Os(2E)-C(16E)	99.8(14)	C(8E)-C(3E)-C(2E)	127(4)
C(19E)-Os(2E)-C(16E)	92.8(14)	C(5E)-C(4E)-C(3E)	124(5)
C(18E)-Os(2E)-C(17E)	92.9(13)	C(4E)-C(5E)-C(6E)	118(5)
C(19E)-Os(2E)-C(17E)	172.7(14)	C(7E)-C(6E)-C(5E)	127(4)
C(16E)-Os(2E)-C(17E)	87.5(13)	C(8E)-C(7E)-C(6E)	104(4)
C(18E)-Os(2E)-W(1E)	104.4(9)	C(7E)-C(8E)-C(3E)	133(4)
C(19E)-Os(2E)-W(1E)	85.1(9)	O(9E)-C(9E)-Os(3E)	170(2)
C(16E)-Os(2E)-W(1E)	155.8(11)	O(10E)-C(10E)-Os(3E)	175(3)
C(17E)-Os(2E)-W(1E)	91.7(8)	O(11E)-C(11E)-Os(3E)	179(2)
C(18E)-Os(2E)-Os(1E)	166.7(9)	O(12E)-C(12E)-Os(3E)	170(3)
C(19E)-Os(2E)-Os(1E)	86.4(11)	O(13E)-C(13E)-Os(1E)	178(5)
C(16E)-Os(2E)-Os(1E)	93.4(11)	O(14E)-C(14E)-Os(1E)	174(4)
C(17E)-Os(2E)-Os(1E)	86.3(8)	O(15E)-C(15E)-Os(1E)	175(3)
W(1E)-Os(2E)-Os(1E)	62.39(5)	O(16E)-C(16E)-Os(2E)	174(3)
C(9E)-Os(3E)-C(11E)	94.5(11)	O(17E)-C(17E)-Os(2E)	172(3)
C(9E)-Os(3E)-C(10E)	94.9(16)	O(18E)-C(18E)-Os(2E)	170(3)
C(11E)-Os(3E)-C(10E)	96.0(11)	O(19E)-C(19E)-Os(2E)	177(3)
C(9E)-Os(3E)-C(12E)	163.8(13)	C(21E)-C(20E)-C(24E)	112(4)
C(11E)-Os(3E)-C(12E)	96.7(11)	C(21E)-C(20E)-C(25E)	128(5)
C(10E)-Os(3E)-C(12E)	95.4(14)	C(24E)-C(20E)-C(25E)	119(3)
C(9E)-Os(3E)-C(1E)	86.1(14)	C(21E)-C(20E)-W(1E)	70(3)
C(11E)-Os(3E)-C(1E)	90.7(9)	C(24E)-C(20E)-W(1E)	73(2)

C(10E)-Os(3E)-C(1E)	173.1(10)	C(25E)-C(20E)-W(1E)	114(3)
C(12E)-Os(3E)-C(1E)	82.2(12)	C(20E)-C(21E)-C(26E)	134(5)
C(9E)-Os(3E)-Os(1E)	81.1(8)	C(20E)-C(21E)-C(22E)	107(5)
C(11E)-Os(3E)-Os(1E)	175.1(8)	C(26E)-C(21E)-C(22E)	115(3)
C(10E)-Os(3E)-Os(1E)	86.6(9)	C(20E)-C(21E)-W(1E)	80(3)
C(12E)-Os(3E)-Os(1E)	87.2(7)	C(26E)-C(21E)-W(1E)	129(4)
C(1E)-Os(3E)-Os(1E)	86.8(5)	C(22E)-C(21E)-W(1E)	74(2)
O(1E)-W(1E)-O(2E)	106.7(12)	C(23E)-C(22E)-C(27E)	137(3)
O(1E)-W(1E)-C(21E)	87.3(16)	C(23E)-C(22E)-C(21E)	104(2)
O(2E)-W(1E)-C(21E)	111.9(14)	C(27E)-C(22E)-C(21E)	119(3)
O(1E)-W(1E)-C(22E)	100.0(11)	C(23E)-C(22E)-W(1E)	75.6(19)
O(2E)-W(1E)-C(22E)	139.6(10)	C(27E)-C(22E)-W(1E)	117(2)
C(21E)-W(1E)-C(22E)	39.2(16)	C(21E)-C(22E)-W(1E)	66.9(19)
O(1E)-W(1E)-C(24E)	142.5(11)	C(24E)-C(23E)-C(22E)	108(3)
O(2E)-W(1E)-C(24E)	85.9(10)	C(24E)-C(23E)-C(28E)	129(4)
C(21E)-W(1E)-C(24E)	55.6(16)	C(22E)-C(23E)-C(28E)	122(3)
C(22E)-W(1E)-C(24E)	55.3(10)	C(24E)-C(23E)-W(1E)	71(2)
O(1E)-W(1E)-C(20E)	109.9(12)	C(22E)-C(23E)-W(1E)	72(2)
O(2E)-W(1E)-C(20E)	86.1(11)	C(28E)-C(23E)-W(1E)	134(3)
C(21E)-W(1E)-C(20E)	30.1(14)	C(23E)-C(24E)-C(20E)	109(3)
C(22E)-W(1E)-C(20E)	56.1(11)	C(23E)-C(24E)-C(29E)	125(4)
C(24E)-W(1E)-C(20E)	34.3(13)	C(20E)-C(24E)-C(29E)	126(3)
O(1E)-W(1E)-C(23E)	132.6(14)	C(23E)-C(24E)-W(1E)	76(2)
O(2E)-W(1E)-C(23E)	115.8(12)	C(20E)-C(24E)-W(1E)	73(2)
C(21E)-W(1E)-C(23E)	58.7(19)	C(29E)-C(24E)-W(1E)	127(2)
C(22E)-W(1E)-C(23E)	32.9(12)		

Atomic Coordinates and equivalent isotropic displacement coefficients ($Å^2 \times 10^3$) for 11.

	X	y	z	U(eq)
Os(1E)	1.5066(1)	0.6436(1)	-0.1967(1)	29(1)
Os(2E)	1.4856(1)	0.5445(1)	-0.1049(1)	30(1)
Os(3E)	1.5201(1)	0.7387(1)	-0.2899(1)	31(1)
W(1E)	1.3752(1)	0.6252(1)	-0.1481(1)	23(1)
O(1E)	1.3555(11)	0.6868(14)	-0.1161(9)	39(7)
O(2E)	1.4091(9)	0.6584(11)	-0.2113(7)	33(7)
O(9E)	1.4414(15)	0.6652(15)	-0.3261(8)	80(14)
O(10E)	1.6667(11)	0.6430(13)	-0.3165(10)	46(8)
O(11E)	1.5243(15)	0.8379(15)	-0.3910(10)	51(9)
O(12E)	1.5730(14)	0.8135(13)	-0.2300(10)	52(8)
O(13E)	1.4600(20)	0.7670(30)	-0.1471(10)	114(18)
O(14E)	1.6487(14)	0.6169(18)	-0.1786(9)	61(11)
O(15E)	1.5502(10)	0.5338(12)	-0.2625(6)	23(5)
O(16E)	1.6420(20)	0.4940(20)	-0.0903(12)	104(15)
O(17E)	1.5079(16)	0.4422(17)	-0.1728(8)	65(11)
O(18E)	1.4392(16)	0.4517(12)	-0.0126(6)	64(10)
O(19E)	1.4600(11)	0.6647(13)	-0.0491(9)	46(8)
C(1E)	1.4167(14)	0.8027(14)	-0.2637(9)	17(8)
C(2E)	1.3780(20)	0.8548(16)	-0.2897(12)	69(18)
C(3E)	1.3156(17)	0.8960(20)	-0.2682(15)	41(11)
C(4E)	1.2820(20)	0.9470(30)	-0.2971(19)	80(18)
C(5E)	1.2230(30)	0.9840(30)	-0.2838(13)	78(18)
C(6E)	1.1930(20)	0.9680(20)	-0.2340(13)	59(15)
C(7E)	1.2190(20)	0.9140(20)	-0.1979(17)	58(14)
C(8E)	1.2810(20)	0.8830(20)	-0.2213(14)	49(12)
C(9E)	1.4770(20)	0.6899(14)	-0.3089(10)	61(15)
C(10E)	1.6111(17)	0.6769(15)	-0.3044(10)	39(11)
C(11E)	1.5223(12)	0.7999(11)	-0.3522(7)	22(8)
C(12E)	1.5482(14)	0.7910(13)	-0.2517(9)	9(6)
C(13E)	1.4780(30)	0.7220(20)	-0.1645(11)	74(18)
C(14E)	1.5979(19)	0.6231(16)	-0.1856(13)	45(13)
C(15E)	1.5355(17)	0.5720(20)	-0.2363(11)	55(15)
C(16E)	1.5800(20)	0.5115(17)	-0.0976(12)	32(10)
C(17E)	1.5045(15)	0.4790(20)	-0.1490(9)	34(11)
C(18E)	1.4516(14)	0.4881(15)	-0.0496(9)	25(8)
C(19E)	1.4694(15)	0.6150(20)	-0.0704(11)	47(14)
C(20E)	1.2790(20)	0.6310(20)	-0.1836(11)	41(12)
C(21E)	1.2610(20)	0.6390(30)	-0.1401(17)	83(19)
C(22E)	1.2914(16)	0.5686(14)	-0.1053(8)	13(7)
C(23E)	1.3320(20)	0.5281(18)	-0.1385(13)	52(14)
C(24E)	1.3264(15)	0.5660(20)	-0.1866(10)	36(11)
C(25E)	1.2666(18)	0.6851(17)	-0.2333(11)	39(11)

C(26E)	1.2021(17)	0.6900(20)	-0.1142(16)	61(15)
C(27E)	1.2759(17)	0.5627(19)	-0.0513(8)	32(9)
C(28E)	1.3600(30)	0.4533(18)	-0.1224(14)	59(15)
C(29E)	1.3560(20)	0.5385(16)	-0.2341(12)	37(10)

Appendix A.12

Structure Determination Summary for $[Os_3W(CO)_8(\mu\text{-}O)_2(Cp^*)]_2$ **12**		
Empirical Formula	$Os_6W_2O_{20}C_{36}H_{30}$	
Crystal size (mm)	0.2 x 0.05 x 0.08	
Crystal System	Triclinic	
Space Group	*P*-1	
Unit Cell Dimensions	$a = 8.83290(10)$ Å	$\alpha = 101.68(1)$
	$b = 10.56540(10)$ Å	$\beta = 93.17(1)$
	$c = 13.82410(10)$ Å	$\gamma = 94.07(1)$
Volume $(Å)^3$	1256.99(2)	
Z	1	
Formula Weight	2291.67	
Density (calc.) $(g\ cm^{-3})$	3.246	
Absorption Coefficient (mm^{-1})	19.94	
λ(Mo-Kα)	0.70930 Å	
Temperature (°C)	-100	
2θ Range (deg)	57.3	
Index Ranges	$-11 \le 11, 0 \le 14, -18 \le 18$	
Reflections Collected	14621	
Independent Reflections	6421	
Observed Reflections [$I > 2.5\ \sigma(I)$]	5443	
Weighting Scheme	$\omega^{-1} = \sigma^2(F_o) + 0.0001\ F_o^2$	
Number of Parameters Refined	316	
Final *R* Indices (obs. Data)	$R = 0.033$; $R_W = 0.038$	
Final *R* Indices (all data)	$R = 0.033$; $R_W = 0.038$	
Goodness of Fit	1.58	
Largest and Mean Δ/σ	0.000	
Largest Difference Peak/Hole $(e/Å^3)$	-2.700/2.390	

Bond lengths (Å) for 12

Os(1)-Os(1)a	2.7982(6)	O(30)-C(30)	1.158(11)
Os(1)-Os(2)	2.7759(5)	O(31)-C(31)	1.129(10)
Os(1)-Os(2)a	2.8184(5)	O(32)-C(32)	1.158(11)
Os(1)-Os(3)	2.8668(5)	C(40)-C(41)	1.427(12)
Os(1)-W	2.8586(5)	C(40)-C(44)	1.438(12)
Os(1)-O(1)	2.144(5)	C(40)-C(45)	1.502(12)
Os(1)-C(10)	1.910(8)	C(41)-C(42)	1.432(12)
Os(1)-C(11)	1.878(8)	C(41)-C(46)	1.478(12)
Os(2)-Os(1)a	2.8184(5)	C(42)-C(43)	1.415(11)
Os(2)-Os(3)	2.8585(5)	C(42)-C(47)	1.507(12)
Os(2)-W	2.9468(4)	C(43)-C(44)	1.425(12)
Os(2)-O(2)	2.170(5)	C(43)-C(48)	1.511(12)
Os(2)-C(20)	1.949(9)	C(44)-C(49)	1.511(12)
Os(2)-C(21)	1.915(9)	C(45)-H(45a)	1.081(8)
Os(2)-C(22)	1.885(8)	C(45)-H(45b)	1.092(9)
Os(3)-W	2.6634(5)	C(45)-H(45c)	1.080(9)
Os(3)-C(30)	1.875(9)	C(46)-H(46a)	1.081(8)
Os(3)-C(31)	1.972(8)	C(46)-H(46b)	1.082(9)
Os(3)-C(32)	1.870(9)	C(46)-H(46c)	1.080(9)
W-O(1)	1.805(5)	C(47)-H(47a)	1.085(8)
W-O(2)	1.781(5)	C(47)-H(47b)	1.078(9)
W-C(40)	2.424(7)	C(47)-H(47c)	1.089(9)
W-C(41)	2.420(7)	C(48)-H(48a)	1.082(8)
W-C(42)	2.401(7)	C(48)-H(48b)	1.082(9)
W-C(43)	2.391(7)	C(48)-H(48c)	1.083(9)
W-C(44)	2.418(8)	C(49)-H(49a)	1.074(8)
O(10)-C(10)	1.156(10)	C(49)-H(49b)	1.092(9)
O(11)-C(11)	1.151(9)	C(49)-H(49c)	1.079(9)
O(20)-C(20)	1.124(12)	C(Cl)-Cl(1)	1.757(11)
O(21)-C(21)	1.150(11)	C(Cl)-Cl(2)	1.739(10)
O(22)-C(22)	1.139(10)	Cl(1)-Cl(2)	2.879(5)

Bond angles (deg) for 12

Os(1)a-Os(1)-Os(2)	60.745(12)	O(1)-W-O(2)	106.41(24)
Os(1)a-Os(1)-Os(2)a	59.237(14)	O(1)-W-C(40)	139.34(24)
Os(1)a-Os(1)-Os(3)	121.519(16)	O(1)-W-C(41)	109.2(3)
Os(1)a-Os(1)-W	94.969(14)	O(1)-W-C(42)	82.21(25)
Os(1)a-Os(1)-O(1)	90.03(14)	O(1)-W-C(43)	90.4(3)
Os(1)a-Os(1)-C(10)	164.6(3)	O(1)-W-C(44)	124.1(3)
Os(1)a-Os(1)-C(11)	91.78(22)	O(2)-W-C(40)	88.21(25)
Os(2)-Os(1)-Os(2)a	119.982(15)	O(2)-W-C(41)	81.56(24)
Os(2)-Os(1)-Os(3)	60.848(13)	O(2)-W-C(42)	109.8(3)
Os(2)-Os(1)-W	63.045(14)	O(2)-W-C(43)	138.86(25)
Os(2)-Os(1)-O(1)	93.59(15)	O(2)-W-C(44)	121.7(3)
Os(2)-Os(1)-C(10)	134.4(3)	C(40)-W-C(41)	34.3(3)
Os(2)-Os(1)-C(11)	90.03(24)	C(40)-W-C(42)	57.1(3)
Os(2)a-Os(1)-Os(3)	177.197(13)	C(40)-W-C(43)	57.3(3)
Os(2)a-Os(1)-W	122.171(15)	C(40)-W-C(44)	34.6(3)
Os(2)a-Os(1)-O(1)	86.49(14)	C(41)-W-C(42)	34.5(3)
Os(2)a-Os(1)-C(10)	105.6(3)	C(41)-W-C(43)	57.3(3)
Os(2)a-Os(1)-C(11)	91.74(24)	C(41)-W-C(44)	57.2(3)
Os(3)-Os(1)-W	55.445(13)	C(42)-W-C(43)	34.3(3)
Os(3)-Os(1)-O(1)	90.79(14)	C(42)-W-C(44)	57.1(3)
Os(3)-Os(1)-C(10)	73.5(3)	C(43)-W-C(44)	34.5(3)
Os(3)-Os(1)-C(11)	90.94(24)	Os(1)-O(1)-W	92.35(22)
W-Os(1)-O(1)	39.13(14)	Os(2)-O(2)-W	95.95(22)
W-Os(1)-C(10)	91.62(24)	Os(1)-C(10)-O(10)	173.5(8)
W-Os(1)-C(11)	143.67(24)	Os(1)-C(11)-O(11)	176.3(6)
O(1)-Os(1)-C(10)	86.3(3)	Os(2)-C(20)-O(20)	174.4(8)
O(1)-Os(1)-C(11)	176.4(3)	Os(2)-C(21)-O(21)	166.7(8)
C(10)-Os(1)-C(11)	91.1(3)	Os(2)-C(22)-O(22)	177.0(8)
Os(1)-Os(2)-Os(1)a	60.018(13)	Os(3)-C(30)-O(30)	179.0(7)
Os(1)-Os(2)-Os(3)	61.148(12)	Os(3)-C(31)-O(31)	177.3(8)
Os(1)-Os(2)-W	59.849(13)	Os(3)-C(32)-O(32)	178.6(8)
Os(1)-Os(2)-O(2)	88.97(14)	W-C(40)-C(41)	72.7(4)
Os(1)-Os(2)-C(20)	138.3(3)	W-C(40)-C(44)	72.5(4)
Os(1)-Os(2)-C(21)	131.9(3)	W-C(40)-C(45)	121.1(5)
Os(1)-Os(2)-C(22)	94.0(3)	C(41)-C(40)-C(44)	107.9(7)
Os(1)a-Os(2)-Os(3)	121.093(16)	C(41)-C(40)-C(45)	125.8(7)
Os(1)a-Os(2)-W	92.624(14)	C(44)-C(40)-C(45)	126.2(8)
Os(1)a-Os(2)-O(2)	88.97(15)	W-C(41)-C(40)	73.0(4)
Os(1)a-Os(2)-C(20)	160.3(3)	W-C(41)-C(42)	72.0(4)
Os(1)a-Os(2)-C(21)	71.9(3)	W-C(41)-C(46)	118.7(5)
Os(1)a-Os(2)-C(22)	95.6(3)	C(40)-C(41)-C(42)	107.6(7)
Os(3)-Os(2)-W	54.593(12)	C(40)-C(41)-C(46)	124.3(8)
Os(3)-Os(2)-O(2)	87.34(14)	C(42)-C(41)-C(46)	128.0(8)
Os(3)-Os(2)-C(20)	77.4(3)	W-C(42)-C(41)	73.5(4)
Os(3)-Os(2)-C(21)	166.4(3)	W-C(42)-C(43)	72.5(4)

Os(3)-Os(2)-C(22)	90.96(24)	W-C(42)-C(47)	119.0(5)
W-Os(2)-O(2)	36.95(14)	C(41)-C(42)-C(43)	108.4(7)
W-Os(2)-C(20)	93.66(25)	C(41)-C(42)-C(47)	126.9(7)
W-Os(2)-C(21)	125.07(24)	C(43)-C(42)-C(47)	124.7(8)
W-Os(2)-C(22)	143.12(24)	W-C(43)-C(42)	73.2(4)
O(2)-Os(2)-C(20)	84.9(3)	W-C(43)-C(44)	73.8(4)
O(2)-Os(2)-C(21)	89.1(3)	W-C(43)-C(48)	119.3(5)
O(2)-Os(2)-C(22)	175.4(3)	C(42)-C(43)-C(44)	108.4(7)
C(20)-Os(2)-C(21)	89.2(4)	C(42)-C(43)-C(48)	125.9(8)
C(20)-Os(2)-C(22)	90.5(4)	C(44)-C(43)-C(48)	125.7(8)
C(21)-Os(2)-C(22)	91.6(3)	W-C(44)-C(40)	73.0(4)
Os(1)-Os(3)-Os(2)	58.004(13)	W-C(44)-C(43)	71.8(4)
Os(1)-Os(3)-W	62.122(12)	W-C(44)-C(49)	133.4(5)
Os(1)-Os(3)-C(30)	159.0(3)	C(40)-C(44)-C(43)	107.6(7)
Os(1)-Os(3)-C(31)	95.90(24)	C(40)-C(44)-C(49)	124.9(8)
Os(1)-Os(3)-C(32)	107.4(3)	C(43)-C(44)-C(49)	125.5(8)
Os(2)-Os(3)-W	64.391(12)	C(40)-C(45)-H(45a)	110.1(7)
Os(2)-Os(3)-C(30)	103.3(3)	C(40)-C(45)-H(45b)	110.2(8)
Os(2)-Os(3)-C(31)	94.87(24)	C(40)-C(45)-H(45c)	110.1(7)
Os(2)-Os(3)-C(32)	164.1(3)	H(45a)-C(45)-H(45b)	108.5(7)
W-Os(3)-C(30)	102.62(24)	H(45a)-C(45)-H(45c)	109.4(8)
W-Os(3)-C(31)	155.17(24)	H(45b)-C(45)-H(45c)	108.5(8)
W-Os(3)-C(32)	104.3(3)	C(41)-C(46)-H(46a)	109.6(7)
C(30)-Os(3)-C(31)	95.1(3)	C(41)-C(46)-H(46b)	109.6(7)
C(30)-Os(3)-C(32)	89.9(4)	C(41)-C(46)-H(46c)	109.7(7)
C(31)-Os(3)-C(32)	92.8(3)	H(46a)-C(46)-H(46b)	109.2(7)
Os(1)-W-Os(2)	57.106(11)	H(46a)-C(46)-H(46c)	109.4(8)
Os(1)-W-Os(3)	62.434(13)	H(46b)-C(46)-H(46c)	109.3(7)
Os(1)-W-O(1)	48.53(16)	C(42)-C(47)-H(47a)	109.9(7)
Os(1)-W-O(2)	94.83(16)	C(42)-C(47)-H(47b)	110.4(7)
Os(1)-W-C(40)	170.02(19)	C(42)-C(47)-H(47c)	109.9(7)
Os(1)-W-C(41)	155.64(20)	H(47a)-C(47)-H(47b)	109.2(8)
Os(1)-W-C(42)	129.85(19)	H(47a)-C(47)-H(47c)	108.5(7)
Os(1)-W-C(43)	123.12(19)	H(47b)-C(47)-H(47c)	108.9(8)
Os(1)-W-C(44)	139.45(20)	C(43)-C(48)-H(48a)	109.8(7)
Os(2)-W-Os(3)	61.017(12)	C(43)-C(48)-H(48b)	109.8(7)
Os(2)-W-O(1)	95.95(16)	C(43)-C(48)-H(48c)	109.9(7)
Os(2)-W-O(2)	47.10(15)	H(48a)-C(48)-H(48b)	109.2(8)
Os(2)-W-C(40)	120.25(19)	H(48a)-C(48)-H(48c)	109.1(8)
Os(2)-W-C(41)	127.80(19)	H(48b)-C(48)-H(48c)	109.1(7)
Os(2)-W-C(42)	155.51(20)	C(44)-C(49)-H(49a)	110.3(7)
Os(2)-W-C(43)	169.11(20)	C(44)-C(49)-H(49b)	108.9(7)
Os(2)-W-C(44)	137.03(21)	C(44)-C(49)-H(49c)	110.1(7)
Os(3)-W-O(1)	105.87(16)	H(49a)-C(49)-H(49b)	109.0(8)
Os(3)-W-O(2)	102.41(16)	H(49a)-C(49)-H(49c)	110.0(7)
Os(3)-W-C(40)	107.64(19)	H(49b)-C(49)-H(49c)	108.6(7)

Os(3)-W-C(41)	141.92(19)	Cl(1)-C(Cl)-Cl(2)	110.9(6)
Os(3)-W-C(42)	143.03(19)	C(Cl)-Cl(1)-Cl(2)	34.3(3)
Os(3)-W-C(43)	108.73(20)	C(Cl)-Cl(2)-Cl(1)	34.7(3)
Os(3)-W-C(44)	90.75(20)		

Atomic Coordinates and equivalent isotropic displacement coefficients ($Å^2$ x 10^3) for 12.

	X	y	z	U(eq)
Os1	0.86893(3)	0.53873(3)	0.046117(20)	1.339(12)
Os2	1.12229(3)	0.71538(3)	0.064908(21)	1.434(11)
Os3	0.86088(3)	0.79219(3)	0.167697(21)	1.543(12)
W	1.01956(3)	0.62227(3)	0.239366(21)	1.378(12)
O1	0.9423(6)	0.4640(5)	0.1724(4)	1.65(22)
O2	1.2027(6)	0.6493(5)	0.1959(4)	1.66(21)
O10	0.5529(7)	0.5335(7)	0.1263(5)	3.2(3)
O11	0.7417(6)	0.6357(6)	-0.1307(4)	2.10(23)
O20	1.2428(8)	0.9850(7)	0.1835(5)	3.6(3)
O21	1.4439(7)	0.7156(7)	-0.0039(5)	3.3(3)
O22	1.0179(7)	0.8346(6)	-0.1058(4)	2.4(3)
O30	0.9760(8)	1.0468(7)	0.3049(5)	3.1(3)
O31	0.7220(7)	0.9216(6)	0.0050(4)	2.8(3)
O32	0.5666(8)	0.7923(7)	0.2701(5)	3.4(3)
C10	0.6737(9)	0.5431(9)	0.0989(6)	2.1(3)
C11	0.7936(9)	0.5968(8)	-0.0655(5)	1.5(3)
C20	1.1913(11)	0.8880(9)	0.1409(6)	2.3(4)
C21	1.3206(10)	0.6998(9)	0.0167(6)	2.2(3)
C22	1.0551(9)	0.7866(8)	-0.0427(6)	1.8(3)
C30	0.9317(10)	0.9502(9)	0.2518(6)	2.2(4)
C31	0.7723(9)	0.8716(8)	0.0626(6)	1.9(3)
C32	0.6802(10)	0.7929(8)	0.2321(6)	2.3(4)
C40	1.1248(9)	0.7271(8)	0.4041(5)	1.6(3)
C41	1.1726(9)	0.5987(8)	0.3843(5)	1.7(3)
C42	1.0394(10)	0.5103(8)	0.3737(5)	1.7(3)
C43	0.9108(9)	0.5831(8)	0.3863(5)	1.8(3)
C44	0.9618(10)	0.7174(9)	0.4061(6)	2.0(3)
C45	1.2273(10)	0.8503(9)	0.4210(6)	2.6(4)
C46	1.3322(10)	0.5679(9)	0.3734(6)	2.2(4)
C47	1.0331(11)	0.3643(9)	0.3508(6)	2.5(4)
C48	0.7472(10)	0.5279(9)	0.3803(6)	2.4(3)
C49	0.8689(10)	0.8273(9)	0.4489(6)	2.3(3)
CCl	0.4860(11)	0.2282(11)	0.2500(8)	3.4(5)
Cl1	0.4476(4)	0.2131(4)	0.37064(22)	5.18(15)
Cl2	0.6547(4)	0.1616(4)	0.2164(3)	6.63(20)
H45a	1.263	0.881	0.499	3.2
H45b	1.328	0.835	0.379	3.2
H45c	1.168	0.926	0.397	3.2
H46a	1.384	0.561	0.444	3.2
H46b	1.335	0.476	0.322	3.2
H46c	1.395	0.643	0.346	3.2
H47a	1.044	0.329	0.419	3.2
H47b	0.927	0.324	0.311	3.2
H47c	1.126	0.332	0.306	3.2

H48a	0.716	0.516	0.453	3.2
H48b	0.673	0.593	0.354	3.2
H48c	0.733	0.434	0.330	3.2
H49a	0.871	0.840	0.528	3.2
H49b	0.917	0.917	0.430	3.2
H49c	0.753	0.808	0.417	3.2

Claims to original research

1. Synthesis and characterization of $[Os_3W(\mu\text{-}H)(\mu\text{-}\eta^1\text{-}C{=}CHPh)(CO)_{10}(O)(\mu\text{-}O)(Cp^*)]$ (**1**).
2. Synthesis and characterization of $[Os_3W(\mu\text{-}H)(\textit{trans}\text{-}\mu\text{-}\eta^1\text{-}C{=}CHPh)(CO)_9(O)(Cp^*)(\mu_3\text{-}O)]$ (**2**)
3. Synthesis and characterization of $[Os_3W(\mu\text{-}H)(\textit{cis}\text{-}\mu\text{-}\eta^1\text{-}C{=}CHPh)(CO)_9(O)(Cp^*)(\mu_3\text{-}O)]$ (**3**)
4. Synthesis and characterization of $[Os_3W(CO)_{10}(O)(\mu\text{-}\eta^1,\eta^2\text{-}CH{=}CHPh)(\mu\text{-}O)(Cp^*)]$ (**4**)
5. Synthesis and characterization of $[Os_3W(\mu\text{-}H)(\textit{anti}\text{-}\mu\text{-}\eta^1\text{-}CHCH_2Ph)(CO)_9(O)(Cp^*)(\mu_3\text{-}O)]$ (**5**)
6. Synthesis and characterization of $[Os_3W(\mu\text{-}H)(\textit{gauche}\text{-}\mu\text{-}\eta^1\text{-}CHCH_2Ph)(CO)_9(O)(Cp^*)(\mu_3\text{-}O)]$ (**6**)
7. Synthesis and characterization of $[Os_3W(CO)_9(\mu\text{-}\eta^1,\eta^2\text{-}CH{=}CHPh\{\textit{W-Os}\})(\mu\text{-}O)_2(Cp^*)]$ (**7**)
8. Synthesis and characterization of $[Os_3W(CO)_9(\mu\text{-}\eta^1,\eta^2\text{-}CH{=}CHPh\{\textit{Os}\cdots\textit{Os}\})(\mu\text{-}O)_2(Cp^*)]$ (**8**)
9. Novel synthesis of $[Os_3W(\mu\text{-}H)(CO)_9(\mu\text{-}O)_2(Cp^*)]$ (**9**)
10. Synthesis and characterization of $[Os_3W(CO)_{10}(O)(\mu\text{-}\eta^1,\eta^2\text{-}CH{=}CHPh)(\mu\text{-}O)(Cp^*)]$ (**10**)
11. Synthesis and characterization of $[Os_3W(\eta^1\text{-}CH{=}CHPh)(CO)_{11}(O)(\mu\text{-}O)(Cp^*)]$ (**11**)
12. Synthesis and characterization of $[Os_3W(CO)_8(\mu\text{-}O)_2(Cp^*)]_2$ (**12**)